

**Advances made in the understanding of the biology
and genetics of *Phytophthora rubi* and *Phytophthora
fragariae***

Aurélia Bézanger

This thesis is submitted for the degree
of Doctor of Philosophy (PhD)
to the University of Dundee

September 2021

Table of Contents

List of Figures	VII
List of Tables	X
List of Abbreviations	XII
Acknowledgements	XV
Declaration	XVII
SUMMARY	XVIII
CHAPTER 1. INTRODUCTION	1
1.1. The current challenges and food crisis	1
1.1.1. Temperature rising.....	2
1.1.2. Adapting to climate change: towards greener solutions and decrease in carbon footprint	2
1.1.2.1. Hydroponics: a better growing alternative and a valuable tool for the study of root pathogens	2
1.1.2.2. Eating locally	5
1.2. Soft Fruits: raspberries and strawberries	5
1.2.1. Increasing demand for soft fruits.....	5
1.2.2. Production of raspberries and strawberries.....	6
1.2.3. A brief history of raspberry and strawberry cultivation	8
1.3. <i>Phytophthora</i> diseases of raspberry and strawberry.....	9
1.3.1. <i>Phytophthora</i> root rot (PRR): <i>Phytophthora rubi</i> and <i>Phytophthora fragariae</i>	9
1.3.2. <i>Phytophthora rubi</i> , cause of raspberry root rot	10
1.3.3. <i>Phytophthora fragariae</i> , cause of strawberry red stele	13
1.3.4. Hosts of <i>P. rubi</i> and <i>P. fragariae</i>	13
1.3.5. Root rot in the UK	14
1.4. Oomycete pathogens	14
1.4.1. Characterisation of Oomycetes.....	14
1.4.1.1. Oomycetes phylogeny	14
1.4.1.2. Oomycetes and fungi	15
1.4.1.3. Oomycetes host range	16
1.4.2. The <i>Phytophthora</i> genus	16
1.4.3. Reproduction and infection structures of <i>Phytophthora</i> spp.	17
1.5. Molecular Plant-Pathogen Interactions.....	20
1.5.1. MAMPs and PAMP- triggered Immunity (PTI).....	20
1.5.2. Effector Triggered Susceptibility (ETS)	21
1.5.3. Oomycete effectors.....	23
1.5.3.1. Oomycete apoplastic effectors	25

1.5.3.2. Translocated oomycete effectors	26
1.5.4. Effector Triggered Immunity (ETI).....	29
1.5.4.1 Oomycete Effector Recognition.....	30
1.5.4.2. Co-evolution and adaptation of the plant and pathogen.....	31
1.6. Potential methods of controlling root rot diseases	32
1.6.1. Growth conditions.....	33
1.6.2. Chemical control.....	34
1.6.3. Identifying and deploying durable resistances.....	35
1.6.4. Understanding the genetics, epidemiology and lifestyle of the pathogen	35
1.7. Summary of the project aims.....	37
CHAPTER 2. PHENOTYPIC STUDIES OF <i>P. RUBI</i> AND <i>P. FRAGARIAE</i>: ASSESSING RESPONSES TO AGRICULTURALLY IMPORTANT FACTORS	38
2.1. Introduction	38
2.2. Materials and methods	43
2.2.1. Cultures of <i>Phytophthora rubi</i> and <i>Phytophthora fragariae</i>	43
2.2.1.1. <i>P. rubi</i> isolation from infected raspberry canes	43
2.2.1.2. Growth media and culturing conditions for <i>P. rubi</i> and <i>P. fragariae</i>	46
2.2.1.3. Short- and long-term storage of <i>P. rubi</i> and <i>P. fragariae</i> isolates	48
2.2.1.4. <i>P. rubi</i> and <i>P. fragariae</i> isolates assessed in phenotypic assays.....	48
2.2.2. Chemical sensitivity testing.....	48
2.2.3. Inoculation and growth conditions.....	50
2.2.4. Hyphal growth measurements	51
2.2.5. Sporangia production and sporangia count.....	52
2.2.6. Chemical target genes sequences alignment.....	53
2.2.7. Statistical analysis	53
2.3. Results.....	53
2.3.1. Five new isolates of <i>P. rubi</i> infecting raspberry fields were successfully isolated from diseased canes in the summer	53
2.3.2. Effect of temperature on <i>in vitro P. rubi</i> life cycle stages: hyphal development and sporulation.....	56
2.3.2.1. Effect of temperature on hyphal growth: <i>P. rubi</i> hyphal development increases with temperatures rising to 21 °C but is inhibited above 25 °C.	56
2.3.2.2. Effect of temperature on <i>P. rubi</i> sporulation – <i>P. rubi</i> sporulation is successful and statistically similar in efficiency at all temperatures checked.....	57
2.3.3. Effects of chemicals on <i>P. rubi</i> and <i>P. fragariae</i> isolates.....	58
2.4. Discussion and Conclusions	69

CHAPTER 3. DIVERSITY STUDY USING PATHOGEN ENRICHMENT SEQUENCING (PENSEQ)	75
3.1. Introduction	75
3.1.1. Current Assessment of Diversity of <i>P. rubi</i> and <i>P. fragariae</i>	75
3.1.2. Pathogen Enrichment Sequencing (PenSeq).....	77
3.2. Materials and methods.....	81
3.2.1. <i>P. rubi</i> and <i>P. fragariae</i> samples preparation.....	81
3.2.1.1. Isolate selection and preparation for Pathogen Enrichment Sequencing	81
3.2.1.2. Sequenced reference genomes of <i>P. rubi</i> and <i>P. fragariae</i>	82
3.2.2. Designing the bait library	83
3.2.3. Enrichment: PenSeq Library preparation, hybridization and sequencing.....	84
3.2.4. Computational analyses	85
3.2.4.1. Preparation of reads prior to analysis	85
3.2.4.2. Mapping and cross-species mapping of reads to reference genomes	85
3.2.4.3. Preparation of reference genomes for coverage analysis: intersecting baits with reference genes.....	85
3.2.4.4. Function identification for gene of interest	86
3.2.4.5. Coverage analysis for genes of interest.....	86
3.2.4.6. Heterozygous Single Nucleotide Polymorphism (SNP) analysis.....	87
3.2.4.7. Inter- and intra-species diversity: presence / absence analyses	87
3.2.4.8. General effector diversity: k-mer analysis.....	87
3.2.5. Validation of observations made through PenSeq	88
3.2.5.1. Conventional PCR for PenSeq validation	88
3.2.5.2. Sequencing of PCR products for nucleotide sequence and SNP confirmation.....	89
3.3. Results.....	89
3.3.1. Mapping and coverage analyses	90
3.3.1.1. RXLR gene predictions	90
3.3.1.2. Same-species mapping and coverage for intra-species analyses.....	90
3.3.1.3. Cross-species mapping and coverage for inter-species analyses.....	93
3.3.2. Non-effector genes: housekeeping and drug target genes.....	95
3.3.2.1. PenSeq labelled <i>CoxI</i> species-specific SNPs were confirmed with PCR and sequencing	95
3.3.2.2. Inter-species diversity analysis of housekeeping and drug target genes	96
3.3.2.3. Intra-species diversity analysis of housekeeping and drug target genes	99
3.3.3. Intra-species studies of effector genes showed diversity amongst species.....	102
3.3.3.1. Diversity of effectors in <i>P. fragariae</i>	103
3.3.3.2. Diversity of effectors in <i>P. rubi</i>	105

3.3.4. Inter-species studies revealed core effectors as well as diversity between the two closely related species	108
3.3.5. Overall diversity analyses emphasized distinction between the two closely related species	111
3.3.6. K-mer analysis confirms PenSeq observations but does not cluster <i>P. rubi</i> according to race, year or location.	113
3.3.7. <i>In silico</i> PenSeq analyses highlighted several <i>P. rubi</i> and <i>P. fragariae</i> genes of interest	117
3.3.7.1. Comparison of expressed <i>P. fragariae</i> RXLR candidates in <i>P. rubi</i>	118
3.3.7.2. Gene coverage of <i>P. fragariae</i> effectors with published orthologs	122
3.3.7.3. <i>P. rubi</i> RXLR effectors.....	127
3.3.7.4. <i>P. rubi</i> PAMP and effectors involved in infections.....	136
3.4. Discussion and conclusions	142
CHAPTER 4. HYDROPONIC INFECTION OF RASPBERRIES USING <i>P. RUBI</i> EXPRESSING A FLUORESCENT MARKER	148
4.1. Introduction	148
4.2. Material and Methods.....	151
4.2.1. Preparation of <i>P. rubi</i> for infections.....	151
4.2.1.1. Culture of Phytophthora for infection assays	151
4.2.1.2. <i>P. rubi</i> culture for sporulation assays.....	151
4.2.1.3. Sporulation solutions	152
4.2.1.4. Induction of sporulation	153
4.2.1.5. Sporulation assays	153
4.2.1.6. Zoospore release for <i>P. rubi</i> and <i>P. fragariae</i>	154
4.2.2. <i>P. rubi</i> transformation for expression of fluorescent markers	154
4.2.2.1. Preparation of transformation plasmids pTOR-eGFP and pTOR-tdT	154
4.2.2.2. Pre-screening for <i>P. rubi</i> geneticin sensitivity	155
4.2.2.3. <i>P. rubi</i> hyphal preparation for transformation method 1	155
4.2.2.4. <i>P. rubi</i> hyphal preparation for transformation method 2	156
4.2.2.5. PEG – protoplast transformation method.....	156
4.2.2.6. Confirmation of <i>P. rubi</i> transformation using fluorescent assessment.....	158
4.2.3. Plant collection and growth conditions	158
4.2.3.1. Hydroponic raspberries	158
4.2.3.2. Plant leaves for infiltration assays	160
4.2.4. Hydroponic infection assay	160
4.2.5. <i>P. rubi</i> PTI leaf infiltration assays.....	161
4.2.6. Microscopic observation of <i>P. rubi</i> infection progression inside raspberry roots... ..	162
4.2.6.1. Confocal microscopy and calcofluor staining	162
4.2.6.2. Trypan blue and light microscopy	162

4.2.7. RNA extraction from infected raspberry roots (hydroponic infection).....	163
4.2.7.1. TriReagent RNA extraction method.....	163
4.2.7.2. Qiagen Rneasy Plant Mini Kit RNA extraction method	163
4.2.7.3. CTAB RNA extraction (Yu et al., 2012a).....	164
4.2.8. Expression of specific genes during hydroponic infection of raspberries.....	164
4.2.8.1. Gene selection	164
4.2.8.2. Primer design.....	164
4.2.8.3. cDNA synthesis.....	166
4.2.8.4. qRT-PCR	166
4.2.9. Statistical analyses	167
4.3. Results.....	167
4.3.1. Preparation of <i>Phytophthora</i> for inoculation assays	168
4.3.1.1. Identifying the most effective sporulation media	168
4.3.1.2. Younger cultures of <i>P. rubi</i> optimized the sporangia production	169
4.3.1.3. Identifying the most effective sporulation solution.....	169
4.3.1.4. Sporulation soil solutions could be stored at 20 °C or -80 °C prior to use	170
4.3.2. <i>P. rubi</i> transformation via two PEG-protoplast methods was confirmed	171
4.3.3. Rooting success of raspberry cultivars used for infection assays.....	174
4.3.4. <i>In planta</i> lifecycle of <i>P. rubi</i>	179
4.3.5. Investigation of resistance in Latham	184
4.3.6. <i>P. rubi</i> gene expression studies in susceptible raspberry cultivars.....	188
4.3.6.1. The CTAB RNA extraction method from Yu et al. (2012) was the most suitable for raspberry root samples	188
4.3.6.2. Expression of <i>P. rubi</i> life markers	188
4.3.6.3. Expression of four <i>P. rubi</i> RXLR genes in susceptible raspberry roots	191
4.4. Discussion & conclusions.....	197
CHAPTER 5. CONCLUSIONS: ANSWERING QUESTIONS ABOUT RASPBERRY ROOT ROT	204
5.1. Conclusions on <i>P. rubi</i> raspberry root rot	204
5.2. Concluding remarks and future work.....	208
REFERENCES	211
APPENDICES.....	234
Appendix A. PHENOTYPIC STUDIES OF <i>P. RUBI</i> AND <i>P. FRAGARIAE</i>: ASSESSING RESPONSES TO AGRICULTURALLY IMPORTANT FACTORS – Chapter 2.....	234
Appendix B. <i>P. RUBI</i> AND <i>P. FRAGARIAE</i> EFFECTOR GENES DIVERSITY STUDIED THROUGH PENSEQ – Chapter 3.....	235
Appendix C. HYDROPONIC INFECTION OF RASPBERRIES – Chapter 4.....	248

List of Figures

Figure 1. 1. Schematic views of different hydroponic systems.	4
Figure 1. 2. Raspberry production worldwide.	7
Figure 1. 3. Strawberry production worldwide.	7
Figure 1. 4. <i>Phytophthora</i> clades.	10
Figure 1. 5. Red stele and Root rot symptoms on strawberries and raspberries.	12
Figure 1. 6. <i>P. rubi</i> and <i>P. fragariae</i> hosts.	13
Figure 1. 7. Oomycetes phylogeny.	15
Figure 1. 8. Potato field infected by <i>Phytophthora infestans</i>	17
Figure 1. 9. Schematic representation of root-infecting <i>Phytophthora</i> life cycle.	18
Figure 1. 10. Oomycetes infection strategies.	19
Figure 1. 11. Effector functions.	22
Figure 1. 12. Schematic representation of oomycete effector secretion and host-haustorium interactions (Dodds et al., 2009).	24
Figure 1. 13. Review and examples of oomycete effector structures.	25
Figure 1. 14. Wang et al. (2019) figure of virulence test of <i>P. infestans</i> RXLR candidate effectors.	27
Figure 1. 15. The zig-zag-zig model for plant-pathogen interactions from Hein et al. (2009).	30
Figure 1. 16. Disease triangle.	33
Figure 1. 17. Flood located near a raspberry polytunnel infected with root rot.	34
Figure 2. 1. Weather data in Invergowrie, Scotland, between 1991 and 2019.	39
Figure 2. 2. Temperatures in raspberry (a.) and strawberry (b.) cultures in 2020.	40
Figure 2. 3. Photos of the <i>P. rubi</i> isolation process from infected canes.	45
Figure 2. 4. Representation of the location and year of isolation of <i>P. rubi</i> and <i>P. fragariae</i> isolates.	47
Figure 2. 5. Representation of the colony diameter measurements for the study.	51
Figure 2. 6. Photo representing a field of view for counting <i>P. rubi</i> / <i>P. fragariae</i> sporangia (microscope).	52
Figure 2. 7. Photos of infected raspberry canes sampled during April and August 2018.	54
Figure 2. 8. Alignment of <i>CoxI</i> sequences from samples isolated from infected raspberry canes.	55
Figure 2. 9. Boxplot representation of the effect of temperature on the mycelial growth of 12 isolates.	56
Figure 2. 10. Boxplot representation of the effect of temperature on the sporulation of five <i>P. rubi</i> isolates.	58
Figure 2. 11. Effect of Fluazinam on isolates growth.	60
Figure 2. 12. Effect of Fluopicolide on isolates growth.	61
Figure 2. 13. Effect of Propa mocarb on isolates growth.	63
Figure 2. 14. Effect of Ametoctradin on isolates growth.	64
Figure 2. 15. Effect of Phorce on isolates growth.	65
Figure 2. 16. Effect of Dimethomorph on isolates growth.	66
Figure 2. 17. Effect of Metalaxyl on isolates growth.	67
Figure 2. 18. Effect of seven chemicals on <i>P. rubi</i> and <i>P. fragariae</i> isolates.	72
Figure 2. 19. Photos illustrating chemical screening plates.	72

Figure 3. 1. Example of overall coverage graphs from 0 % mismatch mapping.....	92
Figure 3. 2. Example of overall coverage graphs from 3 % mismatch mapping.....	92
Figure 3. 3. Example of overall coverage graphs from 0 % mismatch cross-mapping.....	94
Figure 3. 4. Example of overall coverage graphs from 3 % mismatch cross-mapping.....	94
Figure 3. 5. Validation of PenSeq SNPs for <i>CoxI</i> gene.....	96
Figure 3. 6. Coverage for housekeeping / drug target genes at 0 % mm from cross-species mapping.....	97
Figure 3. 7. Coverage for housekeeping / drug target genes at 0 % mm.	100
Figure 3. 8. <i>P. fragariae</i> coverage of genes when mapped to BC-16.....	111
Figure 3. 9. <i>P. rubi</i> coverage of genes mapped to SCRP333.....	112
Figure 3. 10. <i>P. rubi</i> coverage of genes when mapped to <i>P. fragariae</i> reference genome BC-16.....	113
Figure 3. 11. (Overleaf) Representation of the k-mer analysis clustering of the 24 isolates (k=12).....	114
Figure 3. 12. Coverage graphs for eight <i>P. fragariae</i> RXLR.	119
Figure 3. 13. Agarose electrophoresis gels (2 % agarose) testing the BC-16_g19167 primers.....	121
Figure 3. 14. Validation of PenSeq SNPs and nucleotides sequences for BC-16_g19167.	121
Figure 3. 15. Coverage graph for eight <i>P. fragariae</i> apoplastic genes.	125
Figure 3. 16. Agarose electrophoresis gels for BC-16_contig_38_F2468 and BC-16_g2112.	126
Figure 3. 17. Validation of PenSeq nucleotides sequences for BC-16_g2112 and BC-16_contig_38_F2468.....	127
Figure 3. 18. Coverage graph for eight <i>P. rubi</i> RXLR.	130
Figure 3. 19. Agarose electrophoresis gels for SCRP333_contig_4275_F7.	133
Figure 3. 20. Validation of PenSeq SNPs for SCRP333_contig_4275_F7 gene.....	134
Figure 3. 21. Nucleotide alignment for BC-16_contig_51_F623 RXLR gene.	135
Figure 3. 22. Agarose electrophoresis gel following PCR of BC-16_contig_51_F623.....	136
Figure 3. 23. Coverage graph for eight <i>P. rubi</i> apoplastic genes.	139
Figure 3. 24. Agarose electrophoresis gels for SCRP333_g28651.	140
Figure 3. 25. Sequencing to confirm nucleotide sequences for SCRP333_g28651.	141
Figure 3. 26. Nucleotide sequences alignment for SCRP333_g8655, matching <i>P. sojae</i> PsXLP1.....	141
Figure 4. 1. Illustration of leaf infiltration inoculation points.....	162
Figure 4. 2. Layout of microscope slides.....	162
Figure 4. 3. Effect of medium on growth and sporulation of <i>P. rubi</i> SCRP333.	168
Figure 4. 4. Effect of SCRP333 culture age on sporulation.....	169
Figure 4. 5. Effect of different solutions on <i>P. rubi</i> SCRP333 sporulation.	170
Figure 4. 6. Effect of storage conditions of solutions on sporulation of <i>P. rubi</i> SCRP333....	171
Figure 4. 7. <i>P. rubi</i> isolate SCRP333 mycelium expressing fluorescent proteins.....	172
Figure 4. 8. Sporangia and zoospores of transformed <i>P. rubi</i> isolates.....	172
Figure 4. 9. Effect of SCRP333_tdT culture age on sporulation.....	173
Figure 4. 10. Effect of raspberry root exudates on sporulation for transgenic <i>P. rubi</i> SCRP333_tdT.....	174
Figure 4. 11. Progress of hydroponic-raspberry cultures.....	175

Figure 4. 12. Data for success of hydroponics during the two-years of trials.....	176
Figure 4. 13. Average percentage of cuttings surviving and rooting over the two-years trial.	176
Figure 4. 14. Survival rates of hydroponic raspberries.....	177
Figure 4. 15. Photos of infected Glen Dee and Glen Moy at 3 dpi.....	180
Figure 4. 16. Photos of infected Glen Dee, Glen Moy and Latham at 7 dpi.....	181
Figure 4. 17. Photos of infected Glen Dee, Glen Moy and Latham at 9 and 10 dpi.....	182
Figure 4. 18. Photos of infected Glen Dee, Glen Moy and Latham at 11 dpi.....	182
Figure 4. 19. Photos of infected Glen Dee, Glen Moy and Latham at 14 dpi.....	183
Figure 4. 20. Photos of infected Glen Dee and Glen Moy at 22 and 30 dpi.....	184
Figure 4. 21. Photos of infected Glen Dee and Glen Moy plants at 30 dpi.....	184
Figure 4. 22. <i>N. benthamiana</i> leaf infiltration with <i>P. rubi</i> and <i>P. infestans</i> culture filtrates.	186
Figure 4. 23. Potato leaf infiltration with <i>P. rubi</i> and <i>P. infestans</i> culture filtrates.....	186
Figure 4. 24. Raspberry leaf infiltration with <i>P. rubi</i> and <i>P. infestans</i> culture filtrates.....	187
Figure 4. 25. Relative expression of <i>P. rubi</i> haustoria-specific membrane protein PrHmp1.	189
Figure 4. 26. Relative expression of <i>P. rubi</i> sporulation marker PrCDC14.....	190
Figure 4. 27. Relative expression of <i>P. rubi</i> marker RUB1.....	191
Figure 4. 28. Relative expression of <i>P. rubi</i> SCRP333_contig_4275_F7 RXLR gene during the September 2019 infection time course.....	192
Figure 4. 29. Relative expression of <i>P. rubi</i> RXLR genes SCRP333_g22109, SCRP333_g22154 and SCRP333_g24428 at 7 dpi from RNASeq samples.....	194
Figure 4. 30. Relative expression of <i>P. rubi</i> RXLR genes SCRP333_g22109, SCRP333_g22154 and SCRP333_g24428 in infection time courses from qRT-PCR.....	196
Figure 4. 31. Intact Glen Dee root and root tip (photo taken with ZEISS LSM 710, x10)....	199
Figure 4. 32. Spectral power distributions of various light sources.....	200

List of Tables

Table 1. 1. Franceschetti et al. (2017) examples of predicted effectors of pathogens	23
Table 1. 2 Chepsergon et al. (2020) predicted number of cytoplasmic RXLR and CRN effectors in <i>Phytophthora</i> spp.	26
Table 2. 1. Details of chemicals used in this study.....	44
Table 2. 2. Details of <i>P. rubi</i> and <i>P. fragariae</i> isolates used in the phenotypic study assessing the effects of temperatures and chemicals.	47
Table 2. 3. List and description of the fungicides incorporated into media and their mode of action. (N/A: non-applicable)	49
Table 2. 4. Statistical analyses on the effect of temperature.	57
Table 2. 5. Average colony diameter for <i>P. rubi</i> and <i>P. fragariae</i> grown on media incorporated with seven chemicals.	59
Table 2. 6. Half-inhibitory doses of the seven chemicals tested against <i>P. fragariae</i> and <i>P. rubi</i> isolates	68
Table 3. 1. List of <i>P. rubi</i> and <i>P. fragariae</i> sequenced genomes.....	78
Table 3. 2. Effector gene predictions in sequenced isolates of <i>P. fragariae</i> and <i>P. rubi</i> (Table from Adams et al., 2020).....	81
Table 3. 3. Details of <i>P. fragariae</i> and <i>P. rubi</i> isolates used in this PenSeq study	82
Table 3. 4. Total numbers and types of genes incorporated into the input for bait library design.....	83
Table 3. 5. Housekeeping, drug target and pathogenic genes incorporated into the input for bait library design.	84
Table 3. 6. Colour code used for coverage tables	86
Table 3. 7. Primers designed for a subset of <i>P. fragariae</i> and <i>P. rubi</i> genes of interest	88
Table 3. 8. Average mapping of reads at several Bowtie mismatch mapping rates.....	91
Table 3. 9. Average mapping of reads at several Bowtie mismatch mapping rates.....	93
Table 3. 10. (Overleaf) Inter-species polymorphism for housekeeping / drug target genes. .	97
Table 3. 11. Intra-species polymorphism for housekeeping / drug target genes	101
Table 3. 12. Number of isolate-unique genes for <i>P. fragariae</i>	104
Table 3. 13. Coverage for ten diversified <i>P. fragariae</i> RXLR genes.....	104
Table 3. 14. Coverage for ten diversified <i>P. rubi</i> genes.....	106
Table 3. 15. Polymorphism in RXLR genes from Perthshire (farm A) <i>P. rubi</i> isolates.....	107
Table 3. 16. Polymorphism in RXLR genes from Perthshire (farm C) <i>P. rubi</i> isolates.....	108
Table 3. 17. Coverage data for the 12 <i>P. fragariae</i> unique RXLR genes.....	109
Table 3. 18. Coverage data for the 11 <i>P. rubi</i> unique RXLR genes.....	110
Table 3. 19. Coverage data for eight <i>P. fragariae</i> genes.....	118
Table 3. 20. Description of eight <i>P. fragariae</i> effectors	122
Table 3. 21. Coverage data for eight <i>P. fragariae</i> apoplastic genes.....	124
Table 3. 22. <i>P. rubi</i> RXLR effectors of interest.....	128
Table 3. 23. Coverage data for selected <i>P. rubi</i> RXLR genes.....	129
Table 3. 24. Polymorphism in four <i>P. rubi</i> genes of interest.....	132
Table 3. 25. Description of eight <i>P. rubi</i> apoplastic effector of interest	136
Table 3. 26. Coverage data for eight <i>P. rubi</i> genes.....	138

Table 3. 27. Summary table. 145

Table 4. 1. List of *P. rubi* isolates used in various infection assays 152

Table 4. 2. List and details of transformations carried out on *P. rubi*..... 155

Table 4. 3. Media used for PEG-protoplasts transformation of *P. rubi*..... 156

Table 4. 4. Raspberry cultivars tested in hydroponic conditions. 159

Table 4. 5. Details of primers used to screen for genes of interest in qRT-PCR assays..... 165

Table 4. 6. RNA results from three extraction methods. 188

Table 4. 7. Coverage of 10 *P. rubi* RXLR genes expressed at 7 dpi. 193

List of Abbreviations

ANOVA	Analysis of Variance
Avr	Avirulence
BCP	1–Bromo–3–Chloropropane
BLASTn/p	Basic Local Alignment Search Tool for nucleotide / proteins sequences
BP	Base-pair
CAA	Carboxylic Acid Amide
CoxI	Cytochrome C oxidase subunit I
CRN	Crinkler
CT	Cycle Threshold
CV	Cultivar
DAMP	Damage Associated Molecular Pattern
ddNTPs	Dideoxynucleotide triphosphates
DEFRA	Department for Environment, Food and Rural Affairs
DEPC	Diethyl Pyrocarbonate
DMSO	Dimethyl Sulfoxide
DNA	Deoxyribonucleic Acid
dNTPs	Deoxynucleotide triphosphates
DPI	Days Post-Inoculation
DOTMA	(N-[1-(2,3-dioleyloxy)propyl]-N,N,N-trimethylammonium chloride)
eGFP	Enhanced Green Fluorescent Protein
EDTA	Ethylenediaminetetraacetic Acid
EER	Glutamic acid- Glutamic acid– Arginine
ETI	Effector-Triggered Immunity
ETS	Effector-Triggered Susceptibility
FAO	Food and Agriculture Organization of the United Nations
FBA	French Bean Agar
FRAC	Fungicide Resistance Action Committee
FPKM	Fragments Per Kilobase of transcript per Million mapped reads
G. Dee	Glen Dee

G. Fyne	Glen Fyne
GHG	Greenhouse Gas
G. Moy	Glen Moy
HCl	Hydrochloride
HeSNP	Heterozygous SNP
HPI	Hours Post-Inoculation
HR	Hypersensitive Response
HSP	Heat Shock Protein
KOH	Potassium Hydroxide
ITS	Internal Transcribed Spacer
IPM	Integrated Pest Management
JA	Jasmonic Acid
JHI	The James Hutton Institute
LB	Luria-Bertani medium
LTRs	Long Terminal Repeat retrotransposons
LXLFLAK	Leucine-any amino acid-Leucine-Phenylalanine-Leucine-Alanine-Lysine
MAMP	Microbe-Associated Molecular Pattern
MAPK	Mitogen-Activated Protein Kinases
NaCl	Sodium chloride
NB-LRR	Nucleotide-Binding, Leucine-Rich Repeat
NCBI	National Center for Biotechnology Information
NOAA	National Oceanic and Atmospheric Administration
PAMP	Pathogen-Associated Molecular Pattern
PEG	Polyethylene Glycol
PCD	Programmed Cell Death
PCR	Polymerase Chain Reaction
PRR	<i>Phytophthora</i> Root Rot
PRRs	Pattern-Recognition Receptors
PTI	Pattern-Triggered Immunity
PVP	Polyvinylpyrrolidone
PVPP	Polyvinylpolypyrrolidone
qPCR	Quantitative Polymerase Chain Reaction

QTL	Quantitative Trait Locus
rDNA	Recombinant DNA
RNA	Ribonucleic Acid
ROS	Reactive Oxygen Species
RXLR	Arginine-X-Leucine-Arginine
SA	Salicylic Acid
SDS	Sodium Dodecyl Sulfate
SDW	Sterile Distilled Water
SNP	Single Nucleotide Polymorphism
SOLA	Specific Off Label Approval
ssDNA	Single-stranded Deoxyribonucleic acid
tdT	Tander-dimer Tomato
Tris-HCl	Hydroxymethyl-aminomethane hydrochloride
TSL	The Sainsbury Laboratory
UNG	Uracil-N-glycosylase
UK	United Kingdom
UV	Ultraviolet
WT	Wild type

Acknowledgements

First and foremost, I would like to thank my supervisors Dr Eleanor Gilroy, Dr Ingo Hein and Dr Steve Whisson; for securing the funding, accepting me for the project, and for their most helpful guidance and friendship. Eleanor has taught me a lot through her insight and knowledge, while continuously encouraging me in my PhD and as a friend, reminding me that “success is going from failure to failure without losing your enthusiasm”.

Thanks to our partner at NIAB-EMR, Dr Richard Harrison, Dr Charlotte Nellist and Dr Thomas Adams, for sharing their genome data on *P. rubi* and *P. fragariae*, and for always happily help and answer any questions.

Thanks to my funders, AHDB, and my AHDB supervisors, Cathryn Lambourne and Dr Katja Maurer, for this opportunity and for their feedback.

I would also like to thank Ross Mitchell for his guidance and vision into the soft fruit industry.

I need to thank the members of my Thesis committee, Dr Jennie Brierley and Dr Alison Roberts, for their advice and comments on my project.

There are always so many people behind a successful project, and I would like to thank all the members of The James Hutton Institute who have assisted me, particularly Lydia Welsh, who tremendously helped with discovering *P. rubi*'s secrets, generously sharing her expertise in *Phytophthora* and molecular tools; Dr Miles Armstrong, who taught me about bioinformatics and helped with the PenSeq analyses along with Dr Paolo Ribeca; Alison Dobson, with whom I shared the enthusiasm and excitement of the hydroponics raspberries (finally!) growing and brainstormed ideas to improve this technique, which eventually promoted further hydroponics work at The James Hutton Institute. I also want to thank Ruth D'Urban Jackson at ADAS, for sharing protocols, as well as the joys (and tears!) of working with slow growing and difficult pathogens like *P. rubi* and *P. fragariae*, and for keeping me informed on their work.

On a more personal note, I want to thank the many people that helped me during my PhD journey. Special thanks to Dr David Kenyon for his guidance and keen support towards me starting a PhD. I thank all my friends, from all over the world, at SASA and

at JHI, who have been very helpful from the moment I decided to pursue a PhD to the application and throughout my project, always there for me and reminding me that true friends are never apart.

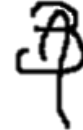
I am also very thankful to my family, including my parents, my brothers, and my family here in Scotland, for encouraging me into these challenging times.

Most of all, I want to thank my partner, Martin, who has always been positive about me following my dreams and has patiently backed me up during my PhD quest. His constant reminder that with my motivation I could achieve anything I wanted has pushed me further towards my goals and positively lifted me up. I want to thank him for listening to me, excitingly explaining parts of my research, and for giving me the confidence to comeback from any setbacks.

Declaration

Candidate

The candidate is the author of the thesis. Unless otherwise stated, all references cited have been consulted by the candidate. The work of which the thesis is a record has been done by the candidate and has not been previously accepted for a higher degree.

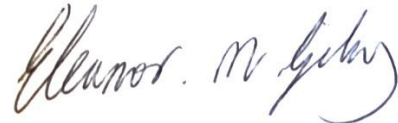


.....

Aurélia Bézanger

Supervisor

The conditions of the relevant ordinances and regulations have been fulfilled.



.....

Dr Eleanor Gilroy (JHI)

SUMMARY

Agriculture is facing many challenges: a 20 % predicted growth in the world's population by 2050 that will require a rise in land and resources use, with a 70 % to 110 % food production increase, global warming with rising carbon dioxide emissions and temperatures, as well as more stringent regulations on disease control. This means that managing and mitigating diseases in the field will be harder as environmental factors might influence the pathogen's populations and genetics through selective pressure.

Raspberry root rot, caused by *Phytophthora rubi*, and strawberry red stele, caused by *Phytophthora fragariae*, are two oomycete pathogens that have decimated soft fruits production, there are few commercially available cultivars with resistance and limited chemical control options. Although both pathogens appeared in the 1930s in the UK, they still remain under-studied in terms of phenotypes, genotypes, and infection mechanisms.

This project aimed to increase the understanding of *P. rubi* and *P. fragariae*, particularly their potential to overcome external pressures caused by higher temperatures or chemicals. Phenotypic studies (Chapter 2) showed here that *P. rubi* and *P. fragariae* possess the potential to adapt to current control chemicals and to changing climatic conditions. Parallel genetic studies (Chapter 3), using target enrichment sequencing on pathogen sequences associated with virulence (PenSeq), found evidence for variation in the effector families between and within species. In this study, effectors unique to just one of the sister species were uncovered, indicating a role in determining host range. Core effectors conserved between the two pathogens and predicted to be essential for virulence were identified. Altogether, these results suggest that *P. rubi* and *P. fragariae* have great potential for adaptation and evolution to adjust to environmental stresses in the field.

Common problems for the study of root infecting pathogens reside in developing infection assays: often, these pathogens only sporulate in non-sterile solutions, and start infecting the crop by entering the root at the elongation zone. A clean method to propagate raspberries was developed here (Chapter 4), using hydroponics systems, which showed a great potential to grow soft fruits disease-free in fully controlled environments. This new system was used to infect raspberry cultivars with various

levels of resistance, with a strain of *P. rubi* that had previously been genetically modified to emit a red fluorescent protein, trackable in real time in the plant roots through confocal microscopy. This was the first report of a fluorescent *P. rubi* strain used for raspberry roots infection assays. Complete life cycle of *P. rubi* was observed on susceptible raspberries, while limited life stages were detected on resistant cultivar. Four effectors of a particularly important class, called RxLR, were up-regulated during infection, conceivably indicating some essential virulence function as well as some more specific early infection roles, like plant immunity suppression or host selection functions.

This work has enhanced our understanding of *P. rubi* and *P. fragariae* of raspberries and strawberries while reviewing and expanding the methodology to work with such diseases. It provides scientific knowledge to strengthen the horticultural industry and to decrease the crop losses due to pathogens through various strategies such as breeding and development of novel pathogen control approaches.

CHAPTER 1. INTRODUCTION

1.1. The current challenges and food crisis

According to NOAA (National Oceanic and Atmospheric Administration) National Centres for Environmental information, the global temperature has been rising between 0.3 °C and 1 °C every year since 1990 (NOAA, 2020). At the moment, it is feared that carbon dioxide emissions and following increased temperatures could lead to a 5 °C of warming by the end of the century (Matthews et al., 2009; O'Neill et al., 2017; Tollefson, 2020). Turning towards alternative growing methods, growing your own (use of allotments) and eating locally are all food-related practices that can help reduce the carbon footprint.

However, by 2050, there will be a 20 % predicted growth in the world's population, reaching just over 9 billion, needing a subsequent increase in global food production projected between 70 % and 110 % (FAO, 2009; Tilman et al., 2011). Nevertheless, this crucial crop production rise faces many additional challenges. Diets need to be rebalanced, both on a worldwide and an individual level, while reducing food related emissions by 70 % by 2050 (WWF, 2017). While around 660 million people are malnourished in the world, there are close to 2 billion who are overweight, and a third of the produced food is wasted (FAO, 2016). The livewell 2020 diet established by WWF recommends around 35 % of fruits and vegetables, 9 % of fatty food and drinks, 15 % of dairy products, 29 % of starchy food (pasta, rice, breads, potato etc.) and 12 % of non-dairy protein (meat, fish, eggs etc.). It highlights the importance of healthy fruits and vegetables consumption and is planned to help decrease GHG (greenhouse gas) emissions.

An essential part of producing more food is to reduce the crop loss associated with pests and pathogens, which is considered to be the biggest threat to food security (BBC-News, 2011; Savary et al., 2019). Worldwide yield loss for crops is estimated to reach between 20 % and 40 % annually, leading to billions of pounds lost (Savary et al., 2012; Savary et al., 2019). Current Integrated Pest Management (IPM) Strategies combine management practices to reduce diseases and pests while maintaining

environmental integrity. Strategies can be preventive, cultural, physical / mechanical, biological, or chemical.

1.1.1. Temperature rising

Climate change can affect crop pests and pathogens: survival, geographical distribution, population size, disease intensity and development are all susceptible to change following shifts in factors such as temperature and rainfall. In the UK, the average temperatures have increased by 0.8 to 1 °C since the 80s, while the winter rainfall appears to have increased (UKRI-NERC, 2016). It is therefore critical to keep research up to date on the effects of such variations to pathogenic populations, while trying to mitigate the problems.

1.1.2. Adapting to climate change: towards greener solutions and decrease in carbon footprint

As well as studying the effects of global warming on diseases, solutions can arise to decrease the carbon footprint, thus slowing down the temperature increase. Such solutions include alternative growing method employing less resources and diminishing waste as well as eating locally and in season.

1.1.2.1. Hydroponics: a better growing alternative and a valuable tool for the study of root pathogens

Even though soil is the natural and most common agricultural plant growth medium, providing everything that plants need (drainage, airflow, nutrients, water retention, and medium for root growth), alternative substrates (coco coir, rockwool etc.) are more and more common. All components of soil can be provided by other alternatives that might be better for controlling pathogens and excellent systems for producing disease free material (Barker and Pilbeam, 2007). For example, hydroponic systems provide adequate and targeted amounts of water, oxygen, and nutrients to the plant, while recycling the water and nutrient solution by recirculating it. In hydroponics, alternative growing media can be used to provide a substrate for root growth and nutrient uptake. It needs to have good moisture retention (nutrient uptake function) and air porosity (drainage function) (Ferguson et al., 2014). The most common growth media are coconut fibre (coir), perlite, vermiculite and rockwool, and they are usually composites

of natural materials (Treftz and Omaye, 2015). Growing fruits in hydroponics has a very positive connotation amongst consumers due to the numerous benefits that it offers compared to soil-based systems, such as lower water consumption and waste: up to 85 % less water used in hydroponics compared to traditional agriculture (Mpusia, 2006), more efficient use of nutrient / fertilisers with controlled application and no run-off (Howland et al., 2012), reduced amount of pesticides, and high yields (Resh, 2012), thus making it a good option for sustainable food production in non-arable regions of the world. Furthermore, hydroponic systems provide an all-year-round growing season. Commonly, there are six different types of hydroponics: Drip System, Ebb and Flow (or Flood and Drain), Nutrient Film Technique (NFT), Deep Water Culture (DWC), Aeroponics, and Wick. Drip systems are one of the most widely commercially used systems around the world, as it is very versatile and effective, especially for plants requiring a lot of root space. A drip system works by dripping nutrient solution onto the plant roots (Figure 1.1.a). Unlike other hydroponic systems, the Ebb and Flow (Figure 1.1.b) does not constantly expose roots to nutrient solution but works on periodic floods. Water is pumped onto the roots a few times a day to soak them, until the level reaches the height of an overflow outlet, when it then drains back down into the reservoir and gets recirculated. Nutrient Film Technique, or NFT, is a popular system for both commercial and home hydroponics (Figure 1.1.c). In NFT, plants are placed into the channel using a growing medium, where a shallow solution is running along the bottom, enabling bare roots to absorb nutrients and water. NFT allows the roots to remain moist and have good access to water, nutrient and oxygen but prevent them from being completely submerged. Deep Water culture, or DWC, is one of the easiest and most basic types of hydroponics (Figure 1.1.d). Plants are placed into growing medium inside net pots and the roots are suspended in the nutrient solution, where an air pump and air stone are placed and distribute oxygen. Aeroponics systems are similar to NFT in that the roots are suspended in the air, but in Aeroponics, nutrient solution is distributed via a constant mist sprayed onto the roots (Figure 1.1.e). In this system, roots get maximum oxygen, and the system generally uses less water than other types of hydroponics. The Wick system, also known as passive hydroponics, uses capillary action (via wicks) to bring nutrient and water from a reservoir to the plant (Figure 1.1.f). Wick systems are usually used for smaller plants which do not require so much water or nutrients.

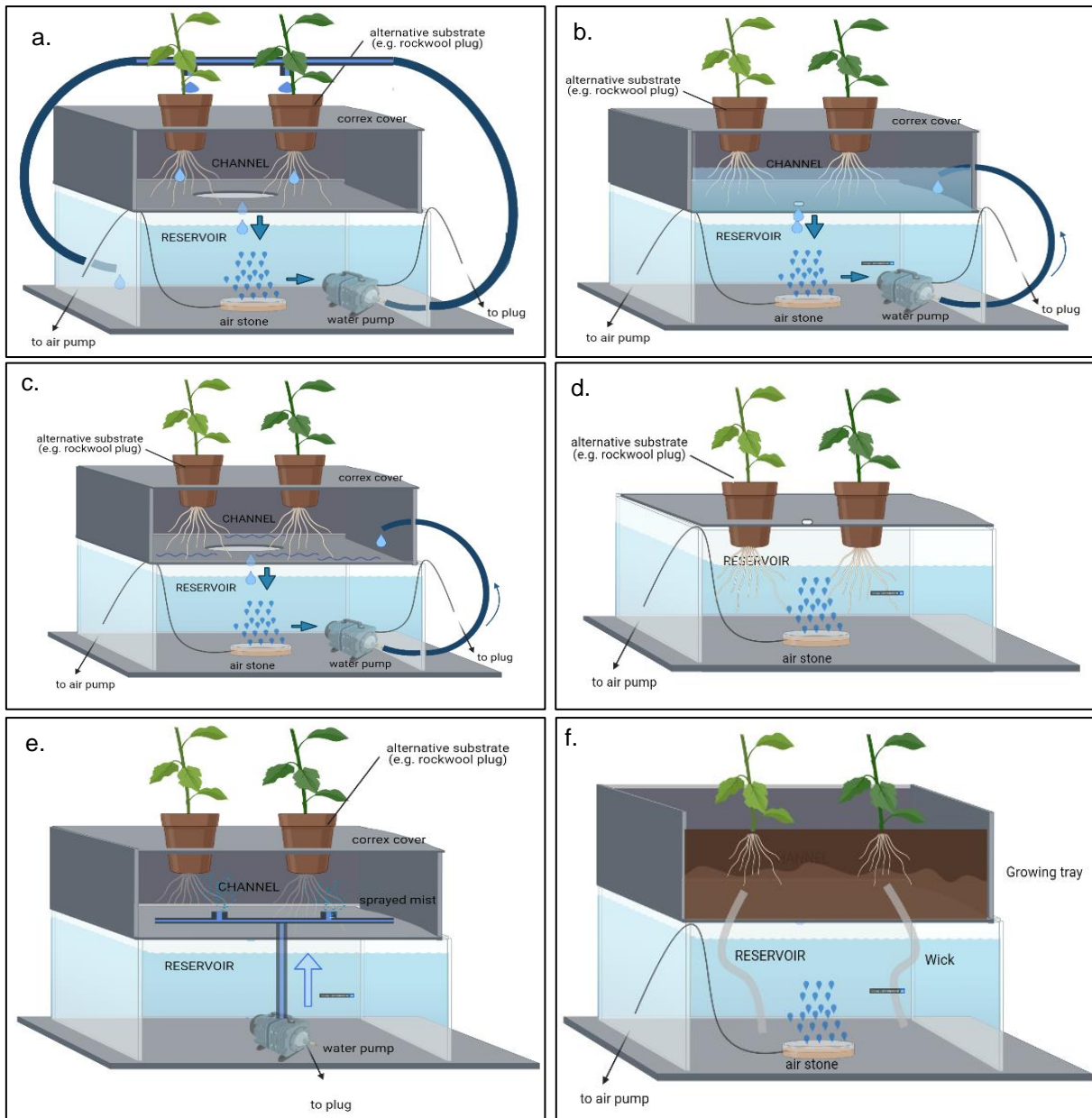


Figure 1. 1. Schematic views of different hydroponic systems. a. Drip Hydroponic system; **b.** Ebb & Flow (Or Flood & Drain) Hydroponic system; **c.** Nutrient Film Technique Hydroponic system; **d.** Deep Water culture (DWC) Hydroponic system; **e.** Aeroponics system (photo from medigrowinnovation.com); **f.** Wick Hydroponic system. Figures were made in BioRender.com

As cultivated land is declining (Pandey and Seto, 2015; Toulaitos et al., 2016), new growing methods emerge, like vertical farming. More and more popular, vertical farming systems (VFS) most often use vertical hydroponics, referred to as vertical columns, and show many improvements over conventional growing methods. They offer the ability to grow plants in small spaces while maintaining high yields, and regularly lead to a better product that is therefore marketable faster, due to the controlled environment granting optimal conditions (Liu et al., 2005; Resh, 2012;

Touliatos et al., 2016). The controlled environment allows the best conditions to grow all year around while final yields are not dependant on external biotic and abiotic factors, thus limiting loss due to extreme temperatures, drought, or disease. The systems reduce soil-borne diseases (as hydroponics) and the automatic feeding and watering simplify the farming process. They can be running on renewable energy to considerably decrease GHG emissions and move towards a greener agriculture. Those numerous benefits make vertical columns very attractive and numerous plants have already been trialled (Arias et al., 2000; Liu et al., 2005; Hayden, 2006; Linsley-Noakes et al., 2006; Coolong, 2012; Ramírez Gómez et al., 2012; Resh, 2012; Ferguson et al., 2014; Treftz and Omaye, 2015; Touliatos et al., 2016). They can be used for commercial growth or for research purposes, due to the wide range of variables that can be controlled. Since soil-less growing conditions produce clean roots that are easy to access and assess without causing damage, it can improve research of root-based pathosystems that usually involve manipulation of roots, many washing steps, de-contamination, that can all lead to root breakage.

1.1.2.2. Eating locally

Growing food in vertical farms is a good way to get local food, that would otherwise not be in season. Eating more locally and in season can increase the healthfulness of foods while helping to reduce the carbon footprint by lessening the packaging, processing, and transport. Investment is being made in new agriculture platforms that can help the UK intensification and widen the range of foods that can be propagated and grown (Agriculture 4.0) in a sustainable manner (Rose and Chilvers, 2018). This means that the UK should take advantage of local products, like fruits and vegetables, which constitute a third of the diet.

1.2. Soft Fruits: raspberries and strawberries

1.2.1. Increasing demand for soft fruits

Another challenge agriculture has to face is the push from populations to seek more variety, fresh and healthful produce for their diets, such as fruits and vegetables, as recommended by the livewell 2020 diet (WWF). At present in the UK, soft fruit represents approximately a quarter of all consumer fruit purchases (22 %) (DEFRA).

Raspberries and strawberries are particular favourites, due to their many health benefits. Indeed, studies have found that raspberries contain high levels of many beneficial vitamins (A, E, B1, B2, B3, B5, B6, and Vitamin K) while strawberries contain high levels of vitamin C. Raspberries and strawberries also contain a variety of polyphenolic compounds, including anthocyanins (responsible for the red colour in the fruit flesh), mostly pelargonidin for strawberries and cyanidin for raspberries (Aaby et al., 2007; Sariburun et al., 2010; Fang, 2015; Ponder and Hallmann, 2019), that can suppress the inflammation that leads to cardiovascular and coronary artery diseases, reduce heart diseases, and inflammation such as postprandial inflammation (Mink et al., 2007; Sesso et al., 2007; Huntley, 2009; Basu et al., 2010; Edirisinghe et al., 2011; Ellis et al., 2011; Wallace, 2011; Schaeffer, 2013; Basu et al., 2014; Ponder and Hallmann, 2019), improve memory and prevent mental declines due to aging (Thomasset et al., 2009; Spencer, 2010; Takanori, 2012). Plants from the *Rosaceae* family (raspberry, strawberry, blackberry, sour cherry etc.), show some of the highest levels of antioxidants (Halvorsen et al., 2002). These antioxidants have displayed anti-carcinogenic properties (Stoner and Mukhtar, 1995; Waladkhani and Clemens, 1998; Gundesli et al., 2019), improve eye health (Snodderly et al., 1991; Snodderly, 1995; Mozaffarieh et al., 2003), improve blood antioxidant status and decrease oxidative stress (Aaby et al., 2007; Henning et al., 2010; Tulipani et al., 2011; Basu et al., 2014). As a result of the research revealing the numerous health benefits of raspberry and strawberry consumption, they have become increasingly desirable to consumers, and more attractive to growers, as they become a higher value product.

1.2.2. Production of raspberries and strawberries

Following the increasing popularity of raspberries, it is not surprising to see an increase in both the fruit demand and the production. Over the past 20 years, the consumption of soft fruits in the UK has grown from 67,000 tonnes of strawberries and 13,000 tonnes of raspberries in 1996, to 168,000 tonnes of strawberries and 29,000 tonnes of raspberries in 2015: a 150 % increase for the former and a 123 % increase for the latter (Anderson, 2017). Similarly, as availability must match the demand, the production of soft fruit in the UK has also increased significantly, from 60,000 tonnes of soft fruit (strawberries, raspberries and “other berries”) produced in 1996, to 140,000 tonnes in 2015, representing a 131 % increase in the UK production of berries

(DEFRA, 2016). Amongst soft fruits, strawberries and raspberries are the most produced and currently showing the fastest growing popularity on the UK market (DEFRA, 2016). On a worldwide scale in 2016, the UK is the 11th largest producer of raspberries and 14th largest producer of strawberries (Figures 1.2 and 1.3). Raspberry production is an important high-value industry in the UK, providing processed produce (pulp for jam manufacture, canning or freezing) as well as fresh fruits, that have now become the focus.

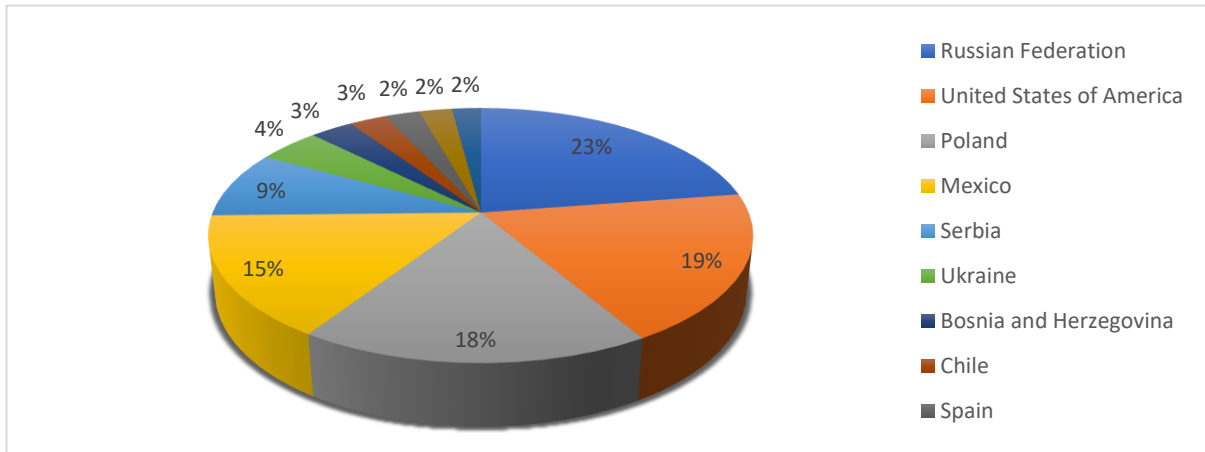


Figure 1. 2. Raspberry production worldwide. Pie chart representing the tonnes of raspberries produced worldwide for the 11 first producer countries and the corresponding percentage in 2016 (DEFRA, 2016).

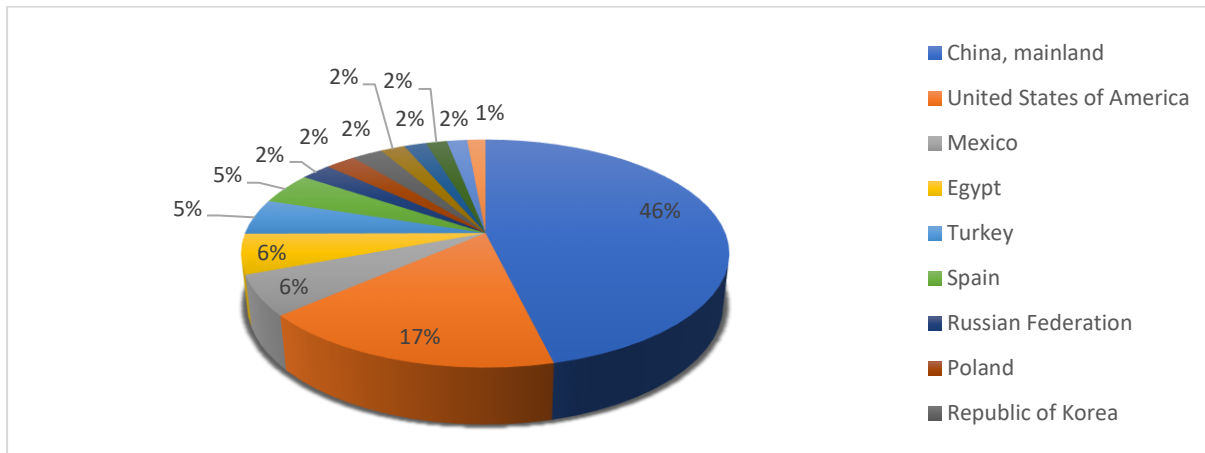


Figure 1. 3. Strawberry production worldwide. Pie chart representing the tonnes of strawberries produced worldwide for the 11 first producer countries and the corresponding percentage in 2016 (DEFRA, 2016).

Soft fruit production methods have evolved in recent years, as growers face wage inflation and shortage of lower-cost labour due to Brexit, whilst market prices remain stationary (Anderson, 2017). Growers are pushed to generate almost all year round

supplies of high-quality fresh produce at low cost while also adapting to the risks of diseases and loss of active compounds that help control pests and pathogens due to changes in regulations. These factors have driven the increased use of pot-based production systems in polytunnels for extending the soft fruit growing season. In the tunnels, alternative artificial substrate such as peat or coir rather than soil, is increasingly used to grow crops such as strawberries or raspberries (Anderson, 2017). Consequently, there is an increase in demand for new varieties that are better suited to this short and intensive method on top of the constant demand for better yield, quality, and disease resistant varieties.

1.2.3. A brief history of raspberry and strawberry cultivation

The Virginia strawberry, *Fragaria virginiana*, was brought to England from America in the 16th century. During the early 19th century, it was cross bred with a Chilean strawberry, *Fragaria chiloensis* in France, giving the strawberry we know today, *Fragaria ananassa*, before being brought to England. *Fragaria virginiana* and *Fragaria chiloensis* both diverged from an older strawberry, which resulted from the hybridization of four different species: two from Japan, *Fragaria iinumae* and *Fragaria nipponica*, a Eurasian species, *Fragaria viridis*, and a North american species, *Fragaria vesca* (Bertioli, 2019).

Red raspberry, *Rubus idaeus*, is native to Turkey. After the Romans spread raspberries throughout their empire, the British kept propagating them before exporting the plants to America, with the first plant nursery in the American colonies in 1737 in New York. In the late 1800s, a breeding program for raspberry started in New York and by 1925, more than 400 varieties were available with thousands of acres of raspberries grown in north-eastern America. *Rubus strigosus*, the American red raspberry has often been treated as a descendant variety of its European relative, as *Rubus idaeus* var. *strigosus*, but is now thought of as a distinct species (Malcolm, 2013).

Four raspberry cultivars were used throughout this study: Glen Dee, Glen Moy, Glen Fyne and Latham. Latham was bred in the USA in 1920 using a complex series of *Rubus* spp. hybrids (*Rubus strigosus*, American raspberry and *Rubus idaeus*, European). It is not a current commercial cultivar as it lacks many desirable traits required by modern growers: more than one crop a year, good yields, attractive

appearance and flavour of the fruits. However, it does possess a durable resistance to *Phytophthora* root rot (*P. rubi*) and has been used in genetic crosses that have identified the microsatellite resistance marker Rub118b, that has consequently been used in commercial breeding programmes (Graham et al., 2011). Still, not all cultivars with the Rub118b markers are symptoms-free for root rot. For instance, Glen Fyne, which possesses the marker, is susceptible to root rot, and not only to specific races, with symptoms quickly showing in the field. The 'Glen' series of raspberries were bred by the Raspberry Breeding Consortium (a partnership of growers, marketing groups, propagators, AHDB and Scottish Government) managed by James Hutton Limited at the James Hutton Institute. Glen Moy was first introduced in 1981 in Scotland, Glen Fyne in 2007 and Glen Dee in 2014. The immediate generations of crossing of those cultivars are from *Rubus idaeus*, although Glen Dee has a *Rubus strigosus* ancestor (nine generations prior). These three cultivars are susceptible to *Phytophthora* root rot.

More research is presently carried out for raspberry breeding in programmes like the one at the James Hutton Institute, in order to gain root rot resistance. At the moment, none of the commercial varieties have resistance against the disease, although the Canadian variety Cowichan seems to partially tolerate it. Genomic regions significantly associated with resistance are identified through mapping (Quantitative Trait Loci, or QTL, mapping) to keep developing molecular markers that will be used in breeding where selections displaying resistance phenotypes will be quickly identified.

1.3. *Phytophthora* diseases of raspberry and strawberry

Strawberry red stele is a disease caused by the oomycete pathogen *Phytophthora fragariae*. A similar disease of raspberry, root rot, is majorly caused by the oomycete *Phytophthora rubi*.

1.3.1. *Phytophthora* root rot (PRR): *Phytophthora rubi* and *Phytophthora fragariae*

P. fragariae Hickman (Hickman, 1940) was originally described as a pathogen of strawberry (*Fragaria x ananassa*), causing red core disease. Isolates were later

obtained from *Rubus idaeus* (red raspberry) and described as *P. fragariae* var. *rubi* (Waterson, 1937; Wilcox et al., 1993). The two species are very similar morphologically and physiologically and cause very comparable symptoms on the different hosts (strawberry and raspberry). It is only following genetics studies in 2007 (Man in't Veld, 2007) that *P. rubi* was identified as a separate species, infecting raspberries. Man in't Veld (2007) tested whether *P. fragariae* var. *fragariae* and *P. fragariae* var. *rubi* were reproductively isolated by genetic barriers to gene flow. From that study, unique alleles were found in strains of *P. fragariae* var. *fragariae* whereas different unique alleles were found in strains of *P. fragariae* var. *rubi*, demonstrating that there are no gene flows between the two varieties under laboratory conditions. The analysis was completed by determination of the cytochrome oxidase I (CoxI) sequences of some of these strains and showed consistent differences between the strains at 15 distinct positions.

Both *P. rubi* and *P. fragariae* belong to Clade 7 of the *Phytophthora* genus (Figure 1.4). *P. rubi* and *P. fragariae* are currently listed as A2 pests by the European and Mediterranean Plant Protection Organisation (EPPO) which recommends treating and regulating them as quarantine pests.

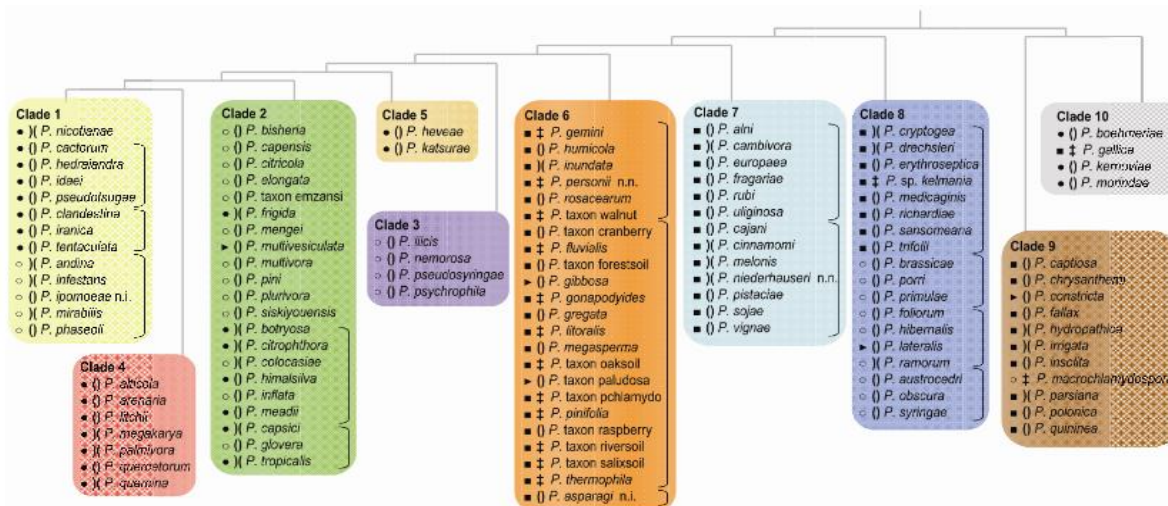


Figure 1. 4. *Phytophthora* clades. A genus-wide phylogeny for *Phytophthora* representing the different clades (Kroon et al., 2012) Heterothallic species are described as)(and homothallic as (). Sterile species have an #.

1.3.2. *Phytophthora rubi*, cause of raspberry root rot

Raspberry root rot, primarily caused by *Phytophthora rubi*, is currently the most economically damaging of all pests and diseases that affect raspberries in the UK.

Several *Phytophthora* species can cause root rot symptoms on raspberries, such as *P. rubi*, *P. idaei*, *P. syringae*, *P. drechsteri*, *P. cactorum*, *P. cambivora*, *P. megasperma*, *P. citricola*, *P. cryptogea*, *P. citrophthora*, and *P. gonopodyides*, though *P. rubi* is the most common and devastating (Wilcox, 1989; Wilcox et al., 1993; Wilcox and Latorre, 2002; Stewart et al., 2014; Ellis, 2016).

P. rubi is a soil-borne pathogen that infects raspberry through the roots. The disease will eventually affect every part of the plant, leading to wilt and death of the plant. Once established, it could be locally spread, and oospores, which are reproductive spores, could remain dormant in the soil for years. As field tolerance to PRR is only seen in a few raspberry cultivars, most of which are not used commercially, highly susceptible cultivars are planted, contributing to the rapid progress of the disease. Symptoms can sometimes be confused with other diseases such as *Verticillium* wilt, *Armillaria* root rot, or cane blight. Once in the root, *P. rubi* targets the vascular cylinder. Lesions form and extend above and below the point of infection. Infected roots often show a reddish colour and start to decay quickly, dying from the root tip upwards. Eventually the root becomes necrotic and lateral and new roots will be poorly developed and weak (Stewart et al., 2014) (Figure 1.5). Meanwhile, leaves on infected canes appear yellow and scorched. They will soon start to wilt, and blackish / purple lesions appear at the base of the cane (Figure 1.5). Severely affected canes will produce little to no new spawn in the spring and those that develop will wilt, making a typical “shepherd’s crook” shape (Figure 1.5). Ultimately, the infected plant ceases to grow and dies, forming patches of dead material in the field, called “disease pockets” (Stewart et al., 2014) (Figure 1.5). In less severe infection, early senescence and loss of vigour can be the only symptoms observed (Fordyce, 1991). Infections create opportunities for secondary fungi to attack the plant which might mask the initial *Phytophthora* pathogen, making disease diagnosis more difficult.

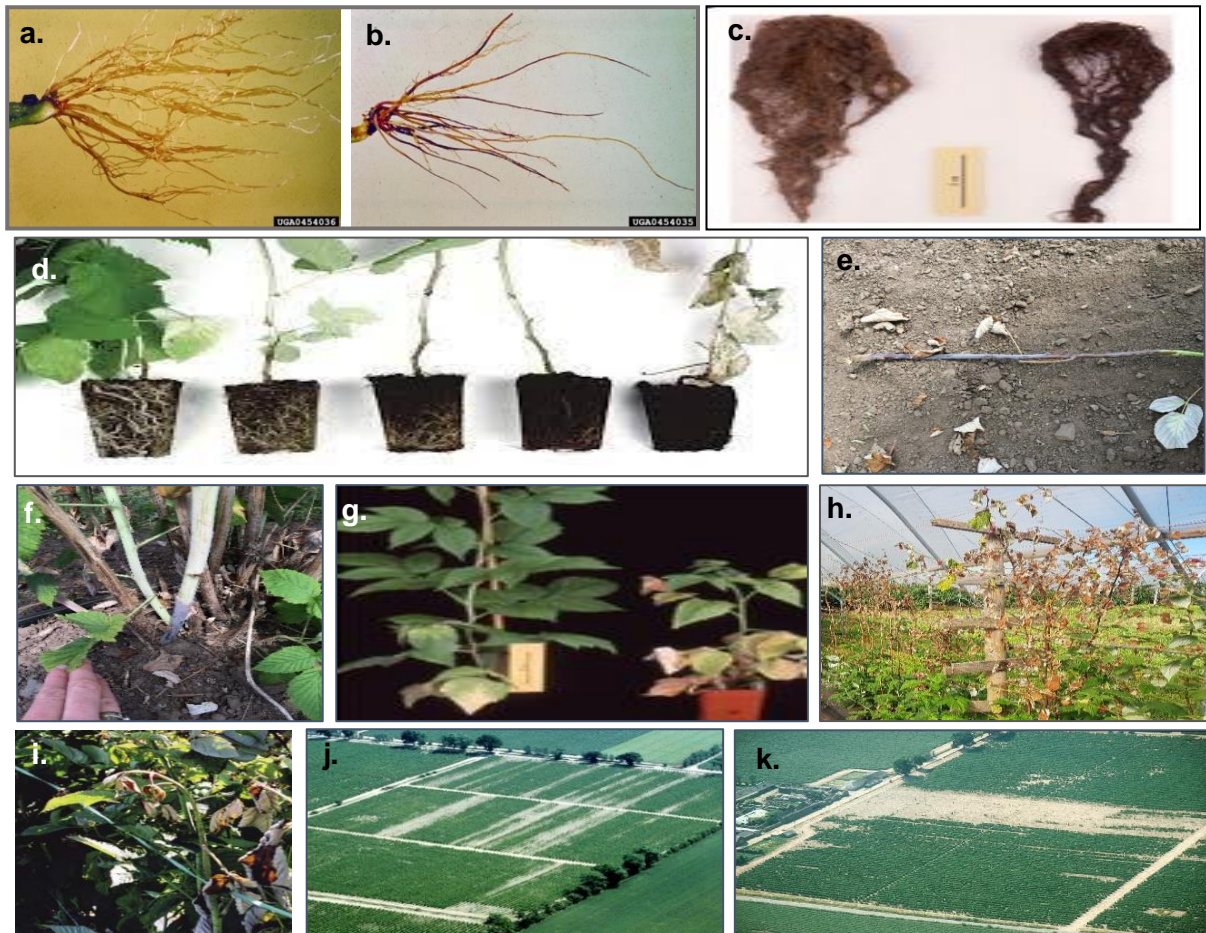


Figure 1. 5. Red stele and Root rot symptoms on strawberries and raspberries. **a.** Non-infected strawberry roots. **b.** Strawberry roots infected with *P. fragariae*, causing red stele disease. Roots have a typical “rat tail” appearance and vigour is reduced. **c.** Raspberry roots: on the left non-infected roots, on the right, roots infected with *P. rubi* causing root rot. Root vigour is reduced in the infected plant. **d.** Declining root volume in raspberry plants caused by increasing levels of *P. rubi* infection. **e-f.** Canes infected with *P. rubi*: purple lesions appear at the base of the cane, just above the ground. **g.** Whole raspberry plants infected with *P. rubi* ceasing to grow and wilting. **h.** Wilted and dying infected raspberry canes. **i.** Infected raspberry canes showing the typical ‘shepherd’s crook’ effect. **j-k.** Aerial view of raspberry fields infected with root rot: as plants die, they leave patches in the field, called disease pockets. (Photos a-c, g and j-k from The James Hutton Institute; Photos e-f and h from Aurelia Bezanger; Photos d and i from Raffle and Allen (2007)).

There are two known races of *P. rubi* (race 1 and 3) with distinct levels of disease on several raspberries, that could be identified using three cultivars: Latham, Autumn Bliss and EM5605/12. Race 1 is avirulent on the cultivars Latham and Autumn Bliss whereas race 3 is avirulent on the cultivars Latham, Autumn Bliss and EM5605/12 (Kennedy & Duncan, 1993).

1.3.3. *Phytophthora fragariae*, cause of strawberry red stele

Very closely related to *P. rubi*, *P. fragariae* is a pathogenic disease of strawberry, causing red core root rot (also known as red stele or red stele root rot). The life cycle is very similar to *P. rubi*. *P. fragariae* attacks and progresses inside strawberry roots, leading to plant decline and collapse. Roots get discoloured to a typical reddish tint, where the disease gets its name, and roots produce “rat tails” symptoms (Figure 1.5). Numerous studies have looked at racing of *P. fragariae* and have finally identified eleven races and hypothesised resistance genes (Adams, 2019; Adams et al., 2020).

1.3.4. Hosts of *P. rubi* and *P. fragariae*

P. fragariae natural hosts include two different soft fruit species: cultivated strawberries (*Fragaria x ananassa*) and loganberry (*Rubus x loganobaccus*) (Figure 1.6), a hybrid of the North American blackberry (*Rubus ursinus*) and the European raspberry (*Rubus idaeus*) (Hickman, 1940; McKeen, 1958; Pepin, 1967). Artificial infections of other *Rubus* members indicate that *P. fragariae* can survive on hosts such as European blackberry (*Rubus fruticosus*). However, even though *P. fragariae* has been isolated from loganberries, most cases of root rot in *Rubus* are caused by *P. rubi* (Wilcox, 1989) (Figure 1.6). *P. rubi* naturally infect cultivated raspberries (*Rubus idaeus*) and possibly other *Rubus* hybrid berries, like loganberries or tayberries, a cross between a blackberry and a red raspberry (*Rubus fruticosus x idaeus*), even though disease could not be reproduced in inoculation experiments on tayberries (Figure 1.6) (EPPO; Duncan et al., 1987).

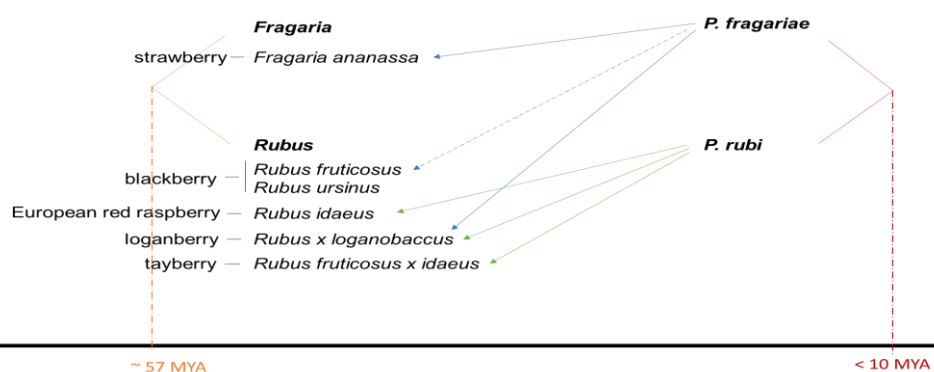


Figure 1. 6. *P. rubi* and *P. fragariae* hosts. *P. fragariae* can infect hosts from the *Fragaria* and *Rubus* genus while *P. rubi* infects *Rubus* species. MYA stands for Million years ago. Red lines indicate divergence between *P. fragariae* and *P. rubi*; orange lines indicate divergence between *Fragaria* and *Rubus* in the Rosaceae family. Blue lines indicate *P. fragariae* hosts, while green lines are *P. rubi* hosts. Full lines are natural hosts while dash lines are hosts infected through artificial infections.

1.3.5. Root rot in the UK

Strawberry red stele disease first appeared in the UK in 1920, caused by *Phytophthora fragariae* (Alcock and Howells, 1936), and similar symptoms were observed on raspberry shortly after, in 1937 (Waterson), caused by *P. fragariae* var. *rubi*. But it is only in the 1980s, following years of agriculture intensification, that several disease outbreaks appearing on raspberries all around the world brought *Phytophthora* root rot (PRR) and its global impacts back to attention, when Europe, the UK, North America, South America, and Australia all had reports of PRR (Alcock and Howells, 1936; Waterson, 1937; Hickman, 1940; Waterhouse, 1963; Barritt et al., 1979; Montgomerie and Kennedy, 1980; Seemüller et al., 1986; Duncan and Kennedy, 1987; Duncan et al., 1987; Nourisseau and Baudry, 1987; Washington, 1988; Duncan and Kennedy, 1989; Heiberg et al., 1989; Wilcox, 1989; Latorre and Muñoz, 1993). The disease spread fast and was locally carried to other growers through infected soil, water or equipment, rapidly infecting susceptible plants across fields, regions and ultimately countries. Furthermore, as homothallic species, *P. rubi* and *P. fragariae* can rapidly produce oospores. These survival structures can stay dormant in the soil for many years, therefore making root rot control difficult once the disease has been established in a field. In 2003, a survey conducted in Scotland concluded that 89% of raspberry growers had *Phytophthora* in their crop (Cooke, personal communication, 2017). Presently, more than 70% of the UK's soil-based raspberry production is affected by PRR, forcing growers to adopt different growing systems.

1.4. Oomycete pathogens

1.4.1. Characterisation of Oomycetes

1.4.1.1. Oomycetes phylogeny

Oomycetes form a distinct phylogenetic line of filamentous eukaryotic fungus-like microorganisms belonging to the Stramenopiles-Alveolata-Rhizaria (SAR) supergroup (Cavalier-Smith, 2018). The Oomycota are broadly divided into two subclasses: the *Saprolegniomycetidae* and the *Peronosporomycetidae* (Figure 1.7, McCarthy and Fitzpatrick, 2017).

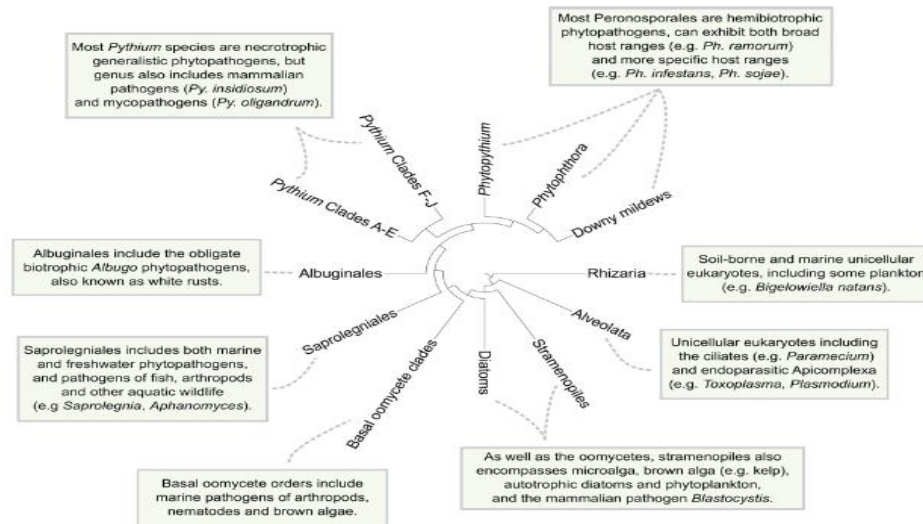


Figure 1. 7. Oomycetes phylogeny. Consensus phylogeny of the oomycetes class within the greater SAR grouping, including information pertaining to various taxa. The cladogram is from McCarthy and Fitzpatrick, (2017).

Saprolegniomycetidae are usually referred to as the “water molds” and include the orders Eurychasmales, Leptomitales, and Saprolegniales. The *Peronosporomycetidae* orders are mostly plant pathogens: the Rhipidiales, Pythiales, and Peronosporales (Fawke et al., 2015). Oomycete pathogens can infect leaf, stem and root tissues.

1.4.1.2. Oomycetes and fungi

Although oomycetes are morphologically similar to fungi, they are genetically more closely related to brown algae and diatoms, based on analyses of the 18S rRNA (Baldauf et al., 2000; van West, 2006; Diéguez-Urbeondo et al., 2009; Beakes et al., 2012). Differences between true fungi and oomycetes include cell walls composition, as fungi have chitin while oomycetes possess β -1,3-glucans, β -1,6-glucans and cellulose. The cellular organisation within hyphae also differs, with oomycetes displaying aseptate and coenocytic tubular hypha and fungi displaying single-cell septate hyphae (Latijnhouwers et al., 2003). Other differences between oomycetes and fungi include a diploid vegetative mycelial stage for oomycetes and a haploid or dikaryotic one for fungi (Emerson, 1941; Lévesque et al., 2010). Oomycete mitochondria possess tubular cristae as opposed to the flattened cristae of fungal mitochondria (Taylor, 1978).

1.4.1.3. Oomycetes host range

Oomycetes host range greatly varies between species. For example, *P. cinnamomi* can infect up to 3,000 different species (Hardham, 2005), while *Phytophthora fragariae* natural hosts include two different soft fruit species (McKeen, 1958; Pepin, 1967). Some oomycetes are biotrophic and establish a feeding relationship with a living host. Obligate biotrophs solely rely on living host tissues, restricting their host range with highly specific infection mechanisms (Fawke et al., 2015). On the other hand, hemi-biotrophic oomycetes, such as *Phytophthora* species, invade living host tissue before switching their feeding strategy to kill the cells as the infection progresses. Oomycetes can also be necrotrophic, such as *Pythium ultimum* (Fawke et al., 2015), which rapidly kills host tissue to obtain nutrients from the dying cells.

1.4.2. The *Phytophthora* genus

The *Phytophthora* genus has been first described by Heinrich Anton de Bary in 1875. *Phytophthora* spp. belong to the Peronosporales order of oomycetes. There are over 120 known species of *Phytophthora* (Martin et al., 2014) which are all plant pathogens, but Brasier (2009) estimated that there are likely to be between 200 and 600 *Phytophthora* species. Most *Phytophthoras* are plant pathogens, and the name *Phytophthora* comes from Greek, meaning “plant destroyer”, a term that is particularly well suited as some of the most destructive plant diseases are caused by *Phytophthora* species. Indeed, *Phytophthoras* have caused some of the most socially, economically and environmentally devastating plant disease outbreaks. The infamous Irish potato famine in 1840s, which was caused by *Phytophthora infestans*, first arriving from Mexico to Europe, where there were no resistant cultivars being grown on a large scale and subsequently destroyed most of the main European potato cultivars (Figure 1.8).



Figure 1. 8. Potato field infected by *Phytophthora infestans*. Damage visible in field of potatoes infected by *P. infestans* (TSL, Jonathan Jones Group, tsl.ac.uk)

Ireland was hit the hardest as many poor farmers relied on potato as a staple food and the disease therefore led to the death of one million people and the exodus of another million (Yoshida et al., 2013). *Phytophthora ramorum* emerged in the mid-1990s, causing ‘sudden oak death’ and ‘sudden larch death’ in America and Europe, leading to great losses of these tree species (Grunwald et al., 2012). *Phytophthora colocasiae* is another example of the dramatic impacts of *Phytophthora* spp., as it wiped out taro production in the Samoan islands in the mid-1990s (Lamour, 2013). *Phytophthora* species are divided into ten different clades, which include sub-clades (Figure 1.4) (Blair et al., 2008; Kroon et al., 2012; Martin et al., 2014; Yang et al., 2017).

1.4.3. Reproduction and infection structures of *Phytophthora* spp.

Oomycetes and *Phytophthoras* can reproduce sexually and/or asexually. In many species, sexual structures have never been observed, or only in laboratories. Homothallic species have both male and female reproductive structures on the same thallus e.g. *P. rubi* and *P. fragariae*; whereas heterothallic species have different mating types, e.g. *P. infestans*, named A1 and A2. Sexual reproduction occurs via the production of gametangia: oogonia and antheridia. When mated, antheridia introduce gametes into oogonia thus producing oospores. Oospores (Figure 1.9) are thick-walled long-term survival structures that usually result from sexual reproduction but can also be produced through apomixis (asexual reproduction without fertilization) (Lamour and Kamoun, 2009). Similar thick-walled resting spores, called chlamydospores, are produced from asexual reproduction. Under the right conditions,

chlamydospores or oospores germinate to form sporangia. These sporangia can either germinate directly, and form invasive hyphae or additional sporangia, or indirectly, which leads to the release of zoospores (Figures 1.9 and 1.10). Zoospores swim towards the host and encyst (Figures 1.9 and 1.10), shedding their flagella to form a cell wall, strongly attaching themselves to the surface with secreted adhesives (Hardham and Shan, 2009). The cyst forms a germ tube that grows across the plant surface and may develop into an appressorium (Latijnhouwers et al., 2003; Boevink et al., 2020) (Figures 1.9 and 1.10) or penetrate between plant cell walls (Figure 1.10 B.).

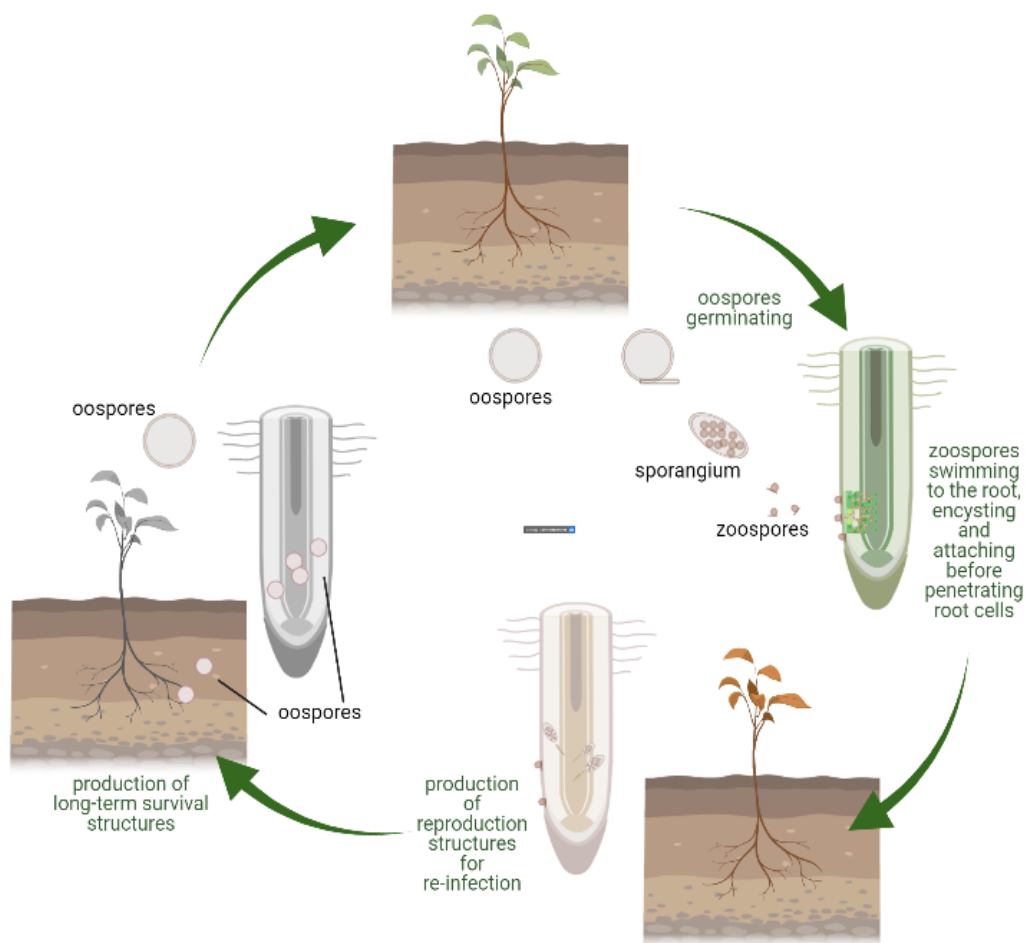


Figure 1. 9. Schematic representation of root-infecting *Phytophthora* life cycle. Oospores germinate, producing sporangia, full of zoospores. Under the right conditions, sporangium bursts and release zoospores, that swim towards a host root. They encyst, attach, and penetrate the cells with appressorium and haustorium. Pathogen progresses inside the host, generating more reproduction structures for re-infection. In later stages, long-term survival structures, oospores, are released, and can remain dormant for many years. Image made with BioRender.

Plant defenses sparked by pathogen penetration might result in the formation of a papilla or the death of the infected cell (Figure 1.10 B.) and during the biotrophic stage of infection, structures called haustoria are formed (Figure 1.10). However, these structures have not yet been observed for *P. rubi* and *P. fragariae* infections of raspberry and strawberry plants.

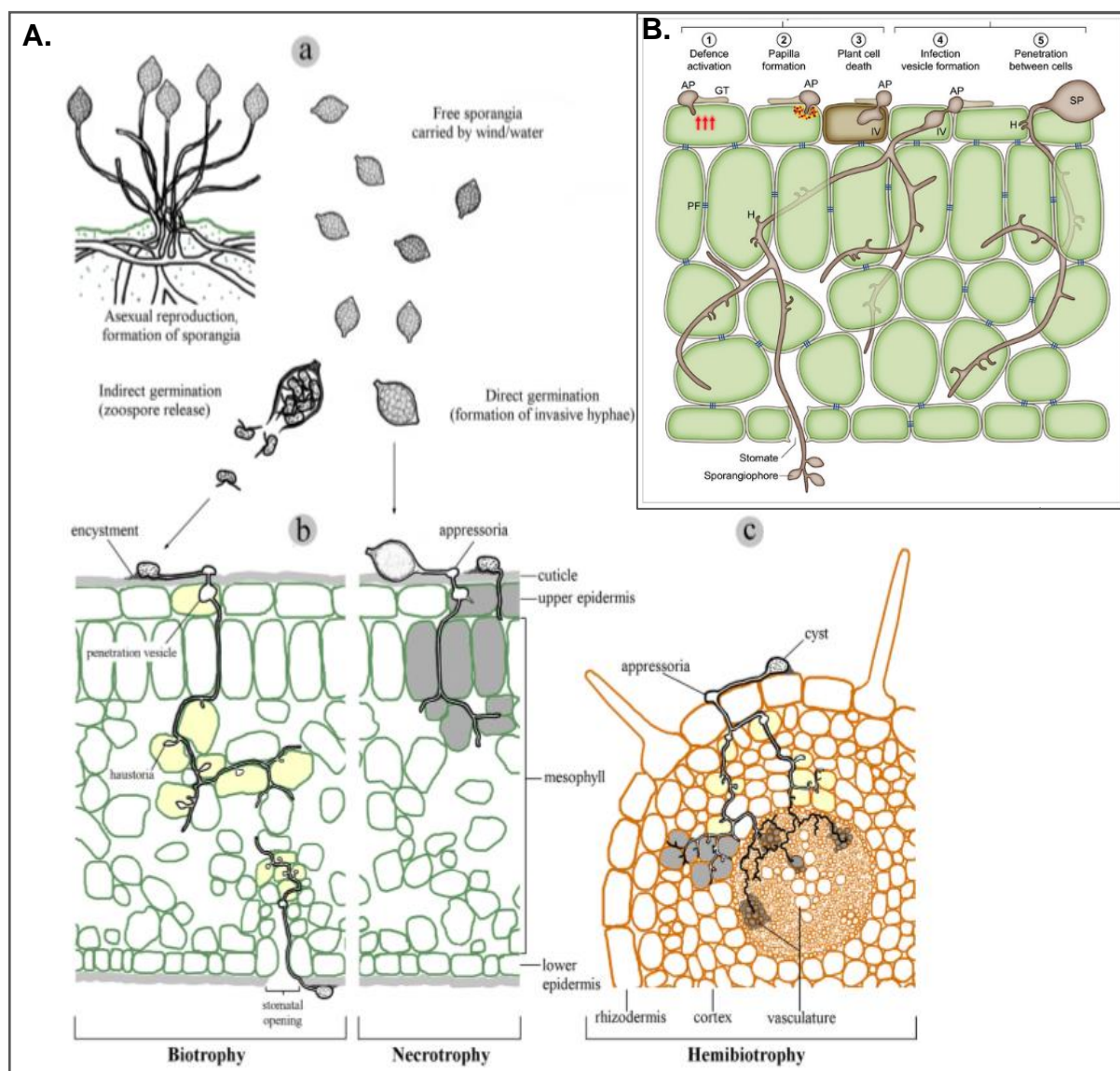


Figure 1. 10. Oomycetes infection strategies. **A.** Fawke et al. (2015) schematic representation of the different infection strategies of oomycetes according to their lifestyle. (a) Typical asexual *Phytophthora* dispersal structures. (b) Leaf colonization. (c) Root colonization. (Fawke et al., 2015). **B.** Boevink et al. (2020) *Phytophthora* infection process. SP: sporangia; GT: germinating tube; AP: appressorium; IV: Infection Vesicle; H: haustoria; PF: pit fields (Boevink et al., 2020).

1.5. Molecular Plant-Pathogen Interactions

1.5.1. MAMPs and PAMP- triggered Immunity (PTI)

Pathogens perception occurs when conserved exogenous molecular motifs of pathogens, like pathogen-associated molecular patterns (PAMPs, also sometimes referred to microbe-associated molecular patterns MAMPs) or host endogenous DAMPs (Damage Associated Molecular Patterns), are recognized by the plant pattern-recognition receptors (PRRs), which results in PAMP-triggered immunity (PTI). PAMPs / MAMPs can be proteins, unsaturated fatty acids or carbohydrates (Henry et al., 2012). PAMPs are structurally conserved and essential for the pathogen life cycle and can adapt and co-evolve with PRRs (Kamoun et al., 1998; Jones and Dangl, 2006; Hein et al., 2009). Examples of PAMPs include the well-known *P. infestans* INF1, leading to cell death (Hein et al., 2009; Chaparro-Garcia et al., 2011), PEP-13 eliciting defense responses (Nürnbergger et al., 1994), or β -glucans, which can trigger the biosynthesis of phytoalexins, secondary metabolites from the plant with antimicrobial activity. Additionally, some proteins are characterized with dual activity, as both PAMP and effector, such as PsXEG1 and PsXLP1. This recognition of PAMPs / MAMPs / DAMPs initiates several events inside the host plant, such as calcium influx (Ca^{2+}), ROS burst, stomatal closure, MAPK signalling and changes in phytohormones jasmonic acid (JA) and salicylic acid (SA). Calcium influx is one of the earliest responses to PAMP recognition, causing alkalization and a depolarization of the plasma membrane (Jeworutzki et al., 2010; Bigeard et al., 2015; Naveed et al., 2020). This event was found to be required for the following extracellular production of reactive oxygen species (ROS burst), components that can be toxic to pathogens and involved in a programmed cell death response (O'Brien et al., 2012; Larroque et al., 2013; Kadota et al., 2014; Bigeard et al., 2015). Also following calcium changes, MAPK (mitogen-activated protein kinases) are activated. MAPK heat shock proteins HSP70 and HSP90 are for instance involved in INF1 induced HR, the hypersensitive response characterized by cell death (Kanzaki et al., 2003; Naveed et al., 2020). Hormones like SA and JA are commonly involved in plant defenses: SA brings resistance to biotrophic and hemi-biotrophic pathogens, while JA plays a role in defenses against necrotrophic pathogens. Tempering of these hormones thus reduces the host defenses. Finally, stomatal closure, linked to PAMP signalling and SA

homeostasis, occurs as part of the plant immune response (Melotto et al., 2008; Bigeard et al., 2015). These various pathways that trigger transcriptional reprogramming lead to the PAMP-triggered immunity (PTI) response, through HR (cell death), with callose deposition (with formation of papilla), biosynthesis of phytoalexins etc. (Collinge, 2009; Larroque et al., 2013; Chang et al., 2015; Du et al., 2015; van den Berg et al., 2018; Boevink et al., 2020). In non-host plants, pathogens cannot overcome the PTI response (non-host interactions).

1.5.2. Effector Triggered Susceptibility (ETS)

When pathogens enter the host, they must evade or suppress the PTI that follows perception of MAMPs / PAMPs and DAMPs, before feeding from the host tissues nutrients. To do so, they secrete various effectors that are generally species- or family-specific microbial proteins, delivered into the hosts to manipulate their molecular and biochemical pathways to cause disease. In the absence of host resistance proteins (or R proteins), the effector function is to overcome plant defenses in a wide variety of ways, but all ultimately aim to induce effector-triggered susceptibility (ETS).

In the absence of host R proteins, the alteration and overcoming of plant defenses leads to effector-triggered susceptibility (ETS), and can occur through many various processes: interaction with GTPase, stabilization of specific proteins, RNA interference, prevention of the secretion of plant defense proteases, interactions with cell death regulators, hormone regulation and suppression of salicylic-acid-mediated defenses, targeting of the ubiquitination system, disruption of the attachment between the plant cell wall and the plasma membrane, calcium and MAPK signalling (Figure 1.11), and many more mechanisms (Mackey et al., 2002; Axtell et al., 2003; Zhao et al., 2003; Brooks et al., 2005; Eulgem, 2005; Kim et al., 2005; Bos et al., 2010; Bozkurt et al., 2011; Caillaud et al., 2013; King et al., 2014; Chaparro-Garcia et al., 2015; He et al., 2020; Naveed et al., 2020). One mechanism through which plant gain defenses is the deployment of RNA interference (RNAi). However, pathogens like oomycetes have developed effectors targeting and inhibiting these RNAi. Regulation of the host transcription can also happen when effectors directly bind to host DNA (Ahmed et al., 2018a; Ahmed et al., 2018b). Furthermore, effectors can alter the host metabolism at different stages, particularly JA and SA. As SA and JA are antagonist to each other,

pathogen usually regulates one or the other to interfere with host defenses (Melotto et al., 2008; Jaswal et al., 2020; Naveed et al., 2020).

Once a pathogen effector is recognized by the plant, it is termed an avirulence protein (Avr protein) and effector-triggered immunity (ETI) follows (see 1.5.4). Examples of well-studied predicted effectors include *Phytophthora* Avr effectors: *Cladosporium fulvum* AVR2, *Pseudomonas syringae* AvrRpt2, AvrRPM1, AvrB, AvrPtoB, *Xanthomonas campestris* AvrBs3 and many others (Table 1.1, Franceschetti et al., 2017). Nevertheless, many effectors functions remain unknown.

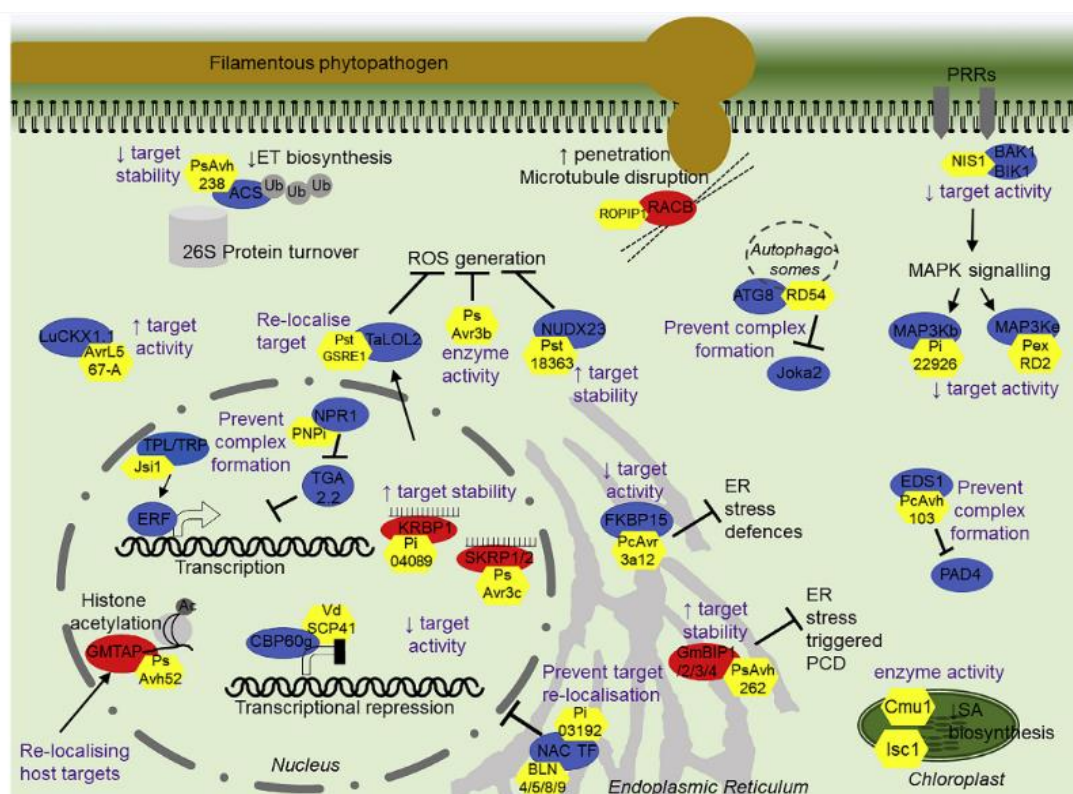


Figure 1. 11. Effector functions. A. He et al. (2020) schematic representation of different functions of effectors. Effectors are shown in yellow. Positive regulators of immunity are shown in blue, and negative regulators of immunity are shown in red. The mode of action of the effectors is written in purple text, with an upward arrow denoting increase and a downward arrow denoting decrease.

Table 1. 1. Franceschetti et al. (2017) examples of predicted effectors of pathogens

Effector class	Hyphal pathogen	Example(s)
Chorismate mutases	<i>Ustilago maydis</i>	Cmu1
Lipase effector	<i>Fusarium graminearum</i>	FGL1
Enzyme inhibitors		
Protease inhibitors	<i>Cladosporium fulvum</i>	Avr2
Cystatin-like protease inhibitor domains	<i>Phytophthora infestans</i>	EPIC1, EPIC2B
Chitinase inhibitor	<i>Cladosporium fulvum</i>	Avr4
Proteases and peptidases		
Proteases	<i>Zymoseptoria tritici</i> (<i>Mycosphaerella graminicola</i>) <i>Colletotrichum</i> sp.	
Secreted peptidases	<i>Zymoseptoria tritici</i> (<i>Mycosphaerella graminicola</i>)	Astacin (peptidase family M12A), serine carboxypeptidase S28
Serine protease	<i>Fusarium oxysporum</i> f. sp. <i>lycopersici</i>	Sep1
Alkaline serine protease alp1	<i>Sclerotinia sclerotiorum</i>	Peptidase inhibitor I9
Metalloproteases		
Zinc metalloprotease	<i>Magnaporthe oryzae</i>	AVR-Pita (AVR2-YAMO)
Deuterolysin metalloprotease	<i>Sclerotinia sclerotiorum</i>	Deuterolysin metalloprotease (M35) family (PF02102) homolog of <i>M. oryzae</i> AVR-Pita
Metalloprotease	<i>Fusarium oxysporum</i> f. sp. <i>lycopersici</i>	Mep1
Nudix hydrolases	<i>Phytophthora sojae</i> <i>Colletotrichum truncatum</i> <i>Melampsora lini</i>	Avr3b CtNUDIX AvrM14
Crinklers		
Kinase activity	<i>Phytophthora infestans</i>	CRN8

1.5.3. Oomycete effectors

When oomycetes colonize plants, they introduce effectors via haustorium, a finger-like projection that forms an enclosed intimate contact point between the oomycete and the host plant plasma membrane (Figure 1.12). Just like any pathogen effectors, oomycetes effectors can have many roles: they can be structural (formation of haustoria), involved in nutrient leakage, dispersal, modification or suppression of recognized elicitors, reduction of salicylic acid etc., and numerous effectors have enzyme activities (kinases, proteases, hydrolases) (Badel et al., 2002; Schulze-Lefert and Panstruga, 2003; Jones and Dangl, 2006; He et al., 2020). Effector size is typically small (less than 300 amino acids), with a high cysteine content. Effectors that are most essential for infection will be highly upregulated during early *in planta* stages (Jaswal et al., 2020). Oomycetes effectors can act outside (apoplastic effectors) or inside (cytoplasmic effectors) the host plant cells.

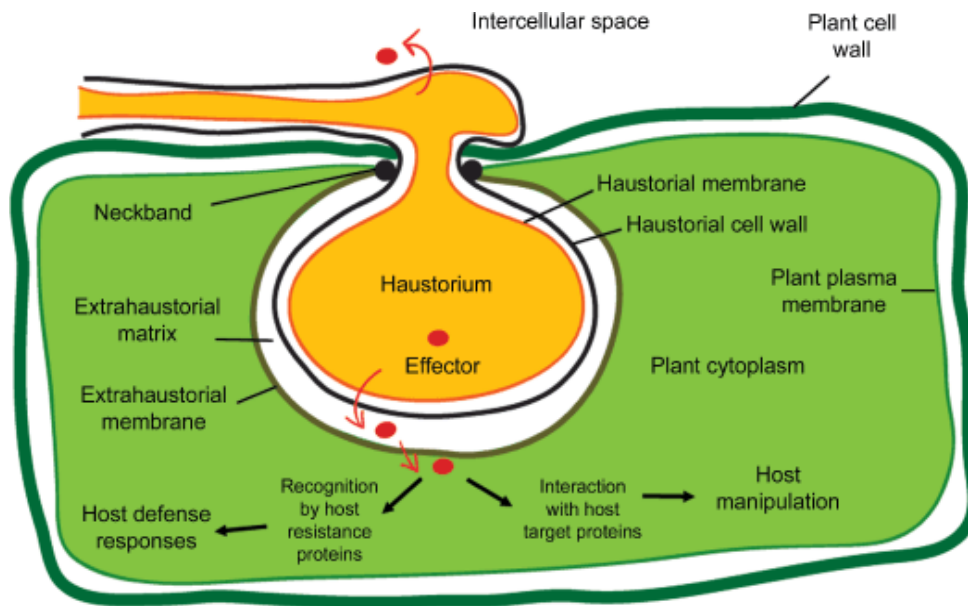


Figure 1. 12. Schematic representation of oomycete effector secretion and host-haustorium interactions (Dodds et al., 2009).

Dodds et al. (2009) host-haustorium interactions. During haustorium development, the pathogen penetrates the plant cell wall and invaginates the host plasma membrane which becomes the extrahaustorial membrane. The region between the haustorial cell wall and the extrahaustorial membrane is called the extrahaustorial matrix (a gel-like layer enriched in carbohydrates). Effectors (red dots) are secreted into the apoplast, including the extrahaustorial matrix, and must cross the extrahaustorial membrane before entering the plant cytoplasm.

Cytoplasmic and apoplastic effectors have an N-terminal signal peptide of usually 18-30 amino acids, allowing them to exit the cell, and a C-terminal domain carrying the effector bioactivity (Damasceno et al., 2008; Schornack et al., 2009; Oh et al., 2010; Schornack et al., 2010; Jiang et al., 2013; Arif et al., 2018), although there has been reports of cytoplasmic effectors that do not contain a predictable signal peptide (Stam et al., 2013) (Figure 1.13). Cytoplasmic effectors, such as CRN or RXLR, are translocated into host cells by a still debated mechanism (Birch et al., 2006; Kamoun, 2006; Kamoun, 2007; Birch et al., 2008; Dodds et al., 2009; Petre and Kamoun, 2014; Fawke et al., 2015; Whisson et al., 2016); while apoplastic effectors remain in the extra-cellular space (apoplast) (Birch et al., 2006; Birch et al., 2008; Dodds et al., 2009; Schornack et al., 2009; Petre and Kamoun, 2014).

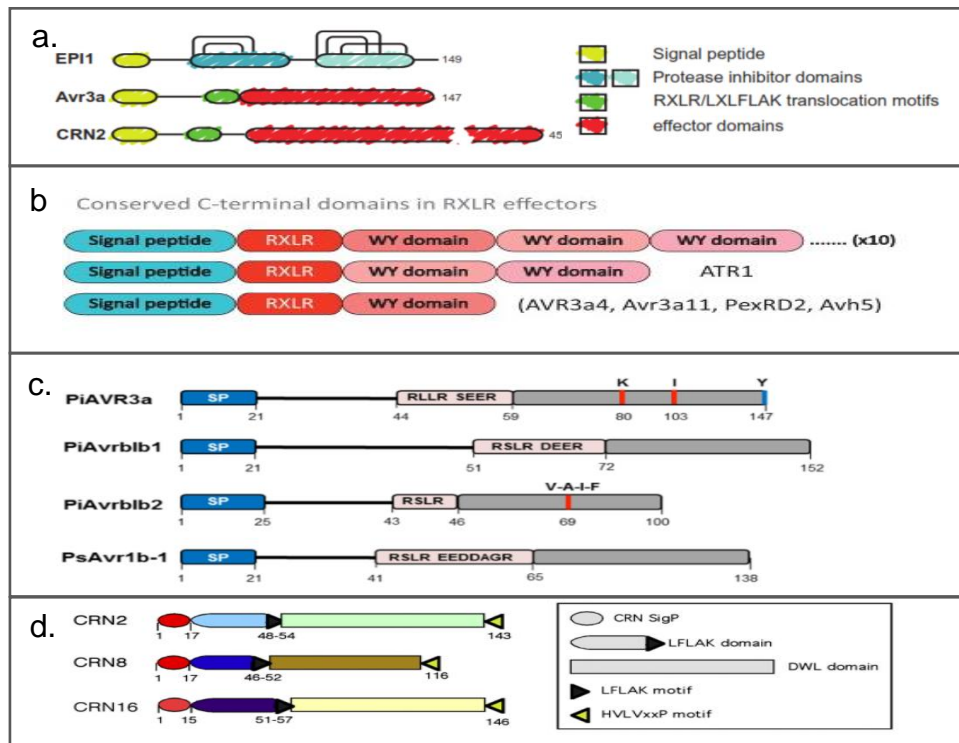


Figure 1. 13. Review and examples of oomycete effector structures. **a.** Schornack et al. (2009) figure showing the modularity of oomycetes effectors. All known effectors carry N-terminal signal peptides for secretion (yellow). Cytoplasmic effectors also have conserved motifs in their N-termini (RXLR or LXLFLAK for Crinkler effectors). The C-terminal domain carries the module with biochemical effector activity. EPI1 is a *P. infestans* apoplastic effector, an extracellular protease inhibitor; Avr3a is a *P. infestans* RXLR avirulence factor and CRN2 is a *P. infestans* CRN effector. Numbers indicate protein length. **b.** Jiang et al. (2013) figure of RXLR effectors structure, showing the signal peptide, RXLR motif and WY domain. **c.** Arif et al. (2018) figure of examples of RXLR effector structures: *P. infestans* PiAVR3a (Bos et al., 2006), *P. infestans* PiAvrblb1 and PiAvrblb2 (Vleeshouwers et al., 2008; Oh et al., 2009; Oh et al., 2010) and *P. sojae* Avr1b-1 (Shan et al., 2004). Numbers indicate the amino-acid positions and grey domains highlights the regions of the effector proteins that are involved in secretion and targeting. **d.** Schornack et al. (2010) figure of CRN effectors modular structure and examples: *P. infestans* CRN2, CRN8, and CRN16.

1.5.3.1. Oomycete apoplastic effectors

Apoplastic effectors can be enzymatic or non-enzymatic proteins, secondary metabolites or small RNAs, and include glucanases, glucanase inhibitors, serine and cysteine protease inhibitors, as well as small cysteine-rich proteins (Rose et al., 2002; Tian et al., 2004; Tian et al., 2005; Kamoun, 2006; Tian et al., 2007; Damasceno et al., 2008), and generally show a higher cysteine content than cytoplasmic effectors. Apoplastic effectors are also usually smaller than cytoplasmic effectors. β -glucans which compose oomycetes cell walls, are PAMPs, which a host might recognize and

inhibit using chitinases and β -glucanases, abundantly present in the apoplast. Pathogenic apoplastic effectors can thus modify elements of the cell wall to evade recognition by the host. Examples in the *Phytophthora* genus include EPIC1, EPIC2B, which inhibit host cysteine proteases, EPI1, an extracellular protease inhibitor (Figure 1.13), or GIP1, inhibiting the host endoglucanases (Rose et al., 2002; Tian et al., 2004; Tian et al., 2005; Rocafort et al., 2020). However, studies have also shown that apoplastic effectors can interfere with the host glycan-triggered immunity. *P. sojae* PsXEG1 and PsXLP1 constitute interesting examples: PsXEG1 is essential for *P. sojae* virulence but is targeted by the host endoglucanase inhibitor protein GmGIP1. *P. sojae* uses PsXLP1, an apoplastic effector similar to PsXEG1 but with a shortened GH12 domain disabling the glucanase activity, as a decoy to protect PsXEG1 from GmGIP1 (Ma et al., 2015; Ma et al., 2017).

1.5.3.2. Translocated oomycete effectors

Effectors translocated inside host cells are cytoplasmic effectors, such as RXLR and Crinkler (CRN) (Figure 1.13). Different species of *Phytophthora* have different predicted cytoplasmic effector repertoires and various numbers of predicted RXLR and CRNs effectors (Table 1.2, (Chepsergon et al., 2020)).

Table 1. 2 Chepsergon et al. (2020) predicted number of cytoplasmic RXLR and CRN effectors in *Phytophthora* spp.

<i>Phytophthora</i> spp	Genome Size (Mb)	RxLR	CRN
<i>P. cactorum</i>	121.5	199	77
<i>P. capsici</i>	64	357	84
<i>P. cinnamomi</i>	58	171	45
<i>P. infestans</i>	240	563	450
<i>P. litchii</i>	38	245	14
<i>P. megakarya</i>	126.8	336	152
<i>P. multivora</i>	41	84	60
<i>P. palmivora</i>	151.2	415	137
<i>P. parasitica</i>	64.5	172	80
<i>P. ramorum</i>	65	350	60
<i>P. sojae</i>	95	350	202

- RXLR effectors

Cytoplasmic RXLR effectors carry conserved peptide motifs: the RXLR and EER motifs, following the N-terminal signal peptide (Figure 1.13). Protein sequence comparisons between oomycete avirulence proteins recognized inside plant cells by resistance (R) proteins revealed that, although they were each dissimilar at the primary

sequence level, they share a signal peptide for secretion, then an RXLR motif defined by the amino acid sequence arginine (R) - any amino acid (x) – leucine (L) – arginine (R). This is often but not always followed by an EER motif: glutamic acid (E) – glutamic acid (E) – arginine (R) (Figure 1.13), within a certain amino acid distance (Allen et al., 2004; Shan et al., 2004; Armstrong et al., 2005; Rehmany et al., 2005; Birch et al., 2008), indicative of a similar RxLxED/Q motif than malaria parasites (Hiller et al., 2004). In some cases, the RXLR motif can be absent or replaced by motifs such as QxLR or RxLQ, with Q representing the glutamine amino acid (Fabro et al., 2011). RXLR effectors show adaptive selection in their C-terminal and approximately half of the C-terminal regions of these proteins contain repeat units made up of W, Y and L motifs, respectively tryptophan, tyrosine and leucine (Jiang et al., 2008; Jiang et al., 2013; Zhao et al., 2018). RXLR effectors have been demonstrated to enhance colonization (Figure 1.14, Wang et al., 2019).

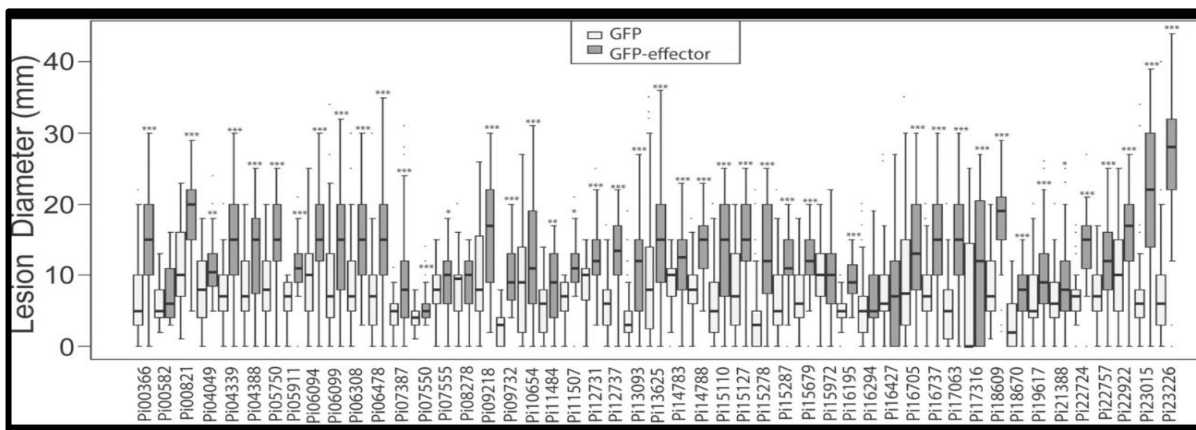


Figure 1. 14. Wang et al. (2019) figure of virulence test of *P. infestans* RXLR candidate effectors. Of the 51 candidate RXLR effectors tested, 44 boosted the growth of *P. infestans* significantly (indicated with asterisks). Two effectors are not shown as they caused cell death. P-values were from a one-way Student's t-test (* $P < 0.05$, ** $P < 0.01$, *** $P \leq 0.001$). Each effector is represented by a minimum of 72 replicates.

During infection, RXLR effectors are highly and differentially expressed, usually during the biotrophic phase (Bhattacharjee et al., 2006; Haas et al., 2009; Schornack et al., 2009; Bozkurt et al., 2011; Gilroy et al., 2011; Evangelisti et al., 2013; McLellan et al., 2013; Na et al., 2013; Oliva et al., 2015; Evangelisti et al., 2017; Guo et al., 2020; Naveed et al., 2020). To date, all identified oomycete avirulence effectors (effector recognized by the plant) have been cytoplasmic RXLR effectors.

Translocation mechanisms are not yet fully understood. Indeed, not all oomycetes form haustoria and studies have shown that oomycete RXLR effectors may not require pathogen structures to be delivered inside host cells (Dou et al., 2008b), whereas contradictory conclusions consistently showed that haustoria are major sites for effector delivery and that RXLR effectors do not enter plant cells in the absence of the pathogen's translocation machinery (Bos et al., 2006; Whisson et al., 2007; Haas et al., 2009; Oh et al., 2009; Schornack et al., 2010; Gilroy et al., 2011; Liu et al., 2014; Whisson et al., 2016; Wang et al., 2017). It is currently believed that the signal peptide sequence of RXLR effectors might be sufficient for their secretion, and that the RXLR motif might be necessary but not the only system for translocation (Bhattacharjee et al., 2006; Whisson et al., 2007; Wang et al., 2017; Boevink et al., 2020). For instance, the oomycete *H. arabidopsidis* effector ATR5 presents an EER motif without an associated RXLR; and is recognized by *Arabidopsis* RPP5 and translocated into the host cell without the RXLR motif (Bailey et al., 2011). Furthermore, the roles of RXLR-EER motifs in recognition of the Avr effector by the plant are still discussed, as the recognition of Avr3a by R3a has been shown to be independent of the RXLR-EER motif (Bos et al., 2006).

- Crinkler effectors

CRN effectors (Figure 1.13) are named after their crinkling and necrosis effects (Torto et al., 2003) and are also believed to have a conserved translocation motif, LXLFLAK (Leucine-any-Leucine-Phenylalanine-Leucine-Alanine-Lysine) (Whisson et al., 2007; Haas et al., 2009). Most CRN effectors carry a diversified DWL domain, located after the LXLFLAK motif and characterized by a specific and conserved amino acid sequence at its end, the HVLVXXP motif, that is defined by Histidine-Valine-Leucine-Valine-any-any-Proline (Haas et al., 2009; Schornack et al., 2009; Schornack et al., 2010). This HVLVXXP motif forms a connection to a wide range of C-terminal domains, holding the effector activity (Haas et al., 2009; Schornack et al., 2009). Examples of *Phytophthora* CRN effectors include *P. sojae* CRN108, inhibiting the plant heat shock proteins, CRN63 and CRN115, interacting with host catalases to alter the hydrogen peroxide (reactive oxygen species) pathways involved in plant defenses, with the former inducing cell death and the latter suppressing it; and CRN70, suppressing cell death triggered by Avh241 (Kuźniak and Urbanek, 2000; Liu et al., 2011; Rajput et al., 2014; Zhang et al., 2015; Song et al., 2016; Ai et al., 2021). Other

examples in *P. infestans* include CRN2 or CRN8 localized in the host nucleus and causing cell death (van Damme et al., 2012; Du et al., 2015). Several studies show that similarly to RXLR, CRN effectors are highly and differentially expressed during infection, at early and / or late stages (Haas et al., 2009; Shen et al., 2013; Stam et al., 2013; Amaro et al., 2017; Adams, 2019; Ai et al., 2021).

CRN and RXLRs are frequently organised in clusters in the genome and localized in repeat-rich regions with transposable elements (Jiang et al., 2006; Haas et al., 2009; Schornack et al., 2009). These effectors have the capacity to rapidly diversify, with high polymorphism rates, leading to non-synonymous amino acid substitutions and contributing to the pathogen's adaptation. The RXLR effector class seems to be phylogenetically restricted to *Phytophthora* species and downy mildews within the Peronosporales, while missing in *P. ultimum* and *A. euteiches* (Gaulin et al., 2008; Lévesque et al., 2010). Following observations of RXLR accumulating at haustoria during infection (Lévesque et al., 2010; Wang et al., 2017), Levesque et al. (2010) hypothesized that RXLR effectors have evolved recently in the *Phytophthora* and downy mildew groups, as haustoria were emerging. In contrast, the CRN family is ubiquitous in oomycetes (Cheung et al., 2008; Gaulin et al., 2008; Lévesque et al., 2010), suggesting that the CRN effector group appeared early in oomycete evolution, before the evolution of haustoria. The fact that *P. ultimum* and *A. euteiches* do not possess RXLR effectors and do not produce haustoria reinforces this hypothesis (Schornack et al., 2010). Zhang et al. (2016) further demonstrate that CRN effectors occur in non-pathogenic eukaryotic organisms.

1.5.4. Effector Triggered Immunity (ETI)

R proteins, usually nucleotide-binding leucine-rich-repeat proteins, also known as NBS-LRRs or NLRS, encoded in the plant genome by resistance genes (or R genes), can directly recognize specific effectors or indirectly recognize effector activities (Figure 1.15). Indirect recognition happens when effector-mediated alterations of host target proteins are detected (Jones and Dangl, 2006; Birch et al., 2008). Once a pathogen effector or its activity is recognized by the plant, it is termed an avirulence protein (Avr protein). This confers effector-triggered immunity (ETI). ETI is usually accompanied by a localised and programmed hypersensitive response (HR) or cell death. Recognition of the Avr genes by the host R genes triggers further waves of

changes in the plant, such as rebalancing of phytohormones JA and SA, calcium signalling with further Ca²⁺ influx, and subsequent MAPK signalling (Jaswal et al., 2020; Naveed et al., 2020). With pathogen and host co-evolution, further ETS and ETI might ensue. Studies have shown that the cell death triggered by RXLRs during ETI can be suppressed by pathogens CRNs effectors, such as *P. sojae* CRN70 and RXLR Avh241 (see 1.5.3).

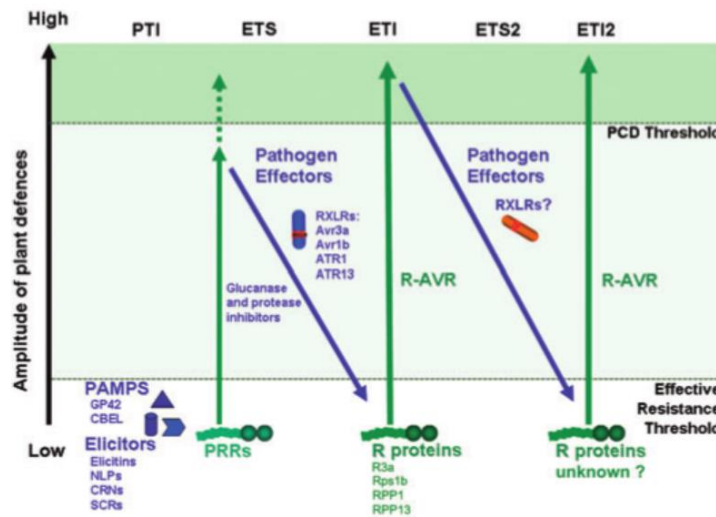


Figure 1. 15. The zig-zag-zig model for plant-pathogen interactions from Hein et al. (2009).

Although this zig-zag-zig model involving effectors and R genes is now well known, there are many processes involved during plant-pathogen interactions, where PTI and ETI responses overlap (hormonal manipulation, calcium and MAPK signalling etc.), eliminating the boundaries between them.

1.5.4.1 Oomycete Effector Recognition

RXLR effectors have been proved to act as avirulence factors, and some corresponding host R genes responsible for recognition and triggering cell death have been identified. This includes *P. infestans* Avr1, Avr2, Avr3a, Avr3, Avrblb1, Avrblb2, Avr4 and PexRD2 (Armstrong et al., 2005; van Poppel et al., 2008; Vleeshouwers et al., 2008; Oh et al., 2009; Bos et al., 2010; Gilroy et al., 2011; King et al., 2014; Du et al., 2015); or *P. sojae* Avr1a, Avr1b, Avr1d, Avr3a, Avr3b, Avr3c, Avr4/6, Avr5 and Avh241 (Shan et al., 2004; Dong et al., 2009; Qutob et al., 2009; Dou et al., 2010; Dong et al., 2011; Yu et al., 2012b; Yin et al., 2013). For instance, *P. infestans* Avr1 RXLR effector suppresses host defense by potentially disturbing vesicle trafficking, suppresses CRINKLER2 (CRN2)-induced cell death and triggers R1-mediated

resistance (Du et al., 2015). *P. infestans* Avr3a is another interesting RXLR, that was shown to target the E3 ubiquitin ligase CMPG1 to suppress plant immunity. Avr3a is encoded by two alleles, Avr3aKI and Avr3aEM, that differs by three amino acids. Avr3aKI is recognised by the host R3a resistance gene while Avr3aEM eludes recognition by R3a (Bos et al., 2006). Similarly, *P. sojae* Avr1d, which triggers a hypersensitive response in the presence of the host R gene Rps1d, is polymorphic, though both alleles are avirulent. This highlights *Phytophthora*'s ability to diversify their effectors arsenal and the importance for polymorphism screening on effector genes.

1.5.4.2. Co-evolution and adaptation of the plant and pathogen

To infect plants, pathogens must constantly adapt and change their effector molecules to avoid being recognized by the plant inducing immunity responses. While pathogens diversify their effector arsenal, altering the recognized effectors or acquiring more effectors to suppress ETI, new or modified R proteins are found in plant, which will activate ETI when facing new effectors and so on (Jones and Dangl, 2006; Hein et al., 2009).

By diversifying their set of effectors, oomycetes can rapidly overcome the R-gene based resistance. It has been shown that the C-terminal half of RXLR effectors have high rates of amino acid polymorphisms, leading to mutation and diversification (Allen et al., 2004; Rehmany et al., 2005; Win et al., 2007; Allen et al., 2008). Facing these quick changes in effectors, the plant expands the R protein repertoire. However, this is a long process and agricultural problems arise while the pathogen is overcoming plant resistance. Indeed, resistance in crop varieties is only durable if the required Avr gene is critical to the pathogen's success. Research focussing on crop resistance has found diverse ways to improve the survival and resistance of plants in the lab and in the field, such as assembling multiple R genes within one variety (Zhu et al., 2012), using variety mixtures (Zhu et al., 2000) or multi-lines (several lines of the same variety but showing different R-gene combinations) (Brunner et al., 2012), as well as R-gene engineering, expanding the plant recognition potential (Chapman et al., 2014; Segretin et al., 2014). While research on plant genetics is crucial, it is also essential to identify pathogenic effectors required for virulence and infection (Vleeshouwers et al., 2011). This is the plant-pathogen co-evolutionary arms race (Kamoun, 2007; Hogenhout et al., 2009), sometimes also referred to as the Red Queen Hypothesis, where organisms must continuously adapt and evolve to survive against ever-evolving opposing

organisms in a constantly changing environment. It is named after a phrase in Lewis Carroll's book *Through the Looking-Glass*, where the Red Queen says to Alice "Now, here, you see, it takes all the running you can do, to keep in the same place".

1.6. Potential methods of controlling root rot diseases

Seeing the complex interactions between pathogen and host, it is crucial to explore the effects of the environment on all the components of the disease triangle and the severity of the infection to mitigate diseases in the field. Such studies evaluate the effects of climate and climate change (temperature, humidity, drought, flood), as well as man-made pressures, like agricultural practices, chemical control, use of resistant cultivar etc. When trying to manage disease in the field, it is important to study and act on all parameters. The disease triangle (Figure 1.16) is a simple representation of the factors that can influence the success and severity of a disease: the environment, the host, and the pathogen. Research on every aspect will enable an IPM approach for disease management. IPM integrates several techniques like targeted use of fungicides, biocontrol, improvement of agricultural practices, habitat management and use of resistant varieties and cultivars. While some of these alternative have been assessed to control *Phytophthora* root rot, such as cultivar choice, planting techniques and biocontrol, options remain limited (Wilcox et al., 1999). Fungicides represent the majority of pesticides applied to soft fruit crops in the UK, compared to herbicides, insecticides and other treatments, illustrating the major threats that fungi and oomycetes pose on the crops (Ridley et al., 2018) and further highlighting the risk of the emergence of resistance. A combination of prevention, novel chemical products and resistance-bred cultivars increases the chance to reduce the spread of *Phytophthora* root rot (Wilcox et al., 1999; Anandhakumar and Zeller, 2008; Wedgwood and Woodhall, 2013).

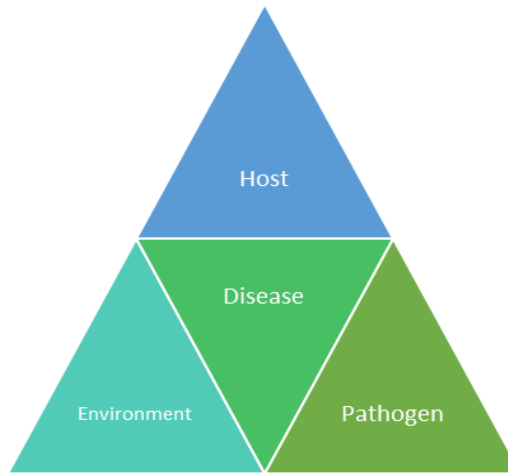


Figure 1. 16. Disease triangle. The disease triangle includes parameters that influence the success and severity of a disease: the host, the environment and the pathogen.

1.6.1. Growth conditions

The best form of control for *P. rubi* is prevention, as once it is established, getting rid or even containing the disease is very difficult. Choosing cultivars with high tolerance to *Phytophthora* root rot and planting clean material are other ways to control the disease. New clean raspberries need to be planted in soil where raspberries have not been grown before (Duncan et al., 2000; Duncan and Cooke, 2002) and infected plants, on which the pathogen depends for reproduction, need to be destroyed as soon as possible. Raspberry growers have thus been forced to adapt to a pot-based annual or short-term production in substrate. Since the disease thrives in wet conditions such as badly drained soils (Figure 1.17), techniques improving drainage or aeration, like hilling (planting raspberries on ridges) are good practices that should minimize root rot spread (Maloney et al., 1993; Heiberg, 1995; Heiberg, 1999; Wilcox et al., 1999). Adapting to growing techniques such as indoor vertical farming using hydroponics also enables better control and prevention of diseases, eliminating potentially contaminated soil and using sterilization methods easy to put in place. However, as

mentioned before, it is always best to adopt an integrative management approach, combining different control measures.



Figure 1. 17. Flood located near a raspberry polytunnel infected with root rot. Photo was taken at a field sampled in August 2018 in Kincardineshire (farm B) (see Chapter 2).

1.6.2. Chemical control

Unfortunately, there is a lack of effective chemical control treatments for PRR. Since raspberry crop production is such a small part of the overall agro-industry, fungicides are not specifically developed to control raspberry root rot but for similar diseases affecting major crops. Nevertheless, these fungicides can and have been tested since the 1980s with ‘off-label’ approval for use on raspberries. For example, Ridomil Plus (Metalaxyl + copper nitrate) was introduced and tested in the 1980s but was shortly discarded as the level of control was not consistent (Maloney et al., 1993; Heiberg, 1995; Wilcox et al., 1999). Following the let-down of the first product, Recoil (Oxadixyl + mancozeb) was developed as a replacement and large-scale fields trials in the 1990s were promising, proving the product’s efficacy against *Phytophthora*, though the level of control varied with the severity of the disease. However, in 2002 Recoil was withdrawn. Lately, more chemicals have been tested in trials before approval for use on raspberries against root rot. Rotation in chemical applied is important in order to avoid the potential build-up of resistant pathogen populations (Wilcox et al., 1999; Pinkerton et al., 2009; Stewart et al., 2014). Indeed, selection pressure built through chemical application of the same products over time can push pathogens to evolve and adapt, resulting in the development of resistant isolates. Hunter et al. (2018) explain the factors and implications of chemical-associated adaptive evolution of pathogens. They define adaptive evolution by “the process by which an organism changes in response to exposure to novel selection pressures”. By repeatedly being

the target of a same chemical treatment, fast evolving pathogens like *Phytophthora* spp. can develop tolerance to it (McDonald and Stukenbrock, 2016; Hunter et al., 2018).

1.6.3. Identifying and deploying durable resistances

Research into the host's genome can identify sources of resistance and can be combined with characterization of resistance in specific cultivar using phenotypic infection assays. Current breeding projects screen raspberries and other *Rubus* species in infected plots to identify sources of PRR resistance in existing cultivars e.g., Latham, Winkler's Sämling; in wild *Rubus* species like *R. strigosus*, *R. occidentalis* and *R. ursinus* (Barritt et al., 1979; Graham et al., 2011) ; and in hybrids like the Tayberry (raspberry–blackberry hybrid) (Duncan and Kennedy, 1987; Duncan et al., 1987). Some level of resistance has been identified against *P. rubi* but other *Phytophthora* species can cause PRR and the level of resistance in the cultivars can vary with the pathogen species (Stewart et al., 2014). Mechanisms of resistance existing in raspberry and strawberry remain to be determined. For example, there are at least several known races of *P. fragariae* in existence and efforts in elucidating strawberry resistance Rpf1-5 (Resistance to *Phytophthora fragariae* race 1-5) and markers for breeding are in progress. This has suggested that NBS-LRR and effector gene recognition plays a part in the resistance of soft fruit to *Phytophthora* pathogens.

1.6.4. Understanding the genetics, epidemiology and lifestyle of the pathogen

Current breeding projects assess cultivars of raspberries to identify sources of PRR resistance though without knowing the genotypes, phenotypes and genetics of the pathogen populations present. Research into pathogen's genomes and isolate variation using bioinformatic tools is essential to identify key virulence factors that might be required to cause infection and likely to be highly conserved in all strains examined. Genes under significant diversifying selection indicate a selection pressure and may be recognized in some potentially resistant host. Therefore, predictions on the evolutionary potential of *Phytophthora* spp. are essential before the successful deployment of wide scale resistance. Numerous mechanisms are deployed for Avr genes mutation: polymorphism between isolates allows for mutation (SNP, Single Nucleotide Polymorphism) and amino acid changes, epigenetic selection under host

resistance (R) gene pressure, allelic variation etc, can all alter the effector protein to elude the plant ETI. Truncation or complete, though reversible, loss of Avr genes are also common for *Phytophthora* species (Gijzen et al., 2014).

A small number of genetic studies have focussed on *P. rubi* and *P. fragariae* genomes (Man in't Veld, 2007; Gao et al., 2015; Tabima et al., 2017; Tabima et al., 2018; Adams, 2019; Adams et al., 2020; Gao et al., 2021). These studies generally use whole genome sequencing to look at genome content and evolution and are essential to predict effectors. Estimations revealed that around 1 % of *Phytophthora*'s genome typically encode effectors. New information on *P. rubi* and *P. fragariae* effectors diversity could be discovered using novel technique like Pathogen Enrichment Sequencing (PenSeq), only targeting effectors and specific genes of interest (Thilliez et al., 2019) in an attempt to understand the diversifying pressures that can lead to mutation. As well as diversity assessment, genetic studies can identify genes such as candidate Avr, or genes that could be involved in host recognition (Adams, 2019; Adams et al., 2020). Along with transcriptomic data, these studies could shed some light onto the pathogen's infection mechanisms and the key effectors associated with the disease.

Combined with research on such genes, phenotypic studies greatly add to the understanding of the pathogen and its evolutionary potential. In the current global warming context, it is important to follow and predict pathogens response to a changing environment. These changes include man-made pressures like chemical applications, which have led to the emergence of resistance in the past (Parra and Ristaino, 2001; Gisi and Sierotzki, 2008; Pérez et al., 2009; Randall et al., 2014). When insensitivity to an active is found amongst isolates, it can sometimes be traced back to specific target proteins (Randall et al., 2014) which can then be used to develop screening methods to assess the evolutionary potential of the pathogen to overcome control. *P. rubi* and *P. fragariae* current responses to external stresses like warmer temperatures and commonly used chemicals need to be assessed to identify population changes and potential resistance.

To date, studies of *Phytophthora* infections *in planta* have used model plants and focussed on aboveground infected tissues, easier to inoculate and use for downstream analyses (Maor et al., 1998; Dumas et al., 1999; Sexton and Howlett, 2001; Chen et al., 2003; Si-Ammour et al., 2003; Vallad and Subbarao, 2008; Li et al., 2011; Njoroge

et al., 2011; Dunn et al., 2013; Yu et al., 2013; Zhou et al., 2014; Häkkinen et al., 2015; Lu et al., 2015; Ochoa et al., 2019). Certain infection assays utilize fluorescent strains of pathogens to follow the disease progression in real time and identify specific structures (haustoria, hyphae, sporangia) (Le Berre et al., 2008; Evangelisti et al., 2017). *P. rubi* and *P. fragariae* would benefit from similar surveys, with reviewed approaches using hydroponics, transgenic fluorescent pathogen strains, and qRT-PCR to screen for life markers and effectors identified with genome and effectors studies.

1.7. Summary of the project aims

Following the description of important factors that might influence a disease in the field, and with the identification of knowledge gaps in *P. rubi* and *P. fragariae* phenotypes, genotypes, and infection mechanisms, several aims will be addressed in this research project:

- Following the current temperature increase and usage of chemical control in the field, the knowledge gap in the behaviour of *P. rubi* and *P. fragariae* needs to be addressed. Responses of recent and old *P. rubi* and *P. fragariae* isolates to these environment pressures (temperatures and chemicals) will be assessed.
- *P. rubi* and *P. fragariae* isolates genomes will be studied to identify conserved effectors genes as well as those that have diversified due to selection pressure, and thus evaluate the ongoing threat to the soft fruit industry.
- To allow a detailed first real time infection study of raspberry roots, transformation assays on *P. rubi* isolates using green and red fluorescent proteins (eGFP and tdTomato) will be carried out.
- The lifecycle on susceptible and resistant raspberry cultivars using hydroponics raspberries and transgenic fluorescent *P. rubi*, will then be investigated with confocal microscopy and qRT-PCR, screening for key *Phytophthora* life stages and gene expression.

Methods and data resulting from this work will feed back into studies on raspberry root rot (*P. rubi*) and strawberry red stele (*P. fragariae*) by providing scientific knowledge to underpin the horticultural industry with the development of novel pathogen control strategies.

CHAPTER 2. PHENOTYPIC STUDIES OF *P. RUBI* AND *P. FRAGARIAE*: ASSESSING RESPONSES TO AGRICULTURALLY IMPORTANT FACTORS

2.1. Introduction

Phytophthora root rot of raspberry is a soil-borne disease, with the causal pathogen starting its infection cycle in the soil. There is thus a delay between the start of the infection in the roots, and the visible above-ground symptoms on raspberry plants. The first signs of *P. rubi* disease on raspberries include leaf chlorosis, lack of or reduced fruit production, and can be noticeable from spring, although the pathogen would have started to infect the root tips during late autumn (Bain and Demaree, 1945). If disease prevails, new cane growth will be limited, and present canes will wilt and show discolouration in late summer and autumn. It is thought that *P. rubi* is active and benefits from winter weather, with cool temperatures and wet climate, ideal conditions for sporangia and zoospore formation (Bain and Demaree, 1945; Duncan and Kennedy, 1987; Duncan and Kennedy, 1989; Kennedy and Duncan, 1993; Wilcox et al., 1993). However, this opinion is based on older publications of *P. rubi* and *P. fragariae*, when information on the pathogens was limited, leaving a knowledge gap in the behaviour of isolates present in the field today, as well as in the adaptation of older isolates to current environmental factors and temperatures. Moreover, evidence has been found that the pathogens could also be actively associated with summer symptoms, indicating their ability to infect new plants during warmer weather (Weiland et al., 2018; Graham et al., 2020). Several temperature studies for *P. rubi* and *P. fragariae*, principally looking at hyphal development, confirmed the optimal growth temperature to be between 18 °C and 22 °C with declining growth from 25 °C (Leonian, 1934; Bain and Demaree, 1945; Duncan, 1985; Wilcox et al., 1993; Wilcox and Latorre, 2002; Graham et al., 2020). *P. rubi* is a widespread disease in Scotland, leading to root rot symptoms in the summer, which is usually characterized by temperatures between 11 °C and 21 °C, and higher rain fall (21 to 125 mm / month averaging 70 mm) compared to winter (-2 °C to 8 °C and 8 to 118mm rain / month averaging 59 mm) (Figure 2.1).

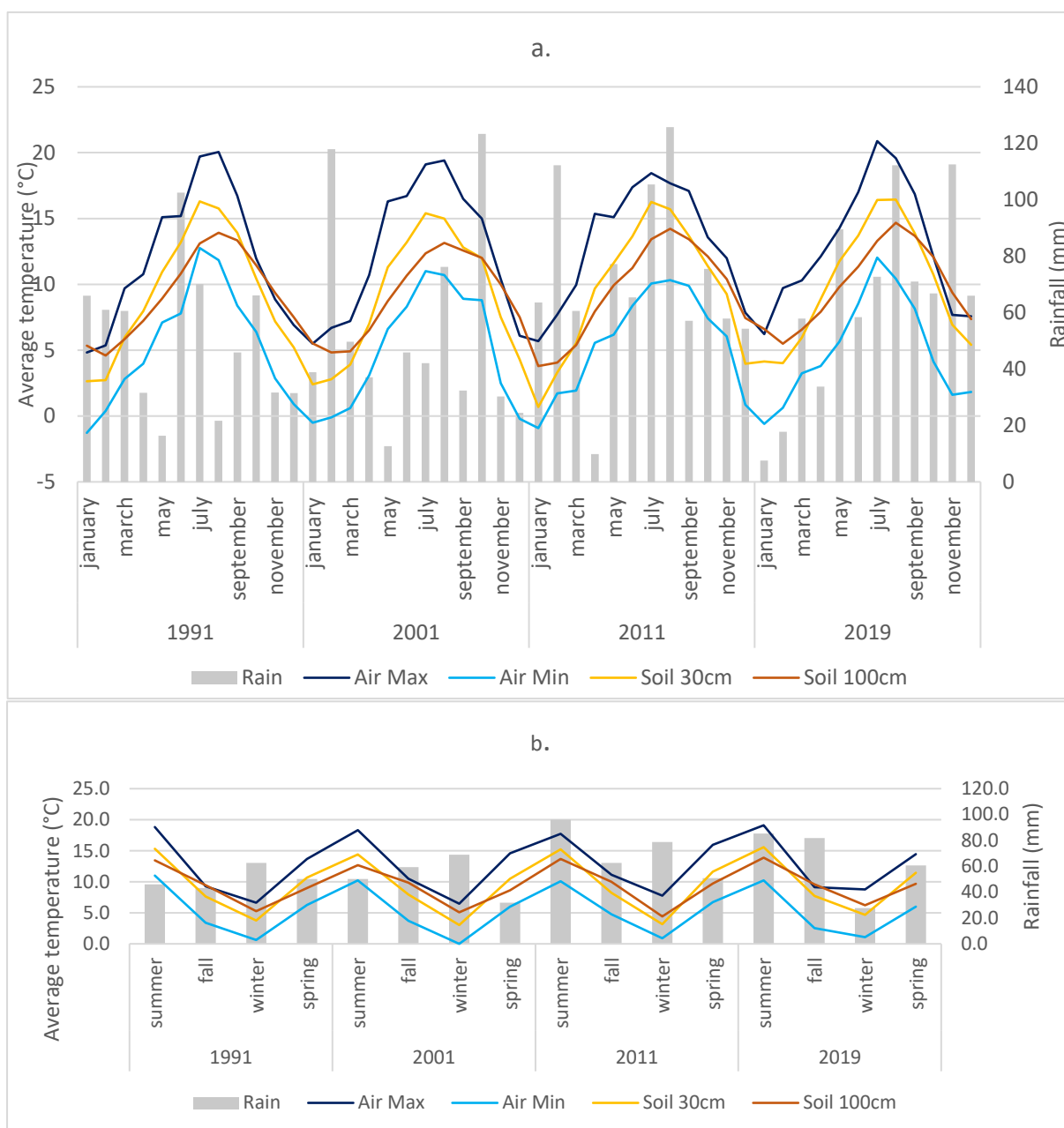


Figure 2. 1. Weather data in Invergowrie, Scotland, between 1991 and 2019. Data shows the average minimum air temperature (Air Min), the average maximum air temperature (Air Max), the soil temperatures at 30 cm and 100 cm depth and the rainfall. a. per month b. per season.

Overall, this suggests that *P. rubi* and *P. fragariae* might thrive in warmer environments, a particularly important question with the current global warming threat that could not only impact crop yields but also pathogens behaviour.

According to NOAA (National Oceanic and Atmospheric Administration) National Centres for Environmental information, the global temperature has increased at an average of 0.08 °C every decade since 1880 (NOAA, 2020). Data from soil temperatures taken at 30 and 100 cm depth from a weather station in Invergowrie, Dundee, from 1991 to 2019, show an average soil temperature increase of 1.2 °C at 30 cm and 0.6 °C at 100 cm between 1991 and 2019; while the increase in air temperature is similar to the one stated by NOAA (between 0.2 °C and 0.8 °C in that time frame) (Figure 2.1). Therefore, the first objective of this study is to assess the effect of temperatures on two important life stages of *P. rubi* and *P. fragariae*: hyphal growth and sporulation. While hyphae are formed when the pathogen infects the roots and is essential for the disease to develop and grow, formation of sporangia is necessary for the pathogen to reproduce and spread from plant to plant. Data compiled from raspberry polytunnels and pots, strawberry polytunnels and substrate bags, and soil temperatures at 30 cm and 100 cm depth showed that soil-borne diseases infecting these hosts could be exposed to temperatures as high as 30 °C in pots or substrate bags, with highest averages between 17 °C and 20 °C (Figure 2.2).

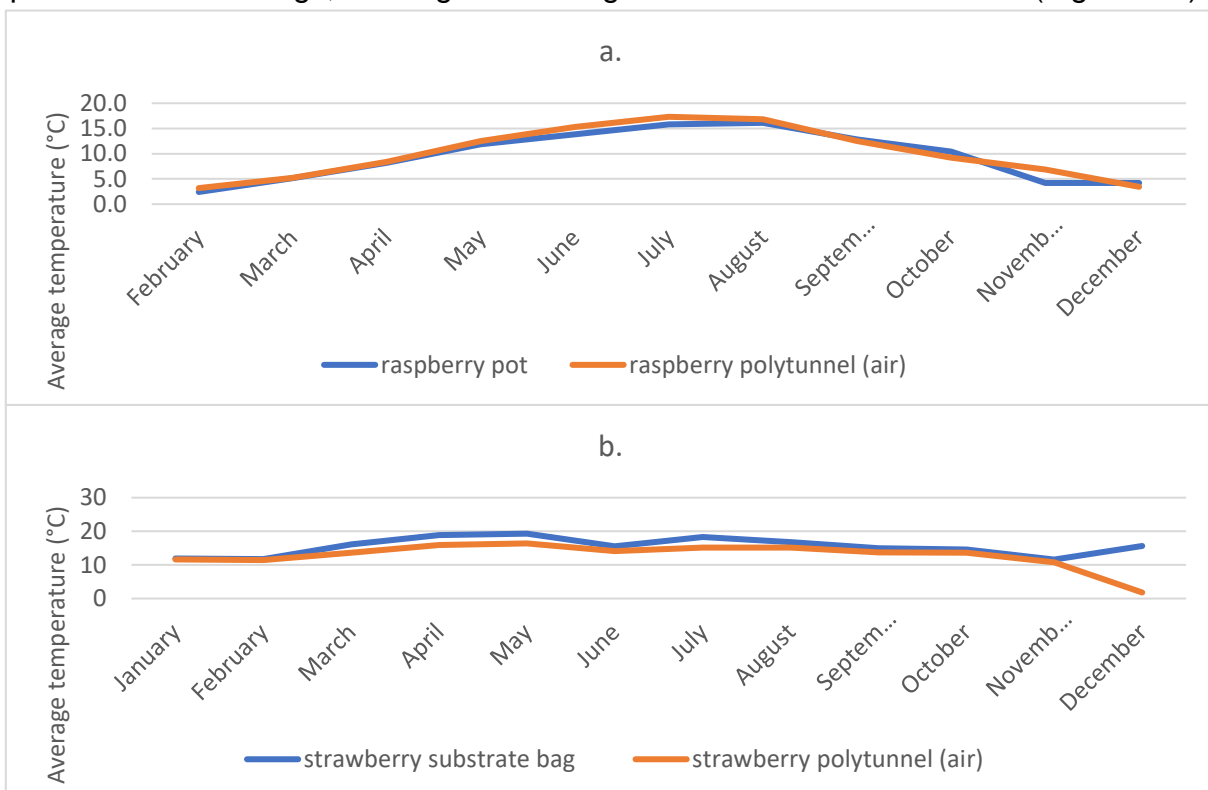


Figure 2. 2. Temperatures in raspberry (a.) and strawberry (b.) cultures in 2020. a. shows the air temperature in the raspberry polytunnel and the soil temperature in the raspberry pots (Invergowrie, Scotland). b. shows the air temperature in the strawberry polytunnel and the soil temperature in the strawberry substrate bags (Laurencekirk, Scotland).

Accordingly, five temperatures were chosen for this study: a low culturing temperature of 15 °C that has also been reported to induce sporulation (Bain and Demaree, 1945; Goode, 1956; Converse, 1962; Felix, 1962; Mussel and Fay, 1973), a typical culturing and control temperature of 18 °C, a high culturing temperature of 21 °C under which we believe *P. rubi* and *P. fragariae* could still thrive, and two higher temperatures of 25 °C and 28 °C. While climate change and temperature rising can affect microbial communities and disease development, other stresses can likewise build selection pressure, pushing pathogens to evolve and adapt. Man-made stress like chemical treatment, widely used in agriculture, can be an important selection pressure and may lead to the emergence of resistant isolates. As under-studied pathogens, there is a lack of information on the current *P. rubi* and *P. fragariae* behaviour and intra-species variation of responses to chemical treatments. Such survey would give us insights to their sensitivity to chemicals registered for use on raspberries and strawberries to treat *Phytophthora*, and their potential for adaptation. Consequently, the second objective of this study is to assess the effect of several chemicals on *P. rubi* and *P. fragariae* mycelial growth and sporulation. Seven different treatments were used: Fluazinam, Dimethomorph, Metalaxyl-M (Mefenoxam), Phorce, Fluopicolide, Propamocarb (Propamocarb hydrochloride) and Ametoctradin. The first four treatments are still registered for use on raspberries. Metalaxyl-M, first registered in 1979, is a fungicide used against oomycetes, though resistance to the chemical has now been demonstrated multiple times (Maloney et al., 1993; Heiberg, 1995; Wilcox et al., 1999; Parra and Ristaino, 2001; Gisi and Sierotzki, 2008; Randall et al., 2014). Metalaxyl-M belongs to the FRAC class of phenylamides (PA-fungicides) and likely acts on RNA polymerase I and ribosomal RNA synthesis. Ridomil Plus using Metalaxyl-M and copper nitrate was first used shortly after the root rot outbreaks in the mid-1980s and had off-label use after trials performed at The James Hutton Institute (Duncan and Kennedy, 1987). Following the reports of resistance to Ridomil, Recoil, a replacement using Oxadixyl (another phenylamide fungicide targeting RNA polymerase) and mancozeb (dithiocarbamate, with multi-sites activity) emerged in the 1990s and was promptly accepted as the fungicide of choice until it was withdrawn in 2002. An extension of authorisation for minor use (EAMU) on raspberries and strawberries of SL567A® (Syngenta), a product containing Metalaxyl-M was given in the UK in 2002, even though resistance and sensitivity levels should be carefully monitored. Fluazinam (targeting respiration) surfaced from a newer generation of chemical treatments

against oomycetes (mid 1990s) and showed promising efficacy. Fluazinam was first registered as a pesticide in 1992 and is the active ingredient of Shirlan® (Syngenta) and Tizca® (Cheminova), fungicides, developed for the control of potato blight (*P. infestans*). Tizca® was released in 2014 and a 'Specific Off Label Approval' (SOLA) was obtained for its use on raspberries, since its predecessor Shirlan®, released in 1993, lost approval. Fluazinam belongs to the uncoupler of oxidative phosphorylation FRAC (Fungicide Resistance Action Committee) class and is thought to act on respiration. Dimethomorph was first registered in 1998 and is the main active ingredient of Paraat® (BASF), a fungicide used against strawberry crown rot (*Phytophthora cactorum*) and raspberry / blackberry root rot (*Phytophthora spp.*). Paraat® was released in 2011 and is still currently approved for use on raspberry root rot. Dimethomorph belongs to the carboxylic acid amides FRAC classification (CAA fungicides) and targets cell wall cellulose biosynthesis. Fluopicolide (2007) and Propamocarb (1984) are active ingredients of Infinito® (Bayer Group), fungicide released in 2007 and generally used against oomycetes such as *Pythium spp.* and *Phytophthora spp.* on vegetables and potatoes. Nevertheless, while Infinito® once had a raspberry approval, it has now been revoked. Fluopicolide is thought to act on cytoskeleton and motor protein (delocalisation of spectrin-like proteins) while Propamocarb may act on the cell membrane permeability. Ametoctradin is the most recently registered pesticide (2009) of the ones tested in this study and is the active ingredient of fungicides controlling major oomycete pathogens, such as Initium® (BASF, 2010) or Zampro® (BASF, 2012). Ametoctradin is thought to inhibit the cytochrome bc1 and act on zoospores and sporangia by stopping the differentiation within the zoosporangium, the release of zoospores from the zoosporangium, the motility of any released zoospores and the germination of encysted zoospores. Most of these chemicals are used in foliar application or drip irrigation at doses ranging between 0.1 and 1 ppm. Due to higher restrictions on chemicals and doses applied to crops, growers use a variety of more natural products, such as fertiliser, with some thought to have biocidal effects on certain pathogens. For instance, numerous studies on phosphite (Phi; H_2PO_3^-) showed that this compound used in fertilisers could control many pathogens, like *Phytophthora infestans*, *Phytophthora plurivora*, *Fusarium solani*, *Erwinia carotovora* (Lobato et al., 2008; Lobato et al., 2010; Lobato et al., 2011; Silva et al., 2011; Burra et al., 2014; Dalio et al., 2014; Aćimović et al., 2015; Gómez-Merino and Trejo-Téllez, 2015; Groves et al., 2015). Consequently, Phorce, a

phosphite-based fertiliser, was additionally screened against *P. rubi* and *P. fragariae* in this study.

In summary, this chapter aims to describe the phenotypic responses of *P. rubi* and *P. fragariae* to agriculturally important factors and major stresses that can exert pressure on the populations by:

- Assessing the hyphal growth and sporulation of several isolates of *P. rubi* and *P. fragariae* from different countries and years, under a range of temperatures realistically found in the UK in raspberry and strawberry crops
- Examining hyphal development in response to several doses of old and newer chemical treatments
- Exploring the variation between the two closely related species as well as variation within these species to these environmental factors to yield indications of their potential for evolution

2.2. Materials and methods

2.2.1. Cultures of *Phytophthora rubi* and *Phytophthora fragariae*

2.2.1.1. P. rubi isolation from infected raspberry canes

- Collection of samples

To isolate soil borne *Phytophthora* species, Schmitthenner and Bhat (1994) suggested sampling stems with active lesions, just above ground level, rather than roots, in order to minimize possible contamination by *Pythium*, another oomycete often present on raspberry roots and canes. Stems of Glen Dee (susceptible to PRR) were sampled in April (spring) and August (summer) 2018 from a commercial grower in Kincardineshire (farm B), from plants showing symptoms of root rot. This field was in arable rotation before raspberries (Glen Dee) were planted for the first time in 2017, and symptoms showed very quickly. Two other varieties that are tolerant to the disease were planted at the same time in adjacent fields and remained healthy with no signs of PRR disease. Raspberry stems were sampled, as opposed to roots, and a cane-based isolation method adapted from Stewart et al. (2014) was trialled.

- Isolation technique

Isolation from canes was carried out using a protocol adapted from Stewart et al. (2014) using a modified V8 medium with a mix of antibiotics and fungicides to inhibit growth of contaminant such as fungi, bacteria or *Pythium spp* (David Cooke, The James Hutton Institute, personal communication, 2017). Calcium carbonate (0.03 g/mL) was added to V8 juice, mixed well and allowed to settle for 15 minutes. The resultant slurry was filtered through a cheesecloth and volume was made back up to 100 mL. The modified V8 medium was mixed with distilled water (10 % solution) before adding agar (15 g/L), and pH was corrected with potassium hydroxide (KOH) or hydrochloric acid (HCl) to 7.0-7.4 before being autoclaved (media cycle, 121 °C for 15 mins). A total of 5 mL of antibiotics stock made with pentachloronitrobenzene, pimaricin, rifampicin, nystatin, hymexazol and ampicillin, was added per litre of autoclaved medium (Table 2.1).

Table 2. 1. Details of chemicals used in this study. Chemical names, nature, supplier and quantities used for the selection media for *P. rubi* isolation from infected raspberry canes

Chemical	Nature	Supplier	Quantity (mg) in 10 mL of 80 % ethanol	Final concentration in V8 plates
Pentachloronitrobenzene (PCNB)	fungicide	Sigma Aldrich	50 mg	25 µg/mL
Pimaricin (also known as Natamycin)	fungicide		20 mg	10 µg/mL
Rifampicin	antibiotic		20 mg	10 µg/mL
Ampicillin	antibiotic		400 mg	200 µg/mL
Nystatin	fungicide	Melford Laboratories	50 mg	25 µg/mL
Hymexazol	fungicide	VWR	100 mg	50 µg/mL

Raspberry cane pieces of approximately 5 mm length from the margin of the disease lesion were cut and surface sterilized, using a 2-minutes wash in 0.5 % sodium hypochlorite, followed by a 2-minutes wash in 70 % ethanol. After washing, the stem pieces were buried in the antibiotic-containing agar (Figure 2.3.a), incubated at 18 °C in the dark, and checked regularly until growing hyphae were visible. At the first signs of growth, candidate *P. rubi* were quickly sub-cultured onto more of the same selection medium. The morphology of hyphae was examined under the microscope to confirm *Phytophthora*-like structures, such as coenocytic hyphae, oospores or sporangia

(Erwin and Ribeiro, 1996) (Figure 2.3. b-c). Once the mycelia grew actively and contamination-free, it was cultured on rye agar containing 100 µg/mL of ampicillin before DNA was extracted.



Figure 2. 3. Photos of the *P. rubi* isolation process from infected canes. **a.** Small pieces of surface-sterilised stems buried in agar showing 'fungus-like' growth; **b.** re-isolated mycelia growing in a Petri dish (rye agar); **c.** aseptate mycelia sampled from plate in b. observed under microscope.

▪ DNA extraction

Once the pathogen had been isolated and growing without contamination, it was sub-cultured in a Petri dish of liquid lima bean medium (Bruck et al., 1981) amended with 100 µg/mL of ampicillin for two weeks. When a mycelial 'mat' had formed, it was removed from the medium, blotted dry and frozen in liquid nitrogen before being stored at -80 °C. Between 20 and 40 mg of frozen mycelium was ground in liquid nitrogen and used for DNA extraction. DNA extraction buffer was made of 200 mM Tris HCl, 250 mM NaCl, 25 mM EDTA and 0.5 % SDS (chemicals from Sigma Aldrich, UK). Ground mycelium was transferred to a 2 mL micro-centrifuge tube, 1 mL of extraction buffer was added and vortexed thoroughly until completely suspended. Equilibrated phenol (700 µL) was added to the sample, vortexed, and then chloroform (300 µL) was added and vortexed further. The sample was then centrifuged for 10 minutes at 10,000 x g at room temperature. The upper phase was transferred to a new 1.5 mL tube, where 1 volume of chloroform was added and mixed. The sample was centrifuged for 5 minutes at 10,000 x g at room temperature and the upper aqueous phase was transferred to a new tube, where 0.5 volume of isopropanol was added to precipitate DNA. The sample was incubated at -20 °C for one hour, then centrifuged for 5 minutes at 10,000 x g at room temperature. The supernatant was discarded, all remnants removed by pipetting and the final pellet was re-suspended in 60 µL of AE buffer from a DNeasy Plant Mini Kit (QIAGEN, UK). To remove RNA and increase the purity of DNA, 1.2 µL of RNase A (100 mg/mL, from DNeasy Plant Mini Kit, QIAGEN,

UK) was added and incubated for 20 minutes at room temperature. DNA was then purified as per the DNeasy Plant Mini Kit (QIAGEN, UK) protocol using spin columns. Finally, DNA was eluted twice in 20 µL of buffer AE and assessed for purity using a NanoDrop (NanoDrop 1000 Thermo Fisher Scientific).

- Identifying *P. rubi* from field samples with *CoxI* PCR and sequencing

Newly extracted DNA was used in a PCR with Cytochrome C oxidase subunit I (*CoxI*) primers OomCoxI-Levup and OomCoxI-Levlo from Martin and Tooley (2003). Phusion High-Fidelity (HF) reagents and PCR protocol from BioLabs were used, with 3 µL of 10 µM primers and 20 - 80 ng of DNA template. After initial denaturation at 98 °C for 30 seconds, the following steps were repeated for 40 cycles: 98 °C for 10 seconds, 52 °C for 30 seconds and 72 °C for 20 seconds. Lastly, the final extension was maintained at 72 °C for 10 minutes. Agarose gel electrophoresis (2 % agarose) was used to confirm PCR products of appropriate size (~ 700 bp) and run at 80 V for 50 mins. Subsequent PCR products were purified using the QIAGEN Mini-Elute PCR Purification kit. Purified products were assessed on a NanoDrop (NanoDrop 1000 Thermo Fisher Scientific, UK) and dilutions were made to get 20 ng / µL of DNA in nuclease-free water, before being sequenced (Sanger Sequencing at The James Hutton Institute). Resulting *CoxI* sequences were compared to known *P. rubi* (SCR1202 and SCR324) and *P. fragariae* (NOV-9 and SCR245) isolates and aligned using BioEdit v. 7.0.5.3.

2.2.1.2. Growth media and culturing conditions for *P. rubi* and *P. fragariae*

Several isolates of *P. rubi* and *P. fragariae* were used throughout this study (Table 2.2 and Figure 2.4.).

Table 2. 2. Details of *P. rubi* and *P. fragariae* isolates used in the phenotypic study assessing the effects of temperatures and chemicals. Isolates in bold were designated as the twelve main studied isolates.

Sample species	Sample name	Country	Year	Race
<i>P. rubi</i>	SCR333	Scotland	1985	Race 3
	SCR1202	The Netherlands	2010	Unknown
	SCR1208	Scotland	2017	Unknown
	SCR1213	Scotland	2018	Unknown
	SCR324	Scotland	1991	Race 1
	SCR249	Germany	1985	Unknown
	SCR296	Scotland	1993	Unknown
	SCR339	France	1985	Race 3
	SCR1212	Scotland	2018	Unknown
SCR1207	Scotland	2017	Unknown	
<i>P. fragariae</i>	BC-1	Canada	1991	Race 1 (CA1)
	BC-16	Canada	1992	Race 2 (CA3)
	NOV-9	Canada	1986	Race 3 (CA2)
	SCR245	England	1945	Unknown

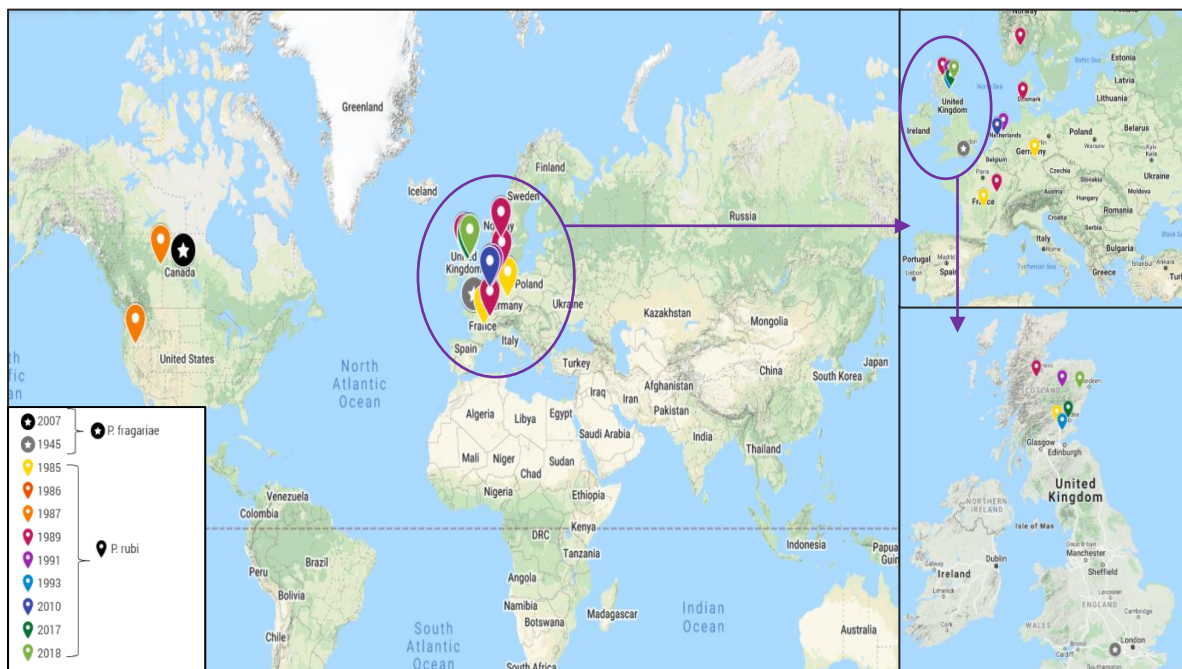


Figure 2. 4. Representation of the location and year of isolation of *P. rubi* and *P. fragariae* isolates.

P. rubi isolate SCR333 was considered a reference isolate, as studies from other research groups used it as a representative of *P. rubi* (Schena and Cooke, 2006; Koprivica et al., 2009; D'Urban-Jackson, 2018; Adams, 2019). A historic culture collection containing more than 120 *P. rubi* isolates has been maintained at The James Hutton Institute, representing a wide range of years and countries / regions of isolation. These isolates were regularly brought out of collection and sub-cultured to expand the

list of actively growing *P. rubi* that could be used in research assays. This work was done collaboratively with L. Welsh, The James Hutton Institute. Cultures were stored on various media: rye and French bean agar (FBA) slopes, oil slopes or liquid nitrogen. Plugs of agar from the stored isolate were cut out and placed onto French bean agar amended with 100 µg/mL of ampicillin, 5 µg/mL of pimarinic acid (in 70 % ethanol) and 2 µg/mL of rifampicin (in 96 % ethanol). Once the culture was growing without contaminants, DNA was extracted and the *CoxI* region was sequenced along with positive controls to confirm identity of *P. rubi*, as described previously.

2.2.1.3. Short- and long-term storage of *P. rubi* and *P. fragariae* isolates

Actively growing isolates of *P. rubi* and *P. fragariae* regularly used for experiments were stored at 18 °C in the dark, on rye agar with ampicillin (100 µg/mL). Each isolate that was positively recovered and identified as *P. rubi* / *P. fragariae* was cultured on slopes of rye agar and ampicillin (100 µg/mL) and stored at 4 °C in the dark, for long-term storage. Isolates were successfully recovered in collaboration with L. Welsh and kept in the James Hutton Institute collection and include *P. fragariae* isolates obtained from NIAB-EMR. A total of 56 % were successfully retrieved, sequenced (*CoxI* gene), and confirmed to be *P. rubi*. However, difficulties were encountered during the recovery, with some isolates that did not grow back, and thus, agar slopes of isolates that were not regularly employed in assays were kept at 15 °C and 18 °C instead of 4 °C for long-term storage.

2.2.1.4. *P. rubi* and *P. fragariae* isolates assessed in phenotypic assays

Following recent cane isolation (2017 and 2018) and recovery of *P. rubi* and *P. fragariae* isolates, a total of ten *P. rubi* (SCR249, SCR296, SCR324, SCR333, SCR339, SCR1202, SCR1207, SCR1208, SCR1212 and SCR1213) and four *P. fragariae* were used in this phenotypic study (BC-1, BC-16, NOV-9 and SCR245).

2.2.2. Chemical sensitivity testing

Seven different treatments were used in this study: Fluazinam, Fluopicolide, Propamocarb, Ametoctradin, Phorce, Dimethomorph and Metalaxyl-M (Mefenoxam) (Table 2.3). All chemicals except Ametoctradin were screened against the twelve main isolates (Table 2.2). Due to previously reported resistance in *Phytophthora* (Nickerson,

1998; Parra and Ristaino, 2001; Vawdrey et al., 2004; Elansky et al., 2007; Gisi and Sierotzki, 2008; Zhu et al., 2008; Pérez et al., 2009; Rekanović et al., 2012; Randall et al., 2014), two more *P. rubi* isolates, SCRP1207 (isolated in Scotland in 2017) and SCRP1212 (isolated in Scotland in 2018) were added to the Metalaxyl-M assay to increase the number of recent *P. rubi* and assess the effect of the fungicide on newer strains. Ametoctradin, a chemical impacting the zoospores and sporangia life stage of oomycetes, was screened on four *P. rubi* isolates as part of an initial mycelial growth test: SCRP333, SCRP324, SCRP1202 and SCRP1212 (from 1985 to 2018, Table 2.2). This selection provided preliminary insights into the effect of Ametoctradin on mycelia of *P. rubi* isolated over a long period of time. Fluazinam, Dimethomorph, Fluopicolide, Propamocarb and Ametoctradin were sourced from Sigma Aldrich. Metalaxyl-M (Mefenoxam) was obtained from Syngenta and Phorce from Nutriphite®. Rye agar with 100 µg/mL of ampicillin was used as a base medium for growing *P. rubi* and *P. fragariae* isolates for both assays. Stock solutions of 100,000 ppm were prepared for each chemical, using dimethyl sulfoxide (DMSO) as a solvent.

Table 2. 3. List and description of the fungicides incorporated into media and their mode of action. (N/A: non-applicable)

Treatment common name	Chemical name	Chemical formula	Year first described	Chemical FRAC classification number	Action
Fluazinam	3-chloro-N-(3-chloro-2,6-dinitro-4-trifluoromethylphenyl)-5-trifluoromethyl-2-pyridinamine	$C_{13}H_4Cl_2F_6N_4O_4$	1992	29	Action on respiration (uncoupler of oxidative phosphorylation)
Fluopicolide	2,6-dichloro-N-[[3-chloro-5-(trifluoromethyl)-2-pyridinyl]methyl]benzamide	$C_{14}H_8Cl_3F_3N_2O$	2007	43	Action on cytoskeleton and motor protein (delocalisation of spectrin-like proteins)
Propamocarb	Propyl [3-(dimethylamino)propyl]carbamate	$C_9H_{20}N_2O_2$	1984	28	Action on cell membrane permeability

Treatment common name	Chemical name	Chemical formula	Year first described	Chemical FRAC classification number	Action
Ametoctradin	5-ethyl-6-octyl[1,2,4]triazolo[1,5-a]pyrimidin-7-amine	C ₁₅ H ₂₅ N ₅	2009	45	Action on respiration (inhibition of complex III, cytochrome bc1 - ubiquinone reductase- at Qo site stigmatellin binding sub site)
Phosphite		H ₂ PO ₃ ⁻	1950	N/A	N/A
Dimethomorph	3-(4-chlorophenyl)-3-(3,4-dimethoxyphenyl)-1-morpholin-4-ylprop-2-en-1-one	C ₂₁ H ₂₂ ClNO ₄	1998	40	Action on cell wall biosynthesis (cellulose synthase)
Metalaxyl-M	N-(methoxyacetyl)-N-(2,6-xylyl)-DL-alaninate	C ₁₅ H ₂₁ NO ₄	1979	4	Action on nucleic acid synthesis (RNA polymerase I)

Appropriate amounts of each chemical were incorporated into this base medium, similarly to previously reported methods (Lee et al., 1999; Groves and Ristaino, 2000; Randall et al., 2014; Saville et al., 2015)). An equivalent dose of DMSO was added to the controls. Four doses were used for each chemical: 0 ppm (control), 0.1 ppm, 1 ppm and 10 ppm (Appendix A, Table A.1). To further investigate resistance to Metalaxyl-M that had been previously reported in *Phytophthora spp.*, an additional dose of 100 ppm was included in the screening.

2.2.3. Inoculation and growth conditions

Agar plugs of 9 mm diameter of *P. rubi* and *P. fragariae* were taken from the actively growing colony margin and placed onto rye agar medium (described in 2.2.2) in 50 mm diameter Petri dishes. Three replicates were used for each study (chemical and temperature screening). For chemicals with results showing potential resistance (Fluazinam and Metalaxyl-M), screening was carried out three times.

Plates were randomized, using the GenStat (19th edition v.19.1) random block design tool, and incubated in the dark, at 18 °C for the chemical study and 15 °C, 18 °C (control), 21 °C, 25 °C and 28 °C for the temperature assay. Several publications looking at hyphal toxicity effect of fungicides against *Phytophthora* species, mention an incubation period of one to two weeks (Groves and Ristaino, 2000; Saville et al., 2015) and carried out a similar method to screen pathogen growth than the one described here. Wilcox and Latorre (2002) used an incubation period of 8 days for *P. rubi* on plates when assessing the growth response to different temperatures. Initial tests for growth of *P. rubi* and *P. fragariae* isolates on control plates (50 mm) at 18 °C in the dark revealed that a week of growth was indeed best to assess chemical and temperature effects.

2.2.4. Hyphal growth measurements

Following a week's growth at the appropriate temperature in the dark, the colony diameter of *P. rubi* and *P. fragariae* isolates was measured along two perpendicular axes (Figure 2.5). The average of the two measurements was calculated and results were expressed in percentage of control's growth, where no chemical was incorporated into the base medium / the incubation temperature was set at 18 °C. After a week of incubation, plates showing no growth at all at 25 °C and 28 °C were placed back at 18 °C for a further 10 days and re-assessed.

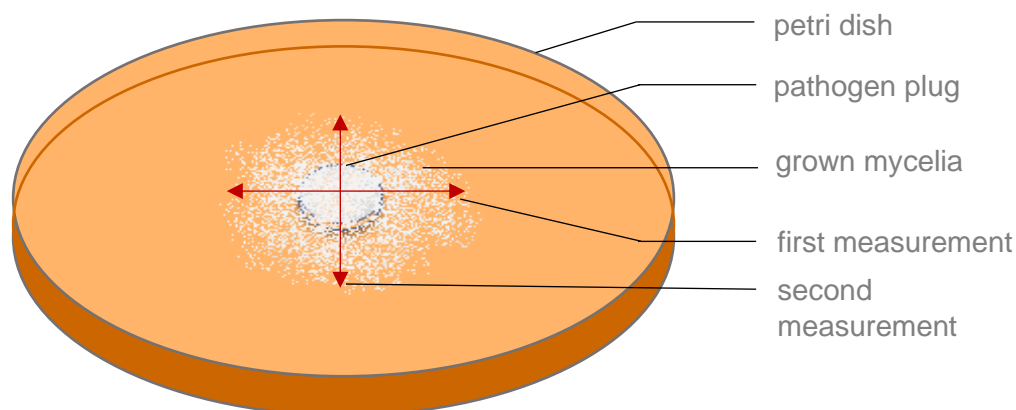


Figure 2. 5. Representation of the colony diameter measurements for the study. Two measurements were recorded per plug per plate, perpendicular to each other, measuring the diameter of the colony. The average of the two measurements was calculated and results were expressed in percentage of control's growth, where no chemical was incorporated.

2.2.5. Sporangia production and sporangia count

Sporulation was tested under temperatures of 15 °C, 18 °C and 21 °C, for five *P. rubi* isolates chosen to represent a variety of old and new strains: SCRP1212, SCRP1213, SCRP296, SCRP324 and SCRP333. Single agar plugs from clean cultures growing on rye agar with ampicillin (100 µg/mL) were transferred onto French bean agar (FBA), containing 100 µg/mL of ampicillin. FBA plates were incubated at 18 °C in the dark for one week. Sporulation solutions were generated by mixing 150 g of standard compost mix (Appendix A, Table A.2), ordered from ICL (Gretna, Scotland), in 1.5 L of distilled water for 30 minutes at room temperature before being passed twice through Whatman filter paper (grade 2V, from Sigma Aldrich, UK) to remove large soil particles. Sporulation solutions were stored at – 20 °C. Ten square plugs (~ 5 mm²) of mycelia actively growing onto ampicillin-amended FBA were then placed into a sterile 150 mm Petri dish. Two 150 mm plates were used per isolate and per temperature. Plates were flooded with sporulation solution and incubated at 15 °C, 18 °C and 21 °C in the dark. Solutions were replaced twice in the following 24 hours, as this was known to increase final number of sporangia (Mussel and Fay, 1973): once after 14 to 16 hours and a second time after a further 6 to 9 hours. Four days later, plates with cut plugs of agar in sporulation solution were placed under a standard microscope and number of sporangia per field of view per plug was recorded for each of the ten plugs per plate (Figure 2.6).



Figure 2. 6. Photo representing a field of view for counting *P. rubi* / *P. fragariae* sporangia (microscope). A plate containing 5 mm² plugs of agar with sporangia is put under the microscope. Sporangia (pointed by the arrows) are counted in the field of view to observe most of the plug from the corner as well as mycelial branches growing out and showing sporangia.

2.2.6. Chemical target genes sequences alignment

Chemical target genes for fungicides that showed diversity in hyphal growth responses were retrieved using NCBI and PenSeq data (Chapter 3). Cellulose synthase genes Cesa1, Cesa3 and Cesa4 were retrieved from *P. sojae* sequences found on NCBI and similar protein and nucleotide sequences were found for *P. rubi* isolates of interest using the BLAST tool BLASTx and BLASTp (PsCesA1: ABP96906.1; PsCesA3: EF563999.1; PsCesA4: ABP96909.1). Cellulose synthase gene Cesa2 sequences were extracted from PenSeq data. Genes encoding subunits of RNA polymerase (RNAPol) in *P. infestans* as listed in Randall et al. (2014) were likewise retrieved from NCBI for *P. rubi* and *P. fragariae* isolates of interest, using the BLASTx and BLASTp tools (NCBI): RPABC23 (PITG_12877), RPABC27 (PITG_10445), RPA190 (PITG_03855), RPA135 (PITG_02420), RPAC19 (PITG_05854) and RPA12.2 (PITG_06706). Nucleotide sequences were aligned using Clustal Omega alignment in Geneious v2020.2.1. When SNPs (Single Nucleotide Polymorphisms) were identified between sequences in different isolates, protein sequences were similarly aligned to assess potential resulting changes in amino acids.

2.2.7. Statistical analysis

Statistical analyses (ANOVA and Tukey's HSD tests) and boxplots were performed using R Studio v1.1.383. Statistical differences were considered significant if the p-value was lower than 0.05 (using a 95 % confidence interval). Dose-response models were fitted using the drm function (drc version 2.5-12). The half maximal inhibitory dose (ID50) was calculated when the growth reached 50 % of the untreated. Bar chart and line graphs were performed in Excel (v. 2102 for Microsoft Office 365).

2.3. Results

2.3.1. Five new isolates of *P. rubi* infecting raspberry fields were successfully isolated from diseased canes in the summer

In 2018, two samplings were carried out in Kincardineshire (farm B), from a field of susceptible cultivar Glen Dee affected by *Phytophthora* root rot (*P. rubi*). Crop symptoms were more noticeable in August (summer sampling) compared to April

(spring sampling), where cane isolation did not yield any new isolates of *P. rubi* (Figure 2.7). From August 2018, when purplish lesions at the base of the raspberry canes were sampled, five new *P. rubi* isolates were recovered.

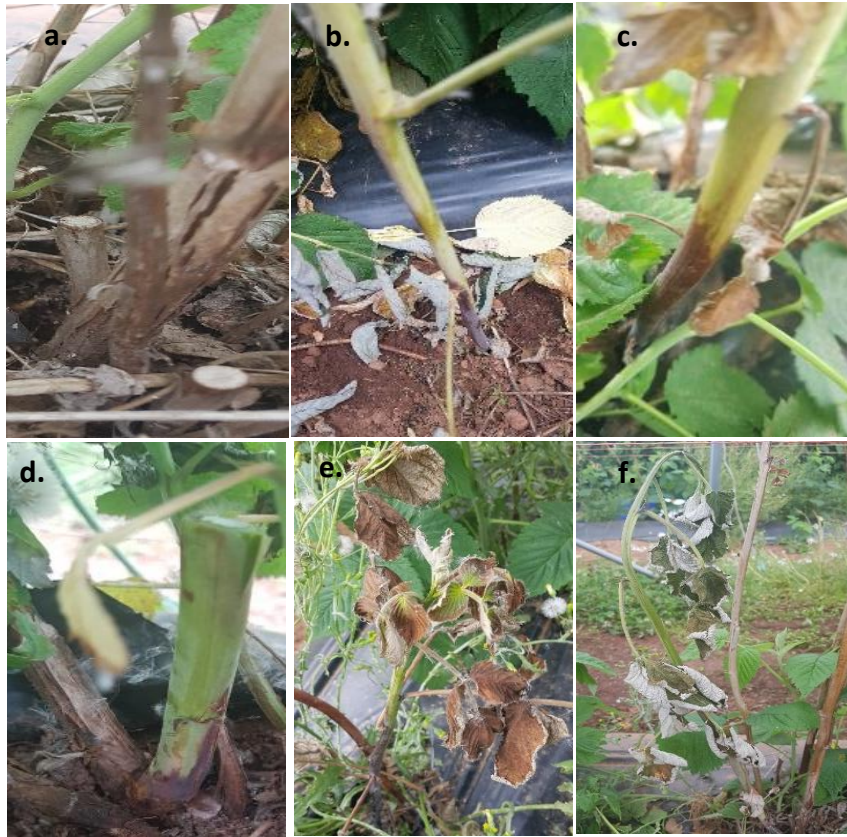


Figure 2. 7. Photos of infected raspberry canes sampled during April and August 2018. a. Cane sampled in April 2018; **b-d.** Canes sampled in August 2018, showing typical PRR purple lesion; **e-f.** Wilted infected canes from August 2018 sampling.

CoxI sequences presented ten SNPs (Single Nucleotide Polymorphism) differentiating *P. rubi* and *P. fragariae*. Interestingly, one additional SNP was identified between the isolates sampled in Perthshire (farm A) in August 2017, using the same isolation method, and those from Kincardineshire (farm B), 2018 (Figure 2.8).

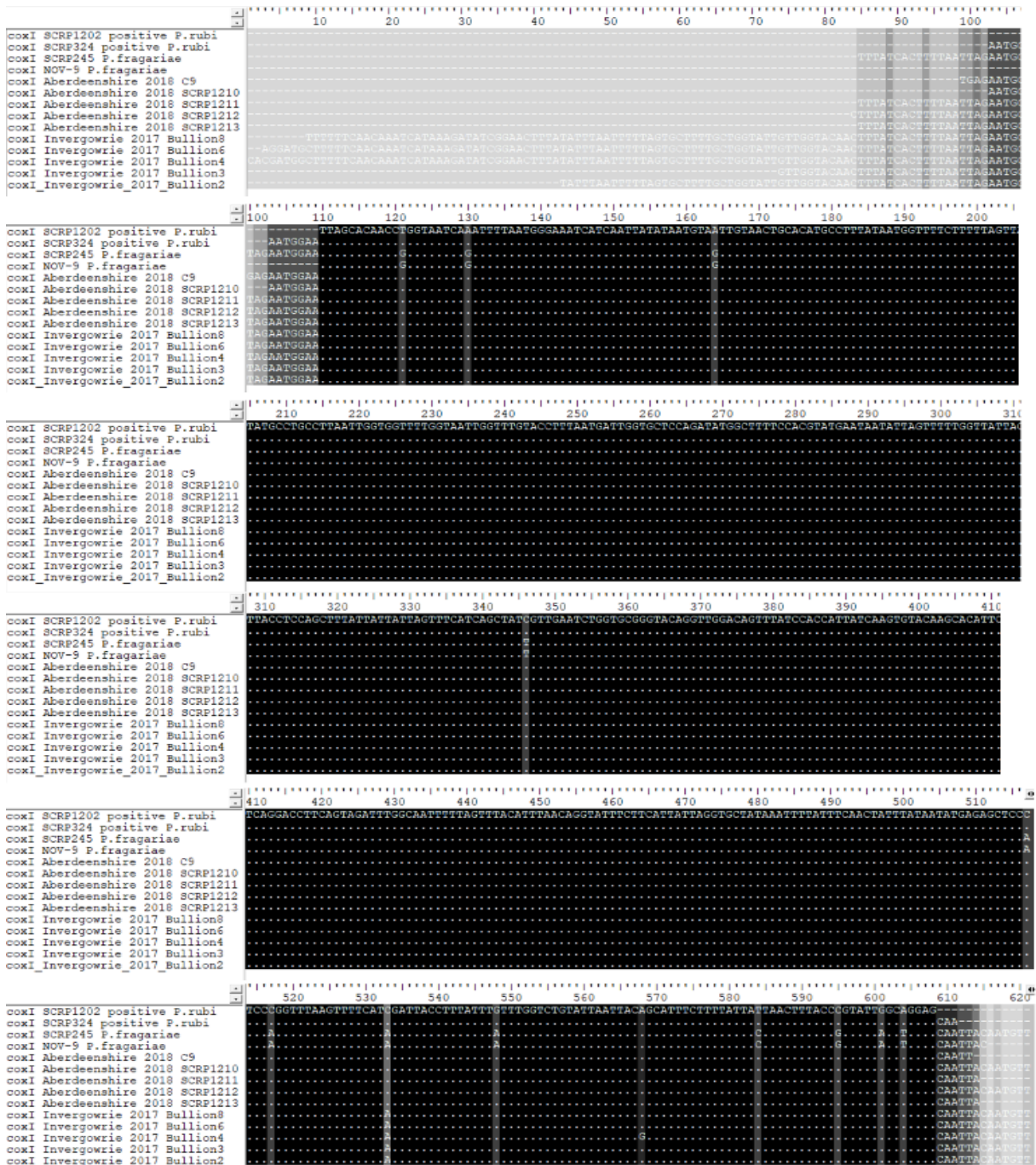


Figure 2. 8. Alignment of *CoxI* sequences from samples isolated from infected raspberry canes. From top line to bottom line: *P. rubi* positive control SCR1202, *P. rubi* positive control SCR324, *P. fragariae* SCR245, *P. fragariae* NOV-9, Kincardineshire (farm B) samples from 2018 C9, SCR1210, SCR1211, SCR1212, SCR1213, Perthshire farm A samples from 2017 Bullion8, Bullion6, Bullion4, Bullion3 and Bullion2. Alignment performed in BioEdit v. 7.0.5.3.

2.3.2. Effect of temperature on *in vitro* *P. rubi* life cycle stages: hyphal development and sporulation

2.3.2.1. Effect of temperature on hyphal growth: *P. rubi* hyphal development increases with temperatures rising to 21 °C but is inhibited above 25 °C.

Overall, hyphal growth increased when the temperature increased from 18 °C to 21 °C, decreased at a temperature of 15 °C and 25 °C compared to controls, and was fully inhibited at 28 °C, with the exception of *P. fragariae* NOV-9, isolated from Canada in 2007 (Figure 2.9).

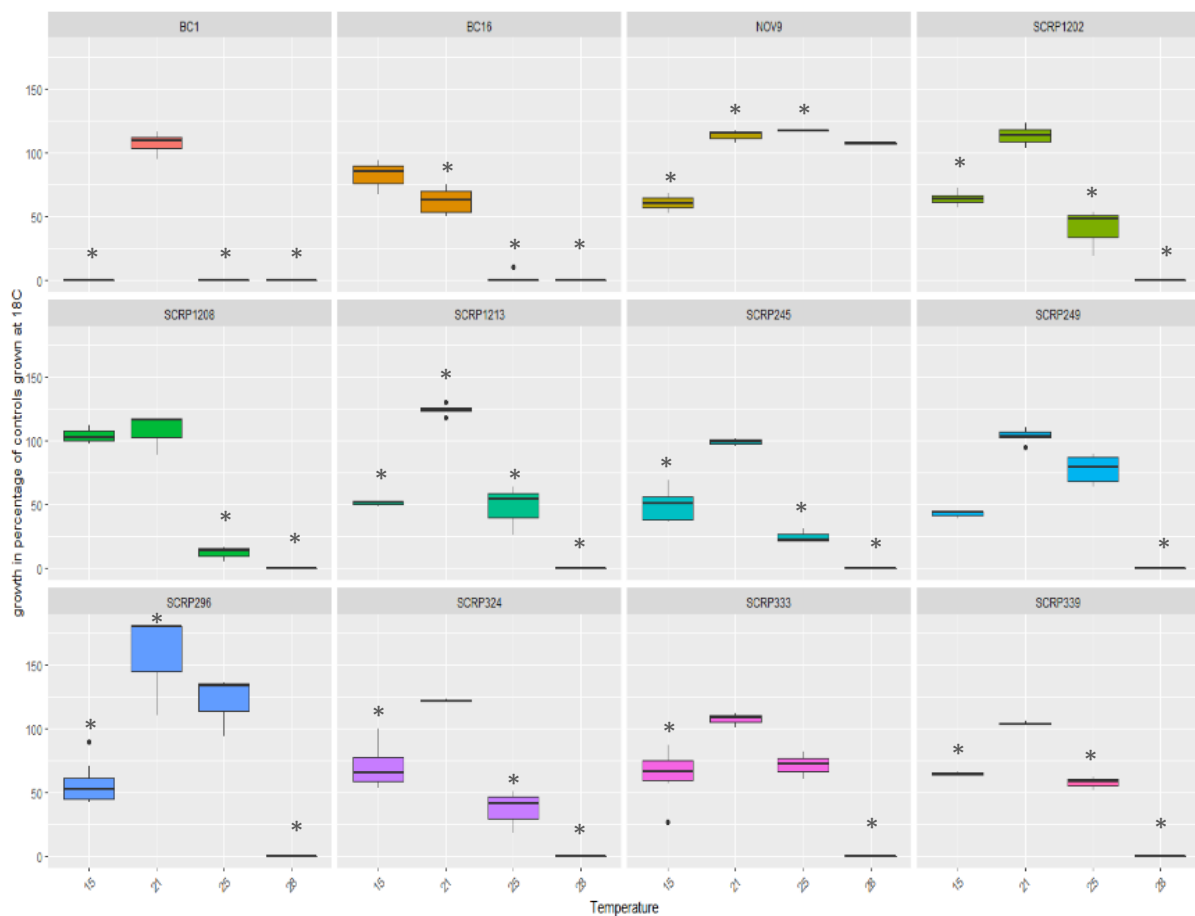


Figure 2. 9. Boxplot representation of the effect of temperature on the mycelial growth of 12 isolates. Effect of temperature (x axis: 15 °C, 21 °C, 25 °C and 28 °C) on four *P. fragariae* and eight *P. rubi* isolates, expressed as percentage of controls (y axis: grown at 18 °C). Three replicates per isolate and temperature were used. Asterix * indicates a statistical difference compared to controls ($p < 0.05$) per isolate.

Statistical analysis showed an effect of the temperature and the isolate on hyphal growth (Table 2.4). Generally, although hyphal growth slightly increases from 18 °C to 21 °C, statistical differences between the two growth temperatures were only observed

for isolates NOV-9, BC-16, SCRP296 and SCRP1213. When temperature raised to 25 °C, hyphal growth was significantly different than the 18 °C controls, except for *P. rubi* isolates SCRP249, SCRP333 and SCRP296. Growth at 15 °C and 25 °C were only significantly different from each other for isolates NOV-9, BC-16, SCRP1208 and SCRP296 (Table 2.4).

Table 2. 4. Statistical analyses on the effect of temperature. ANOVA and Tukeys test (performed in R) analysing effect of temperature on the isolate's mycelial growth (Table is to be read vertically, as per isolate)

Temperature	Isolates											
	BC-1	BC-16	NOV-9	SCRP1202	SCRP1208	SCRP1213	SCRP245	SCRP249	SCRP296	SCRP324	SCRP333	SCRP339
15 °C	b	a	a	b	a	b	b	ab	b	b	b	b
18 °C	a	a	b	c	a	c	c	b	c	c	c	a
21 °C	a	b	c	c	a	a	c	b	d	c	c	a
25 °C	b	c	c	b	b	b	b	b	cd	ab	bc	b
28 °C	b	c	bc	a	b	d	a	a	a	a	a	c

This shows that *P. rubi* and *P. fragariae* hyphal growth thrived at temperatures of 21 °C, and that all *P. rubi* and two *P. fragariae* isolates (isolated in 1945 and 2007) could still grow at 25 °C.

Plates that did not grow under high temperatures were re-incubated at 18 °C for 10 days to determine if the high temperatures were lethal or only inhibitory to *P. rubi* growth. *P. rubi* isolates SCRP333 and SCRP1208 were the only isolates developing mycelia when incubated back at 18°C for 10 days.

2.3.2.2. Effect of temperature on *P. rubi* sporulation – *P. rubi* sporulation is successful and statistically similar in efficiency at all temperatures checked

Since hyphal growth showed statistical differences between temperatures for some isolates, assessing the effect of temperature on another aspect of the *P. rubi* life cycle, here the sporulation, is significant to gain an insight into the pathogen response to climate change induced by temperature fluctuations. Although it seems that there was

an increase in the number of sporangia produced at 18 °C and 21 °C compared to 15 °C, there were no statistical differences for sporulation between the temperatures for any isolate (Figure 2.10).

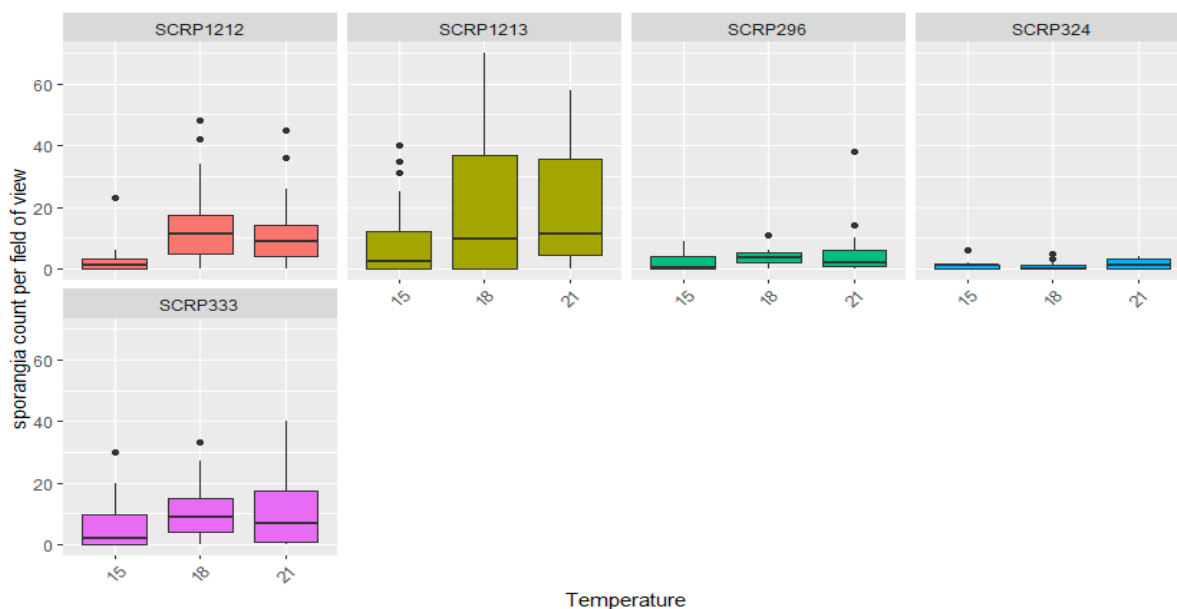


Figure 2. 10. Boxplot representation of the effect of temperature on the sporulation of five *P. rubi* isolates. The vertical axis represents the number of sporangia per field of view; the x axis represents the temperatures: 15 °C, 18 °C and 21 °C. Twenty replicates per isolate and temperature were used, as 10 mycelial plugs in two plates of sporulation solution. Each temperature experiment was performed once.

2.3.3. Effects of chemicals on *P. rubi* and *P. fragariae* isolates

2.3.3.1. *In vitro* inhibition of *P. rubi* and *P. fragariae* hyphal growth greatly depends on the chemical

- Fluazinam

Isolates of *P. rubi* and *P. fragariae* grown with 0.1 ppm of Fluazinam in agar displayed a mean hyphal growth of 75 % to 100 % of controls (90 % on average for *P. rubi* and 93 % for *P. fragariae*, Table 2.5 and Figure 2.11). When the dose increased to 1 ppm, close to the field application dose, the average pathogen growth was 54 % of the controls and only *P. rubi* SCRP324 and SCRP339, and *P. fragariae* SCRP245 and BC-16, show growth below 50 % of controls. At the highest Fluazinam dose (10 ppm), SCRP339 and SCRP245 were the most affected, with growth below 20 % of controls, while other isolates showed a response averaging of a quarter of control growth.

Table 2. 5. Average colony diameter for *P. rubi* and *P. fragariae* grown on media incorporated with seven chemicals. Average is calculated in percentage of controls (grown without chemical, i.e. at a dose of 0 ppm) per treatment and dose for **a. *P. rubi*** isolates and **b. *P. fragariae*** isolates.

<i>a. P. rubi</i>							
Doses	Treatment						
	Ametoctradin	Dimethomorph	Fluazinam	Fluopicolide	Metalaxyl	Phorce	Propamocarb
average	83.0	5.5	56.0	43.0	24.6	105.3	84.1
0.1 ppm	90.0	15.0	89.8	68.3	49.0	107.2	94.7
1 ppm	84.2	1.3	54.1	47.1	27.6	106.5	86.8
10 ppm	74.7	0.0	24.0	13.7	9.6	101.8	70.7
100 ppm	N/A	N/A	N/A	N/A	2.0	N/A	N/A
<i>b. P. fragariae</i>							
Doses	Treatment						
	Dimethomorph	Fluazinam	Fluopicolide	Metalaxyl			
average	0.9	54.1	39.3	41.4			
0.1 ppm	2.7	92.8	79.0	53.4			
1 ppm	0.0	53.6	38.3	47.4			
10 ppm	0.0	19.6	0.5	33.8			
100 ppm	N/A	N/A	N/A	25.6			

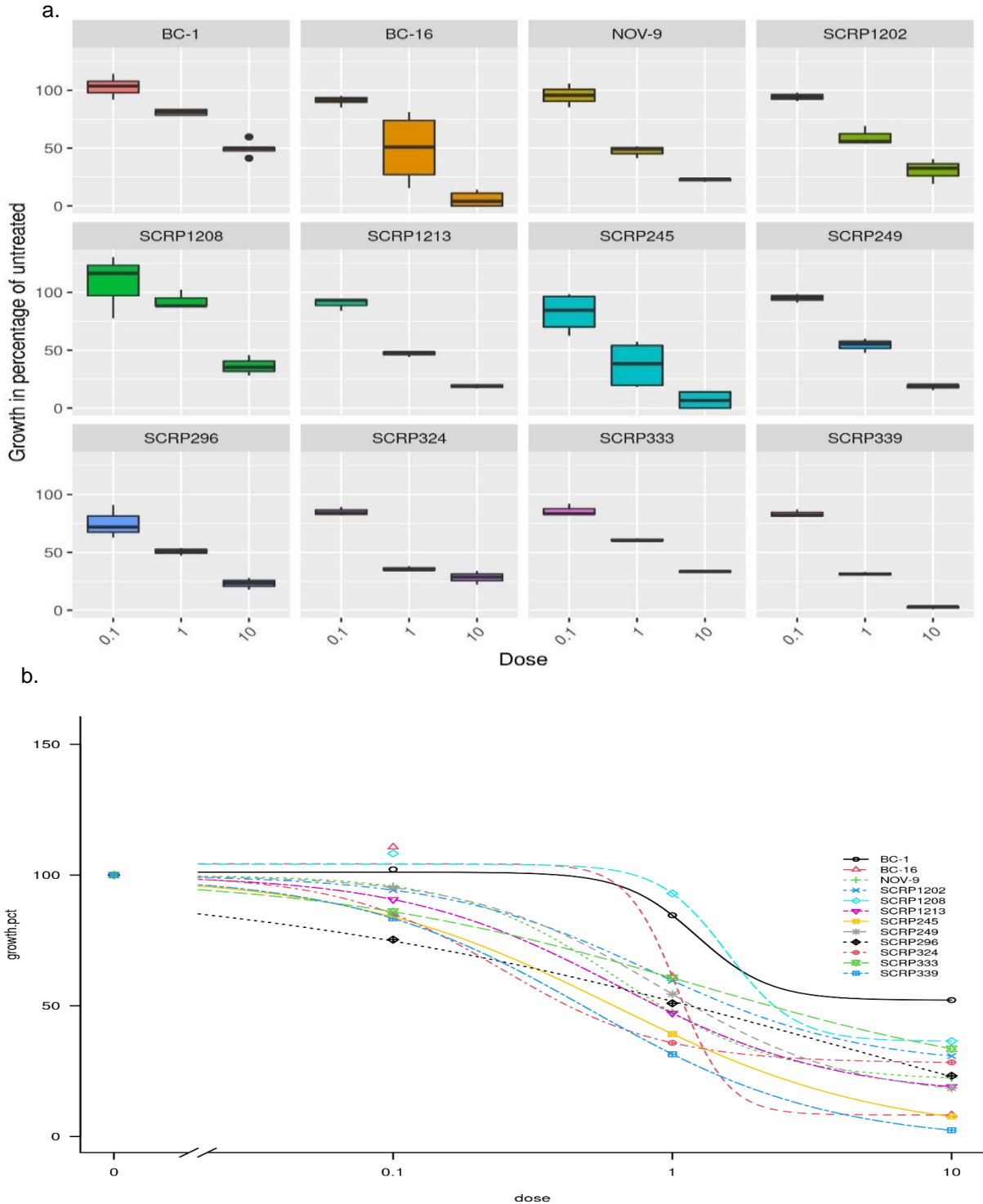


Figure 2. 11. Effect of Fluazinam on isolates growth. **a.** Boxplot representation of the effect of Fluazinam incorporated at different doses (0.1ppm, 1ppm and 10ppm, x axis) on the diametral hyphal growth (expressed in percentage of controls, y axis) of eight *P. rubi* and four *P. fragariae* isolates. **b.** Dose-response model fitted to Fluazinam. Doses are represented on the x axis in ppm and growth in percentage of controls is represented on the y axis (“growth.pct”). Three replicates per isolate and dose were used and experiment was performed once.

- Fluopicolide

Variation of growth inhibition was found between doses with isolates grown on medium incorporating Fluopicolide (Figure 2.12).

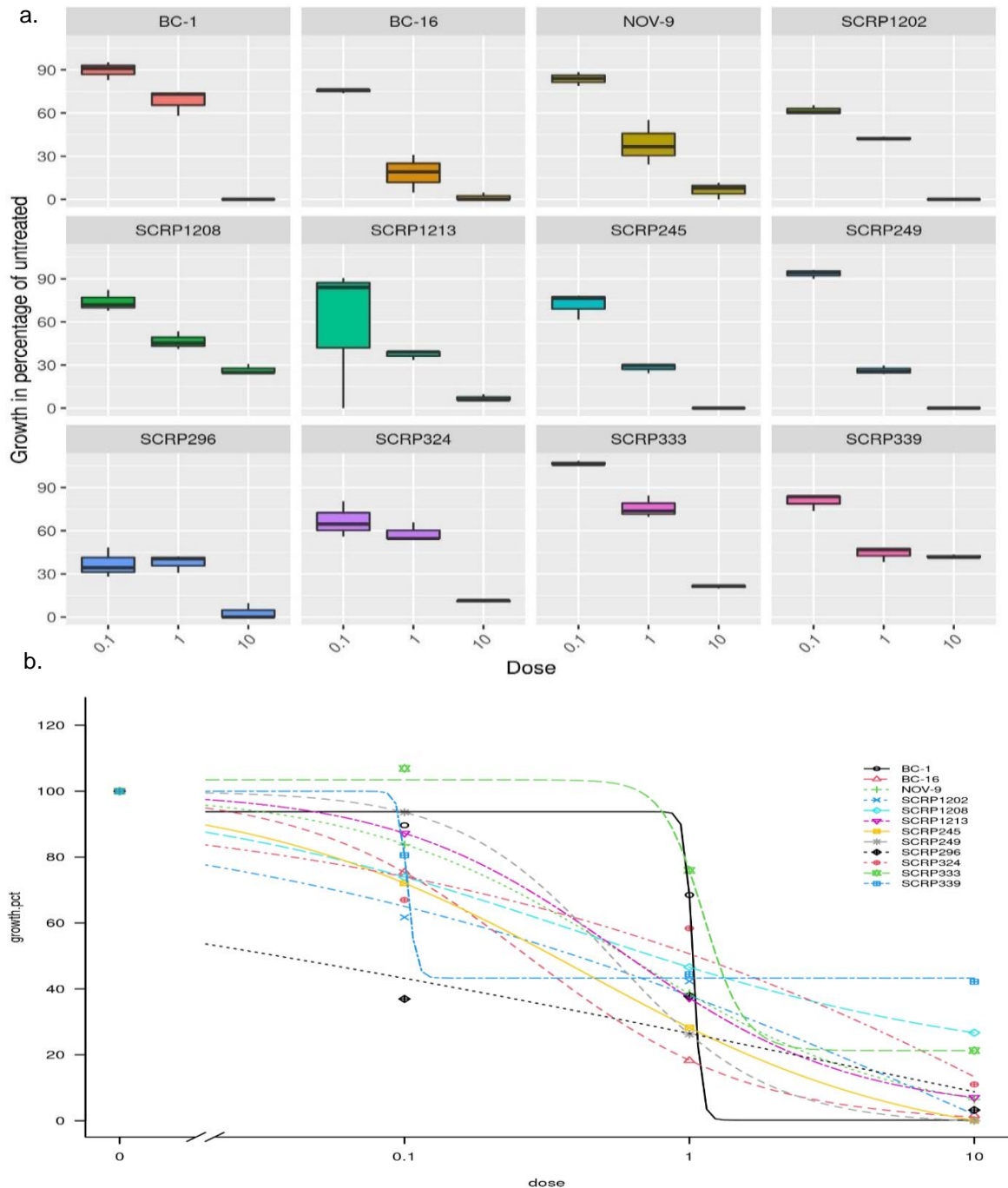


Figure 2. 12. Effect of Fluopicolide on isolates growth. **a.** Boxplot representation of the effect of Fluopicolide incorporated at different doses (0.1ppm, 1ppm and 10ppm, x axis) on the diametral hyphal growth (expressed in percentage of controls, y axis) of eight *P. rubi* and four *P. fragariae* isolates. **b.** Dose-response model fitted to Fluazinam. Doses are represented on the x axis in ppm and growth in percentage of controls is represented on the y axis (“growth.pct”). Three replicates per isolate and dose were used and experiment was performed once.

At 0.1 ppm, most isolates had a mean hyphal growth under 95 % of controls (on average, 68 % for *P. rubi* and 79 % for *P. fragariae*, Table 2.5), although a lot of variation was observed between isolates (Figure 2.12).

At 1 ppm, this dissimilarity is even clearer, while the average growth is under 50 % of controls, except for SCRP1207. At 10 ppm, only *P. fragariae* SCRP245 and BC-1, and *P. rubi* SCRP1202 and SCRP249 showed absence of growth, while all others displayed variable response to the chemical. *P. fragariae* isolates were more sensitive to the chemical at 10 ppm, as the average growth is only 0.5 % of untreated, while the average growth of *P. rubi* cultures was 14 % of untreated. Overall and similarly to Fluazinam, a general decrease is observed in the hyphal growth when the Fluopicolide dose is increased.

- Propamocarb

Unlike the two previous chemicals, Propamocarb did not show a statistically significant decrease of the mean hyphal growth with an increased dose incorporated in the medium (Table 2.5 and Figure 2.13).

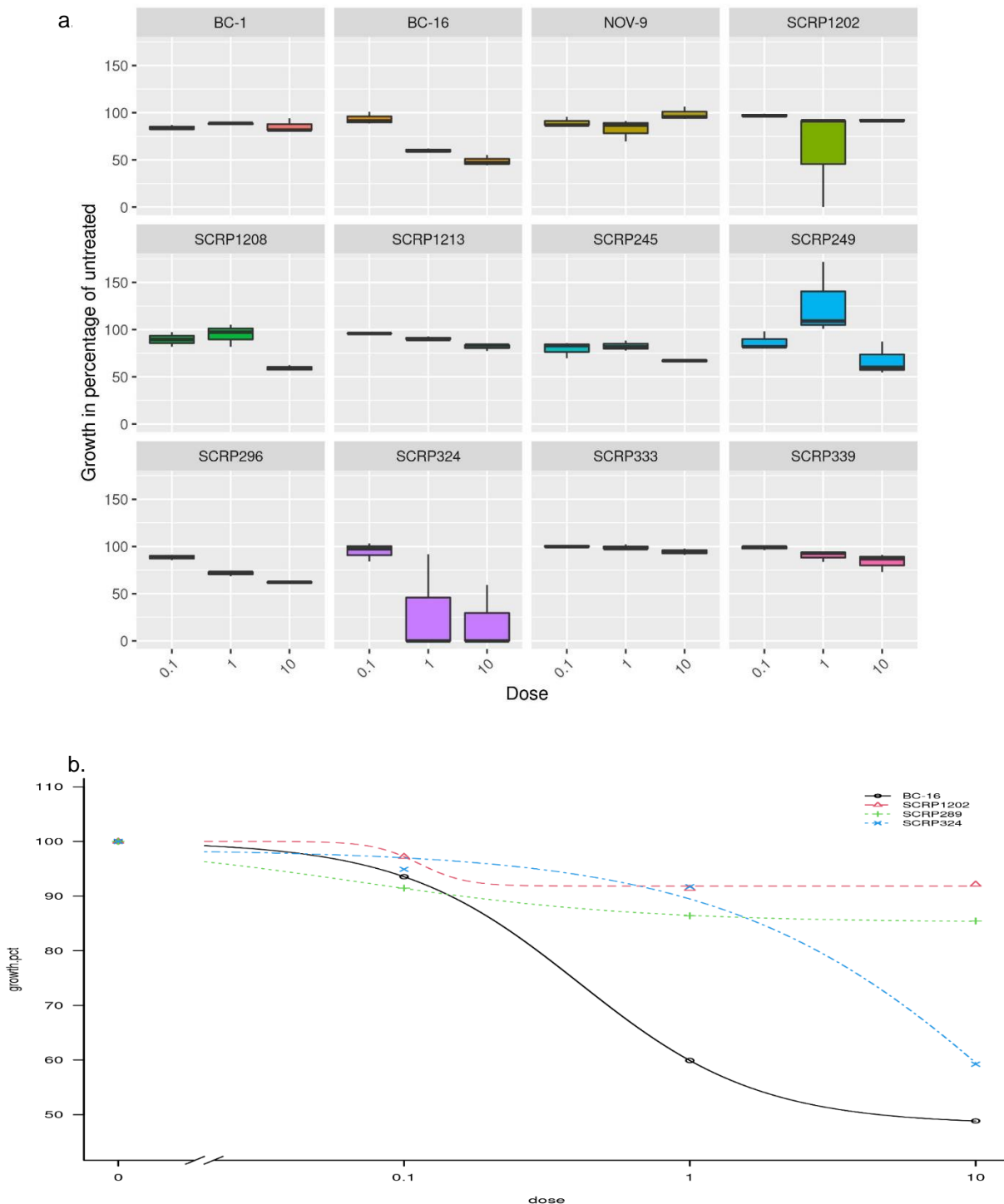


Figure 2. 13. Effect of Propa mocarb on isolates growth. **a.** Boxplot representation of the effect of Propamocarb incorporated at different doses (0.1ppm, 1ppm and 10ppm, x axis) on the diametral hyphal growth (expressed in percentage of controls, y axis) of eight *P. rubi* and four *P. fragariae* isolates. **b.** Dose-response model fitted to Fluazinam. Doses are represented on the x axis in ppm and growth in percentage of controls is represented on the y axis (“growth.pct”). Three replicates per isolate and dose were used and experiment was performed once.

- Ametoctradin

Average hyphal growth on agar incorporating the highest dose (10 ppm) of Ametoctradin stayed at 75 % of the untreated (Table 2.5 and Figure 2.14). Lower doses (0.1 and 1 ppm) of Ametoctradin led to hyphal growth over 80 % of the controls, regardless of the isolates. There was no evident effect of the year of isolation: both SCRP1212 (isolated in Scotland in 2018) and SCRP324 (isolated in Scotland in 1991) showed hyphal growth higher than the controls at 0.1 ppm (up to > 110 % of untreated).

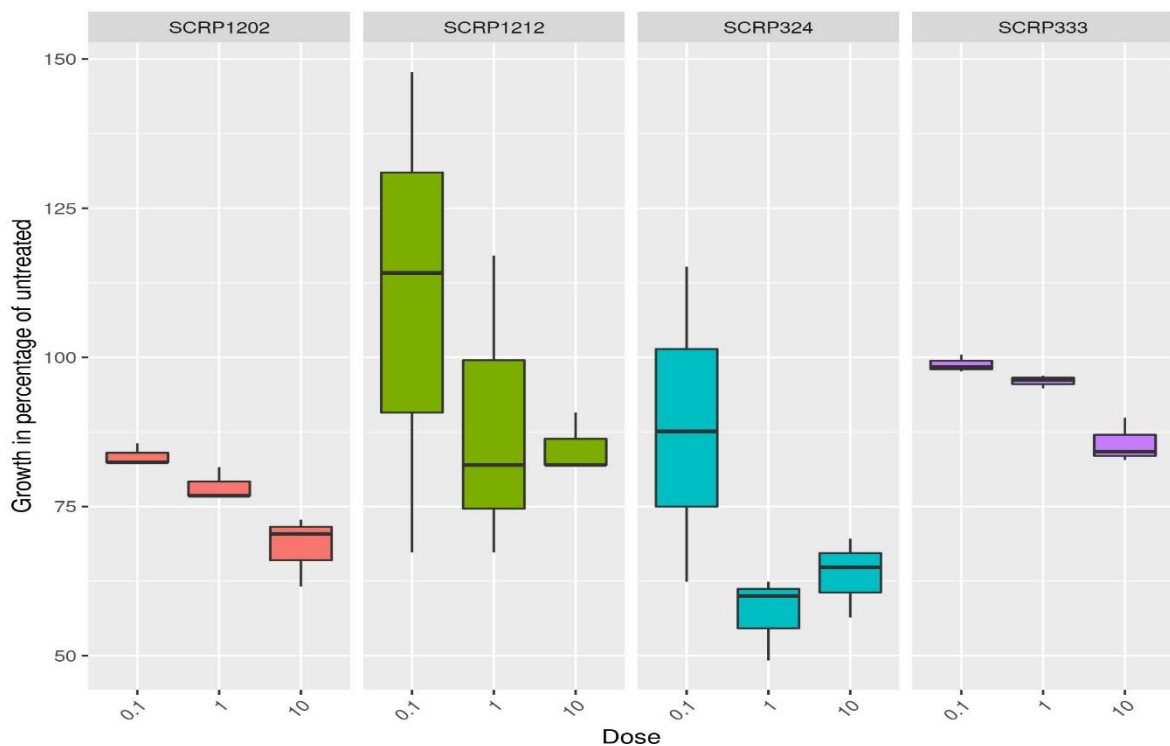


Figure 2. 14. Effect of Ametoctradin on isolates growth. Boxplot representation of the effect of Ametoctradin incorporated at different doses (0.1ppm, 1ppm and 10ppm, x axis) on the diametral hyphal growth (expressed in percentage of controls, y axis) of eight *P. rubi* and four *P. fragariae* isolates. Three replicates per isolate and dose were used and experiment was performed once.

- Phorce

Phorce, a phosphite-based product used as a fertiliser, led to similar growth as observed with Propamocarb (Figure 2.15): the hyphal growth of *P. rubi* isolates did not significantly decrease with an increasing dose. In fact, the average hyphal growth for all isolates was nearly 100 % of the controls (Table 2.5), therefore demonstrating negligible effects of this treatment on hyphal development.

None of the five chemicals described above (Fluazinam, Fluopicolide, Propamocarb, Ametoctradin, Phorce) could fully inhibit *P. rubi* and *P. fragariae* hyphal growth.

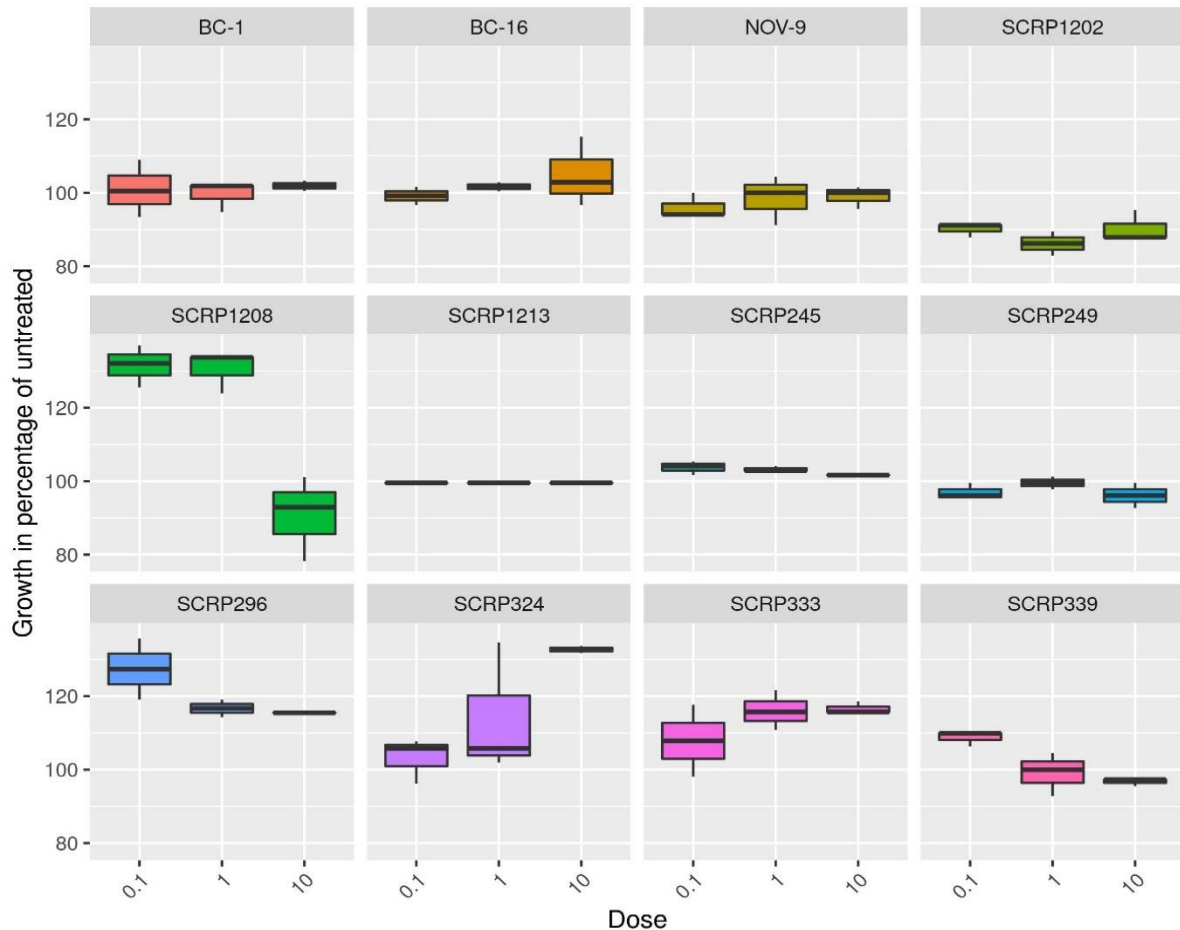


Figure 2. 15. Effect of Phorce on isolates growth. Boxplot representation of the effect of Phorce incorporated at different doses (0.1ppm, 1ppm and 10ppm, x axis) on the diametral hyphal growth (expressed in percentage of controls, y axis) of eight *P. rubi* and four *P. fragariae* isolates. Three replicates per isolate and dose were used and experiment was performed once.

- Dimethomorph

Dimethomorph, the active ingredient of Paraat®, showed strong inhibition of hyphal growth. The lowest dose of Dimethomorph (0.1 ppm) resulted in less than 40 % of the control growth for *P. rubi* and *P. fragariae* isolates, with an average of 15 % of untreated for *P. rubi* and 3 % of untreated for *P. fragariae* (Table 2.5 and Figure 2.16). At 1 ppm, the usual field application dose for Dimethomorph, only *P. rubi* SCRP333 and SCRP324 showed any mycelia development, with an average growth below 2 % of the untreated. At the highest dose, none of the isolates tested grew.

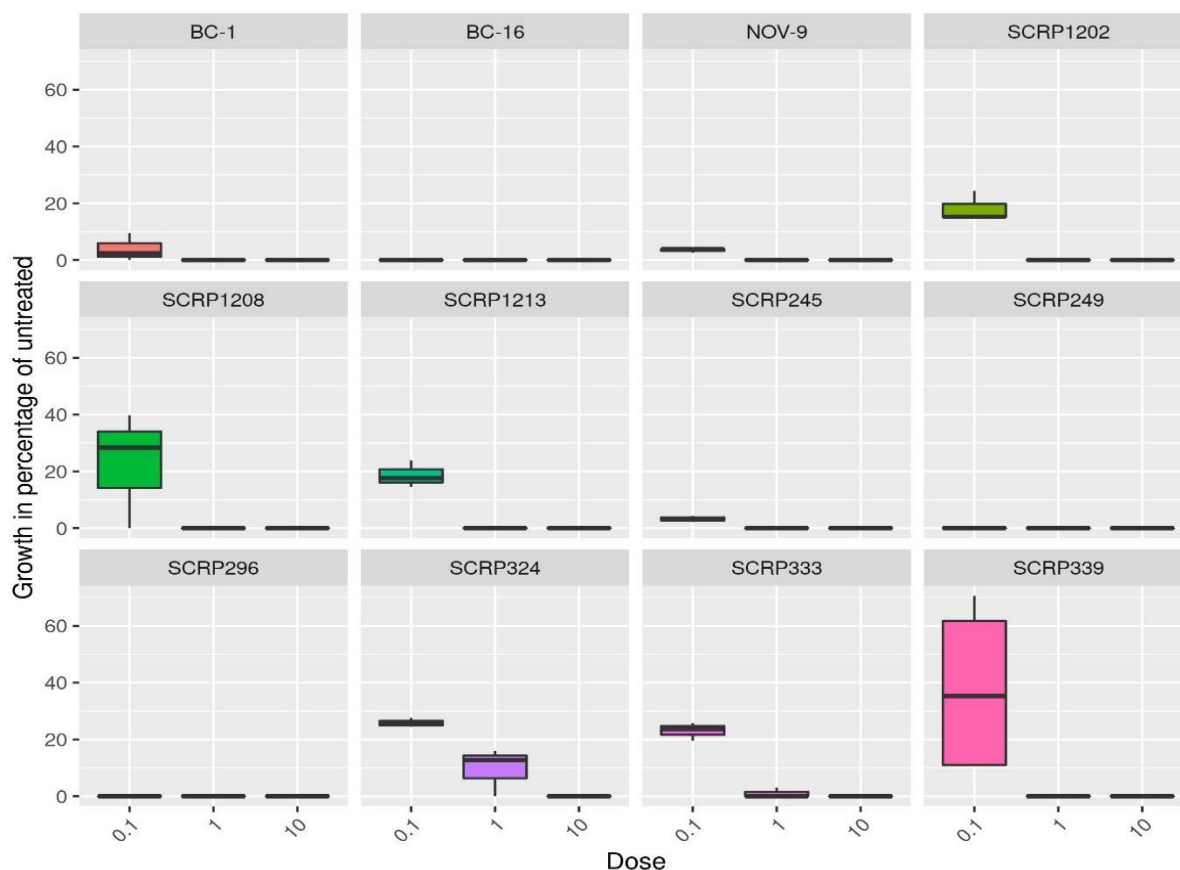


Figure 2. 16. Effect of Dimethomorph on isolates growth. Boxplot representation of the effect of Dimethomorph incorporated at different doses (0.1ppm, 1ppm and 10ppm, x axis) on the diametral hyphal growth (expressed in percentage of controls, y axis) of eight *P. rubi* and four *P. fragariae* isolates. Three replicates per isolate and dose were used and experiment was performed once.

- Metalaxyl-M

Metalaxyl-M, also still approved for use on raspberry, showed great variation in its efficacy amongst the isolates (Table 2.5 and Figure 2.17). Around 86 % of isolates tested could grow on 1 ppm of Metalaxyl-M, with hyphal growth up to 90 % of the untreated ones. At 10 ppm, 50 % of all isolates screened grew, and at 100 ppm, 21 % showed growth. Generally, the colony diameter decreased with increasing doses of Metalaxyl-M, except for *P. rubi* SCRP339, where it plateaued, showing the resistance of some isolates to Metalaxyl-M. *P. fragariae* isolates BC-1 and BC-16, and *P. rubi* SCRP1208 could still grow at a very high dose of the chemical (100 ppm, Figure 2.17). Lee et al. (1999) and Randall et al. (2014) considered isolates sensitive to Metalaxyl-M if they show hyphal growth below 40 % of the untreated under a 10 ppm dose, while isolates with 40 to 50 % of untreated growth were classed as showing an intermediate response and isolates with hyphal growth above 50 % of those untreated were resistant. At 10 ppm and following those criteria, BC-1 and SCRP339 were resistant

to Metalaxyl-M, BC-16 displayed an intermediate response, and all other isolates were sensitive. When the dose was increased to 100 ppm, only BC-16 stayed resistant to the chemical.

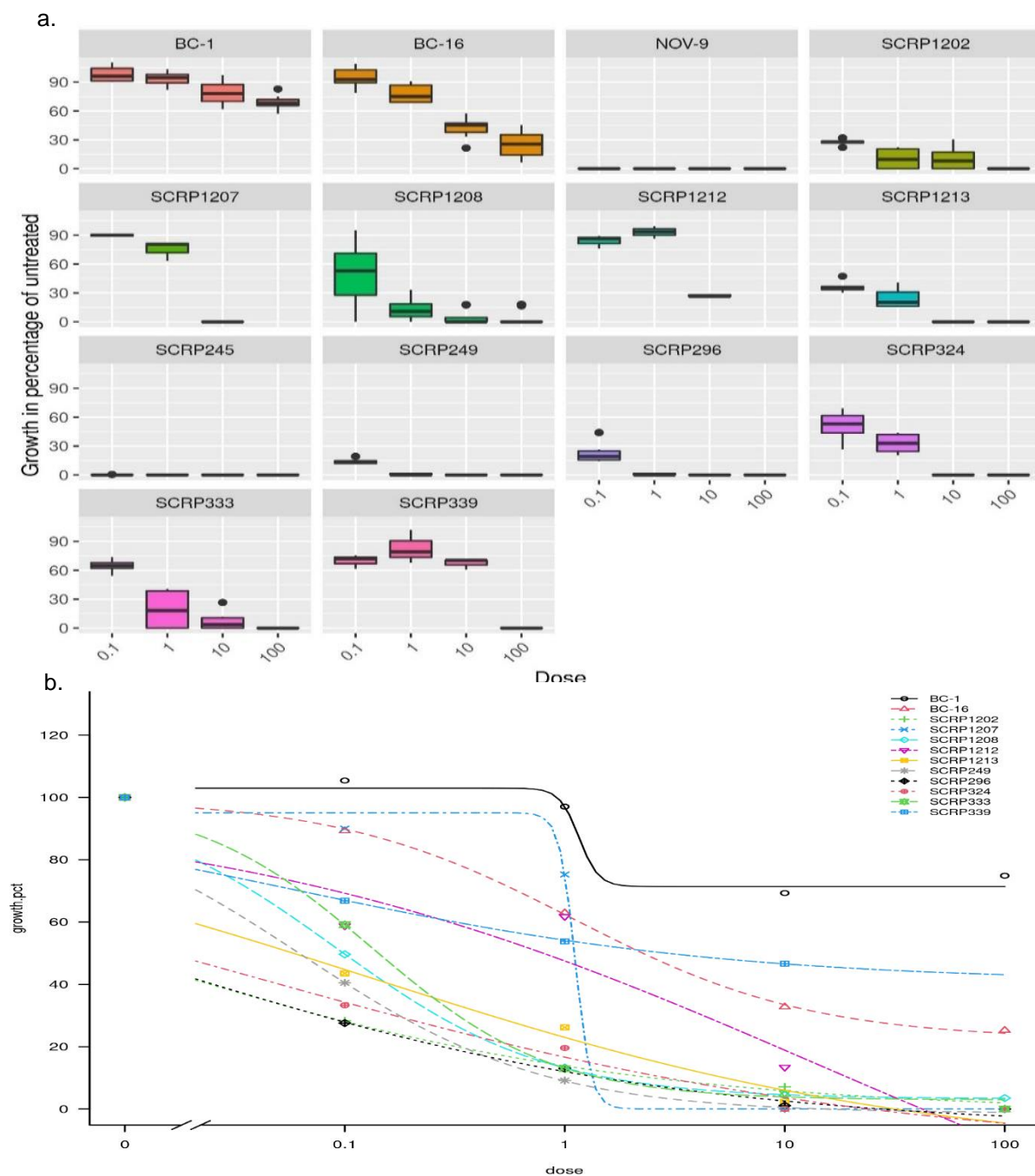


Figure 2. 17. Effect of Metalaxyl on isolates growth. **a.** Boxplot representation of the effect of Metalaxyl-M incorporated at different doses (0.1ppm, 1ppm and 10ppm, 100ppm, x axis) on the diametral hyphal growth (expressed in percentage of controls, y axis) of ten *P. rubi* and four *P. fragariae* isolates. **b.** Dose-response model fitted to Fluazinam. Doses are represented on the x axis in ppm and growth in percentage of controls is represented on the y axis (“growth.pct”). Three replicates per isolate and dose were used and experiment was performed twice for *P. rubi* isolates and three times for *P. fragariae* isolates.

- Half maximal inhibitory dose (ID50)

The half maximal inhibitory dose (ID50) is commonly used to measure the concentration needed to inhibit, *in vitro*, a biological process by 50 % (here hyphal growth). ID50 are often used in chemical screening publications (Parra and Ristaino, 2001; Pérez et al., 2009; Qi et al., 2012; Rekanović et al., 2012). In this study, we observe that Dimethomorph always inhibits 50 % or more of the hyphal growth, compared to the controls, while Phorce, Ametoctradin and Propamocarb almost never inhibit the isolates growth to 50 % or less of the untreated (Table 2.6). Metalaxyl-M, Fluazinam and Fluopicolide provide a variety of intermediate responses (Table 2.6), with ID50 lower than 0.1 ppm (e.g. SCR296 with Fluopicolide) or higher than 10 ppm (e.g. BC-1 with Metalaxyl-M).

Table 2. 6. Half-inhibitory doses of the seven chemicals tested against *P. fragariae* and *P. rubi* isolates

ID50 (ppm)														
Chemical	Isolates													
	<i>P. fragariae</i>				<i>P. rubi</i>									
	BC-1	BC-16	NOV-9	SCR245	SCR1202	SCR1207	SCR1208	SCR1212	SCR1213	SCR249	SCR296	SCR324	SCR333	SCR339
Ametoctradin					> 10			> 10				> 10	> 10	
Dimethomorph	< 0.1	< 0.1	< 0.1	< 0.1	< 0.1		< 0.1		< 0.1	< 0.1	< 0.1	< 0.1	< 0.1	< 0.1
Fluazinam	> 10	1.1 0	0.9 1	0.6 2	1.6 2		2.3 1		0.8 8	1.1 8	1.1 5	0.4 2	2.2 3	0.4 8
Fluopicolide	1.0 3	0.2 7	0.6 2	0.3 3	0.4 0		0.7 5		0.6 1	0.5 3	0.0 4	1.0 5	1.3 3	0.1 1
Metalaxyl-M	> 10	2.2 7	< 0.1	< 0.1	0.0 1	1.1 1	0.1 0	0.8 2	0.0 6	0.0 6	0.0 1	0.0 2	0.1 4	2.9 2
Phorce	> 10	> 10	> 10	> 10	> 10		> 10		> 10	> 10	> 10	> 10	> 10	> 10
Propamocarb	> 10	4.6 0	> 10	> 10	> 10		> 10		> 10	> 10	> 10	> 10	> 10	> 10

2.3.3.2. Chemical target genes for Metalaxyl-M did not explain the phenotypic resistance of *P. rubi* and *P. fragariae* isolates

SNPs and amino acid changes were investigated in the suspected target genes to explain the observed resistance, as previous studies have done before (Randall et al.,

2014). Even though diversity in *P. rubi* responses to Dimethomorph showed that SCRP324 and SCRP333 were growing at 1 ppm, this was not considered target site mediated resistance, for which almost complete insensitivity to the chemical would be expected. Metalaxyl-M screening however detected resistance for two *P. fragariae* isolates: BC-1 and BC-16, that could grow at 100 ppm; while *P. fragariae* isolates SCRP245 and NOV-9 did not grow under the same dose. *P. infestans* RNA Pol genes RPABC23, RPABC27, RPA190, RPA135, RPAC19 and RPA12.2 sequences were used in BLASTx and BLASTp searches on NCBI for the four *P. fragariae* isolates, translated into proteins and aligned. Only RPAC19 showed amino acid differences between the four isolates sequences, though resulting in a different clustering than the resistance observed (data not shown). This means that nucleotide and protein sequences for these RNAPol genes were not enough to explain phenotypic differences in resistance levels to Metalaxyl-M.

2.4. Discussion and Conclusions

Phenotypic studies are important for characterizing under-studied species and assessing the diversity of isolates through variation in responses to different stimuli. This chapter investigates the phenotypic behaviours of several isolates of *P. rubi* and *P. fragariae*, regarding adaptation to rising temperatures and assesses the relevance of several control chemicals, representing modern field conditions.

Five isolates of *P. rubi* causing raspberry root rot in Scotland have been obtained in 2018, providing this study with up-to-date strains for phenotypic and genetic studies.

The temperature screening study in this chapter indicates that *P. rubi* and *P. fragariae* hyphal growth increased from 15 °C to 18 °C and to 21 °C but decreases at 25 °C and is fully inhibited at 28 °C while *P. rubi* sporulation is statistically similar at all temperatures tested. Wilcox and Latorre (2002) found similar patterns for *P. rubi* hyphal growth at 25 °C and reducing at higher temperatures, though no differences amongst isolates were examined. Bain and Demaree (1945) and Leonian (1934) observed the same temperature responses for *P. fragariae*, with an optimum between 18 °C and 22 °C and a declining rate of growth at 25 °C. Similarly, Duncan (1985), found that *P. fragariae* inoculum was detected in drainage water of plants kept at

temperatures between 2 °C and 20 °C but not in water from plants kept at 26 °C. Comparing the two closely related species *P. rubi* and *P. fragariae* shows that the latter does not consistently thrive under temperatures higher than 21 °C. Indeed, the hyphal growth of two *P. fragariae* isolates, BC-1 and BC-16 (isolated from Canada in 2007), is inhibited at 25 °C, while other isolates NOV-9 (Canada, 2007) and SCRP245 (England, 1945), as well as all eight *P. rubi* tested show hyphal development at 25 °C. Although a non-significant increase in sporangia numbers was observed at 18 °C and 21 °C compared to 15 °C, previous studies have used low temperatures for the production of sporangia and zoospores (Bain and Demaree, 1945; Goode, 1956; Converse, 1962; Felix, 1962; Mussel and Fay, 1973). These findings demonstrate the ability of *P. rubi* to survive and reproduce at higher temperatures than the ones commonly observed in cooler winter months. Average winter air temperatures recorded in Invergowrie, Scotland, vary between -2 °C and 8 °C (Figure 2.1) while winter soil temperatures recorded at 30 cm and 100 cm depth at the same location showed an average of 4 °C to 6 °C (Figure 2.1). In the winter (2020), the average temperature for soil in raspberry pot was 4 °C and 13 °C in strawberry substrate bag (Figure 2.2). The range of temperatures studied and under which pathogens lived (15 °C to 21 °C), is in fact, closer to Scottish summer temperatures (11 °C to 21 °C for air temperatures, 13 °C to 16 °C for soil, and 14 °C to 17 °C for pots and bags), where the disease has been prevalent for over 80 years. Presence of active disease on raspberry roots and canes in the summer confirms *P. rubi* as a pathogen that thrives in wetter environment, since rain fall is higher in the summer than in the winter in Scotland. It should be noted that isolates from Kincardineshire in 2018 were recovered from diseased canes near a flooded field (Figure 1.17, Chapter 1).

Overall, this work gives insights into the effect of temperature on *P. rubi* and *P. fragariae* on hyphal growth and sporangia production, including recent isolates (2017 and 2018) and data on variation amongst species. It completes the pathogen's profile by adding information on these diseases and demonstrates that *P. rubi* and *P. fragariae* should not only be associated with cold weather. Other *Phytophthora* species that can be found on raspberries (Duncan et al., 1987; Meszka and Michalecka, 2016) have also been reported to thrive in wetter environment, though their optimal temperature range is diverse. While *P. rubi* and *P. fragariae* optimal temperature ranges between 18 °C and 22 °C and is close to *P. idaei*, *P. cactorum*, *P. cryptogea*

(Waterhouse and Backwell, 1954; Waterhouse, 1956; Waterhouse, 1963; Falloon and Grogan, 1991; Erwin and Ribeiro, 1996a; Haverkort et al., 2009; Grove et al., 1985), other *Phytophthora* species have a lower (*P. syringae*) or higher optimum (*P. drechsleri*, *P. cambivora*, *P. megasperma*, *P. citricola*, *P. citrophthora*) (Erwin and Ribeiro, 1996a; Pane et al., 2001; Mostowfizadeh-Ghalamfarsa et al., 2010; Vannini and Vettraino, 2011; Scanu et al., 2015). Added to the current and foreseeable global warming, these results should encourage growers to be mindful of the disease all year around, and rule out summer temperatures for disease inhibition (Bain and Demaree, 1945). These results raise the question of adaptations to other stresses, such as man-made stresses and chemical pressures, which can commonly lead to resistance (Nickerson, 1998; Parra and Ristaino, 2001; Vawdrey et al., 2004; Elansky et al., 2007; Gisi and Sierotzki, 2008; Zhu et al., 2008; Pérez et al., 2009; Rekanović et al., 2012; Randall et al., 2014).

The chemical screening study in this Chapter highlights different responses showing both inter and intra-species diversity, including resistance to chemicals still used on raspberries, at doses close to field application doses (Figures 2.18 and 2.19).

Dimethomorph exhibits the best inhibitory effect on the hyphal growth of the isolates tested, to an adequate level of control. Elansky et al. (2007), Zhu et al. (2008) and Rekanović et al. (2012) also observed very little or no resistance to Dimethomorph, further confirming these findings. Fluazinam and Fluopicolide treatments lead to a decreased hyphal growth with an increasing dose, showing sensitivity of the *P. rubi* and *P. fragariae* isolates to the chemicals, as observed formerly in studies such as Toquin et al. (2007) and Jackson et al. (2010); with *P. fragariae* generally more sensitive to Fluopicolide than *P. rubi*. Propamocarb, Ametoctradin, and Phorce display very little to no decrease of the hyphal growth with an increasing dose, indicating a lack of sufficient inhibition to growers' standards, as similarly seen in studies by Chan and Kwee (1986), Chase (1993), Hu et al. (2007) and Töfoli et al. (2016). Even though studies have found that higher doses can reduce hyphal development (Löchel and Birchmore, 1990; Samoucha and Cohen, 1990), active compounds are limited in their application and only products like fertilisers (such as Phorce) could realistically be used at much higher concentrations in the field.

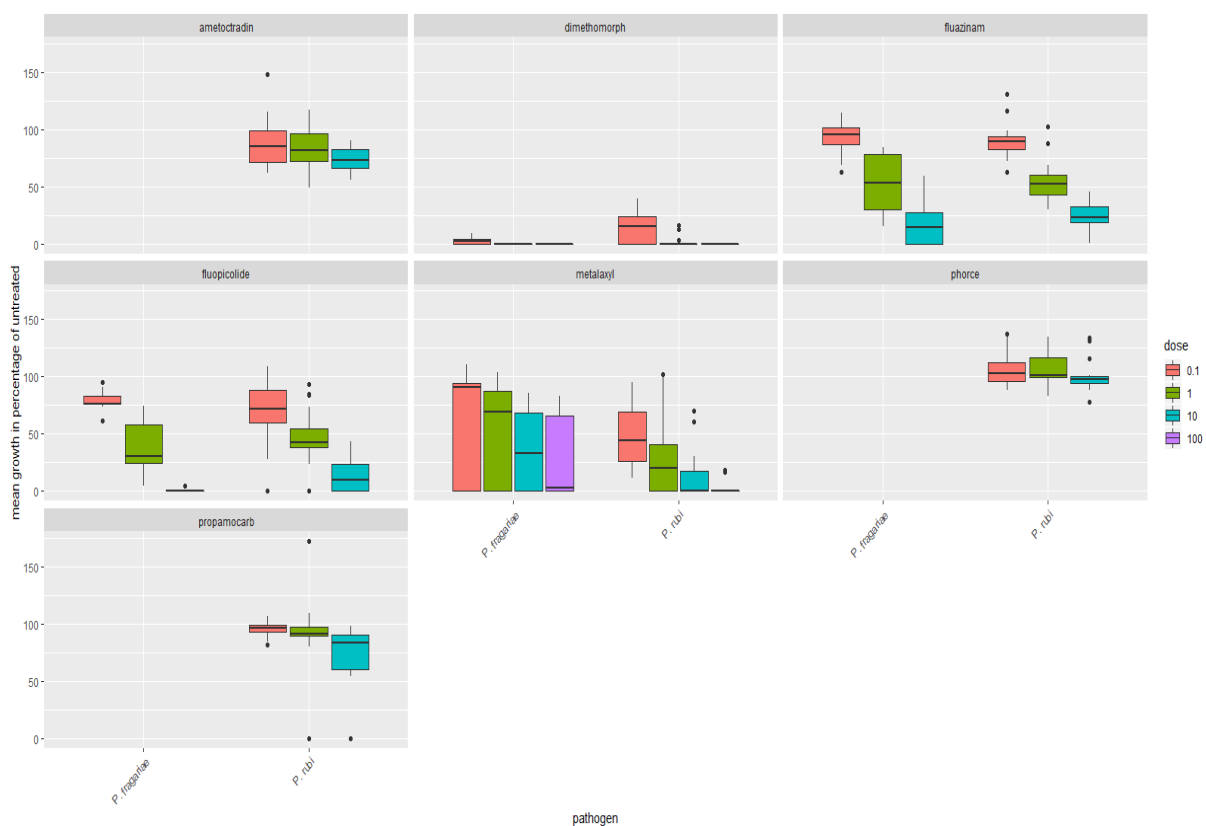


Figure 2. 18. Effect of seven chemicals on *P. rubi* and *P. fragariae* isolates. Boxplot representation of the effect of all chemicals incorporated at different doses (0.1ppm, 1ppm and 10ppm, 100ppm) on the diametral hyphal growth (expressed in percentage of controls, y axis) for *P. rubi* and *P. fragariae* isolates. Three replicates per isolate, dose and chemical were used.

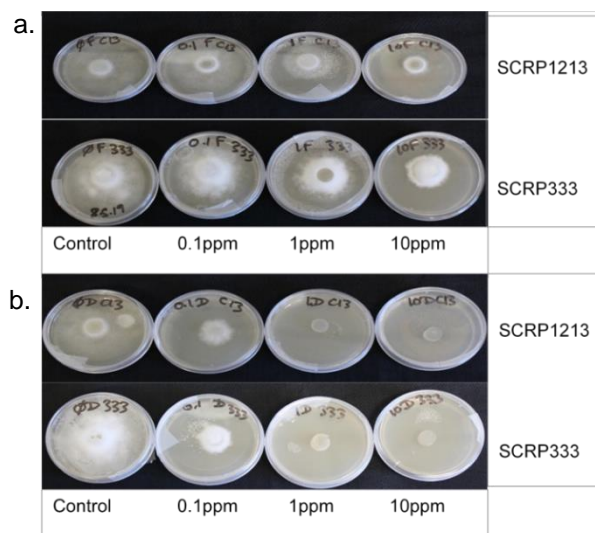


Figure 2. 19. Photos illustrating chemical screening plates. Plates incorporated with a. Fluazinam and b. Dimethomorph for several isolates at 0 ppm (controls), 0.1 ppm, 1 ppm and 10 ppm.

Metalaxyl-M incorporation reveals a variety of responses depending on the isolate screened, with both inhibition under high doses of the chemical, and resistance where isolates grow with no statistical difference compared to controls. Resistance to

Metalaxyl-M has previously been reported by other studies on *Phytophthora* species, such as *P. fragariae* (Nickerson, 1998), *P. infestans* (Elansky et al., 2007; Zhu et al., 2008; Pérez et al., 2009; Rekanović et al., 2012; Randall et al., 2014), *P. capsici* (Parra and Ristaino, 2001; Qi et al., 2012) and *P. palmivora* (Vawdrey et al., 2004). Such emerging resistance, as well as more stringent regulations on pesticides has led to numerous chemical withdrawals, leaving very few chemical control options available, and sometimes relying on single active ingredient (SL567®, Paraat®), which can also increase the chances of new resistance. For example, frequent replacements of control chemicals for raspberry root rot have been made in the last 40 years.

It should also be noted that both phenotypic studies would benefit from further research and replication of experiments looking at the effects of these factors on other cells like sporangia or zoospores, which are the infective propagules for these soil-borne pathogens. However, such experiments can prove difficult and time-consuming, as described in Chapter 4 (Coffey, 1984; Duncan, 1985; Chan and Kwee, 1986; Cohen and Coffey, 1986; Hu et al., 2007; Lawrence et al., 2017; Wu et al., 2020).

Chemical treatments on raspberries and strawberries are usually applied via drip irrigation, one of the most efficient delivery methods for soil fungicide, with a more uniform distribution and a reduction in pesticide application and plant disturbance (Ghidu et al., 2012). However, only a low percentage of the active ingredient(s) will eventually reach the pathogen. This contrasts with *in vitro* studies on hyphal growth that use chemical incorporated directly into the growing medium, thus allowing the full dose to be in contact with the pathogen. Therefore, while ID50 are very useful to compare efficacy of different chemicals, pathogen control to grower's standards should be assessed by looking at the minimum growth for the minimum dosage. Bearing this in mind, this study highlights the control potential of Dimethomorph (Paraat®) at low doses, the variation in tolerance to Fluazinam (Tizca®), and the existence of resistance to high doses of Metalaxyl-M (SL567A®). These findings reflect the current usage of these three treatments still allowed for use on raspberries and strawberries. In fact, pesticides usage surveys show a decrease in use of Fluazinam (from 44 % in 2012 to 10 % in 2018), a low use of Metalaxyl-M (1 % in 2012 and 2 % in 2018) and an increased use of Dimethomorph (2 % in 2012 and 28 % in 2018) (Government, 2019).

In conclusion, this chapter provides novel information on *P. rubi* and *P. fragariae* *in vitro* responses to agriculturally important factors, showing the difference in efficacy of controlling products and the presence of resistance amongst specific isolates. It illustrates the possibility of resistance and thus the impact humans could have on the evolution of pathogens through single-chemical application and selection pressure (Hunter et al., 2018). Generally, as previously stated, a reduction in pesticides has been observed in the UK, with the weight of authorised pesticides applied to soft fruit crops in the United Kingdom going from 350 tonnes in 2010 to 150 tonnes in 2018, of which 35 % were fungicides (Ridley et al., 2018). Pesticide reduction as well as the many withdrawals and replacements due to resistance and toxicity to the environment are evidence that integrated pest management (IPM) is necessary to manage diseases such as *P. rubi* and *P. fragariae*. Control of pathogens should be comprehensive with research on 1) the host's resistance potential by comparing resistance genes in resistant and susceptible cultivars, 2) the pathogen and its essential components (housekeeping genes) and attacking proteins (effectors) and 3) external factors that can influence both the pathogen and the host (temperatures, chemical pressure, examined in this study) (Figure 1.15, Chapter 1). This inclusive approach looking at every element of the plant disease triangle (Figure 1.15) is key to disease control and can lead to resistant or tolerant cultivars (1), the discovery of novel chemicals targeting essential pathogen biology (2) and accordingly amend guidance for growers considering all environmental factors (3). To address pathogen biology, both the phenotype and the genotype should be explored. Pathogen genotype can be assessed through sequence analysis of chemical target genes for mutations that could lead to resistance, as well as pathogenicity effectors and their diversity (see Chapter 3) which could impact the perception by host resistance proteins. In this study, phenotypic variation of isolates to Metalaxyl-M could not be explained with amino acid changes in the genes screened. However, it should be noted that the target proteins for most chemicals used in this study are not fully understood, making conclusions from this data difficult at present.

CHAPTER 3. DIVERSITY STUDY USING PATHOGEN ENRICHMENT SEQUENCING (PENSEQ)

3.1. Introduction

3.1.1. Current Assessment of Diversity of *P. rubi* and *P. fragariae*

P. rubi and *P. fragariae* are two very closely related pathogens that were originally classed as a single species, as detailed in Chapter 1. *P. rubi* is only known to infect species from the *Rubus* genus. *P. fragariae*, although mainly a pathogen of cultivated *Fragaria* (*Fragaria x ananassa*), has been found to naturally infect some *Rubus* species e.g. Loganberry (*Rubus x loganobaccus*) (Figure 1.6, Chapter 1). Intriguingly, the genus *Rubus* diverged from *Fragaria* approximately 57 million years ago (Zhang et al., 2017), while it is estimated that *P. fragariae* and *P. rubi* diverged only 10 million years ago (Xiang et al., 2016). Based on these observations on host range and host divergence, Gao et al. (2021) suggest that *P. fragariae* went through a rare host change to *Fragaria* hosts that could have been driven by divergence within the *Rubus* genus, as opposed to divergence between *Rubus* and *Fragaria* hosts. Schulze-Lefert and Panstruga (2011) proposed that the inability of a pathogen to establish infection in non-host plants could be relative to the phylogenetic distance between host and non-host plants. In distantly related plants, PAMP triggered immunity (PTI) is thought to be the major contribution to resistance as effectors are inappropriately attuned to perturb their orthologous plant targets. In contrast, in non-host plants that are more closely related to the host plants, effector triggered immunity (ETI) and therefore the early *in planta* recognition of successfully delivered effectors could be the major mechanism determining the outcome of an attempted infection. Based on this theory, we hypothesize that ETI (and effectors) should be contributing towards limiting the host range of these sister species of *Phytophthoras* between their related hosts. Similarly, changes in pathogen host range are driven by variation in pathogen effector genes repertoires, which highlights the importance of the study of pathogen genetics. Taken altogether, if Gao et al. (2021) and Schulze-Lefert and Panstruga (2011) are correct, then we hypothesize that there should be some *P. fragariae* effectors that have been lost or diverged compared to *P. rubi* to successfully infect *Fragaria* species;

and that those might be widely conserved in *P. rubi* isolates. Consequently, one important aim of this chapter is to assess the inter-species diversity of effector genes by identifying core effectors conserved in the two species as well as species-specific effectors.

Identifying species of pathogens in the field is important and can be used to inform growers of disease threat before symptoms and important crop losses are incurred. This is particularly valuable for detecting the presence of persistent pathogens contaminating the soil for many years or when disease symptoms are slow to develop, such as *Phytophthora* diseases of raspberries and strawberries. Traditionally, PCR based diagnostic tools have been used to distinguish pathogens at the species level. Until recently, the major way to distinguish *Phytophthora* species like *P. rubi* and *P. fragariae* was using PCR amplification and sequencing of the spacer region between eukaryotic mitochondrial cytochrome c oxidase (*Cox*) subunits I and 2 (Man in't Veld, 2007) or of the *CoxI* encoding region (Peters and Woodhall, 2014). These diagnostic tools rely on the identification of genes with 1) enough variation between the species to be able to design species-specific primers, and 2) that are less likely to evolve to insure the relevance of the diagnostic tool. Genes such as housekeepers, included in this study, that present species-specific polymorphism, could constitute good candidates for PCR based diagnostic tools.

Population genetics is a powerful tool to understand patterns and evolutionary processes that are involved in pathogen emergence and adaptation. Genotyping by sequencing studies on *P. rubi* and *P. fragariae* isolates from Western United States, Canada and EU confirmed hypotheses that *P. rubi* appears to be a monophyletic species (descending from a common evolutionary ancestor) distinct from *P. fragariae* (Tabima et al., 2018). Evaluation using SNP variant analysis revealed very high population differentiation between these two species further supporting previous conclusions that the two *Phytophthoras* are genetically isolated species (Man in't Veld, 2007; Tabima et al., 2018). However, this study highlighted evidence for low genetic diversity between the different isolates of *P. rubi* examined and a lack of evidence for clustering by geographical origin.

P. rubi and *P. fragariae* isolates have been shown to infect multiple cultivars and so the intra-species diversity amongst isolates of a single species is important to assess. *P. rubi* has been tentatively divided into two races, based on virulence / avirulence on

a single raspberry line known as EM5605/12 (Kennedy and Duncan, 1993; van de Weg, 1997). *P. fragariae* has had up to 11 races described, (Kennedy and Duncan, 1993; van de Weg, 1997) and at least three races are of major significance to the UK (UK1-2-3). Therefore, another major aim of this chapter is to identify polymorphic effector genes which could determine avirulence or be used as isolate specific marker.

However, recent PacBio and Illumina sequencing of *P. rubi* and *P. fragariae* genomes indicated little evidence of gene loss or presence of insertions / deletions (INDELS) or Single Nucleotide Polymorphisms (SNPs) in pathogenicity genes (Adams et al., 2020). Adams et al. (2020) indicate that around 26 % of predicted *P. fragariae* RXLRs, 31 % of CRNs and 20% of apoplastic effectors show evidence of expression *in planta*. The study speculates that it is the differential expression of effectors during attempted infection of resistant and susceptible hosts that accounts for race and isolate differences within *P. fragariae*. However, we here use Pathogen Enrichment Sequencing (PenSeq) to focus on effector genes, which can be under significant diversifying selection, and therefore expect polymorphism as well as presence / absence variation of some of these between isolates and species. This should help to identify distinguishing features between isolates at the genome level, rather than transcription level.

3.1.2. Pathogen Enrichment Sequencing (PenSeq)

Various models have been used to predict the number of effectors in *Phytophthora* spp. and have estimated that RXLR effectors are encoded by a small percentage of the genome. Enrichment sequencing deploys bespoke RNA baits combined with short- or long-read sequencing technologies to examine specific gene families of interest. This technology has major advantages over whole genome sequencing: 1) it saves money by sequencing only DNA of interest 2) depending on the application, accurate short read sequencing technologies can be combined with long-read sequencing such as PacBio 3) it ensures sufficient high-quality read coverage for robust analyses of targeted genes. Indeed, the enrichment step significantly increases the read depth of genes of interest usually swamped by the sequences from the rest of the genome (Kozarewa et al., 2015). Since effectors are typically encoded by short sequences, Illumina-based re-sequencing via PenSeq yields cheaper and more accurate results if compared to long-reads sequencing platforms such as PacBio or

MinION, that can also show higher per base error rates (Goodwin et al., 2015; Rhoads and Au, 2015).

PenSeq (enrichment sequencing of pathogen sequences) is a powerful tool that has been developed and deployed in house for analysis of inter- and intra-species diversity of effectors and neutral markers of *P. infestans* and *P. capsici* (Thilliez et al., 2019). The efficiency and power of PenSeq was initially deployed at JHI / TSL using bespoke baits library designed for *P. infestans* and *P. capsici* virulence factors. This was successfully used to examine presence and absence variation, SNP diversity within the effector families, and neutral markers (Thilliez et al., 2019). Due to the diverse nature of effector families across species, the existing baits designed for *P. infestans* and *P. capsici* were not suitable for analysis of *P. rubi* and *P. fragariae* effectors, and a new gene list for bespoke bait design has to be generated. Jupe et al. (2013) previously highlighted that biotinylated RNA baits can be utilized to enrich for target sequences with a minimum of 80 % sequence identity to the bait probes. It is therefore expected that genes highly similar to targets will also be re-sequenced.

This chapter describes the application of PenSeq to *P. rubi* and *P. fragariae*. Here, published genome information (Table 3.1) was used to develop gene lists for a bespoke bait library (Table 3.2) by targeting cytoplasmic and apoplastic effector candidate genes alongside housekeepers. Using such baits in our PenSeq study will enable the genetic variation to be studied, allowing identification of allelic diversity, mutations and revealing patterns of adaptive evolution within and between species.

Table 3. 1. List of *P. rubi* and *P. fragariae* sequenced genomes

Species	Isolate	Isolation date	Isolation country	Submitter	Year of submission	Assembly level	Genome representation	GenBank assembly accession	Sequencing technology	Total sequences length (Mb)
<i>P. fragariae</i>	NOV-9	1986	Canada	NIAB-EMR	2019	Contig	Full	GCA_009729435.1	Oxford Nanopore GridION; Illumina MiSeq	93.7
<i>P. fragariae</i>	BC-16	1992	Canada	NIAB-EMR	2019	Contig	Full	GCA_009729455.1	PacBio RSII; Illumina MiSeq	91

Species	Isolate	Isolation date	Isolation country	Submitter	Year of submission	Assembly level	Genome representation	GenBank assembly accession	Sequencing technology	Total sequences length (Mb)
<i>P. fragariae</i>	BC1	1991	Canada	NIAB-EMR	2019	Scaffold	Full	GCA_009733085.1	Illumina MiSeq	79.1
<i>P. fragariae</i>	NOV-71	1986	Canada	NIAB-EMR	2019	Scaffold	Full	GCA_009733065.1	Illumina MiSeq	78.4
<i>P. fragariae</i>	NOV-27	1986	Canada	NIAB-EMR	2019	Scaffold	Full	GCA_009732985.1	Illumina MiSeq	78.7
<i>P. fragariae</i>	NOV-77	1994	Canada	NIAB-EMR	2019	Scaffold	Full	GCA_009733125.1	Illumina MiSeq	78.8
<i>P. fragariae</i>	ONT-3	1990	Canada	NIAB-EMR	2019	Scaffold	Full	GCA_009733005.1	Illumina MiSeq	79.1
<i>P. fragariae</i>	BC-23	1992	Canada	NIAB-EMR	2019	Scaffold	Full	GCA_009733045.1	Illumina MiSeq	78.3
<i>P. fragariae</i>	A4	unknown	Canada	NIAB-EMR	2019	Scaffold	Full	GCA_009733105.1	Illumina MiSeq	79.1
<i>P. fragariae</i>	SCR245	1945	England (Kent)	NIAB-EMR	2019	Scaffold	Full	GCA_009732925.1	Illumina MiSeq	77.8
<i>P. fragariae</i>	NOV-5	1992	Canada	NIAB-EMR	2019	Scaffold	Full	GCA_009733025.1	Illumina MiSeq	79
<i>P. fragariae</i>	CBS 209.46	unknown	unknown	Oregon State University	2017	Scaffold	Full	GCA_002025845.1	Illumina	77

Species	Isolate	Isolation date	Isolation country	Submitter	Year of submission	Assembly level	Genome representation	GenBank assembly accession	Sequencing technology	Total sequences length (Mb)
<i>P. fragariae</i>	CBS 309.62	unknown	unknown	Shenzhen Entry-Exit Inspection and Quarantine Bureau	2018	Scaffold	Full	GCA_000686205.4	Illumina	76
<i>P. rubi</i>	CBS 109.892	unknown	unknown	Shenzhen Entry-Exit Inspection and Quarantine Bureau	2018	Scaffold	Full	GCA_000687305.2	Illumina	79
<i>P. rubi</i>	SCR333	1985	Scotland (Perthshire, Essendy)	NIAB-EMR	2019	Scaffold	Full	GCA_009733145.1	Illumina MiSeq	78
<i>P. rubi</i>	SCR324	1991	Scotland (Cranslea)	NIAB-EMR	2019	Scaffold	Full	GCA_009732945.1	Illumina MiSeq	78
<i>P. rubi</i>	SCR249	1985	Germany (Munich)	NIAB-EMR	2019	Scaffold	Full	GCA_009732905.1	Illumina MiSeq	77.8
<i>P. rubi</i>	SCR1202/ od101050015038			Oregon State University	2017	Scaffold	Full	GCA_002025925.1	Illumina HiSeq	75

Table 3. 2. Effector gene predictions in sequenced isolates of *P. fragariae* and *P. rubi* (Table from Adams et al., 2020)

	<i>Phytophthora fragariae</i>										<i>Phytophthora rubi</i>			
	A4	BC-1	BC-16	BC-23	NOV-5	NOV-9	NOV-27	NOV-71	NOV-77	ONT-3	SCR245	SCR249	SCR324	SCR333
Secreted proteins ^a	3,637	3,601	4,217	3,611	3,626	3,637	3,690	3,633	3,620	3,658	3,581	3,697	3,683	3,832
RxLR HMM ^b	194	194	218	188	196	186	183	191	166	191	196	197	195	207
RxLR-EER Regex ^c	178	184	208	176	186	174	172	182	150	178	185	188	176	188
RxLR Regex	371	367	445	364	370	356	369	374	341	367	370	363	350	359
Final RxLR effectors ^d	410 (935)	405 (919)	486 (1,052)	402 (928)	408 (918)	397 (951)	405 (899)	412 (931)	378 (934)	403 (898)	407 (882)	407 (882)	395 (861)	410 (826)
CRN LFLAK HMM ^e	85	83	114	86	84	82	87	90	86	90	90	156	93	154
CRN DWL HMM ^e	95	87	121	96	91	96	93	101	83	90	87	139	102	142
Final CRNs ^{d,e}	55 (68)	53 (59)	82 (87)	55 (62)	53 (67)	50 (61)	57 (63)	59 (71)	62 (75)	61 (74)	60 (68)	128 (132)	71 (85)	128 (134)
Apoplast effectors ^{d,f}	991 (3,896)	1,002 (3,798)	1,274 (4,757)	980 (3,630)	986 (3,913)	1,007 (3,983)	1,011 (3,708)	1,007 (3,911)	1,010 (3,922)	982 (3,709)	984 (3,522)	1,017 (3,266)	1,059 (3,607)	1,090 (3,268)

^aSignalP: Nielsen et al., 1997; Bendtsen et al., 2004; Petersen et al., 2011 and Phobius: Kälf et al., 2004. ^bWhisson et al. (2007). ^cArmitage et al. (2018). ^dValues in brackets include low confidence gene models from open reading frames. ^eBoth LFLAK and DWL HMM models present (Armitage et al., 2018). ^fApoplastP: Spersneider et al. (2018).

The main objectives of this chapter are to:

- Apply PenSeq to examine the diversity between species (inter-species) and between isolates (intra-species) of *P. fragariae* and *P. rubi* effectors genes, neutral markers and candidate drug targets.
- Assess the level of diversity in the species and the threat to agriculture, through presence / absence and sequence polymorphism of specific effector genes in *P. rubi* and *P. fragariae*, where other methods have failed.
- Identify core effectors, conserved amongst isolates and species.
- Identify diversifying effectors that are unique to *P. rubi* or to *P. fragariae*, which could be essential for virulence and in limiting host range.

3.2. Materials and methods

3.2.1. *P. rubi* and *P. fragariae* samples preparation

3.2.1.1. Isolate selection and preparation for Pathogen Enrichment Sequencing

A total of 24 isolates were used for Pathogen Enrichment Sequencing (PenSeq) in two runs of 12 samples each: 20 *P. rubi* and four *P. fragariae* (Table 3.3), representing a variety of years and countries of isolation as well as races. DNA was collected from the 24 isolates with a method described in Chapter 2 (2.2.1.1) and yield was assessed with a Qubit fluorometer (ThermoFisher).

Table 3. 3. Details of *P. fragariae* and *P. rubi* isolates used in this PenSeq study

Species	Isolate name	Race	Isolation date	Isolation location		PenSeq run
<i>Phytophthora fragariae</i>	BC-1	Race 1 (CA1)	2007	Canada		1
	BC-16	Race 2 (CA3)	2007	Canada		1
	NOV-9	Race 3 (CA2)	2007	Canada		1
	SCR245	unknown	1945	England		1
<i>Phytophthora rubi</i>	SCR1202	unknown	2010	The Netherlands		1
	SCR1207	unknown	2017	Scotland	Farm A, Perthshire	2
	SCR1208	unknown	2017	Scotland	Farm A, Perthshire	1
	SCR1212	unknown	2018	Scotland	Farm B, Kincardine	2
	SCR1213	unknown	2018	Scotland	Farm B, Kincardine	1
	SCR249	Race 1	1985	Germany		1
	SCR250	unknown	1985	Scotland	Farm C, Perthshire	2
	SCR260	unknown	1986	England		2
	SCR283	Race 3	1987	USA		2
	SCR287	unknown	1989	Scotland		2
	SCR288	unknown	1989	Denmark		2
	SCR290	unknown	1989	France		2
	SCR292	unknown	1989	Norway		2
	SCR293	Race 1	1991	The Netherlands		2
	SCR296	unknown	1993	Scotland	Farm A, Perthshire	1
	SCR323	Race 1	1991	Scotland	Farm D, Perthshire	2
	SCR324	Race 1	1991	Scotland	Farm D, Perthshire	1
	SCR333	Race 3	1985	Scotland	Farm C, Perthshire	1
	SCR338	Race 3	1987	Canada		2
	SCR339	Race 3	1985	France		1

3.2.1.2. Sequenced reference genomes of *P. rubi* and *P. fragariae*

Reference genomes for PenSeq analysis were provided by Adams T. (Adams, 2019). SCR333 constituted the reference genome for *P. rubi* (GenBank accession GCA_009733145.1) and BC-16 was the reference genome for *P. fragariae* (GenBank accession GCA_009729455.1) (Table 3.1).

3.2.2. Designing the bait library

A biotinylated RNA bait library was designed with nucleotide sequences for *P. rubi* and *P. fragariae* genes of interest (Tables 3.4 and 3.5). It included RXLR, CRN and apoplastic effectors, predicted from the genomes of eleven different *P. fragariae* isolates (A4, BC-1, BC-16, BC-23, NOV-5, NOV-9, NOV-27, NOV-71, NOV-77 and ONT3) and three *P. rubi* isolates (SCR249, SCR324 and SCR333) (Adams, 2019). RXLRs were originally predicted by Adams (2019) using three models: the RXLR HMM model by Whisson et al. (2007), and the RXLR and RXLR- EER Regex models by Armitage et al. (2018). CRNs list comprise of CRNs predicted by Adams (2019) with both the CRN LFLAK HMM and the CRN DWL HMM models by Armitage et al. (2018). Finally, apoplastic effectors were predicted using ApoplastP (Sperschneider et al., 2018). In addition, known drug target and housekeeping genes were also included in the bait library compiling data from NIAB-EMR, NCBI BLAST searches and various publications (loos et al., 2006; Schena et al., 2007; Blair et al., 2008; Peters and Woodhall, 2014) and was purposefully inclusive. The resulting list of gene sequences was sent to Arbor Biosciences for bait design and library production: more than 185,732 sequences, covering a gene space of approximately 5 million nucleotides per isolate were provided for bait design, which produced 50,234 baits.

Table 3. 4. Total numbers and types of genes incorporated into the input for bait library design.

The biotinylated RNA bait library was designed with nucleotide sequences for *P. rubi* and *P. fragariae* RXLR, CRN and apoplastic effectors, predicted from the genomes of eleven different *P. fragariae* isolates (A4, BC-1, BC-16, BC-23, NOV-5, NOV-9, NOV-27, NOV-71, NOV-77 and ONT3) and three *P. rubi* isolates (SCR249, SCR324 and SCR333) (Adams, 2019)

Bait type	<i>P. fragariae</i>	<i>P. rubi</i>	Total
Apoplastic effectors	119948	32026	151974
RXLR effectors	25389	6752	32141
CRN effectors	1181	404	1585
Known drug target and housekeeping genes	9	9	18

Table 3. 5. Housekeeping, drug target and pathogenic genes incorporated into the input for bait library design. Genes sequences were obtained from the following papers and partners, either directly for *P. rubi* and *P. fragariae* or via BLAST searches from other *Phytophthora* spp. (such as *P. sojae*): ¹ NIAB-EMR files, ² Blair et al., 2008, ³ Schena et al., 2007, ⁴ loos et al., 2006, ⁵ Peters and Woodhall, AHDB SF130, 2014

Genes names	Genes
<i>RPABC27/Rpb5</i>	large subunit of RNA polymerase I RPABC27 ¹
<i>RPABC23/Rpb6</i>	large subunit of RNA polymerase I RPABC23 ¹
<i>CesA2</i>	cellulose synthase A2 ¹
<i>Bgx1</i>	betaglucosidase ¹
<i>Mft</i>	major facilitator transporter ¹
<i>tigA</i>	glyceraldehyde-3-phosphate dehydrogenase (G3PDH) ²
<i>60S_L10</i>	60S ribosomal protein L10 ²
<i>28S.1</i>	28S ribosomal DNA ²
<i>Btub</i>	betatubulin ²
<i>Ef1α</i>	elongation factor 1 alpha ²
<i>Enl</i>	enolase ²
<i>Hsp90</i>	heat shock protein 90 ²
<i>Ypt1</i>	ras-like ypt1 ^{3,4}
<i>CoxI</i>	Mitochondrial cytochrome oxidase I ⁵
<i>Asf1A</i>	antisilencing factor ⁴
<i>Gpa1</i>	G-protein alpha 1 ⁴
<i>Trp1</i>	indole-3-glycerol-phosphate synthase N-5'-phosphoribosyl anthranilate isomerase ⁴
<i>Nadh9</i>	NADH dehydrogenase subunit 9 ¹
<i>RXLR</i>	Effectors ¹
<i>CRN</i>	
<i>Apoplactic</i>	

3.2.3. Enrichment: PenSeq Library preparation, hybridization and sequencing

For each PenSeq run, 500 ng gDNA was used per isolate. Library preparation, consisting of DNA fragmentation, indexing with adaptor-ligation and fragment size selection was performed following the NEBNext® Ultra™ II FS DNA library Prep Kit (NEB, Ipswich) protocol. AMPure XP purification beads (Beckman Coulter) were used multiple times during the protocol at a 1:0.8 ratio of beads-to-sample to eliminate fragments smaller than ~ 300 bp. After library preparation, each DNA sample was quantified using a Qubit Fluorometer (Thermo Fisher Scientific). Equimolar amounts of DNA from the 12 indexed libraries were combined to achieve 750 ng of total material. Hybridization and target enrichment were carried out with the Total SureSelectXT Target Enrichment System protocol from Agilent Technologies using

the myBaits buffer from Arbor Biosciences. Post-capture amplification was performed with Herculase II polymerase (Agilent Technologies). Enriched samples were sequenced using Illumina MiSeq at The James Hutton Institute using the v.2 reagent kit and 2 x 250 bp conditions.

3.2.4. Computational analyses

3.2.4.1. Preparation of reads prior to analysis

Raw reads resulting from PenSeq were filtered using FastP (Chen et al., 2018) to a minimum length of 100 bp with a minimum quality score of 20 (> 99% certainty) using settings anticipating 3' anchored adapters and overlapping reads correction based on quality score. Filtering resulted in a total of 29,421,901 filtered reads, corresponding to an average of 1,225,913 reads per isolate; and the average read length was 225 bp.

3.2.4.2. Mapping and cross-species mapping of reads to reference genomes

The filtered reads were mapped to reference genomes (FASTA files) sequenced by NIAB-EMR: *P. fragariae* BC-16 (GCA_009729455.1) and *P. rubi* SCRP333 (GCA_009733145.1) (Table 3.1) using Bowtie2 (Langmead and Salzberg, 2012) v.2.2.1 at 0 %, 3 % and 5 % mismatch mapping rates (here referred to as 0 %, 3 % and 5 % “mm”) for each isolate. Same species mapping mapped reads from one species to the corresponding species reference genome (*P. rubi* reads mapped to SCRP333 and *P. fragariae* reads mapped to BC-16); while cross-species mapping used reads from one species mapped to the other species reference genome (*P. rubi* reads mapped to BC-16 and *P. fragariae* reads mapped to SCRP333). The resulting bam alignments were sorted and indexed using samtools v1.3.1 (Li et al., 2009).

3.2.4.3. Preparation of reference genomes for coverage analysis: intersecting baits with reference genes

The 50,234 bait sequences containing baits for both *P. rubi* and *P. fragariae* were mapped to the reference genomes (FASTA files) using Bowtie2 and samtools at 0 % mismatch mapping rate (mm), similarly to 3.2.4.2. This provided a list of genes (and genes ID) for which at least one bait mapped to. The newly created bed files were used for coverage analyses (see 3.2.4.5).

3.2.4.4. Function identification for gene of interest

Proteins obtained from NIAB-EMR had been previously annotated as RXLR, CRN or apoplastic effectors (Adams, 2019). However, we checked RXLR predictions by running all effector proteins used for baits through the Galaxy platform (Cock et al., 2013) using both the strict Whisson et al. (2007) and the more relaxed Win et al. (2007) RXLR prediction models.

3.2.4.5. Coverage analysis for genes of interest

Mapping of baits to the reference genomes resulted in bed files compiling a list of genes that were targeted for enrichment where at least one bait mapped to. Using these conditions, 14,958 genes for *P. fragariae* BC-16 and 14,295 genes for *P. rubi* SCRP333 were targeted. These bed files of enriched genes were used as references for coverage analyses. Coverage of the enriched genes (bed files), was calculated at each mismatch mapping rate (0 %, 3 % and 5 %) for each isolate using Bedtools coverage v. 2.25.0 (Quinlan and Hall, 2010). Coverage graphs were plotted with R Studio v1.1.383. Overall coverage graphs were plotted to give the number of genes and the proportion covered for all genes and per isolate. Coverage graphs for particular genes of interest were plotted to give the read depth (log10 transformed) and the corresponding position (bp) for each gene. Such representations enable quick and easy identification of potential SNPs and gaps compared to the reference sequence for several isolates of one species. Coverage tables were created with the coverage info for each enriched gene, each isolate and at each mismatch mapping rate; and given a colour code based on the proportion covered (Table 3.6).

Table 3. 6. Colour code used for coverage tables

% coverage	colour code
0	grey
0-10	dark grey
10-20	red
20-30	orange-red
30-40	orange
40-50	yellow-orange
50-60	yellow
60-70	light green
70-80	green
80-90	light blue
90-100	blue
100	dark blue

3.2.4.6. *Heterozygous Single Nucleotide Polymorphism (SNP) analysis*

While coverage graphs for specific genes can indicate heterozygous version of SNPs with a lower number of reads at 0 % mm compared to 3 % mm, heterozygous SNP calling was performed to assess true heterozygous SNPs (~ 50 % occurrence) over all genes screened. Overall heterozygous SNP calling (here referred to as HeSNP) was performed using the filtered reads and VarScan.v2.3.7 with a frequency of SNP between 40 % and 60 % for a minimum of 30 reads.

3.2.4.7. *Inter- and intra-species diversity: presence / absence analyses*

Potential SNPs and sequence diversity for specific genes of interest were identified using the 0 % mismatch mapping rate coverage tables and graphs, where a coverage under 100 % would indicate possible SNPs compared to the reference genome used for mapping. For those polymorphic genes, sequences were retrieved with samtools from the 3 % mismatch mapping rate files and translated into amino acid from the start codon with Geneious v2020.2.1 translation tool, to investigate whether SNPs resulted in changes in the amino acid sequences. Nucleotide and protein alignments were made using Clustal alignment in Geneious v2020.2.1.

Absence of genes was identified by screening for genes showing 0 % coverage at the highest mismatch mapping rate (5 %). Genes identified as absent in specific isolates were discarded (not considered truly absent) if heterozygous versions were found using heterozygous SNP calling.

3.2.4.8. *General effector diversity: k-mer analysis*

K-mer analysis was performed by Dr Paolo Ribeca. PenSeq reads were filtered by mapping them against the different gene sets obtained for the baits library: apoplastic genes, CRN and RXLR. Reads were used for k-mer generation using 25 nucleotide length and mapped to the gene sets with the GEM mapper (Marco-Sola et al., 2012) with a 8 % mismatch mapping rate and fast mapping mode selected. Paired-end reads were kept when at least three portions of 25 nucleotides from the pair mapped to the gene set. The resulting read files were then processed to deduce k-mer counts and de-duplicate palindromic k-mers (where complementary sequences read the same in both directions). K=12 was selected after studying cluster convergence as a function of k. K-mer counts were normalised and subjected to Correspondence Analysis (Greenacre, 2016).

3.2.5. Validation of observations made through PenSeq

Presence / absence of genes of interest in specific isolates was verified through conventional PCR, while specific nucleotide sequences and SNPs observed from PenSeq data were confirmed through sequencing.

3.2.5.1. Conventional PCR for PenSeq validation

For general PCR amplification, a Taq polymerase (obtained from Dr Hazel McLellan, JHI) was used with 10x PCR buffer (100nM MgCl₂, 1M KCl, 1M Tris-HCl and 0.1% gelatin) and 2.5mM dNTP mix (New England Biolabs). Primers for genes of interest were designed with Primer3 and secondary structures were checked using NetPrimer. Primers were ordered from Eurofins Genomics (Germany). For genes showing polymorphism, conserved regions were identified using the nucleotide sequences alignment in Geneious. Primers were first tested *in silico* with the Geneious primer testing function on the gene of interest and on reference genomes (Table 3.7).

Table 3. 7. Primers designed for a subset of *P. fragariae* and *P. rubi* genes of interest

Species	Gene of Interest	Primers names	Primers sequences 5'-3'	Amplicon (bp)	Selection criteria
<i>P. rubi</i>	g19167 (PF003_g21231)	Pr_g19167_491F	TAACCACACCCGCATACCAC C	141	<i>P. fragariae</i> RXLR effectors expressed in planta at all time points screened (24, 48, 72 and 96 hpi) for infection assays using isolates BC-1, BC-16 and NOV-9
		Pr_g19167_631R	AGAAGGACGGAAAAGGGCT G		
<i>P. fragariae</i> & <i>P. rubi</i>	BC-16_contig_51_F623 (PF003_g26871)	PrPf_F623_1F	ATGATCTGGCTGCACAGTC C	186	<i>P. rubi</i> RXLR effectors showing interesting inter / intra-species diversity patterns
		PrPf_F623_186R	TCAAGGGCTGGCAGAAATC G		
<i>P. rubi</i>	SCR333_contig_4275_F7 (PR003_g28352)	Pr_4275F7_F	CCTTGGCTACGCTCCTATCA	188	
		Pr_4275F7_R	TCGCTCTTCATCGATGCTAT T		
<i>P. rubi</i>	SCR333_g28651 (PR003_g30919)	Pr_g28651_F	CATGCACAGCGACCAAGAC	111	Apoplastic effectors retrieved for <i>P. rubi</i>
		Pr_g28651_R	GTTTCTCCTCCGCCTGTTC		
<i>P. fragariae</i>	BC-16_contig_	Pf_F2468_1F	ATGAGCTCTGCTGCTTCCG	165	<i>P. fragariae</i> RXLR and apoplastic effectors

Species	Gene of Interest	Primers names	Primers sequences 5'-3'	Amplicon (bp)	Selection criteria
	38_F2468 (PF003_g2 2679)	Pf_F2468_165R	CTATGGGTGCTTGGTGTAT GAAC		showing interesting inter / intra-species diversity patterns
<i>P. fragariae</i>	BC-16_g2112 (PF003_g2 353)	Pf_g2112_F	GGAATCCGTGACGATCAAG A	210	
		Pf_g2112_R	CGTAGCAACTTCTCCATAAC CT		

Conventional PCR assays were usually carried in 25 μ L reaction with 5 μ L of 10x buffer, 4 μ L of 2.5mM dNTPs, 2 μ L of each primer at 10 μ M, 0.8 μ L of Taq polymerase and 10.2 μ L of purified DNase-free water. For sequencing, PCR assays used 50 μ L reactions. The PCR programme consisted of 4 mins at 92 °C, followed by 35 cycles of 30 seconds at 92 °C, 30 seconds at 56 °C, 15 seconds at 72 °C; and a final extension of 10 mins at 10 °C. Agarose gel electrophoreses (2 % agarose) were used to visualise PCR amplicons and run at 80 V for 50 mins. The oomycete *CoxI* gene was used as a positive DNA control and sterile distilled water (SDW) was used as negative control for the PCR.

3.2.5.2. Sequencing of PCR products for nucleotide sequence and SNP confirmation

Following successful PCR amplification, 50 μ L of PCR reactions were purified using the QIAGEN Mini-Elute™ PCR Purification kit. A gel extraction was carried out when gel electrophoresis showed multiple bands, using the NucleoSpin™ Gel and PCR clean up (Macherey-Nagel™). Purified and extracted products were assessed on a NanoDrop (NanoDrop 1000 Thermo Fisher Scientific, UK) and dilutions were made to adjust concentrations to 3 ng / μ L of DNA in nuclease-free water, before being Sanger sequenced (The James Hutton Institute). For *CoxI* sequencing, protocol was carried out as described in Chapter 2 (2.2.1.1).

3.3. Results

An inclusive list of predicted RXLR, CRN and apoplastic effectors, candidate drug targets and housekeeping genes was generated from *P. fragariae* and *P. rubi* genome information provided by NIAB-EMR ahead of publication (Adams et al., 2019). The

customised RNA bait library was designed and produced by Arbor Biosciences. Target enrichment of selected genes was conducted in two runs of 12 individually ‘barcoded’ gDNA samples from 20 *P. rubi* and 4 *P. fragariae* isolates (Table 3.3) under the supervision of Dr Miles Armstrong. Post-enrichment sequencing was performed in house. Raw reads were filtered and mapped at three different mismatch rates (0, 3 and 5%) to *P. rubi* SCRP333 and *P. fragariae* BC-16 reference isolates. Coverage of ~ 15,000 baited genes for each species was assessed.

3.3.1. Mapping and coverage analyses

3.3.1.1. RXLR gene predictions

Predictions of *P. rubi* RXLR genes (using reference isolate SCRP333) identified 177 genes predicted to encode for RXLRs using the Whisson et al. (2007) model and 380 predicted RXLRs with the Win et al., 2007 model from the 14,295 baited genes. Similarly, 182 *P. fragariae* genes were predicted to be RXLRs using Whisson et al. (2007) model and 547 with the Win et al. (2007) model from the 14,958 baited genes (using the reference isolate BC-16). However, since target enrichment allows for sequence variation, with an 80 % sequence similarity to RNA baits, a higher number of genes were retrieved and mapped to reference genomes, allowing the identification of additional RXLR variants, not previously annotated.

3.3.1.2. Same-species mapping and coverage for intra-species analyses

Examination of the average mapping proportions to the same-species reference genome is an essential first step in our data analysis pipeline and a tool to estimate the overall diversity within the target sequences versus the reference genomes. In general, less polymorphism leads to more reads mapped to the reference. Here, filtered reads from each isolate were mapped to reference genomes *P. fragariae* BC-16 and *P. rubi* SCRP333 using Bowtie2 at 0 %, 3 % and 5 % mismatch mapping rates. The resulting alignments were sorted and indexed.

For *P. rubi*, the average ‘on target’ mapping rate of reads back to the reference genome (SCRP333) when no polymorphism was allowed (0 % mm) was 59.5 % (Table 3.8 and Appendix B, Table B.1).

Table 3. 8. Average mapping of reads at several Bowtie mismatch mapping rates. Averages are displayed for *P. rubi* and *P. fragariae* mapped to same-species reference genomes at 0 %, 3 % and 5 % mismatch mapping rates.

Species	Reference mapped to	Average mapping percentages		
		Bowtie mismatch mapping rate		
		0%mm	3%mm	5%mm
<i>P. rubi</i>	SCR333	59.5	90.0	92.2
<i>P. fragariae</i>	BC-16	74.4	91.7	92.5

The average mapping for the *P. fragariae* isolates at 0 % mm was 74.4 % (Table 3.8). This higher percentage is due to lower diversity within target sequences from four *P. fragariae* isolates (although of three different races) being compared to the diversity within target sequences from 20 *P. rubi* isolates (from a range of geographical backgrounds). The influence of isolate sample number on strict average mapping proportions was also seen in Thilliez et al., (2019).

The less stringent 3 % mismatch mapping rate allows inclusion of genes with up to 3 SNPs per 100 bp compared to the reference sequence. *P. fragariae* isolates mapped on average at 91.7 % and *P. rubi* at 90 % under these conditions, which indicates highly efficient targeted sequencing. This revealed that at 3 % mismatch rate the bias caused by isolate sample number was lost. Decreasing the read mapping stringency again, to 5 % mm, made little difference to the average mapping of reads to the references, with 92.2 % for *P. rubi* and 92.5 % for *P. fragariae* (Table 3.8). We conclude that the number of isolates examined within a single species is likely to bias the average mismatch rate at 0 % mm for smaller sample sets but that at 3 % mismatch rate or above this difference plateaued out.

The read coverage is determined by the percentage of nucleotides covered by mapped reads on the total number of nucleotides per gene, for the enriched genes. This was calculated at each mismatch mapping rate for each isolate and coverage graphs were plotted with R Studio using the scripts developed by Thilliez et al., (2019) and with the help of Dr Miles Armstrong. Overall coverage graphs of all selected genes were plotted per isolate at 0 %, 3 % and 5 % mm, following same-species mapping (Appendix B, Figures B.1 and B.2 and Table B.2). This gives an indication of the number of genes and the proportion covered for all genes and per isolate. Most genes showed a coverage between 97.5 % and 100 % (Appendix B, Figures B.1 and B.2 and

Table B.2), as exemplified with *P. fragariae* isolate BC-1 and *P. rubi* isolate SCR1208 (Figures 3.1 and 3.2).

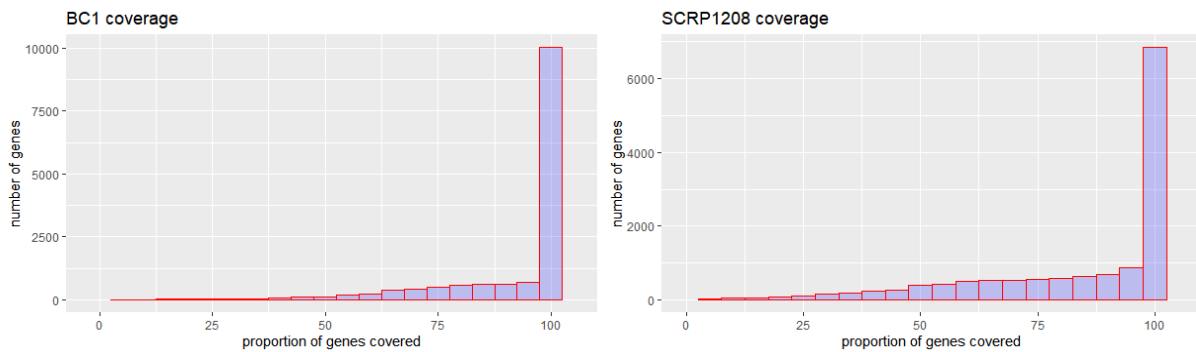
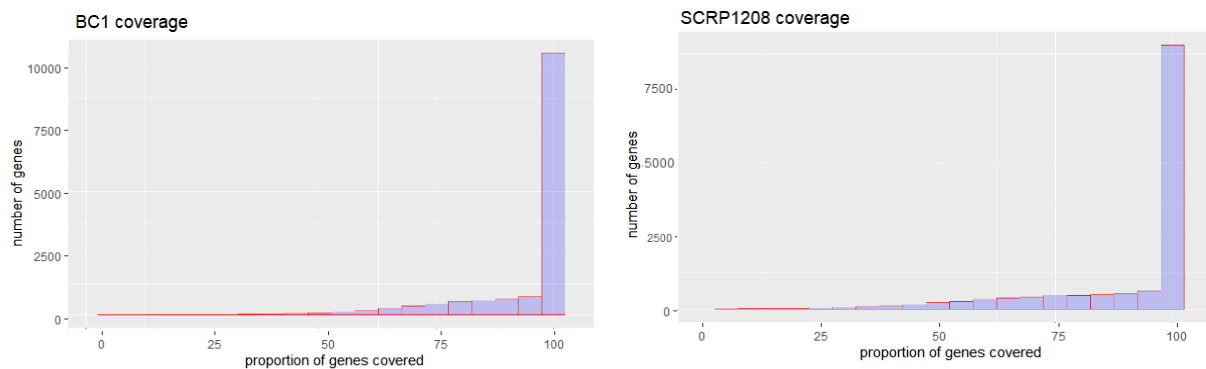


Figure 3. 1. Example of overall coverage graphs from 0 % mismatch mapping. Coverage graphs for *P. fragariae* isolate BC-1 (left) *P. rubi* isolate SCR1208 (right) from mapping at 0 % mismatch mapping rate. Number of genes covered are represented on the y-axis and proportion of gene covered (in percentage) is represented on the x-axis. Coverage graphs were plotted with R Studio



v1.1.383.

Figure 3. 2. Example of overall coverage graphs from 3 % mismatch mapping. Coverage graphs for *P. fragariae* isolate BC-1 (left) *P. rubi* isolate SCR1208 (right) from mapping at 3 % mismatch mapping rate. Number of genes covered are represented on the y-axis and proportion of gene covered (in percentage) is represented on the x-axis. Coverage graphs were plotted with R Studio v1.1.383.

For *P. fragariae*, an average of 160 genes per isolate were not covered (0 % coverage at 5 % mm), including an average of 129 apoplastic genes and 7 RXLR (Win et al., 2007), and thus 14,798 genes were on average partially or fully covered. For *P. rubi*, an average of 108 genes per isolate were not represented (0 % coverage at 5 % mm), including 85 apoplastic and 2 RXLR (Win et al., 2007) effectors, with on average 14,187 genes represented with partial or full coverage. This lack of representation of genes at a high mismatch mapping rate suggests that PenSeq reveals presence / absence variation in these isolates; while the partial coverage is indicative of sequence polymorphisms.

Coverage graphs for particular genes of interest were plotted to give the read depth (log₁₀ transformed) and the position (bp). This allowed the read coverage to be examined to determine the presence and position in the target sequence of potential SNPs, gaps and regions of low coverage, compared to reference genome sequences. These graphs are presented for all isolates and per gene of interest (see 3.3.2). Coverage tables grouping the gene proportion covered per gene, per isolate and at each mismatch mapping rate were generated.

3.3.1.3. Cross-species mapping and coverage for inter-species analyses

The cross-species analysis in this study used reads from the 20 *P. rubi* isolates mapped to the *P. fragariae* reference genome, and *vice versa* (see 3.2.4.2), informing us on the inter-species diversity. If the two species share similar genes, the corresponding reads should map to the other species reference genome, with or without SNPs, determined by using different mismatch mapping rates. On the other hand, if at the highest mismatch mapping rate, no reads are mapped for any of the isolate of one species to the reference genome of the other, it could indicate species-specific genes. As before, percentage of reads mapped at 0 %, 3 % and 5 % mm were calculated (Table 3.9 and Appendix B, Table B.3).

Table 3. 9. Average mapping of reads at several Bowtie mismatch mapping rates. Averages are displayed for *P. rubi* and *P. fragariae* mapped to the other species reference genomes at 0 %, 3 % and 5 % mismatch mapping rates.

Species	Reference mapped to	Average mapping percentages		
		Bowtie mismatch mapping rate		
		0%	3%	5%
<i>P. rubi</i>	BC-16	15.5	70.6	78.1
<i>P. fragariae</i>	SCR333	16.1	70.5	78.7

When all *P. rubi* PenSeq reads were mapped to the *P. fragariae* reference genome, 15.5 % was successfully mapped at 0 % mismatch and the ratio went up to 70.6 % and 78.1 % when using 3 % and 5 % mm respectively. Percentages were similar when *P. fragariae* reads were mapped to *P. rubi* (Table 3.9). Those percentages are consistently much lower than those from the same species mapping, with 59.5 % of reads mapped for *P. rubi* and 74.4 % for *P. fragariae* at 0 % mismatch rate, thus emphasizing the distinction between the two species.

Coverage for each of the 24 isolates at each mismatch mapping rate was calculated and plotted as described in 3.2.4.5 (Figures 3.3 and 3.4 and Appendix B, Figures B.3 and B.4 and Table B.4).

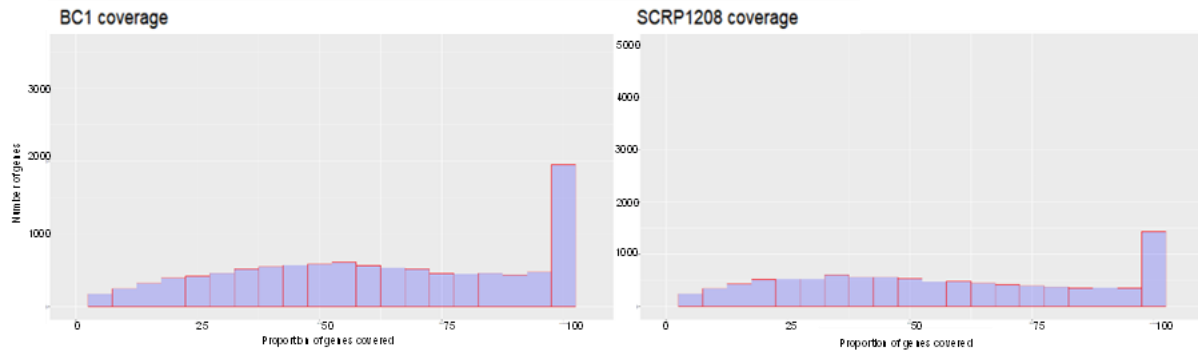


Figure 3.3. Example of overall coverage graphs from 0 % mismatch cross-mapping. Coverage graphs for *P. fragariae* isolate BC-1 (left) *P. rubi* isolate SCRP1208 (right) from cross-mapping at 0 % mismatch mapping rate. Number of genes covered are represented on the y-axis and proportion of gene covered (in percentage) is represented on the x-axis. Coverage graphs were plotted with R Studio v1.1.383.

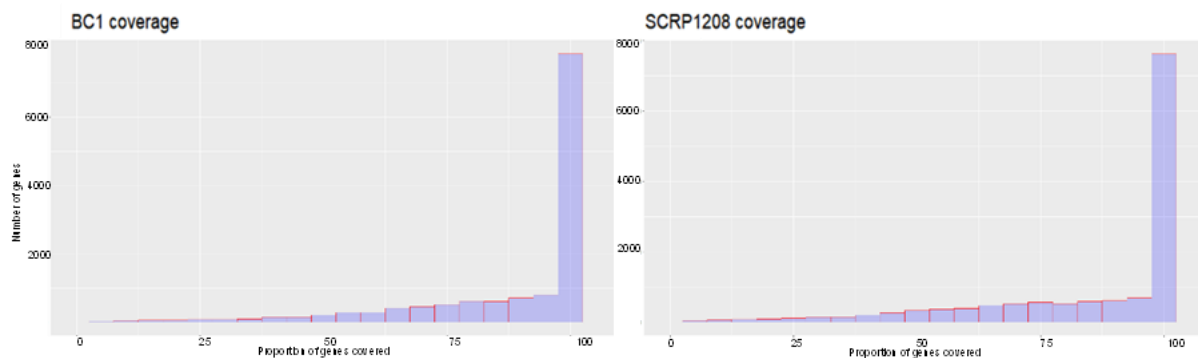


Figure 3.4. Example of overall coverage graphs from 3 % mismatch cross-mapping. Coverage graphs for *P. fragariae* isolate BC-1 (left) *P. rubi* isolate SCRP1208 (right) from cross-mapping at 3 % mismatch mapping rate. Number of genes covered are represented on the y-axis and proportion of gene covered (in percentage) is represented on the x-axis. Coverage graphs were plotted with R Studio v1.1.383.

For *P. fragariae* reads mapped to *P. rubi*, an average of 602 genes per isolate were not covered at 5 % mismatch mapping rate, including a number of predicted genes: 417 apoplastic genes, 6 CRNs and 25 RXLRs; while the rest of the genes (on average 13,693 *P. rubi* genes) were at least partially covered. For *P. rubi* mapped to *P. fragariae*, an average of 594 genes per isolate were not represented at 5 % mm, which included 375 predicted apoplastic, 7 predicted CRN and 47 predicted RXLR genes; with 14,364 genes represented with partial or full coverage.

3.3.2. Non-effector genes: housekeeping and drug target genes

Non-effector genes such as housekeeping or drug target were assessed in all isolates. Diversity between species (inter-species) and between isolates (intra-species) in the nucleotide and protein sequences were evaluated. We hypothesize that although SNPs might be found between isolates in non-effector genes, the inter-species diversity will be higher, identifying candidate genes presenting highly polymorphic regions for future diagnostic tools.

3.3.2.1. *PenSeq* labelled *CoxI* species-specific SNPs were confirmed with PCR and sequencing

CoxI gene is commonly utilised to distinguish oomycetes at the species level, including *P. rubi* and *P. fragariae*. The ability of *PenSeq* to successfully identify *CoxI* SNPs between isolates was examined.

CoxI sequences were extracted from *PenSeq* reads, mapped to reference genomes for each species at 3 % mm, and aligned. A total of 22 species-specific SNPs were identified within those *PenSeq* sequences (Table 3.10). To confirm the *PenSeq* SNPs, the *CoxI* gene was amplified through PCR and sequenced on a subset of eight isolates: NOV-9, SCRP245, SCRP1202, SCRP1208, SCRP1213, SCRP324, SCRP333 and SCRP339, for which SNPs would be present. The cleaned nucleotide consensus sequences obtained were aligned with the *PenSeq* sequences. The overlapping region, representing a part of the *CoxI* gene, presented six species-specific SNPs, in that they are similar in all isolates of one species but different to the other (Figure 3.5). Those six species-specific SNPs were present and identical between *PenSeq*-obtained sequences and sequencing-obtained sequences (Figure 3.5), emphasizing the reliability of the *PenSeq* method to identify real SNPs.

3.6). Genes showing absence of reads mapped to the other species genome, displayed in absence of coverage or “troughs”, from both cross-mapping analyses (*P. rubi* to *P. fragariae* and vice versa) were selected as highly diversified between the two sister species. Nucleotide sequences for the 24 isolates were aligned.

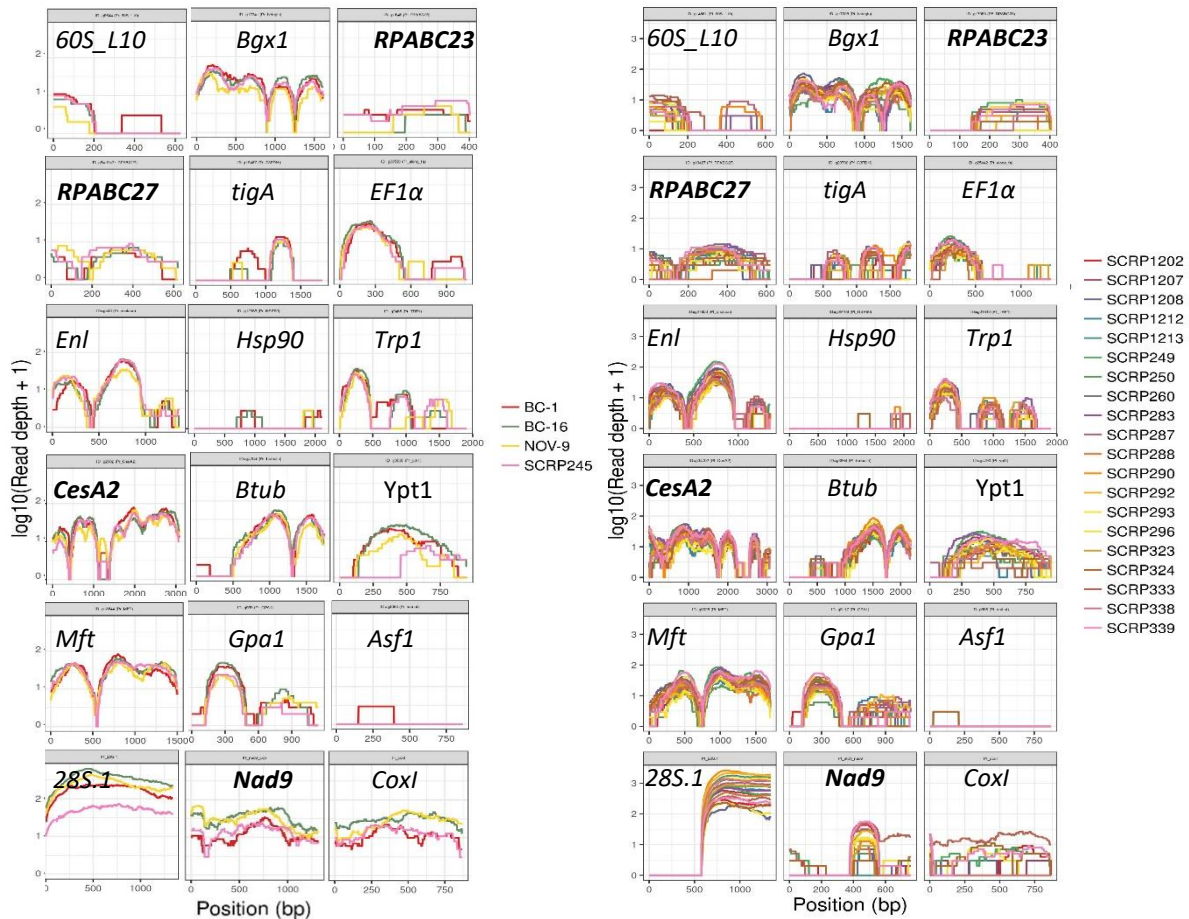


Figure 3. 6. Coverage for housekeeping / drug target genes at 0 % mm from cross-species mapping. Coverage graph at 0 % mm for housekeeping and drug target genes (bold) described in Table 3.5 for *P. fragariae* isolates (left) mapped to *P. rubi* genome and *P. rubi* isolates (right) mapped to *P. fragariae* genome at 0 % mismatch mapping rate.

Seven housekeeping genes were thus selected for high polymorphism: *tigA* (glyceraldehyde-3-phosphate dehydrogenase), *Cox1*, *Bgx1* (betaglucosidase), *Hsp90* (heat shock protein 90), *Gpa1* (G-protein alpha), *Mft* (major facilitator transporter), *60S_L10* (60S ribosomal protein L10) and *Asf1A* (anti-silencing factor) (Table 3.10).

Table 3. 10. (Overleaf) Inter-species polymorphism for housekeeping / drug target genes. Single Nucleotide Polymorphism and Amino Acid changes between *P. fragariae* and *P. rubi*.

Gene name	Nucleotide			
	Position	<i>P. rubi</i>	<i>P. fragariae</i>	
Cytochrome oxidase I (<i>CoxI</i>)	12	C	A	
	43	G	A	
	79	T	C	
	90	C	G	
	96	G	A	
	99	A	T	
	159	C	T	
	162	G	T	
	168	G	A	
	174	T	A	
	213	T	C	
	265	G	T	
	286	G	A	
	360	T	C	
	393	A	G	
	462	G	A	
	516	G	A	
	618	C	T	
	651	T	C	
	681	A	G	
	759	T	C	
	798	T	A	
	G-protein alpha 1 (<i>Gpa1</i>)	39	G	A
		115	C	T
		494	G	T
		554	C	T
		124	A	G
	Glyceraldehyde-3-phosphate dehydrogenase (<i>tigA</i>)	201	G	A
370		T	G	
786		C	T	
925		G	T	
1485		G	A	
1503		T	C	
1513		A	G	
1518		C	T	
1557		G	C	
1563		T	C	
1566		C	T	
1569		T	C	
1570		A	G	
1571		G	A	
1572		C	G	
1575		T	C	
1578		C	T	
1581		T	C	
1584		C	T	
Heat shock protein 90 (<i>Hsp90</i>)		144	C	T
	294	G	C	
	417	C	G	
	570	C	G	
	642	T	G	
	708	C	G	
	732	C	T	
	837	T	C	
	936	C	T	
	1014	C	G	
	1017	G	C	
	1104	T	G	
	1221	T	C	
	1301	C	G	
	1328	T	A	
	1398	C	G	
	1452	C	T	
	1458	T	C	
	1509	T	C	
	Major facilitator transporter (<i>Mft</i>)	88	T	A
104		A	T	
161		C	T	
179		T	C	
188		A	G	
197		T	C	
231		A	C	
60S ribosomal protein L10 (60S_L10)	216	T	C	
	230	C	T	
	333	G	A	
	336	A	G	
	582	A	C	
Antisilencing factor (<i>Asf1A</i>)	30	C	G	
	108	T	C	
	115	A	T	
	116	C	/	
	126	C	T	
	129	C	A	
	148-158	Gap		
	185	T	C	
	258	A	G	
	354	T	C	
	360	T	G	
	504	G	C	
	564	C	G	
	594	G	A	
	612	T	C	
	648	T	C	
	672	T	C	
	693	C	A	
	747	C	G	
	765	C	T	
	777	C	G	
	792	G	A	
	795	T	C	
798	C	T		

This revealed diversity at the genome level between the two species on non-effector genes, with non-synonymous polymorphisms detected. A total of 66 SNPs were detected in those five genes, of which 15 led to non-synonymous amino acid change. *CoxI*, *tigA* and *Hsp90* showed the highest number of species-specific SNPs: 22, 20 and 19 respectively. Housekeeping genes showing several consecutive SNPs could be candidate for species distinction diagnosis tools such as field PCR, using appropriately designed primers. For instance, the *tigA* gene shows a total of 11 SNPs between position 1,557 and 1,584 of the gene (i.e. over 28 bp), while *CoxI* displays four SNPs between nucleotide 159 and 174 (16 bp).

3.3.2.3. Intra-species diversity analysis of housekeeping and drug target genes

Gene coverage of selected housekeeping and drug target genes (Table 3.5) between isolates of the same species was examined. Coverage graphs were plotted per gene for each isolate at 0 % (Figure 3.7). Genes from both sets, housekeepers and drug targets, showed typical SNP “troughs”, where coverage at 0 % mm drops: *Ypt1* (ras-like GTP-binding protein YPT1), *tigA* (glyceraldehyde-3-phosphate dehydrogenase), *TRP1* (indole-3-glycerol-phosphate synthase N-5'-phosphoribosyl anthranilate isomerase), *CesA2* (cellulose synthase A2), *nad9* (NADH dehydrogenase subunit 9) and *Hsp90* (heat shock protein 90) for *P. fragariae*; and *Bgx1* (beta-glucosidase), *Hsp90*, *tigA*, *CesA2*, *EF1 α* (elongation factor 1 alpha), *CoxI* (cytochrome oxidase I), *Gpa1* (G protein alpha 1) and *nad9* for *P. rubi* (Table 3.5).

Naturally, mitochondrial genes such as the *Nad9* and *CoxI*, yielded increased read depth (higher numbers of baited and mapped reads, with a $\log_{10}(\text{read depth}+1) > 2$) as they are highly represented compared to nuclear encoded genes (Avila-Adame et al., 2006; Martin et al., 2007; Cai and Scofield, 2020). Sequences from all isolates of *P. rubi* or *P. fragariae* were extracted, translated and aligned to examine changes.

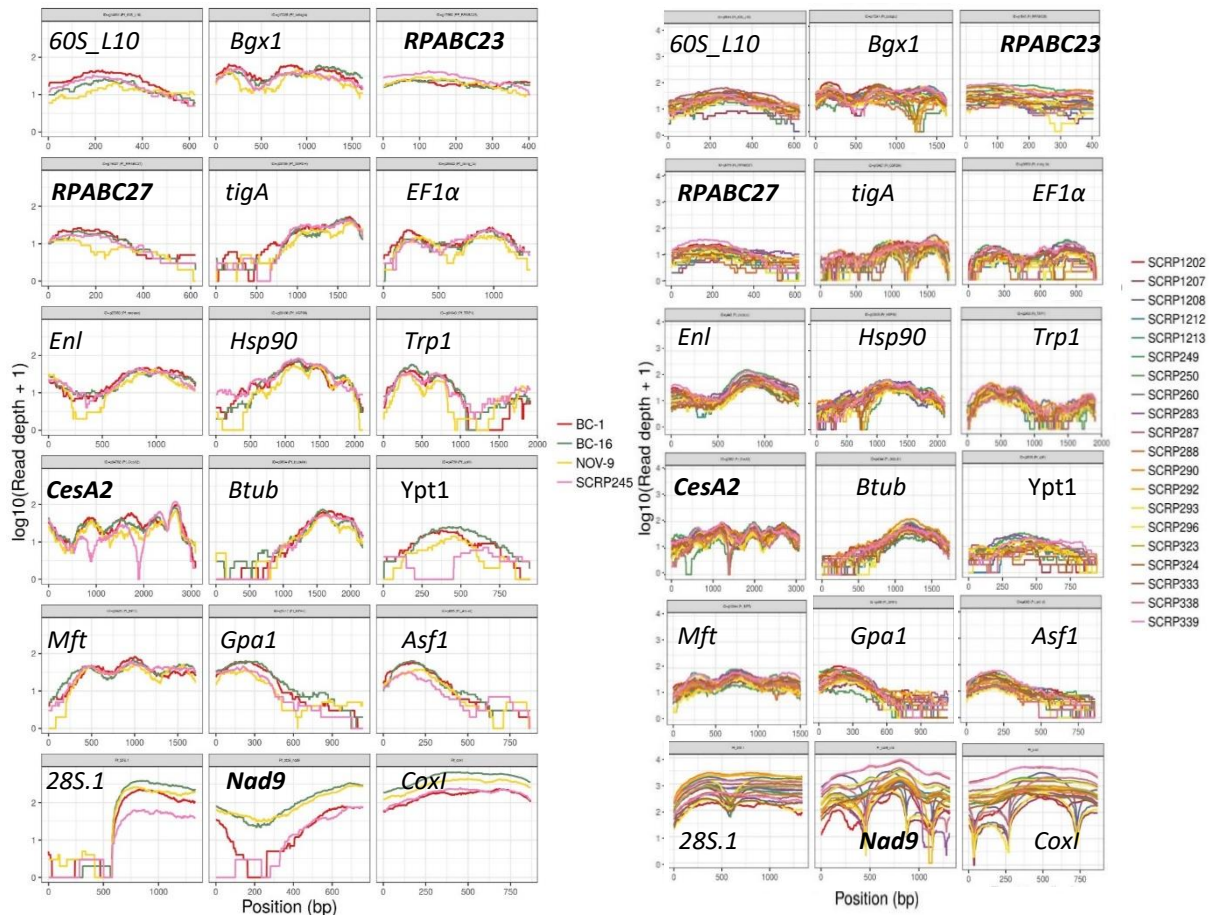


Figure 3.7. Coverage for housekeeping / drug target genes at 0 % mm. Coverage graph at 0 % mm for housekeeping and drug target genes (bold) described in Table 3.5 for *P. fragariae* isolates (left) and *P. rubi* isolates (right), when mapped against same-species genomes at 0 % mismatch mapping rate.

SNPs were confirmed for two *P. fragariae* genes, *Ypt1* and *CesA2*, and for seven *P. rubi* genes: *Bgx1*, *Hsp90*, *CesA2*, *EF1α*, *Cox1*, *Gpa1* and *Nad9* (Table 3.11). Coverage lower than 100 % for genes where the presence of SNPs was not confirmed was due to short gaps in the mapped sequences of those genes or to a lower representation (less reads mapped) of this particular portion of gene. These analyses show that around half of the identified SNPs revealed a non-synonymous change thus inducing a change at the protein level. For any of the species, the number of SNPs per gene stayed low (with a maximum of five SNPs in one gene, for *P. rubi Nad9*). On a total of 18 non-effector genes, seven showed intra-species polymorphism for *P. rubi*, with 22 SNPs in total, including 12 leading to non-synonymous amino acid change; while two genes for *P. fragariae* displayed a total of four SNPs, all of which led to a non-synonymous change.

Table 3. 11. Intra-species polymorphism for housekeeping / drug target genes Single Nucleotide Polymorphism and Amino Acid changes for **a. *P. fragariae*** and **b. *P. rubi*** housekeeping / drug target genes. Nucleotides in yellow are identical to the reference while nucleotides in blue are different from the reference sequence. Two nucleotides (e.g. G/C) indicate heterozygous SNPs, with around 50 % of the reads with each selection. Cons.: Consequence is either S for synonymous (same amino acid, in green) or NS for non-synonymous (amino acid change, in orange). “?” indicates a gap in the nucleotide sequence.

a. <i>P. fragariae</i>																										
Gene name	Nucleotide position on Geneious alignment	Amino acid	Cons.	Ref.	Alt.	<i>P. fragariae</i>																				
						BC-1	BC-16	NOV-9	SCR245																	
ras-like ypt1 (<i>Ypt1</i>)	241	I81V	NS	A	G	A	A	A	G																	
	425	G142E	NS	G	A	G	G	G	A																	
Cellulose synthase A2 (<i>CesA2</i>)	1175	T392I	NS	C	T	C	C	C	T																	
	2172	E724D	NS	G	C	G	G	G	C																	
b. <i>P. rubi</i>																										
Gene name	Nucleotide position on Geneious alignment	Amino acid	Cons.	Ref.	Alt.	<i>P. rubi</i>																				
						SCR1202	SCR1207	SCR1208	SCR1212	SCR1213	SCR249	SCR250	SCR260	SCR283	SCR287	SCR288	SCR290	SCR292	SCR293	SCR296	SCR323	SCR324	SCR333	SCR338	SCR339	
Cellulose synthase A2 (<i>CesA2</i>)	479	V160A	NS	T	C	T	T	T	T	T	T	C	T	T	T	T	T	T	T	T	T	T	T	T	T	T
	1383	V461V	S	A	G	A	A	A	A	A	A	G	A	A	A	A	A	G	A	A	G	G	A	G	A	A
Betaglucosidase (<i>Bgx1</i>)	1249	L417L	S	T	C	T	T	T	T	T	C	C	T	T	T	C	C/T	C	T	T	C	C	T	T	T	T
	33	F11F	S	C	A	C	C	C	C	C	C	C	C	C	C	C	C	C	C	C	C	C	C	A	C	C
Heat shock protein 90 (<i>Hsp90</i>)	34	S12P	NS	T	C	T	T	T	T	T	T	T	T	T	T	T	T	T	T	T	T	T	C	T	T	
	67	I23V	NS	A	G	A	G	?	A	A	A	A	A	A	A	A	A	A	A	A	A	A	A	A	A	A
	107	E36X	S	A	A/G	A/G	A	?	A	A	A	A	A	A	A	A	A	A	A	A	A	A	A	A	A	A
	142	V48I	NS	G	A	A/G	G	A/G	A/G	A/G	A/G	A/G	A/G	A/G	G	A	A	G	A	G	G	A/G	A/G	A/G	A	A
Elongation factor 1 alpha (<i>Ef1α</i>)	560	P187L	NS	C	T	C	C	C	C	C	C	T	C	C	C	C/T	C	T	C	C	T	C/T	C	C	C	C
	561		C	G	G/C	G/C	G/C	G/C	C	C	C	G/C	C	G/C	G/C	G/C	C	G	G/C	C	G/C	G/C	G/C	G/C	G/C	
	28		R10R	S	C	A	C	A	A	C	C	C	C	A	A	C	C	C	A	A	C	C	C	C	A	C
Cytochrome oxidase I (<i>CoxI</i>)	264	S88S	S	G	A	G	A	A	G	G	G	C	A	A	G	G	G	A	G	G	C	G	G	A	G	
	723	I241I	S	T	C	T	C	C	T	T	T	T	C	T	T	T	T	T	C	T	T	T	T	T	T	
	404	P135L	NS	C	T	C	T	T	C	C	C	C	T	T	C	C	C	T	T	C	C	C	C	T	C	
NAD9 NADH dehydrogenase subunit 9 (<i>Nad9</i>)	819	I273M	NS	A	G	A	G	G	A	A	A	A	G	A	A	A	A	A	G	A	A	A	A	A	A	
	985	Q329Q	S	C	T	C	C	C	C	C	C	C	T	C	C	C	C	C	C	C	C	C	C	T	C	
	1049	F350C	NS	T	G	T	T	T	T	T	T	T	T	T	T	T	T	G	T	T	T	T	T	T	T	
	1085	I362T	NS	T	C	T	C	C	T	T	T	T	C	C	T	T	T	C	C	T	T	T	T	C	T	
G-protein alpha 1 (<i>Gpa1</i>)	724	R242W	NS	C	T	C	C	C	C	C	C	C	C	C	C	C	C	C	T	C	C	C	C	C	C	
	925	W309G	NS	T	G	T	T	T	T	T	T	T	G	T	T	T	T	T	?	?	?	?	T	T	T	
	955		T	A	T	T	T	T	T	T	T	A	T	T	T	T	T	?	?	?	?	T	T	T	T	
	976	C326G	NS	T	G	T	T	T	T	T	T	T	G	T	T	T	T	T	?	?	T	T	T	T	T	

Interestingly, isolate SCRP245, the oldest and only UK *P. fragariae* isolate examined here, with unknown race designation, displayed the most SNPs for housekeeping and drug target genes when compared to the three Canadian *P. fragariae*, representatives of three different races. Many factors could influence the diversity found in SCRP245, such as country and year of isolation, host range and latent period / speed of infection, as well as environmental factors like climate or chemical pressures. Chapter 2 did not, however, find that SCRP245 behaved consistently different than all three other isolates for the temperatures and chemicals tested.

P. rubi isolates SCRP293 (collected in 1991, The Netherlands) and SCRP296 (1993, Scotland) shared the most SNPs for polymorphic housekeeping genes compared to reference SCRP333 (Scottish, 1985). This could suggest that this Scottish isolate may be connected to The Netherlands isolate.

We suppose that the analysis of effectors will offer a higher determination of the diversity of isolates than traditional housekeeping genes.

3.3.3. Intra-species studies of effector genes showed diversity amongst species

In order to find higher levels of variation with which to properly examine isolate phylogeny and diversity, more rapidly evolving gene families, such as effectors, were examined. Effectors are constantly under diversifying selection due to their virulence function inside host plants and the risk of recognition. Those with the most essential virulence function may be highly conserved amongst isolates as they are required to overcome the host defense responses and generate the next generation of oospores. On the contrary, if some host plants carry NB-LRR resistances that recognise effectors, it will lead to selection of pathogen strains that will have mutated, lost, down-regulated or suppressed recognised effectors to stay virulent. This leads to diversification of effectors sequences in isolates over time.

Consequently, to assess the diversity, if any, between isolates of the same species, presence / absence of specific effector genes was examined to identify most diverse, most conserved, and most polymorphic effector genes for each species. In addition, it was hypothesised that the PenSeq analyses of the effector gene families may highlight possible geographical, chronological or race patterns.

3.3.3.1. Diversity of effectors in *P. fragariae*

In this PenSeq study, coverage analysis identified 6,417 genes shared identically between all four *P. fragariae* isolates, showing 100 % coverage at 0 % mm, which corresponds to 43 % of the total genes screened. Of those, 50 genes were also found to possess heterozygous SNPs which were revealed at 3 % mm. Amongst those identical *P. fragariae* genes, 4,413 were predicted as apoplastic effectors (Adams, 2019), 77 as CRNs, (Adams, 2019), 344 predicted RXLRs using the relaxed Win et al. (2007) algorithm and an additional 128 predicted by the stringent Whisson et al. (2007) HMM model. This means that 64 % of the *P. fragariae* RXLR genes (including both Win et al., 2007 and Whisson et al., 2007 models) are completely identical between the four *P. fragariae* isolates, separated geographically and historically by 62 years in the field (English SCRP245, 1945 and Canadian BC-1, BC-16, NOV-9, 2007). Additionally, 70 % of the RXLR genes (Win et al., 2007 and Whisson et al., 2007 models) were identical between SCRP245 and the reference isolate BC-16. Looking at coverage at 5 % mm, 83 % of the RXLR genes showed 100 % coverage in all four *P. fragariae*, indicating polymorphism in the nucleotide sequences of those genes present in all strains. Very few genes showed no coverage for the Canadian isolates while present and divergent for SCRP245.

Coverage analysis of effectors discovered *P. fragariae* isolate-unique genes (Table 3.12), as well as genes uniquely absent in isolates, while fully covered and identical in all others. The oldest UK *P. fragariae* isolate SCRP245 displayed the most diversity, though only four *P. fragariae* isolates were compared. In total, 23 genes showed no coverage at 5 % mm in SCRP245, while the same genes were shared and identical in the three Canadian *P. fragariae* isolates. This suggests that the more recent Canadian isolates have gained effectors or that SCRP245 has very diverse variant genes. Only one RXLR gene (Win et al., 2007) was identified as one of the genes absent in SCRP245, and the remaining genes were predicted apoplastic effectors. In comparison, only three and nine genes respectively for BC-1 and BC-16, were absent (at 5 % mm) and fully covered in all other isolates.

Table 3. 12. Number of isolate-unique genes for *P. fragariae*

Number of genes	<i>P. fragariae</i> isolates			
	BC-1	BC-16	NOV-9	SCR245
Present only in this isolate (100 % covered in this isolate at 0 % mm) - absent in all other isolate (0 % covered at 5 % mm)	3	1	0	0
Present only in this isolate (> 80 % covered in this isolate at 0 % mm) - absent in all other isolate (0 % covered at 5 % mm)	4	1	0	0
Present only in this isolate (> 50 % covered in this isolate at 0 % mm) - absent in all other isolate (0 % covered at 5 % mm)	4	2	1	1

In order to examine the variation within more confidently predicted RXLR families, effector gene coverage for baits specifically selected as RXLR effectors (Whisson et al., 2007; Win et al., 2007) were filtered and shown to vary between isolates and mismatch mapping rates, highlighting the existence of diverse RXLR genes (Table 3.13 shows ten diversified RXLR as an example to illustrate this variation).

Table 3. 13. Coverage for ten diversified *P. fragariae* RXLR genes. Coverage data for ten *P. fragariae* BC-16 RXLR genes: five predicted with the Win et al. (2007) model and five with the Whisson et al. (2007) model at 0 %, 3 % and 5 % mismatch mapping rates.

Bowtie mismatch mapping rate		0%mm				3%mm				5%mm				gene type
PenSeq gene ID (BC-16)	NCBI gene ID	BC-1	BC-16	NOV-9	SCR245	BC-1	BC-16	NOV-9	SCR245	BC-1	BC-16	NOV-9	SCR245	
BC-16_g11021	PF003_g12210	100	100	100	0	100	100	100	100	100	100	100	100	RxLR_Whisson2007
BC-16_contig_58_F2062	PF003_g29093	100	100	100	6.49652	100	100	100	100	100	100	100	100	RxLR_Whisson2007
BC-16_g6060	PF003_g6757	100	100	100	34.38486	100	100	100	100	100	100	100	100	RxLR_Whisson2007
BC-16_g21047	PF003_g23292	100	100	100	36.34312	100	100	100	100	100	100	100	100	RxLR_Whisson2007
BC-16_g2282	PF003_g2545	100	100	100	37.3057	100	100	100	100	100	100	100	100	RxLR_Whisson2007
BC-16_contig_30_RC_R23PF003_g19268		0	64.89796	0	0	0	64.89796	0	44.89796	0	64.89796	0	44.89796	RxLR_Win2007
BC-16_contig_76_RC_R14PF003_g33346		50	23.96694	2.892562	0	50	23.96694	2.892562	100	50	23.96694	2.892562	100	RxLR_Win2007
BC-16_contig_12_RC_R19PF003_g9944		32.48731	45.68528	0	0	32.48731	45.68528	0	1.522843	32.48731	45.68528	0	1.522843	RxLR_Win2007
BC-16_contig_49_RC_R28PF003_g26165		11.46789	1.834862	76.14679	0	11.46789	1.834862	76.14679	0	11.46789	1.834862	76.14679	0	RxLR_Win2007
BC-16_contig_4_RC_R414PF003_g4054		0	0	100	2.941176	92.94118	0	100	84.70588	92.94118	0	100	84.70588	RxLR_Win2007

Interestingly, when selecting a more stringent RXLR prediction model (Whisson et al., 2007), compared to the Win et al. (2007) model, the effectors appear less diversified, with higher coverage (gene type RxLR_Whisson2007 in Table 3.13) but isolate SCR245 stands out again as genetically more diverse (Table 3.13).

Taken together, these results suggest that effectors could vary significantly between the four *P. fragariae* isolates at the genomic level. Furthermore, this study has identified some candidates that can be used to demonstrate the intra-species variation. As expected with over time evolution and a different country of isolation, the oldest and only UK *P. fragariae* isolate SCR245 diverged the most from the reference

BC-16. These studies have successfully identified intraspecies variation and have surpassed what has been previously detectable (Adams, 2019; Adams et al., 2020).

3.3.3.2. Diversity of effectors in *P. rubi*

The diversity of *P. rubi* effectors was examined across 20 isolates to identify highly conserved and thus potentially essential effectors as well as effectors under diversifying selection.

Analyses for *P. rubi* found 3,024 genes shared identically between all 20 isolates (100 % coverage at 0 % mm) that did not have any heterozygous allele, which corresponds to 22 % of the total genes examined. Of the 3,024 identical *P. rubi* genes, 2,294 were identified as apoplastic effectors, 31 as CRNs (Adams, 2019) and 170 were predicted RXLR by the Whisson et al. (2007) model and / or the Win et al. (2007) model (31 %).

The coverage analysis of effector families was used to attempt to identify any discernible geographical, chronological or race-associated patterns to possibly predict related pathogen introductions. Of the 20 *P. rubi* isolates, no isolate-unique effector gene was found through coverage analysis, possibly due to the high number of isolates screened.

When selecting specifically for RXLR effectors (Whisson et al., 2007; Win et al., 2007), coverage varied between isolates and mismatch mapping rates, therefore we highlighted RXLR genes with low coverage that are under diversifying selection (Table 3.14).

Race designation has not been thoroughly carried out on *P. rubi* isolates since the 1990s and is based on resistance / susceptibility of a single raspberry line. It is probably not surprising that no race candidate gene could be found through both full and partial coverage analysis and presence vs absence of genes.

Table 3. 14. Coverage for ten diversified *P. rubi* genes. Coverage data for ten *P. rubi* SCRP333 RXLR genes with potential polymorphism: five predicted with the Win et al. (2007) model and five with the Whisson et al. (2007) model at 0 %, 3 % and 5 % mismatch mapping rates.

Bowtie mismatch mapping rate		0%mm																		gene type		
PenSeq gene ID (SCR333)	NCBI gene ID	SCR249	SCR296	SCR324	SCR333	SCR339	SCR1202	SCR1208	SCR1213	SCR250	SCR260	SCR283	SCR287	SCR288	SCR290	SCR292	SCR293	SCR323	SCR338	SCR1207	SCR1212	
SCR333_g15422	PR003_g16584	53.68852	0	51.43443	100	100	100	100	100	0	90.57377	0	100	100	100	0	92.41803	50	0	90.77869	100	RxLR_Whisson2007
SCR333_g24428	PR003_g26341	41.85567	45.36082	52.98969	100	100	100	100	42.68041	0	100	100	100	100	41.64948	100	44.3299	0	100	100	100	RxLR_Whisson2007
SCR333_g24183	PR003_g26066	100	100	0	100	100	100	100	100	0	100	100	100	100	100	100	0	0	49.72376	0	100	RxLR_Whisson2007
SCR333_g26002	PR003_g28078	13.6108	26.65917	56.74916	99.15636	98.76265	98.70641	72.60967	99.77503	39.48256	71.70979	98.87514	99.77503	98.59393	96.73791	89.53881	73.00337	41.78853	99.10011	68.44769	99.32508	RxLR_Whisson2007
SCR333_g27840	PR003_g30058	45.9854	62.48175	67.66423	95.91241	73.21168	88.90511	78.90511	82.70073	97.44526	82.70073	74.67153	89.19708	74.23358	85.62044	82.84672	65.9854	84.0146	95.76642	66.05839	100	RxLR_Whisson2007
SCR333_contig_1133_F10	PR003_g15927	79.67033	98.9011	0	0	30.32967	0	0	0	0	100	56.04396	0	54.3956	100	0	48.35165	58.24176	98.9011	100	100	RxLR_Win2007
SCR333_contig_3826_F1	PR003_g27434	50.54545	0	0	81.09091	46.18182	74.18182	19.27373	49.81818	0	68.72727	36.36364	100	0	0	40	0	42.18182	0	21.81818	4	RxLR_Win2007
SCR333_contig_326_F110	PR003_g7067	0	0	8.737864	94.66019	100	0	15.53388	39.80583	91.74757	100	100	100	89.80583	78.15534	48.54369	94.17476	15.04899	55.33981	37.37864	100	RxLR_Win2007
SCR333_contig_727_RC_R	PR003_g12193	70.05348	0	75.66845	70.05348	100	58.28877	22.99465	100	68.4492	88.50267	100	47.05882	45.9893	91.17647	89.03743	100	44.91979	100	0	0	RxLR_Win2007
SCR333_contig_1135_RC	PR003_g15943	100	67.62402	0	82.50653	100	0	74.67363	87.20627	80.93995	100	75.45692	24.28198	85.37859	43.86423	56.13577	0	68.68841	52.74151	75.71802	100	RxLR_Win2007
Bowtie mismatch mapping rate		3%mm																		gene type		
PenSeq gene ID (SCR333)	NCBI gene ID	SCR249	SCR296	SCR324	SCR333	SCR339	SCR1202	SCR1208	SCR1213	SCR250	SCR260	SCR283	SCR287	SCR288	SCR290	SCR292	SCR293	SCR323	SCR338	SCR1207	SCR1212	
SCR333_g15422	PR003_g16584	53.68852	0	78.07377	100	100	100	100	100	60.65574	100	59.22131	100	100	100	50.40984	100	95.69672	59.01639	0	100	RxLR_Whisson2007
SCR333_g24428	PR003_g26341	98.35052	99.17526	95.05155	100	100	100	100	100	100	37.93814	100	100	100	99.38144	100	95.05155	0	100	100	100	RxLR_Whisson2007
SCR333_g24183	PR003_g26066	100	100	0	100	100	100	100	70.99448	100	100	100	100	100	70.71823	100	74.03315	71.54696	100	100	100	RxLR_Whisson2007
SCR333_g26002	PR003_g28078	28.17773	56.13048	89.82002	100	100	100	92.29471	100	58.66142	100	100	100	99.94376	100	99.15636	76.94038	100	99.49381	99.94376	100	RxLR_Whisson2007
SCR333_g27840	PR003_g30058	75.25547	81.9708	76.71538	95.91241	77.08029	94.52555	96.49635	82.70073	100	100	100	89.19708	98.39416	88.83212	100	86.86131	97.73723	100	75.9854	100	RxLR_Whisson2007
SCR333_contig_1133_F10	PR003_g15927	79.67033	98.9011	0	100	30.32967	0	0	100	0	100	67.58242	38.46154	54.3956	100	0	48.35165	100	100	100	100	RxLR_Win2007
SCR333_contig_3826_F1	PR003_g27434	89.81818	0	0	81.09091	46.18182	100	19.27373	100	0	100	100	100	35.63636	100	99.27273	100	84.72727	95.63636	100	100	RxLR_Win2007
SCR333_contig_326_F110	PR003_g7067	0	0	100	100	100	0	15.53388	39.80583	96.1165	100	100	100	100	78.15534	100	94.17476	22.3301	100	100	100	RxLR_Win2007
SCR333_contig_727_RC_R	PR003_g12193	70.05348	0	75.66845	70.05348	100	88.23529	22.99465	100	84.49198	88.50267	100	71.12299	91.44385	91.17647	89.03743	100	44.91979	100	0	67.1123	RxLR_Win2007
SCR333_contig_1135_RC	PR003_g15943	100	67.62402	0	90.07833	84.8564	100	0	74.67363	100	100	75.45692	50.39164	85.37859	85.11749	99.47781	66.05744	70.75718	94.25587	75.71802	100	RxLR_Win2007
Bowtie mismatch mapping rate		5%mm																		gene type		
PenSeq gene ID (SCR333)	NCBI gene ID	SCR249	SCR296	SCR324	SCR333	SCR339	SCR1202	SCR1208	SCR1213	SCR250	SCR260	SCR283	SCR287	SCR288	SCR290	SCR292	SCR293	SCR323	SCR338	SCR1207	SCR1212	
SCR333_g15422	PR003_g16584	53.68852	0	78.07377	100	100	100	100	100	60.65574	100	76.63934	100	100	100	77.2541	100	95.69672	62.90884	100	100	RxLR_Whisson2007
SCR333_g24428	PR003_g26341	100	100	100	100	100	100	100	100	100	37.93814	100	100	100	100	100	100	100	0	100	100	RxLR_Whisson2007
SCR333_g24183	PR003_g26066	100	100	0	100	100	100	100	70.99448	100	100	100	100	100	70.71823	100	77.90055	81.49171	100	100	100	RxLR_Whisson2007
SCR333_g26002	PR003_g28078	31.72103	65.5793	89.82002	100	100	100	97.58155	100	71.48481	100	100	100	99.94376	100	99.94376	90.55118	100	100	100	100	RxLR_Whisson2007
SCR333_g27840	PR003_g30058	75.25547	81.9708	76.71538	95.91241	77.08029	94.52555	96.49635	82.70073	100	100	100	89.19708	98.39416	90	100	89.27007	98.32117	100	75.9854	100	RxLR_Whisson2007
SCR333_contig_1133_F10	PR003_g15927	79.67033	98.9011	0	100	30.32967	0	0	100	0	100	72.5274	47.25275	54.3956	100	0	43.95604	48.35165	100	100	100	RxLR_Win2007
SCR333_contig_3826_F1	PR003_g27434	89.81818	0	0	81.09091	46.18182	100	19.27373	100	0	100	100	100	100	100	100	100	100	100	100	100	RxLR_Win2007
SCR333_contig_326_F110	PR003_g7067	0	0	100	100	100	0	15.53388	39.80583	96.1165	100	100	100	100	78.15534	100	94.17476	22.3301	100	100	100	RxLR_Win2007
SCR333_contig_727_RC_R	PR003_g12193	70.05348	0	75.66845	70.05348	100	100	22.99465	100	84.49198	88.50267	100	71.12299	91.44385	91.17647	89.03743	100	44.91979	100	0	67.1123	RxLR_Win2007
SCR333_contig_1135_RC	PR003_g15943	100	67.62402	0	90.07833	84.8564	100	0	74.67363	100	100	75.45692	50.39164	85.37859	85.11749	99.47781	66.05744	70.75718	94.25587	75.71802	100	RxLR_Win2007

Most Scottish samples had duplicate isolations from the same sampling trip and could be used to assess diversity existing within a single sampling site. We found six genes absent from the 2017 Perthshire isolates (SCR1207 and SCR1208) and one gene absent in the 2018 Kincardineshire isolates (SCR1212 and SCR1213), while being covered in all other *P. rubi*. This highlights that the current PenSeq analysis is able to detect gene loss for these recent isolates which is also confounded by the fact that PenSeq reads are mapped against reference genomes and no *de novo* assembly has been conducted.

Moreover, isolates sampled from the same location years apart harboured a few genes of interest. *P. rubi* SCR296 was sampled from the same location (Perthshire,1993) than SCR1207 and SCR1208 (2017). Four RXLR genes were found to be 100 % covered in SCR1207 and SCR1208 while showing 0 % coverage for SCR296 at 0 % mm: SCR333_contig_1684_F14 (PR003_g19710, Win et al., 2007 prediction), SCR333_contig_3705_RC_R18 (PR003_g27151, Win et al., 2007 prediction), SCR333_g29970 (PR003_g32342, Whisson et al., 2007 prediction) and SCR333_g9504 (PR003_g10169, Whisson et al., 2007 prediction). Nucleotide and proteins sequences of those four RXLR genes were investigated for SNPs, INDELS

and amino acid changes. SCRP333_contig_1684_F14 and SCRP333_g9504 showed SNPs between the three sequences leading to some amino acid changes in the resulting predicted protein, while SCRP333_contig_3705_RC_R18 SNPs did not lead to protein changes (Table 3.15). SCRP333_g29970 nucleotide's change led to an earlier stop codon for SCRP296 and a shorter protein resulting in the absence of an RXLR motif for *P. rubi* SCRP296 (Table 3.15).

Table 3. 15. Polymorphism in RXLR genes from Perthshire (farm A) *P. rubi* isolates. SNPs and amino acid changes in four RXLR genes (SCRP333_contig_1684_F14/ PR003_g19710, SCRP333_contig_3705_RC_R18/ PR003_g27151, SCRP333_g29970/ PR003_g32342 and SCRP333_g9504/ PR003_g10169) from *P. rubi* isolates sampled from the same location (Perthshire, farm A) in different years: SCRP296, 1993; SCRP1207 and SCRP1208, 2017. Nucleotides in yellow are identical to the reference while nucleotides in blue are different from the reference sequence. Two nucleotides (e.g. G/C) indicate heterozygous SNPs, with around 50 % of the reads with each selection. Cons.: Consequence is either S for synonymous (same amino acid, in green) or NS for non-synonymous (amino acid change, in orange).

Gene name	Gene type	Nucleotide position on	Amino acid	Cons.	Ref.	Alt.					RxLR motif	
							SCR1207	SCR1208	SCR296	SCR333	RxLR	RxLR position
SCRP333_contig_1684_F14	RxLR (Win et al., 2007)	18	L6L	S	G	A	G	G	A	G	RSLR	55-58
		93	N31K	NS	T	G	T	T	G	T		
		127	R43W	NS	C	T	C	C	T	C		
		195	V65V	S	G	A	G	G	A	G		
SCRP333_contig_3705_RC_R18	RxLR (Win et al., 2007)	156	R52R	S	T	C	T	T	C	T	RQLR	52-55
SCRP333_g29970	RxLR (Whisson et al., 2007)	70	K24Q	NS	A	C	A	A	C	A	RFLR (except for SCRP296)	49-52
		84	Stop codon for SCRP296	NS	C	T	C	C	T	C		
SCRP333_g9504	RxLR (Whisson et al., 2007)	45	L15L	S	T	C	T	T	C	T	RFLR	50-53
		50	A17V	NS	C	T	C	C	T	C		
		66	H22Q	NS	C	A	C	C	A	C		
		73	T25G	NS	A	G	A	A	G	A		
		74			C	G	C	C	G	C		
		198	L66F	NS	G	C	G	G	C	G		
		232	E78K	NS	G	A	G	G	A	G		
		251	R84H	NS	G	A	G	G	A	G		
		309	N103K	NS	C	A	C	C	A	C		
		313	K105X	S	A	A/C	A	A	A/C	A		
		317	E106A	NS	A	C	A	A	C	A		
		336	N112K	NS	C	G	C	C	G	C		
		343	G115R	NS	G	A	G	G	A	G		
		346	S116D	NS	A	G	A	A	G	A		
		347			G	A	G	G	A	G		
		417	A139A	S	A	A/G	A	A	A/G	A		
		516	F172F	S	T	C	T	T	C	T		
		661	H221D	NS	C	G	C	C	G	C		
		742	K248Q	NS	A	C	A	A	C	A		
		767	D256G	NS	A	G	A	A	G	A		
774	M258I	NS	G	T	G	G	T	G				
797	G266V	NS	G	T	G	G	T	G				
817	E273K	NS	G	A	G	G	A	G				

Interestingly, RXLR gene SCRP333_g9504 (PR003_g10169) also showed different coverages between SCRP333 and SCRP250, both sampled in 1985, Perthshire, and between SCRP323 and SCRP324, both sampled in 1991, Perthshire. Polymorphism in SCRP333_g9504 in those strains was investigated and revealed amino acid changes between SCRP333 and SCRP250 (Table 3.16); while SCRP323 and SCRP324 had what seemed to be heterozygous versions of the gene. All these findings indicate that RXLR gene SCRP333_g9504 is under high diversification amongst *P. rubi* isolates and that there is some evidence of diversity in isolates from a single sample site over time.

Table 3. 16. Polymorphism in RXLR genes from Perthshire (farm C) *P. rubi* isolates. SNPs and amino acid changes in RXLR gene SCRP333_g9504 (PR003_g10169) from *P. rubi* isolates sampled from the same location (Perthshire, farm C) in 1985: SCRP333 and SCRP250. Nucleotides in yellow are identical to the reference while nucleotides in blue are different from the reference sequence. Cons.: Consequence is either S for synonymous (same amino acid, in green) or NS for non-synonymous (amino acid change, in orange).

Gene name	Gene type	Nucleotide position on	Amino acid (SCRP250/SCRP333)	Cons.	Ref.	Alt.	SCRP250		SCRP333		RxLR motif	
											RxLR	RxLR position
SCRP333_g9504	RxLR (Whisson et al., 2007)	9	L3L	S	G	A	A	A	G	RFLR	50-53	
		27	V9V	S	G	A	A	A	G			
		45	L15L	S	T	C	C	C	T			
		50	V17A	NS	C	T	T	T	C			
		66	Q22H	NS	C	A	A	A	C			
		73	G22T	NS	A	G	G	A				
		74			C	G	G	C				
		198	F66L	NS	G	C	C	G				
		232	K78E	NS	G	A	A	G				
		251	X84R	NS	G	R	R	G				
		309	K103N	NS	C	A	A	C				
		313	Q105K	NS	A	C	C	A				
		317	A106E	NS	A	C	C	A				
		336	K112N	NS	C	G	G	C				
		343	R115G	NS	G	A	A	G				
		346	D116S	NS	A	G	G	A				
		347			G	A	A	G				
		516	F172F	S	T	C	C	T				
		661	D221H	NS	C	G	G	C				
		742	Q248K	NS	A	C	C	A				
		767	G256D	NS	A	G	G	A				
		774	I258M	NS	G	T	T	G				
		797	V266G	NS	G	T	T	G				
		817	K273E	NS	G	A	A	G				

Overall, PenSeq has shown that there is diversity amongst species, though it is hard to quantify this across all gene families examined (close to 15,000 genes in total). This will be addressed later by using k-mer analyses to provide a global analysis of diversity to cluster isolates by relatedness (3.3.6).

3.3.4. Inter-species studies revealed core effectors as well as diversity between the two closely related species

Cross species mapping and the resulting coverage analysis described in 3.2.4. investigated differences in effector genes between the two species. Presence /

absence with *P. rubi* and *P. fragariae* unique genes or highly diversified effectors candidates as well as most conserved effectors were evaluated.

Using *P. rubi* isolates reads mapped to *P. fragariae* BC-16 reference genome, 554 effector genes were found to be identical between the 24 isolates, displaying 100 % coverage at 0 % mismatch mapping rates, i.e., absence of any polymorphism. This corresponds to 3.7 % of the total of effectors included in this study. Of those identical effectors, 474 were apoplastic effectors as predicted by Adams (2019) and 33 were predicted to be RXLR (32 with the Win et al.,2007 model, and one with the Whisson et al.,2007 model: BC-16_contig_61_RC_R2199). The 33 RXLRs were additionally mapped to the *P. infestans* genome of isolate T30-4 with Geneious (medium sensitivity, no trim) to screen for RXLR conserved across more *Phytophthora* species. We found one Win et al. (2007) RXLR gene (BC-16_contig_8_RC_R3463) showing a *P. infestans* matching protein with 83 % identity and RXLR motifs (*P. infestans* accession XP_002909763.1, Appendix B, Figure B.5).

This cross-mapping of *P. rubi* to the *P. fragariae* reference genome also revealed *P. fragariae* unique genes: 218 effectors were not covered in any *P. rubi* isolate for any of the mismatch rates, including 143 apoplastic, 12 predicted RXLR (such as BC-16_g14605 further investigated in 3.3.7) as well as two CRN effectors. These genes are either absent in *P. rubi* or display an extremely high rate of polymorphism and diversification. The 12 RXLRs identified display an average coverage of 94 % for the four *P. fragariae* isolates at 0 % mm and seven of those were conserved and identical between *P. fragariae* (Table 3.17).

Table 3. 17. Coverage data for the 12 *P. fragariae* unique RXLR genes. Coverage data for 0 % mismatch mapping rate (left) and 3 % mismatch mapping rate (right) for genes absent or highly diversified in the 20 *P. rubi* isolates.

Bowtie mismatch mapping rate		0%mm				3%mm			
PenSeq gene ID (BC-16)	NCBI gene ID	BC-1	BC-16	NOV-9	SCR245	BC-1	BC-16	NOV-9	SCR245
BC-16_contig_11_RC_R4163	PF003_g9039	100	100	100	100	100	100	100	100
BC-16_contig_111_F395	PF003_g38964	100	100	100	100	100	100	100	100
BC-16_contig_13_RC_R1406	PF003_g10642	100	100	100	96.62162	100	100	100	100
BC-16_contig_16_F2222	PF003_g8598	100	100	100	100	100	100	100	100
BC-16_contig_36_F753	PF003_g21706	100	100	100	100	100	100	100	100
BC-16_contig_4_RC_R841	PF003_g4026	95.76271	100	0	94.49153	95.76271	100	0	94.49153
BC-16_contig_41_RC_R2774	PF003_g23528	100	100	100	100	100	100	100	100
BC-16_contig_45_RC_R509	PF003_g25084	100	100	100	0	100	100	100	0
BC-16_contig_46_RC_R3016	PF003_g25133	100	100	100	100	100	100	100	100
BC-16_contig_58_RC_R1909	PF003_g28960	100	100	92.45283	93.531	100	100	92.45283	100
BC-16_contig_66_RC_R64	PF003_g27233	68.58639	63.35079	93.19372	61.7801	88.48168	100	93.19372	61.7801
BC-16_g14605	PF003_g16208	100	100	100	100	100	100	100	100

This suggests that those seven *P. fragariae* predicted RXLRs may have an essential function during infection of strawberry, and it could be speculated that they represent determinants of host specificity and pathogen specialisation. On the other hand, two of the 12 RXLR (BC-16_contig_4_RC_R841 and BC-16_contig_RC_R64) displayed presence / absence and sequence variation (SNP) across the four *P. fragariae* isolates.

In a similar manner, *P. fragariae* isolates were mapped to *P. rubi* SCRP333 reference genome and the subsequent coverage was assessed. A total of 217 effectors were absent at any mismatch mapping rate in all four *P. fragariae*, while covered on average 89 % in the *P. rubi* isolates, indicating possible unique *P. rubi* effectors. This included 148 apoplastic (Adams, 2019), 11 predicted RXLR (such as SCRP333_contig_4275_F7 further investigated in 3.3.7) and two CRNs (Adams, 2019). Within the 11 RXLR genes (Table 3.18), one was identical in all 20 isolates examined (SCRP333_contig_2222_F4). This highlights some level of diversity between the species-specific RXLRs isolates of *P. rubi*.

Table 3. 18. Coverage data for the 11 *P. rubi* unique RXLR genes. Coverage data for 0 % mismatch mapping rate (top) and 3 % mismatch mapping rate (bottom) for genes absent or highly diversified in the four *P. fragariae* isolates.

Bowtie mismatch mapping rate		0 % mm																				
PenSeq gene ID (SCRP333)	NCBI gene ID	SCRP249	SCRP296	SCRP324	SCRP333	SCRP339	SCRP1202	SCRP1208	SCRP1213	SCRP250	SCRP260	SCRP283	SCRP287	SCRP288	SCRP290	SCRP292	SCRP293	SCRP323	SCRP338	SCRP1207	SCRP1212	
SCRP333_contig_2222_F4	PR003_g22438	100.0	100.0	100.0	100.0	100.0	100.0	100.0	100.0	100.0	100.0	100.0	100.0	100.0	100.0	100.0	100.0	100.0	100.0	100.0	100.0	100.0
SCRP333_contig_1346_F32	PR003_g17526	100.0	100.0	100.0	100.0	100.0	100.0	100.0	100.0	100.0	100.0	100.0	100.0	100.0	100.0	100.0	100.0	100.0	100.0	100.0	100.0	100.0
SCRP333_contig_349_RC_R98	PR003_g7415	100.0	100.0	100.0	100.0	100.0	100.0	100.0	100.0	100.0	100.0	100.0	100.0	100.0	100.0	100.0	100.0	100.0	100.0	100.0	100.0	95.3
SCRP333_contig_4334_RC_R15	PR003_g28463	100.0	100.0	100.0	100.0	100.0	100.0	100.0	100.0	88.2	100.0	100.0	100.0	100.0	76.5	100.0	100.0	100.0	100.0	100.0	100.0	100.0
SCRP333_contig_462_RC_R66	PR003_g9040	100.0	100.0	97.5	100.0	100.0	100.0	88.0	100.0	100.0	97.5	100.0	100.0	100.0	100.0	100.0	100.0	100.0	100.0	100.0	0.0	100.0
SCRP333_contig_4202_RC_R2	PR003_g28211	80.3	100.0	94.7	100.0	96.6	95.2	93.3	100.0	78.9	91.3	81.7	100.0	90.7	100.0	91.9	94.4	96.9	96.1	90.2	100.0	100.0
SCRP333_contig_1339_RC_R23	PR003_g17480	100.0	100.0	100.0	50.0	100.0	100.0	100.0	100.0	90.2	100.0	100.0	100.0	9.8	100.0	99.4	100.0	100.0	100.0	11.0	91.5	
SCRP333_contig_4275_F7	PR003_g28352	100.0	87.2	90.1	100.0	100.0	100.0	100.0	100.0	43.6	100.0	100.0	100.0	100.0	39.3	100.0	37.7	42.0	100.0	100.0	100.0	
SCRP333_contig_2886_F19	PR003_g24908	100.0	100.0	100.0	100.0	100.0	100.0	38.1	100.0	98.7	38.1	100.0	100.0	100.0	100.0	100.0	16.1	94.1	100.0	38.1	100.0	
SCRP333_contig_737_RC_R14	PR003_g12299	100.0	0.0	0.0	1.3	88.8	94.1	79.6	100.0	0.0	100.0	100.0	100.0	100.0	100.0	100.0	71.7	0.0	100.0	86.8	100.0	
SCRP333_g26255	PR003_g28351	0.0	36.2	49.0	100.0	100.0	100.0	100.0	100.0	0.0	100.0	0.0	100.0	100.0	100.0	100.0	0.0	0.0	45.5	100.0	100.0	
Bowtie mismatch mapping rate		3 % mm																				
PenSeq gene ID (SCRP333)	NCBI gene ID	SCRP249	SCRP296	SCRP324	SCRP333	SCRP339	SCRP1202	SCRP1208	SCRP1213	SCRP250	SCRP260	SCRP283	SCRP287	SCRP288	SCRP290	SCRP292	SCRP293	SCRP323	SCRP338	SCRP1207	SCRP1212	
SCRP333_contig_2222_F4	PR003_g22438	100.0	100.0	100.0	100.0	100.0	100.0	100.0	100.0	100.0	100.0	100.0	100.0	100.0	100.0	100.0	100.0	100.0	100.0	100.0	100.0	100.0
SCRP333_contig_1346_F32	PR003_g17526	100.0	100.0	100.0	100.0	100.0	100.0	100.0	100.0	100.0	100.0	100.0	100.0	100.0	100.0	100.0	100.0	100.0	100.0	100.0	100.0	100.0
SCRP333_contig_349_RC_R98	PR003_g7415	100.0	100.0	100.0	100.0	100.0	100.0	100.0	100.0	100.0	100.0	100.0	100.0	100.0	100.0	100.0	100.0	100.0	100.0	100.0	100.0	100.0
SCRP333_contig_4334_RC_R15	PR003_g28463	100.0	100.0	100.0	100.0	100.0	100.0	100.0	100.0	88.2	100.0	100.0	100.0	100.0	100.0	100.0	100.0	100.0	100.0	100.0	100.0	100.0
SCRP333_contig_462_RC_R66	PR003_g9040	100.0	100.0	100.0	100.0	100.0	100.0	88.0	100.0	100.0	97.5	100.0	100.0	100.0	100.0	100.0	100.0	100.0	100.0	100.0	0.0	100.0
SCRP333_contig_4202_RC_R2	PR003_g28211	100.0	100.0	100.0	100.0	96.6	95.2	100.0	100.0	100.0	100.0	100.0	100.0	100.0	100.0	100.0	100.0	100.0	100.0	100.0	100.0	100.0
SCRP333_contig_1339_RC_R23	PR003_g17480	100.0	100.0	100.0	78.0	100.0	100.0	100.0	100.0	90.2	100.0	100.0	100.0	9.8	100.0	100.0	100.0	100.0	100.0	11.0	100.0	
SCRP333_contig_4275_F7	PR003_g28352	100.0	100.0	100.0	100.0	100.0	100.0	100.0	100.0	100.0	100.0	100.0	100.0	100.0	100.0	100.0	100.0	100.0	100.0	100.0	100.0	100.0
SCRP333_contig_2886_F19	PR003_g24908	100.0	100.0	100.0	100.0	100.0	100.0	100.0	100.0	100.0	100.0	100.0	100.0	100.0	100.0	100.0	100.0	89.8	100.0	100.0	99.2	100.0
SCRP333_contig_737_RC_R14	PR003_g12299	100.0	0.0	34.9	1.3	88.8	94.1	79.6	100.0	0.0	100.0	100.0	100.0	100.0	100.0	100.0	100.0	52.0	100.0	86.8	100.0	
SCRP333_g26255	PR003_g28351	95.9	91.2	96.4	100.0	100.0	100.0	100.0	100.0	88.2	100.0	100.0	100.0	100.0	100.0	100.0	100.0	88.8	82.2	100.0	100.0	

These findings revealed both core and diverse effectors between *P. rubi* and *P. fragariae* and confirmed previously published data (Adams, 2019; Adams et al., 2020), while highlighting species unique RXLRs that might be determinants of host specificity.

3.3.5. Overall diversity analyses emphasized distinction between the two closely related species

Overall diversity for *P. rubi* and *P. fragariae* isolates was summarized in ‘heat-map’ styled coverage tables (Figures 3.8 and 3.9 and Table 3.6).

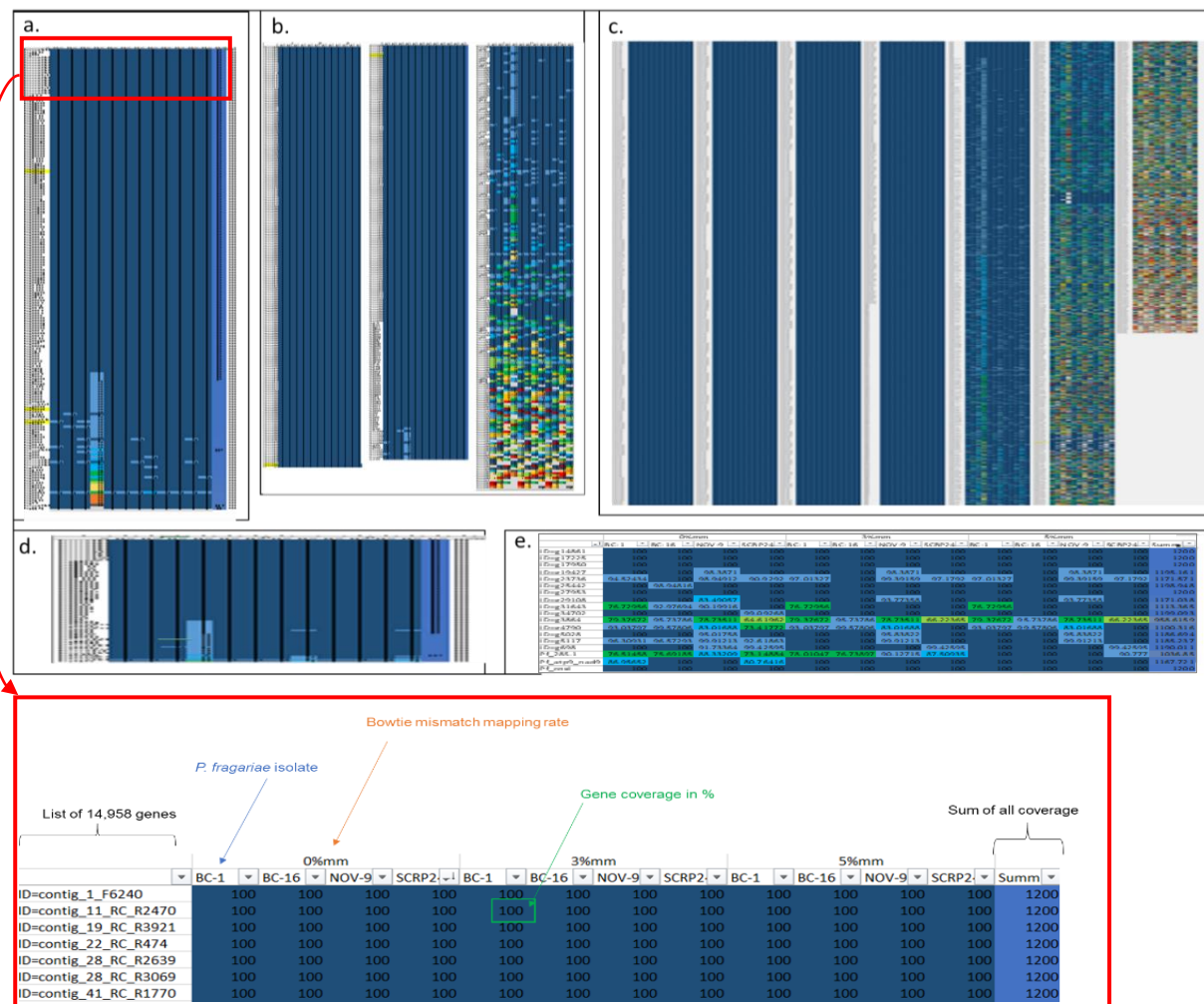


Figure 3. 8. *P. fragariae* coverage of genes when mapped to BC-16. “Zoomed-out” representation of coverage for *P. fragariae* genes. **a.** RXLR predicted with the Whisson et al., 2007 model. **b.** RXLR predicted with the Win et al., 2007 model. **c.** Apoplastic effector genes (predicted by Adams et al., 2019). **d.** CRN genes (predicted by Adams et a., 2019). **e.** Housekeeping and drug target genes. Red box indicates how to read the tables: first column represents the genes; all other columns represent the different isolates coverage. Columns 2, 3, 4 and 5 are coverage at 0 % mm of *P. fragariae* isolates, in order BC-1, BC-16, NOV-9 and SCR245; followed by 3 % mm and 5 % mm. Colour code for coverage described in Table 3.6.

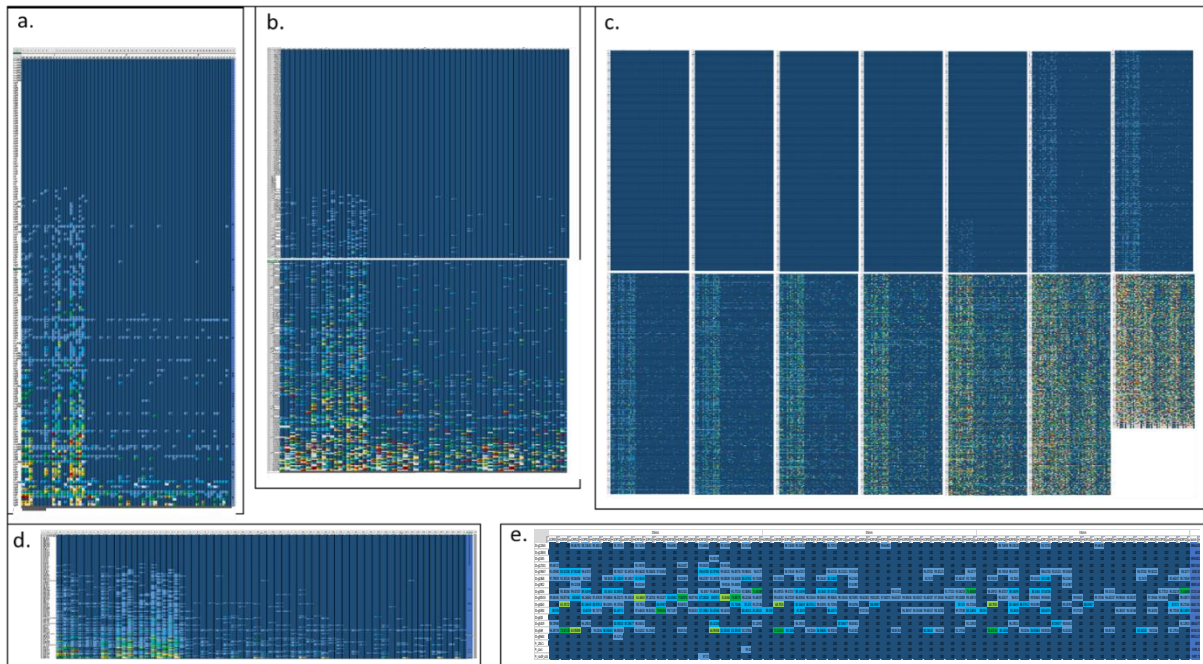


Figure 3. 9. *P. rubi* coverage of genes mapped to SCRP333. “Zoomed-out” representation of coverage for *P. rubi* genes. **a.** RXLR predicted with the Whisson et al., 2007 model. **b.** RXLR predicted with the Win et al., 2007 model. **c.** Apoplastic effector genes (predicted by Adams et al., 2019). **d.** CRN genes (predicted by Adams et a., 2019). **e.** Housekeeping and drug target genes. Layout is the same than Figure 3.8: first column represents the genes; all other columns represent the different isolates coverage. Columns 2 to 21 are coverage at 0 % mm, in order SCRP249, SCRP296, SCRP324, SCRP333, SCRP339, SCRP1202, SCRP1208, SCRP1213, SCRP250, SCRP260, SCRP283, SCRP287, SCRP288, SCRP290, SCRP292, SCRP293, SCRP323, SCRP338, SCRP1207 and SCRP1212; followed by 3 % mm and 5 % mm. Colour code for coverage described in Table 3.6.

Diversity from references is indicated through colour coded coverage (Table 3.6): blue is 100 % covered and thus similar to the reference; while orange, red and white indicate low coverage, indicating of some diversity between isolate and reference. An identical evaluation using cross-mapped reads emphasized the distinction between the two species, displaying much lower coverage for the genes of interest (Figure 3.10). RXLR and apoplastic effectors showed more variation (overall lower coverage) than Crinkler effectors and housekeeping genes (Figure 3.8 to 3.10). Interestingly, Crinkler effectors showed similar or higher levels of conservation between isolates of the same species compared to housekeeping genes, which was not the case between species, where housekeeping genes displayed the least variation.

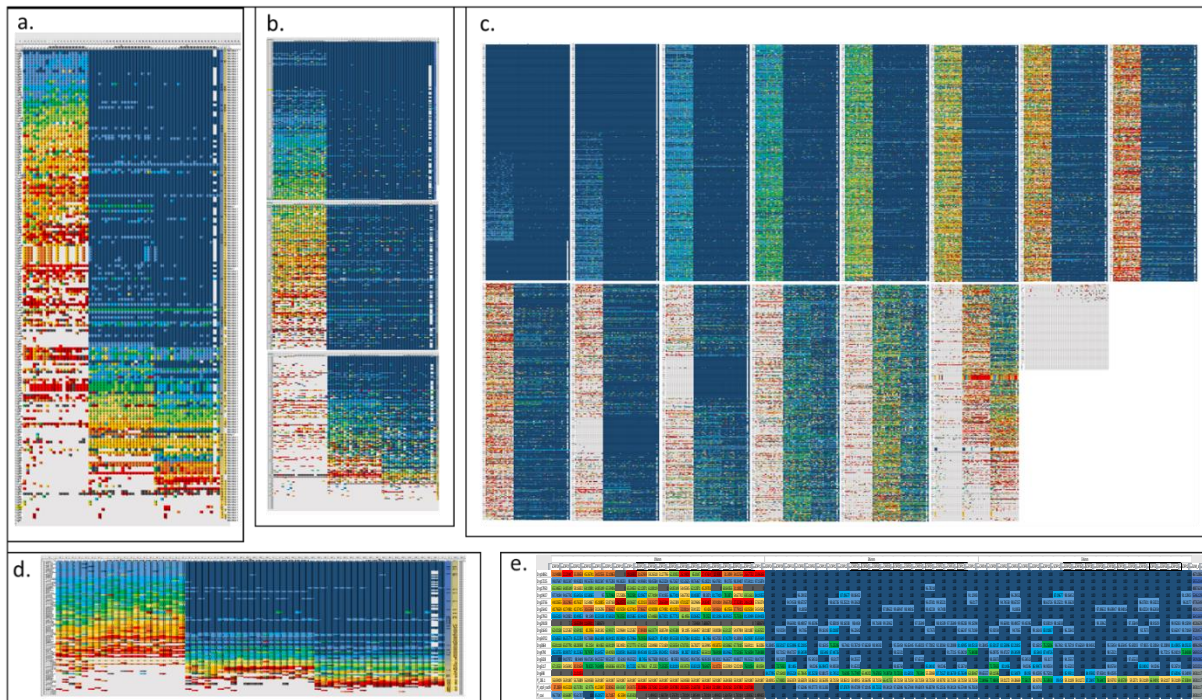


Figure 3. 10. *P. rubi* coverage of genes when mapped to *P. fragariae* reference genome BC-16. “Zoomed-out” representation of coverage for *P. rubi* genes mapped to *P. fragariae*. **a.** RXLR predicted with the Whisson et al., 2007 model. **b.** RXLR predicted with the Win et al., 2007 model. **c.** Apoplastic effector genes (predicted by Adams et al., 2019). **d.** CRN genes (predicted by Adams et a., 2019). **e.** Housekeeping and drug target genes. Layout is the same than Figure 3.9. Colour code for coverage described in Table 3.6.

3.3.6. K-mer analysis confirms PenSeq observations but does not cluster *P. rubi* according to race, year or location.

Although coverage data for the ~ 15,000 genes provides a quick visual representation of the diversity and allows study of a particular subset of genes, it is not the ideal method to identify clustering amongst isolates. Consequently, with the help of Dr Paolo Ribeca from BioSS, a k-mer analysis was conducted using PenSeq-derived reads. Short unique string of nucleotides known as k-mers were identified for enriched sequences mapping to reference genomes. Clusters based on genetic data could give an indication of introduction events. Around 48 % of reads were kept for all the baits during filtering for k-mer analyses: ~ 40 % for apoplastic, ~ 15 % for RXLR and ~ 3 % for CRN effectors, which was in line with the number of genes selected (Table 3.4). A k-mer length of k=12 was used for the clustering analysis.

This k-mer analysis showed grouping of the 24 isolates on two and three dimensions (Figure 3.11). In line with our expectations, *P. rubi* and *P. fragariae* isolates clustered separately, with the most variance (dimension 1, Figure 3.11).

Although the two-dimensional analysis did not separate *P. fragariae* isolates, the 3D plots clustered NOV-9 with BC-16, and BC-1 with SCRP245, revealing that the effectors genes in these two subsets of isolates might be quite similar (Figure 3.11). This suggests that even with a low number of isolates, clustering can be performed with reads from enrichment sequencing methods like PenSeq, which previous studies have struggled with. On the 2D plot and some 3D k-mer plots, BC-1 is placed in the middle of *P. fragariae* isolates, suggesting it could also constitute a good reference isolate. Using PenSeq coverage, a paired comparison of the number of identical effectors between all four *P. fragariae* isolates (paired comparison of genes 100 % covered at 0 % mismatch, for every pair of two *P. fragariae* isolates) confirmed that against each other isolate, *P. fragariae* isolate BC-1 has the highest number of reference-identical genes (100 % covered at 0 % mismatch mapping rate), showing its potential to be a better reference isolate for future research studies.

Global k-mer analysis did not group *P. rubi* isolates per known race or per year but did produce distinct clusters within the species (Figure 3.11) For instance, SCRP283 from USA and SCRP338 from Canada were grouped when looking at RXLR, CRN or apoplastic (x, y axes) set of effectors. This indicates that RXLR sequences are more similar between those two isolates compared to the other *P. rubi* studied, such as shared presence / absence and polymorphism variations. Additionally, *P. rubi* isolates SCRP260 (England, 1986), SCRP293 (Netherlands, 1991) and SCRP1207 (Scotland, 2017) grouped together for all the effector genes sets: apoplastic, RXLR and CRN (Figure 3.11). We also observed the clustering of isolates SCRP333 (Scotland, 1985), SCRP339 (France, 1985), SCRP1202 (Netherlands, 2010) and SCRP1213 (Scotland, 2018) for all the effector genes sets (Figure 3.11).

Figure 3. 11. (Overleaf) Representation of the k-mer analysis clustering of the 24 isolates (k=12).

a. Two-dimensions representation of k-mer analysis (bottom) and details of *P. rubi* isolates (top) with country (red: America; blue: Europe and green: UK), year of isolation and races (yellow rectangles and arrows: race 1; purple: race 3). **b.** Three-dimensions representations of k-mer analyses for all genes (left), RXLR genes (middle) and apoplastic genes (right). On the 3D plots, old sampling names are used: “Bullion-6” represents SCRP1208 and “C13” represents SCRP1213.

These consistent patterns could inform on the spread of the disease. For example, *P. rubi* could have been introduced from the Netherlands to France and England then propagated to Scotland (SCRP293 to SCR260 and then SCR1207; or SCR1202 to SCR339 then SCR333 and SCR1213). Alternatively, introduction could have come from the UK to France and then the Netherlands. Previous similarities between Scottish and Dutch isolates have also been observed on the housekeeping gene *CoxI* with shared SNPs. Introduction scenarios would have to be examined and could be tested like in the study carried out by Tabima et al. (2018) on *P. rubi* isolates from the USA, using DIYABC (a software for analyses of population history using approximate Bayesian computation on DNA polymorphism data) and multiple potential sites of origins to run scenarios. We notice that *P. rubi* reference isolate SCR333 is located as the lowest on the dimension 2 on the 2D plot and stands out on the 3D plot including all baits (Figure 3.11), suggesting that it stands at one end of the clustering, thus being quite different to other *P. rubi* isolates. This raises the question of the relevance of SCR333 (isolated in Scotland, 1985) as a reference isolate in the study of effectors, which should perhaps be replaced by an isolate grouped more closely to the other *P. rubi*, such as SCR290 (isolated in France, 1989). PenSeq coverage data confirmed this when carrying out paired comparison of genes 100 % covered at 0 % mismatch, for every pair of two *P. rubi* isolates. It showed that SCR290 consistently had the highest number of genes 100 % covered and thus identical to the reference genome and to each other *P. rubi* isolate. This indicates that in terms of effectors, SCR290 might have more genes identical to each and every *P. rubi* isolate selected than any of the other ones used in this study and could therefore constitute a good candidate for a new reference. SCR290 also had the lowest number of genes absent or highly polymorphic (0 % covered at 5 % mismatch mapping rate) compared to the reference genome, showing a good representation of the selected genes.

A whole genome study conducted by Tabima et al. (2018) has not highlighted any population differentiation for *P. rubi* at a global or regional scale. We demonstrated through coverage and k-mer analyses that PenSeq does enable the detection of genetic diversity within *P. rubi* and *P. fragariae*, including from isolates sampled from the same country or even the same field at the same sampling time and over time.

3.3.7. *In silico* PenSeq analyses highlighted several *P. rubi* and *P. fragariae* genes of interest

As described previously and throughout this chapter, the presence / absence analyses from same- and cross-species mapping and the coverage analyses with resulting tables give a quick overview of the similarity of genes for numerous isolates. This allows the quick identification of conserved vs diversifying genes before a more in-depth examination of individually selected genes. Here, we have selected four different sets of eight genes of interest for a deeper examination, first *in silico* and then by PCR and PCR-based sequencing, to confirm coverage and polymorphism. Orthologs to other *Phytophthora* species genes were also searched.

Firstly, eight *P. fragariae* RXLR effectors that have been shown to be expressed *in planta* at all time points tested (24, 48, 72 and 96 hpi) in infection assays using *P. fragariae* isolates BC-1, BC-16 and NOV-9 (Adams, 2019; Adams et al., 2020) were selected. Sequences were obtained from NIAB-EMR (courtesy of Dr Thomas Adams and Dr Charlotte Nellist) and subsequent ID numbers retrieved from the BC-16 reference available at the time (PenSeq ID). Coverage of these BC-16 genes for *P. rubi* isolates was found using the cross-species mapping. A second set of eight *P. fragariae* genes from literature (Tian et al., 2004; Tian et al., 2005; Kanneganti et al., 2006; Ma et al., 2017; Guo et al., 2020; Rocafort et al., 2020) and presenting interesting inter / intra-species diversity patterns was selected. In that subgroup, five apoplastic and three RXLR effector genes were studied and coverage for *P. rubi* isolates was retrieved from the cross-species analysis. Thirdly, eight *P. rubi* RXLR effectors, identified with the Whisson et al. (2007) and Win et al. RXLR prediction models (2007) were selected for interesting inter / intra-species diversity patterns. Finally, eight effectors, identified from various literature (Tian et al., 2004; Tian et al., 2005; Kanneganti et al., 2006; Ma et al., 2017; Guo et al., 2020; Rocafort et al., 2020) were retrieved in *P. rubi* using the NCBI BLASTp search. *P. fragariae* equivalent of those genes were found using the cross-species mapping and coverage analyses.

Coverage graphs for each gene for all *P. rubi* and *P. fragariae* were plotted according to 3.2.4.5. Sequences were extracted for a selection of those genes and translated with Geneious translation tool. BLASTx was carried out for protein sequences for

correspondence in other *Phytophthora* species (excluding *P. rubi* and *P. fragariae*), and recovered sequences aligned in Geneious.

To confirm presence / absence patterns, nucleotide sequences and eventual SNPs, six of these genes of interest were chosen to be tested in conventional PCR assay on a subset of isolates and some were further sequenced using Sanger sequencing at The James Hutton Institute.

These selected four sets of interesting effectors were therefore analysed in depth for inter / intra-species differences and polymorphism in order to draw more conclusions on their representation, possible function and evolution.

3.3.7.1. Comparison of expressed *P. fragariae* RXLR candidates in *P. rubi*

The top eight *in planta* expressed *P. fragariae* RXLR effectors are described as potential avirulence genes (Adams, 2019; Adams et al., 2020). The sequence diversity of these eight effectors, revealed by PenSeq, was examined in *P. fragariae* and *P. rubi*. The genes were mapped to the *P. fragariae* reference genome at several mismatch mapping rates. The DNA sequence conservation was confirmed across *P. fragariae* isolates (including a race 1, a race 2 and a race 3). Gene coverage of these eight RXLRs was significantly lower or in some cases null (absent gene) for *P. rubi* isolates (Table 3.19).

Table 3. 19. Coverage data for eight *P. fragariae* genes. Coverage for eight *P. fragariae* genes of interest at 0 % and 3 % mismatch mapping rates for all 24 isolates studied

Published gene ID		PF003_g16234		PF003_g20420		PF003_g21231		PF003_g23640		PF003_g27513		PF003_g35418		PF003_g40916		PF003_g6480	
PenSeq gene ID		BC-16_g14629		BC-16_g18452		BC-16_g19167		BC-16_g21368		BC-16_g24882		BC-16_g32018		BC-16_g36900		BC-16_g5824	
Mismatch mapping rate		0%	3%	0%	3%	0%	3%	0%	3%	0%	3%	0%	3%	0%	3%	0%	3%
<i>P. rubi</i>	SCR1202	67.3	98.5	0.7	52.4	16.3	100.0	0.0	0.0	0.0	3.1	0.0	52.5	0.0	88.9	0.0	93.5
	SCR1207	61.7	98.9	6.7	43.6	27.4	100.0	0.0	0.0	1.0	0.0	51.2	0.0	85.0	16.6	95.7	
	SCR1208	64.6	99.3	0.0	48.5	30.1	100.0	0.0	0.0	0.5	0.0	51.9	38.9	90.5	0.0	99.7	
	SCR1212	60.2	98.2	0.0	51.5	13.2	100.0	0.0	0.0	4.8	0.0	52.3	0.0	71.4	0.0	93.8	
	SCR1213	71.5	98.7	0.0	51.3	29.2	100.0	0.0	62.0	0.0	3.4	0.0	49.0	23.0	79.8	52.7	95.7
	SCR249	78.7	100.0	0.0	51.5	29.8	100.0	0.0	0.0	0.0	37.5	0.0	52.3	25.0	89.5	49.1	100.0
	SCR250	69.2	100.0	0.0	46.4	31.7	100.0	0.0	0.0	0.0	4.8	0.0	52.1	0.0	89.5	0.0	89.9
	SCR260	63.5	98.3	0.0	48.7	17.7	100.0	0.0	0.0	0.0	0.0	0.0	52.5	0.0	66.1	0.0	93.7
	SCR283	69.0	100.0	0.0	51.7	29.2	100.0	0.0	22.3	0.0	4.8	0.0	51.2	0.0	81.8	0.0	92.7
	SCR287	68.1	99.3	0.0	52.2	12.7	100.0	0.0	0.0	0.0	31.0	0.0	49.0	0.0	88.2	0.0	97.2
	SCR288	56.5	98.5	0.0	50.6	18.0	100.0	0.0	0.0	0.0	0.0	0.0	52.3	0.0	89.5	0.0	95.6
	SCR290	67.9	98.8	0.0	51.3	31.1	100.0	0.0	0.0	0.0	0.0	0.0	51.4	0.0	90.2	0.0	95.3
	SCR292	66.8	100.0	0.0	52.2	17.4	100.0	0.0	0.0	0.0	0.0	0.0	52.1	0.0	90.0	18.8	100.0
	SCR293	69.2	100.0	0.0	46.2	0.0	100.0	0.0	0.0	0.0	0.0	0.0	52.1	0.0	75.9	0.0	96.2
	SCR296	70.4	100.0	24.6	51.0	30.0	100.0	91.3	100.0	0.0	35.6	0.0	51.4	0.0	81.1	0.0	92.6
	SCR323	68.3	100.0	0.0	49.7	17.4	100.0	0.0	0.0	0.0	4.4	0.0	50.2	0.0	95.7	0.0	95.6
	SCR324	73.7	100.0	0.0	49.7	62.2	100.0	0.0	4.6	0.0	5.8	0.0	51.9	21.4	87.0	0.0	94.6
	SCR333	74.6	99.1	0.0	50.6	71.5	100.0	0.0	0.0	0.0	36.6	0.0	51.4	0.0	76.1	0.0	93.5
SCR338	69.3	100.0	0.0	51.3	16.6	100.0	0.0	0.0	0.0	3.6	18.1	50.2	0.0	86.4	0.0	95.9	
SCR339	79.3	98.2	6.3	52.9	41.9	100.0	0.0	0.0	0.0	47.9	0.0	51.2	0.0	80.9	0.0	94.1	
<i>P. fragariae</i>	BC-1	100.0	100.0	100.0	100.0	98.9	100.0	100.0	100.0	100.0	100.0	100.0	100.0	100.0	100.0	100.0	100.0
	BC-16	100.0	100.0	100.0	100.0	100.0	100.0	100.0	100.0	100.0	100.0	100.0	100.0	100.0	100.0	100.0	100.0
	NOV-9	100.0	100.0	100.0	100.0	99.8	100.0	100.0	100.0	100.0	100.0	100.0	100.0	100.0	100.0	100.0	100.0
	SCR245	100.0	100.0	97.0	100.0	97.2	100.0	100.0	100.0	96.9	100.0	52.3	100.0	100.0	100.0	95.7	100.0

Graphic representations of coverage at 0 % mm and 3 % mm emphasized which gene were conserved or diverse (with potential SNPs) and how well represented they were (Figure 3.12).

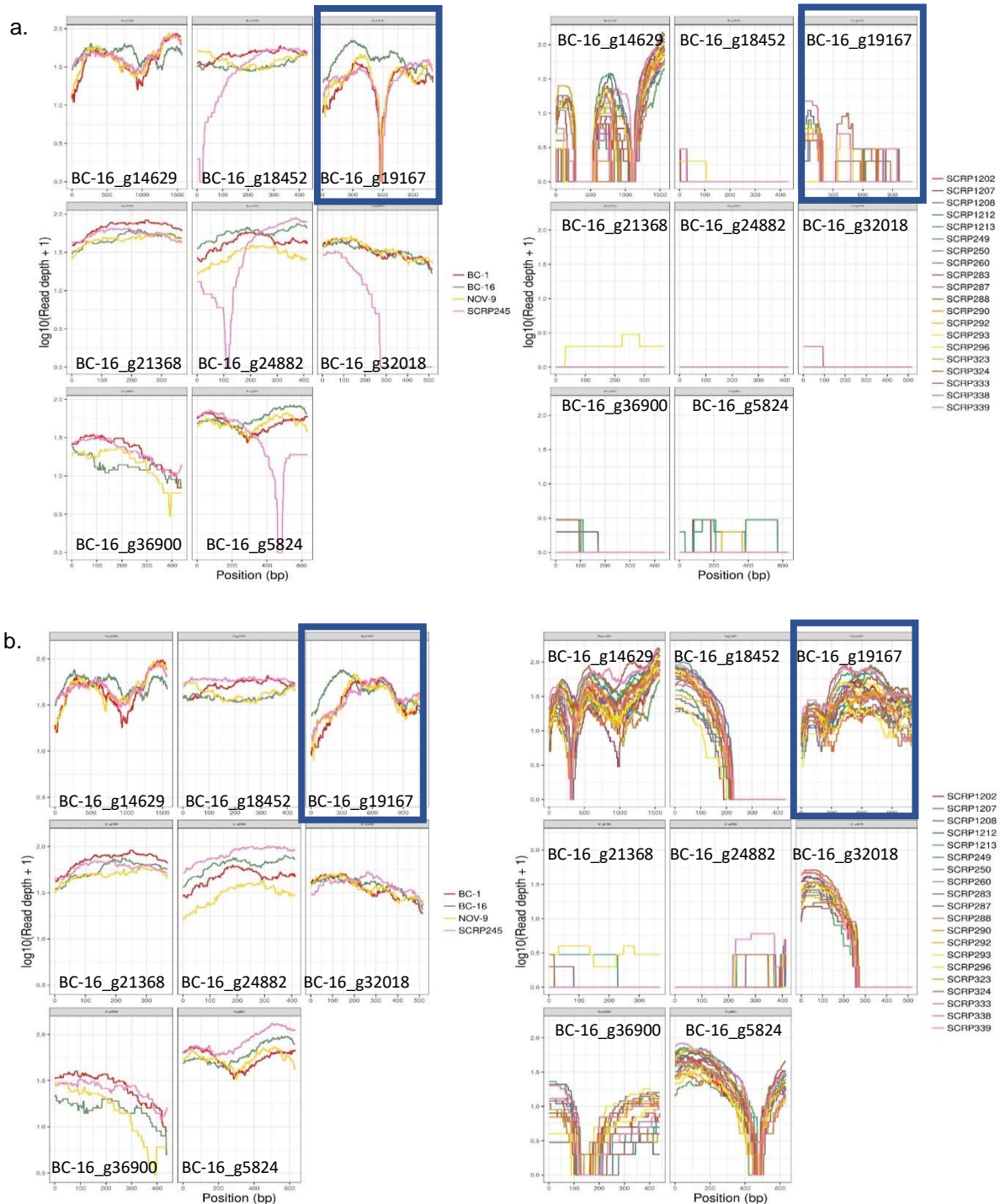


Figure 3.12. Coverage graphs for eight *P. fragariae* RXLR. Left: *P. fragariae* isolates and right: *P. rubi* isolates at **a.** 0 % and **b.** 3 % mismatch mapping rates. Eight *P. fragariae* predicted RXLR genes were selected and their coverage was retrieved at 0 % (**a.**) and 3 % (**b.**) mismatch mapping rates for the four *P. fragariae* isolates (left) using same-species mapping and for the 20 *P. rubi* isolates (right) using cross-species mapping. Blue rectangle highlights BC-16_g19167.

When comparing conservation of these *P. fragariae* expressed RXLRs, we found that isolate SCRP245, which has no current race designation, showed four RXLRs differing in sequence from the other three *P. fragariae* isolates (PF003_g20420/BC-16_g18452; PfAvr2 candidate PF003_g27513/BC-16_g24882, Adams et al., 2020; PF003_g35418/BC-16_g32018 and PF003_g6480/BC-16_g5824). Although none of the eight expressed *P. fragariae* RXLRs were found to be completely identical in *P. rubi*, four were conserved at 3 % mismatch rate (PF003_16234/ BC-16_g14629; PF003_g21231/ BC-16_g19167; PF003_g40916/ BC-16_g36900 and PF003_g6480/ BC-16_g5824) and could be candidates for downstream studies to look at their possible function (Figure 3.12).

A BLASTx search of those RXLRs found that BC-16_g36900 and BC-16_g5824 were the most conserved in other *Phytophthora* spp., with > 80 % of identity with proteins in *P. sojae* and *P. cinnamomi*, evidently showing the importance of those genes amongst other root infecting species of the same clade. Whereas BC-16_g14629 and BC-16_g19167 had low coverage of matching proteins in the same species (~ 45 %). Top-expressed RXLRs BC-16_g21368 and BC-16_g24882 did not yield good coverage in a few *P. rubi* isolates, even at 3 % mm (Figure 3.12 and Table 3.19), and BLASTx searches did not find any close matching proteins (<30 % identity) in other *Phytophthora* spp., showing the possibility of species-specific roles in the infection of strawberry.

As the most conserved RXLR effector, BC-16_g19167 was selected for PCR validation. As described in 3.2.5, primers were designed on conserved region (Table 3.7). *In silico* primer testing with Geneious showed amplification for a subset of 12 isolates (from the first PenSeq run), which was confirmed with PCR and agarose gel electrophoresis (Figure 3.13). Additionally, following the PCR amplification, Sanger sequencing was performed for BC-16_g19167 (see 3.2.5). Cleaned consensus sequences from good quality reads matched the extracted nucleotide sequences from mapped PenSeq reads for each of the isolates, including a species-specific SNP (Figure 3.14), that was thus confirmed between PenSeq and Sanger sequencing methods. Interestingly, the *P. rubi* equivalent of BC-16_g19167, identified as SCRP333_g25584 in our PenSeq data and as PR003_g27614 with a BLASTx search, has also been detected as being expressed in a *P. rubi* infection time-course

(Chapter 4) and is thus thought to be a core effector, that could be key for the infection process of *P. fragariae* and *P. rubi*.

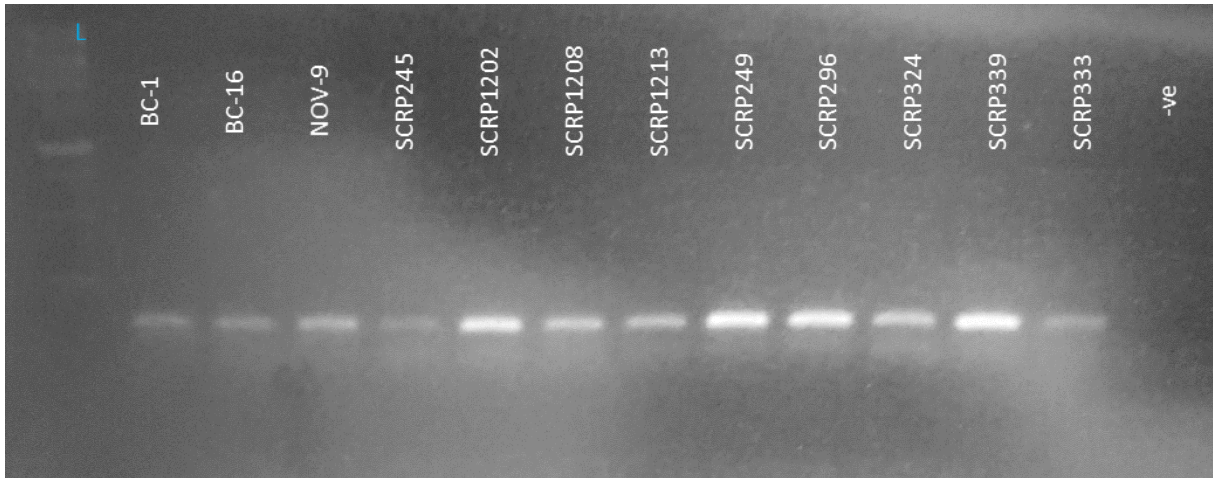


Figure 3. 13. Agarose electrophoresis gels (2 % agarose) testing the BC-16_g19167 primers. BC-16_g19167 amplicon size is 141 bp. Blue ladder (L) is 1 kb. Negative control (-ve) using SdW did not show amplification.

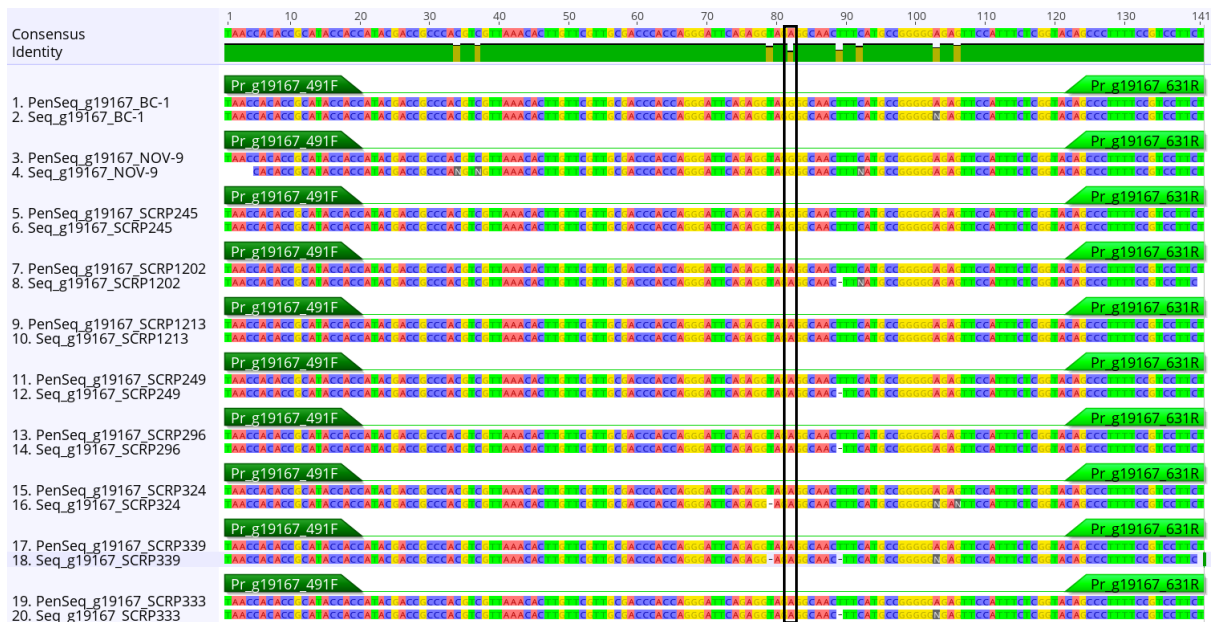


Figure 3. 14. Validation of PenSeq SNPs and nucleotides sequences for BC-16_g19167. Comparison between PenSeq analyses (odd rows, “PenSeq_g19167_[isolate]”) and Sanger sequencing (even rows, “Seq_g19167_[isolate]”) for BC-16_g19167 RXLR gene for isolates of *P. rubi* and *P. fragariae*. Figure also shows where primers bind and a species-specific SNP (black rectangle, position 82). Alignment was performed in Geneious.

3.3.7.2. Gene coverage of *P. fragariae* effectors with published orthologs

A second set of eight *P. fragariae* effectors was selected for in-depth analysis of coverage and levels of polymorphism. These effectors had been identified through the literature (Tian et al., 2004; Tian et al., 2005; Kanneganti et al., 2006; Ma et al., 2017; Guo et al., 2020; Rocafort et al., 2020) and were retrieved in *P. fragariae* using the BLAST tools. The list was completed with additional apoplastic and RXLR *P. fragariae* effectors, identified from the PenSeq analyses (see Tables 3.20 and 3.21).

Table 3. 20. Description of eight *P. fragariae* effectors

Effector name	Function / Gene description	References	PenSeq ID	NCBI ID number
EPIC3	Inhibit host cysteine proteases	Tian et al., 2004; Tian et al., 2005; Rocafort et al., 2020	BC-16_g12621	PF003_g13986
INF1	Elicitor protein inducing HR (necrosis inducing)	Kanneganti et al., 2006	BC-16_g21771 BC-16_g21778	PF003_g24108
BC-16_contig_38_F2468	<i>P. fragariae</i> apoplastic gene absent from BC-16 reference genome and identical in all other <i>P. fragariae</i> isolates		BC-16_contig_38_F2468	PF003_g22679
BC-16_g7853	<i>P. fragariae</i> GIP2 (Glucanase Inhibitor Protein 2)		BC-16_g7853	PF003_g8719
BC-16_g2112	<i>P. fragariae</i> RXLR effector gene (Whisson et al., 2007) identical between all 4 <i>P. fragariae</i>		BC-16_g2112	PF003_g2353
BC-16_g24778	<i>P. fragariae</i> RXLR effector gene (Whisson et al., 2007) with most heterozygous SNPs in the 4 isolates		BC-16_g24778	PF003_g27402
BC-16_g14605	<i>P. fragariae</i> RXLR effector (Win et al., 2007) unique to <i>P. fragariae</i> and conserved across the four isolates		BC-16_g14605	PF003_g16208

Except for BC-16_g14605 (PF003_g16208), a likely unique *P. fragariae* RXLR (0 % coverage in all *P. rubi* at all mismatch mapping rates), selected effector genes were also represented in *P. rubi* with sequence polymorphism (Table 3.21 and Figure 3.15).

GIP2 gene, BC-16_g7853, was found to match to a GIP protein in *P. megakarya* through a BLASTx search (78 % identity).

BC-16_contig_38_F2468 apoplastic gene was the most conserved across isolates (Table 3.21), with identical nucleotide sequences but was absent in BC-16. A BLASTx search revealed that the resulting protein was conserved in clade 1 *Phytophthoras* like *P. infestans* and *P. parasitica* (with 98 % to 100 % match of the protein). However, PenSeq revealed that this gene was not covered in the BC-16 isolate, at 0 %, 3 % and 5 % mismatch mapping rates (Table 3.21 and Figure 3.15), while reads from the three other *P. fragariae* successfully mapped to this gene. This suggests a loss of this

effector gene in lab strains over a short period of time. RXLR genes BC-16_g2112 (PF003_g2353, identical in our four *P. fragariae*) and BC-16_g24778 (PF003_g27402, a diverse gene with heterozygous SNPs) matched to RXLR proteins in *P. palmivora*, *P. innamomi*, *P. sojae* and *P. agathidicida*, showing conservation across *Phytophthora*, though with some sequence variation. The latter matched at 60 % and 52 % respectively to Avh1531a in *P. sojae* and PaRXLR68 in *P. agathidicida*.

Table 3. 21. Coverage data for eight *P. fragariae* apoplastic genes. Coverage for eight *P. fragariae* genes of interest at 0 % and 3 % mismatch mapping rates for all 24 isolates studied

PenSeq gene ID		BC-16_contig_38_F2468		BC-16_g12621		BC-16_g14605		BC-16_g2112		BC-16_g7853		BC-16_g21771		BC-16_g21778		BC-16_g24778	
Predicted function		P. fragariae apoplastic gene absent from BC-16 reference genome and identical in all other P. fragariae isolates		PF003_EPIC3		P. fragariae RxLR effector (Win et al., 2007) unique to P. fragariae and conserved across the four isolates		P. fragariae RxLR effector gene (Whisson et al., 2007) identical between all 4 P. fragariae		GIP2		INF1		P. fragariae RxLR effector gene (Whisson et al., 2007) with most heterozygous SNPs in the 4 isolates			
Mismatch mapping rate		0%	3%	0%	3%	0%	3%	0%	3%	0%	3%	0%	3%	0%	3%	0%	3%
<i>P. fragariae</i>	BC-1	100.0	100.0	100.0	100.0	100.0	100.0	100.0	100.0	100.0	100.0	100.0	100.0	100.0	100.0	100.0	100.0
	BC-16	0.0	0.0	100.0	100.0	100.0	100.0	100.0	100.0	100.0	100.0	100.0	100.0	100.0	100.0	100.0	100.0
	NOV-9	100.0	100.0	100.0	100.0	100.0	100.0	100.0	100.0	100.0	100.0	100.0	100.0	100.0	100.0	100.0	100.0
	SCRP245	100.0	100.0	100.0	100.0	100.0	100.0	100.0	100.0	45.7	100.0	100.0	100.0	97.2	100.0	92.8	100.0
<i>P. rubi</i>	SCRP1202	100.0	100.0	0.0	100.0	0.0	0.0	55.0	100.0	0.0	95.0	0.0	100.0	21.1	100.0	24.6	94.3
	SCRP1207	54.3	100.0	0.0	66.1	0.0	0.0	6.8	100.0	0.0	100.0	0.0	100.0	45.5	100.0	10.1	67.2
	SCRP1208	100.0	100.0	0.0	100.0	0.0	0.0	50.8	100.0	0.0	100.0	0.0	100.0	46.3	100.0	21.1	68.6
	SCRP1212	90.9	100.0	0.0	99.7	0.0	0.0	29.9	100.0	0.0	95.1	0.0	100.0	30.6	100.0	0.0	67.8
	SCRP1213	100.0	100.0	0.0	98.7	0.0	0.0	20.3	100.0	0.0	93.3	0.0	100.0	19.9	100.0	17.2	68.6
	SCRP249	100.0	100.0	0.0	100.0	0.0	0.0	79.7	100.0	0.0	100.0	50.0	100.0	79.5	100.0	15.9	69.3
	SCRP250	100.0	100.0	0.0	100.0	0.0	0.0	68.5	100.0	0.0	95.1	0.0	100.0	47.8	100.0	0.0	63.9
	SCRP260	100.0	100.0	0.0	100.0	0.0	0.0	18.0	100.0	0.0	100.0	0.0	100.0	39.0	100.0	0.0	69.1
	SCRP283	100.0	100.0	0.0	100.0	0.0	0.0	71.1	100.0	0.0	100.0	0.0	100.0	41.0	100.0	8.6	68.0
	SCRP287	75.0	75.0	0.0	99.2	0.0	0.0	72.0	100.0	0.0	95.1	0.0	100.0	33.1	100.0	0.0	68.2
	SCRP288	100.0	100.0	0.0	91.8	0.0	0.0	26.7	100.0	0.0	95.6	0.0	100.0	38.8	100.0	0.0	65.7
	SCRP290	100.0	100.0	0.0	92.1	0.0	0.0	71.4	100.0	0.0	95.0	30.1	100.0	58.1	100.0	10.1	75.9
	SCRP292	96.3	100.0	0.0	100.0	0.0	0.0	0.0	100.0	0.0	100.0	0.0	100.0	44.1	100.0	0.0	68.3
	SCRP293	100.0	100.0	0.0	100.0	0.0	0.0	28.9	100.0	0.0	100.0	0.0	100.0	42.4	100.0	0.0	68.4
	SCRP296	100.0	100.0	0.0	99.0	0.0	0.0	75.2	100.0	0.0	100.0	0.0	100.0	47.2	100.0	7.2	68.4
	SCRP323	100.0	100.0	0.0	100.0	0.0	0.0	26.7	100.0	0.0	95.1	0.0	100.0	50.0	100.0	0.0	68.0
	SCRP324	100.0	100.0	0.0	96.2	0.0	0.0	74.3	100.0	0.0	95.1	0.0	100.0	42.7	100.0	1.9	96.1
	SCRP333	100.0	100.0	0.0	100.0	0.0	0.0	24.1	100.0	0.0	94.0	13.8	100.0	42.7	100.0	12.8	73.0
	SCRP338	100.0	100.0	0.0	92.3	0.0	0.0	12.5	100.0	0.0	100.0	0.0	100.0	50.0	100.0	14.9	68.1
	SCRP339	100.0	100.0	0.0	100.0	0.0	0.0	53.7	100.0	0.0	100.0	0.0	100.0	32.0	100.0	18.4	68.4

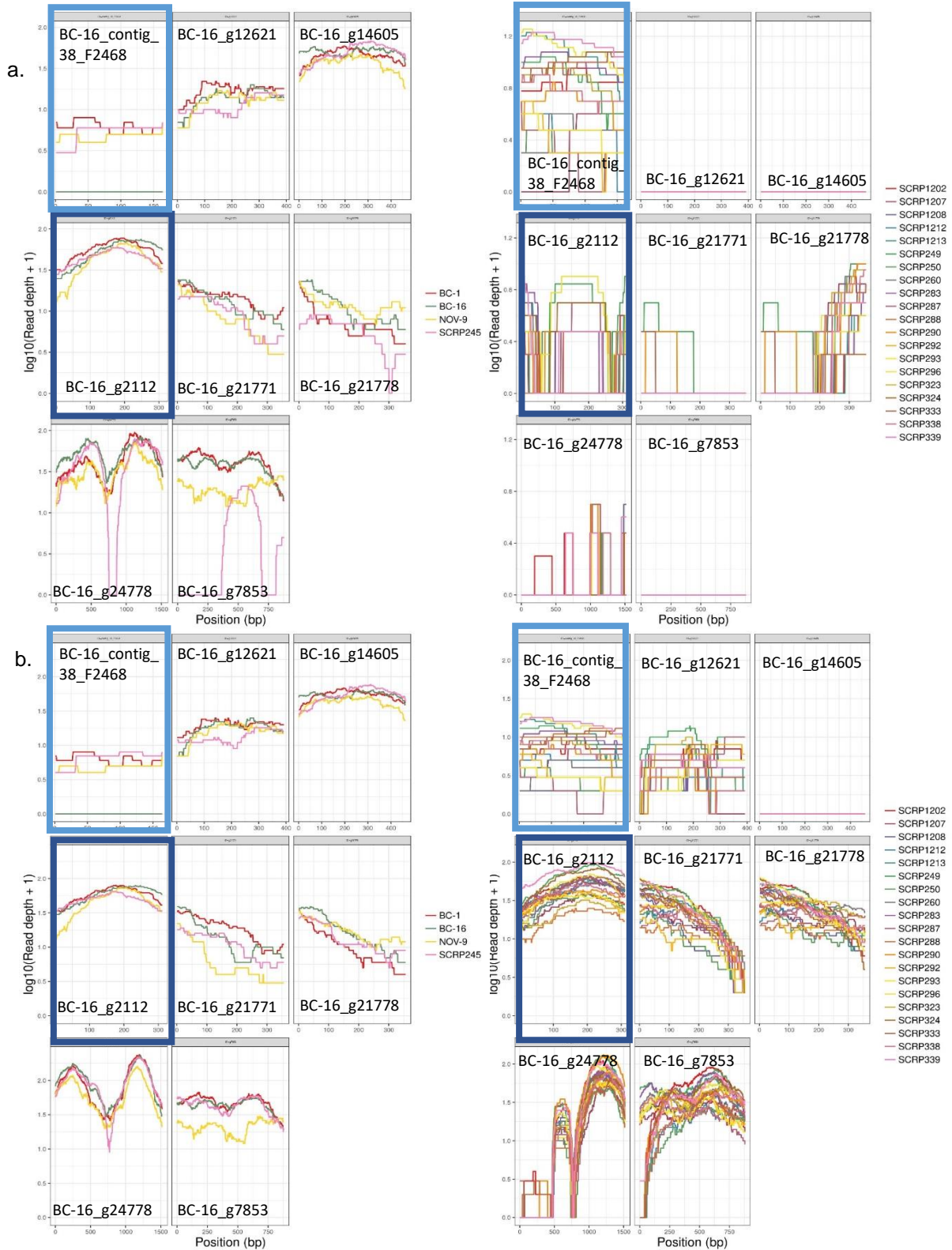


Figure 3. 15. Coverage graph for eight *P. fragariae* apoplastic genes. Left: *P. fragariae* isolates and right: *P. rubi* isolates at **a.** 0 % and **b.** 3 % mismatch mapping rates. Eight *P. fragariae* effector genes were selected and their coverage was retrieved at 0 % (**a.**) and 3 % (**b.**) mismatch mapping rates for the four *P. fragariae* isolates (left) using same-species mapping and for the 20 *P. rubi* isolates (right) using cross-species mapping. Blue rectangle highlights BC-16_contig_38_F2468 and BC-16_g2112.

Two *P. fragariae* genes, one apoplastic BC-16_contig_38_F2468 (PF003_g22679) and one RXLR (Whisson et al., 2007) BC-16_g2112 (PF003_g2353) were selected for PCR validation on *P. fragariae* isolates BC-1, BC-16, NOV-9 and SCR245. According to the coverage data, BC-16_contig_38_F2468 (PF003_g22679) was absent from BC-16; whereas BC-16_g2112 (PF003_g2353) was represented in all four *P. fragariae* isolates. This was confirmed with *in silico* primer testing and by *in vitro* PCR and gel electrophoresis (Figure 3.16).

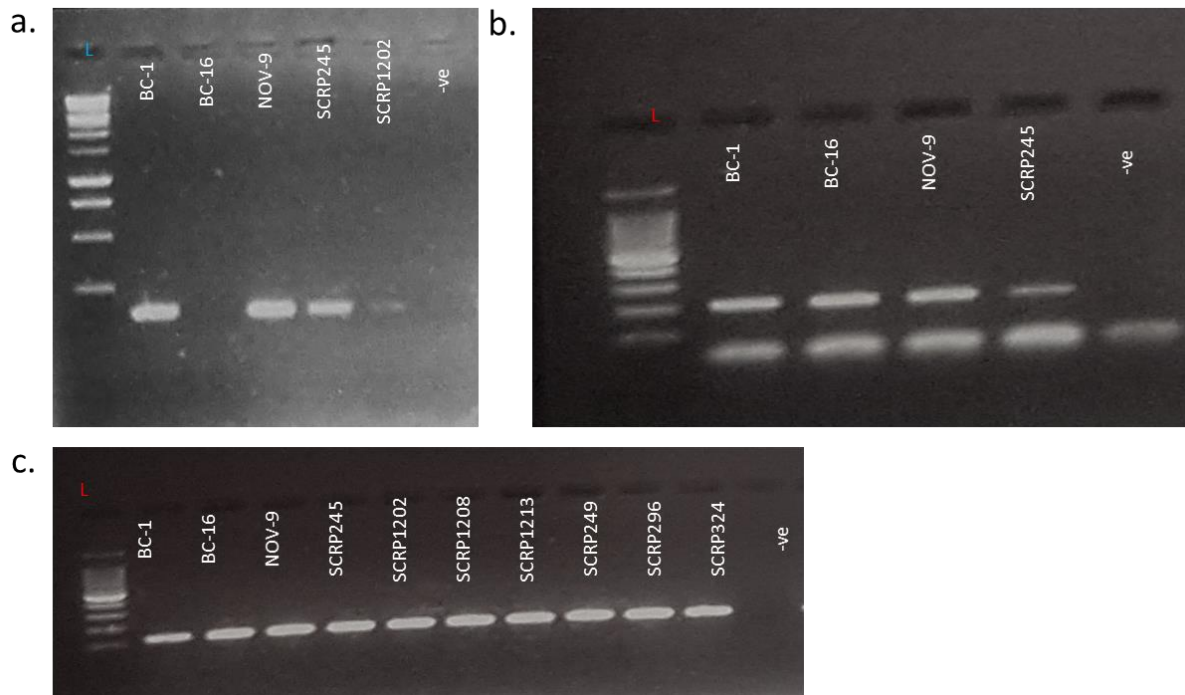


Figure 3. 16. Agarose electrophoresis gels for BC-16_contig_38_F2468 and BC-16_g2112. Agarose electrophoresis gels (2 % agarose) testing **a.** *P. fragariae* gene BC-16_contig_38_F2468, for which PenSeq coverage data indicates absence in isolate BC-16, hereby confirmed with absence of bands on the agarose gel. **b.** Agarose electrophoresis gels (2 % agarose) testing *P. fragariae* conserved gene BC-16_g2112 present in all *P. fragariae* isolates. **c.** *CoxI* was used as a control to check for presence of DNA in *P. fragariae* templates. BC-16_contig_38_F2468 amplicon size is 165 bp, BC-16_g2112 amplicon size is 210 bp and *CoxI* amplicon is 127 bp. Gel a. shows amplification of appropriate size amplicons for all *P. fragariae* isolates tested except BC-16; Gel b. shows amplification of right size amplicons for BC-16_g2112 for all *P. fragariae* isolates. Gel c. shows amplification for all *P. fragariae* isolates, thus proving presence of DNA in all *P. fragariae*.

Furthermore, final consensus sequences from BC-16_g2112 and BC-16_contig_38_F2468 Sanger sequencing were aligned with the corresponding sequences obtained from the mapped PenSeq reads. The alignment confirmed the nucleotide sequences, highlighting the reliability of PenSeq (Figure 3.17).

a.



b.

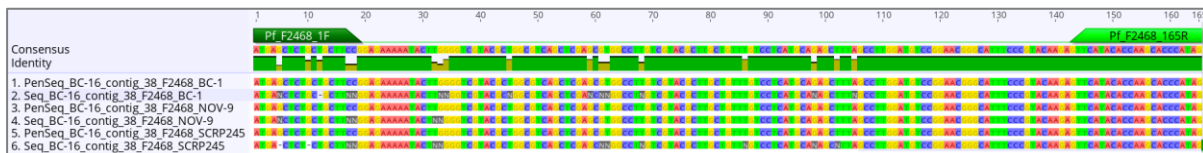


Figure 3. 17. Validation of PenSeq nucleotides sequences for BC-16_g2112 and BC-16_contig_38_F2468. Comparison between PenSeq analyses (odd rows, “PenSeq_[gene]_[isolate]”) and Sanger sequencing (even rows, “Seq-[gene]_[isolate]”) for **a.** BC-16_g2112 and **b.** BC-16_contig_38_F2468 genes for isolates of *P. fragariae*. Figures also show where primers bind. Nucleotide alignments were performed in Geneious and “N” refers to ambiguity (quality of consensus below threshold)

This study of eight more *P. fragariae* genes revealed conservation and diversity amongst genes of different functions and families (apoplastic, RXLRs) across 24 isolates.

3.3.7.3. *P. rubi* RXLR effectors

The third set of effectors included *P. rubi* RXLR genes identified with published prediction models (Whisson et al., 2007; Win et al., 2007). They showed variation in

their coverage across the 20 *P. rubi* isolates and four *P. fragariae* isolates (Tables 3.22 and 3.23 and Figure 3.18).

Table 3. 22. *P. rubi* RXLR effectors of interest

PenSeq gene ID	NCBI ID number	Gene description	Function	Type of diversity
SCR333_contig_4275_F7	PR003_g28352	<i>P. rubi</i> unique RXLR effector gene (Whisson et al., 2007), absent from four <i>P. fragariae</i> and present in all 20 <i>P. rubi</i> isolates	RXLR (Whisson et al., 2007)	species specific - unique to <i>P. rubi</i>
BC-16_contig_51_F623	PF003_g26871	<i>P. fragariae</i> / <i>P. rubi</i> RXLR effector gene (Win et al., 2007), conserved between the two species and the 24 isolates, identical between 23 isolates, polymorphism only in SCR333	RXLR (Win et al., 2007)	most conserved in 2 species
BC-16_contig_61_RC_R2199	PF003_g29701	<i>P. fragariae</i> / <i>P. rubi</i> RXLR effector gene (Whisson et al., 2007) identical between all 24 isolates	RXLR (Whisson et al., 2007)	most conserved in 2 species
SCR333_g19119	PR003_g20604	<i>P. rubi</i> RXLR effector gene (Whisson et al., 2007) identical between all 20 <i>P. rubi</i>	RXLR (Whisson et al., 2007)	most conserved in 1 species - identical between all <i>P. rubi</i>
SCR333_contig_7278_F2	PR003_g32027	<i>P. rubi</i> RXLR effector gene (Win et al., 2007) showing high species-polymorphism (SNPs in 20 <i>P. rubi</i> isolates)	RXLR (Win et al., 2007)	intra-species diversity - most diverse
SCR333_g24428	PR003_g26341	<i>P. rubi</i> RXLR effector gene (Whisson et al., 2007) with diversity and SNPs within <i>P. rubi</i> (RXLR Whisson et al., 2007 with lowest coverage sum)	RXLR (Whisson et al., 2007)	intra-species diversity - most diverse
SCR333_g19264	PR003_g20757	<i>P. rubi</i> RXLR effector gene (Whisson et al., 2007) with diversity and SNPs within <i>P. rubi</i>	RXLR (Whisson et al., 2007)	intra-species diversity - most diverse
SCR333_g28562	PR003_g30828	<i>P. rubi</i> RXLR effector (Whisson et al., 2007), showing SNPs and heterozygous SNPs in 19 isolates	RXLR (Whisson et al., 2007)	intra-species diversity - most diverse

Table 3. 23. Coverage data for selected *P. rubi* RXLR genes. Coverage data for eight *P. rubi* genes of interest at 0 % and 3 % mismatch mapping rates for all 24 isolates studied

PenSeq gene ID	SCR333_contig_4275_F7		BC-16_contig_51_F623		BC-16_contig_61_RC_R2199		SCR333_contig_7278_F2		SCR333_g19119		SCR333_g19264		SCR333_g24428		SCR333_g28562	
Predicted function	RxLR (Whisson et al., 2007)		RxLR (Win et al., 2007)		RxLR (Whisson et al., 2007)		RxLR (Win et al., 2007)		RxLR (Whisson et al., 2007)		RxLR (Whisson et al., 2007)		RxLR (Whisson et al., 2007)		RxLR (Whisson et al., 2007)	
Mismatch mapping rate	0%	3%	0%	3%	0%	3%	0%	3%	0%	3%	0%	3%	0%	3%	0%	3%
<i>P. rubi</i>	SCR1202	100.0	100.0	100.0	100.0	100.0	100.0	35.7	100.0	100.0	100.0	100.0	100.0	100.0	100.0	100.0
	SCR1207	100.0	100.0	100.0	100.0	100.0	100.0	83.1	100.0	100.0	100.0	0.0	100.0	100.0	100.0	100.0
	SCR1208	100.0	100.0	100.0	100.0	100.0	100.0	88.6	100.0	100.0	100.0	64.4	100.0	100.0	100.0	100.0
	SCR1212	100.0	100.0	100.0	100.0	100.0	100.0	88.0	100.0	100.0	100.0	100.0	100.0	100.0	100.0	100.0
	SCR1213	100.0	100.0	100.0	100.0	100.0	100.0	85.4	100.0	100.0	100.0	100.0	100.0	100.0	100.0	100.0
	SCR249	100.0	100.0	100.0	100.0	100.0	100.0	89.6	100.0	100.0	100.0	53.5	100.0	41.9	98.4	100.0
	SCR250	43.6	100.0	100.0	100.0	100.0	100.0	90.9	100.0	100.0	100.0	32.5	100.0	42.7	100.0	97.8
	SCR260	100.0	100.0	100.0	100.0	100.0	100.0	85.1	100.0	100.0	100.0	0.0	100.0	100.0	100.0	100.0
	SCR283	100.0	100.0	93.0	100.0	100.0	100.0	92.5	100.0	100.0	100.0	61.6	100.0	0.0	37.9	94.3
	SCR287	100.0	100.0	100.0	100.0	100.0	100.0	86.7	100.0	100.0	100.0	100.0	100.0	100.0	100.0	100.0
	SCR288	100.0	100.0	100.0	100.0	100.0	100.0	90.9	100.0	100.0	100.0	100.0	100.0	89.7	100.0	97.5
	SCR290	100.0	100.0	100.0	100.0	100.0	100.0	90.9	100.0	100.0	100.0	100.0	100.0	100.0	100.0	100.0
	SCR292	39.3	100.0	100.0	100.0	100.0	100.0	42.2	100.0	100.0	100.0	31.0	100.0	41.6	99.4	98.8
	SCR293	100.0	100.0	100.0	100.0	100.0	100.0	85.1	100.0	100.0	100.0	0.0	100.0	100.0	100.0	100.0
	SCR296	87.2	100.0	100.0	100.0	100.0	100.0	82.8	100.0	100.0	100.0	30.1	100.0	45.4	99.2	100.0
	SCR323	37.7	100.0	100.0	100.0	100.0	100.0	88.3	100.0	100.0	100.0	31.2	100.0	44.3	95.1	100.0
	SCR324	90.1	100.0	100.0	100.0	100.0	100.0	72.4	100.0	100.0	100.0	100.0	100.0	53.0	95.1	99.5
	SCR333	100.0	100.0	100.0	100.0	100.0	100.0	86.7	100.0	100.0	100.0	100.0	100.0	100.0	100.0	100.0
SCR338	42.0	100.0	100.0	100.0	100.0	100.0	85.4	100.0	100.0	100.0	70.7	100.0	0.0	0.0	81.8	
SCR339	100.0	100.0	100.0	100.0	100.0	100.0	89.9	100.0	100.0	100.0	100.0	100.0	100.0	100.0	100.0	
<i>P. fragariae</i>	BC-1	0.0	0.0	100.0	100.0	100.0	100.0	22.4	100.0	0.0	0.0	0.0	96.5	0.0	0.0	65.4
	BC-16	0.0	0.0	100.0	100.0	100.0	100.0	33.1	100.0	97.1	97.1	0.0	97.4	0.0	0.0	58.2
	NOV-9	0.0	0.0	100.0	100.0	100.0	100.0	19.2	100.0	0.0	0.0	0.0	100.0	63.3	85.8	43.0
	SCR245	0.0	0.0	100.0	100.0	100.0	100.0	0.0	100.0	0.0	0.0	40.0	93.4	15.1	68.9	70.3

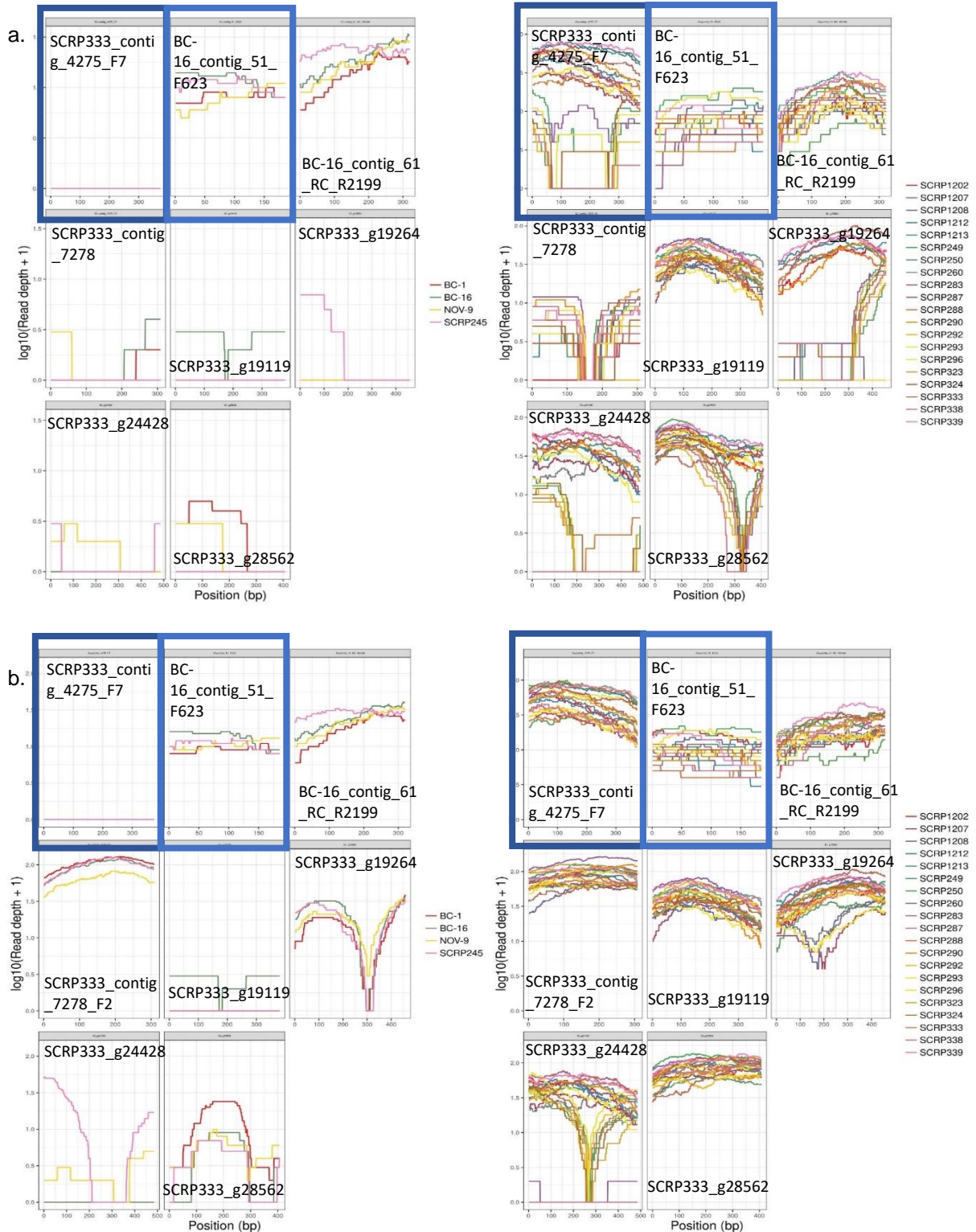


Figure 3. 18. Coverage graph for eight *P. rubi* RXLR. Left: *P. fragariae* isolates and right: *P. rubi* isolates at **a.** 0 % and **b.** 3 % mismatch mapping rates. Eight *P. rubi* predicted RXLR genes were selected and their coverage was retrieved at 0 % (**a.**) and 3 % (**b.**) mismatch mapping rates for the four *P. fragariae* isolates (left) using cross-species mapping and for the 20 *P. rubi* isolates (right) using same-species mapping. Blue rectangle highlights SCRP333_contig_4275_F7 and BC-16_contig_51_F623.

General polymorphism with sequence diversity and resulting amino acid changes were assessed for five diverse *P. rubi* genes of interest (Table 3.24): SCRP333_contig_4275_F7 (PR003_g28352, unique *P. rubi* RXLR), SCRP333_contig_7278_F2 (PR003_g32027, diverse), SCRP333_g24428 (PR003_g26341, diverse RXLR absent in the Canadian isolate), SCRP333_g19264 (PR003_g20757, diverse) and SCRP333_g28562 (PR003_g30828, with heterozygous SNPs). Extraction of nucleotide sequences for SCRP333_contig_7278_F2 only revealed heterozygous SNPs, meaning identical protein sequences between all isolates (hence not shown in Table 3.24).

BLASTx of *P. rubi* RXLR SCRP333_g28562 showed 86 % protein identity with a putative *P. fragariae* RXLR sequence PF003_g37524, explaining the partial coverage of the gene (Table 3.23, Appendix B, Figure B.6). SCRP333_g28562 also matched RXLR effectors in *P. palmivora* (POM74617.1, 59 % protein identity) and in *P. parasitica* P1569 (ETI47704.1, 58 % protein identity). Similarly, BLASTx search of SCRP333_g19264 found matches to other RXLR genes in *P. cinnamomi* (55 % identity) and *P. sojae* (46 %). SCRP333_g24428/ PR003_g26341 was shown to be absent in the Canadian *P. rubi* isolate (SCR338) and highly diversified in USA isolate SCR283, making SCRP333_g24428 a candidate marker for testing regional isolates; a hypothesis that would need a bigger sample size to be confirmed. BLASTx of SCRP333_g24428 revealed distant matches in other species including *P. cinnamomi*, *P. parasitica* and *P. sojae*.

Only one *P. rubi* RXLR, SCRP333_contig_4275_F7 (PR003_g28352) was found to be unique to *P. rubi* and absent in *P. fragariae*, which is displayed by the absence (0 %) of coverage in any of the four *P. fragariae* isolates at any mismatch rates, 0 %, 3 % and 5 % mm (5 % mm not shown here). SCRP333_contig_4275_F7 displayed sequence polymorphism and SNPs across the *P. rubi* isolates (Table 3.23, Figure 3.18). BLASTx of this RXLR found that it shared 71 % identity at the protein level and 83 % at the nucleotide level with another *P. rubi* RXLR (PR003_g29800, PenSeq ID SCRP333_contig_5194_F3) which has a match in *P. fragariae* (PF003_g30833) and shares high homology with *P. sojae* and *P. parasitica*.

Study of the extracted nucleotide sequences for SCRP333_contig_4275_F7 (PR003_g28352) revealed that the low coverage at 0 % mismatch mapping rate was due to the presence of two SNPs, thus preventing appropriate reads to be picked up and matched against the reference genome (Table 3.24). These SNPs led to non-synonymous amino acid substitution (Table 3.24).

SCRP333_contig_4275_F7 was selected for *in vitro* PCR validation (Table 3.7). Coverage data showed that SCRP333_contig_4275_F7 should be amplified for all *P. rubi* but not for any of the four *P. fragariae* (Table 3.23), while polymorphism within *P. rubi* was detected (Table 3.24). Our aim was to first validate the absence of SCRP333_contig_4275_F7 in our four *P. fragariae* isolates compared to selected *P. rubi* isolates, and to confirm at least one of the two SNPs observed in PenSeq sequences. *In silico* primer testing of SCRP333_contig_4275_F7 with Geneious predicted amplification for all *P. rubi* isolates along with lack of amplification for *P. fragariae* isolates BC-1, BC-16, NOV-9 and SCRP245. This was confirmed by *in vitro* PCR and agarose gel electrophoresis (Figure 3.19), showing no amplification in *P. fragariae*.

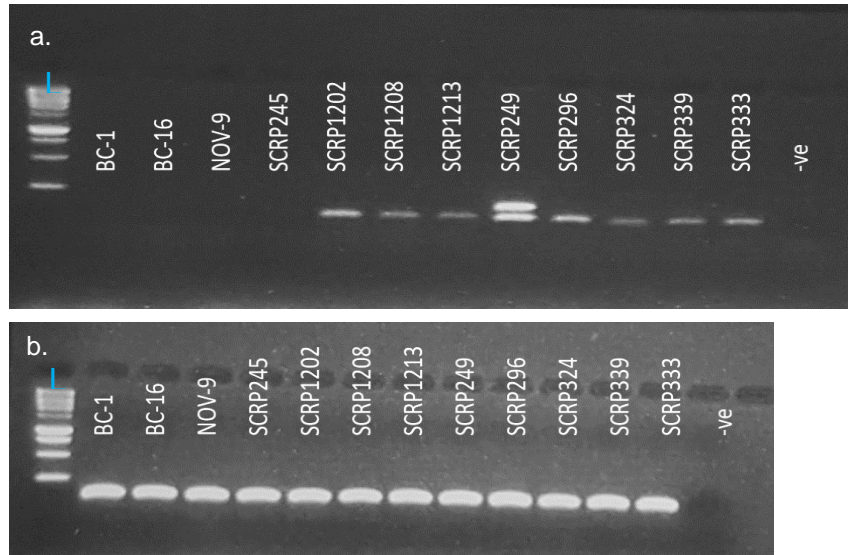


Figure 3. 19. Agarose electrophoresis gels for SCRP333_contig_4275_F7. Agarose electrophoresis gels (2 % agarose) testing **a.** *P. rubi* unique RXLR SCRP333_contig_4275_F7 primers and **b.** *CoxI* control to check presence of DNA in *P. fragariae* isolates templates. SCRP333_contig_4275_F7 amplicon size is 188 bp and *Cox I* amplicon size is 127 bp. Blue ladder (L) is 1 kb. Negative control (-ve) using SdW did not show amplification.

SCRP333_contig_4275_F7 gene was sequenced for a subset of seven *P. rubi* isolates: SCR1208, SCR250, SCR292, SCR296, SCR324, SCR333 and SCR338. Resulting cleaned consensus sequences were aligned and one SNP located within the amplicon was confirmed (Table 3.24 and Figure 3.20). It should be noted that the two bands observed on the SCR333_contig_4275_F7 gel following PCR had been confirmed to be SCR333_contig_4275_F7 gene, using gel extraction (data not shown).

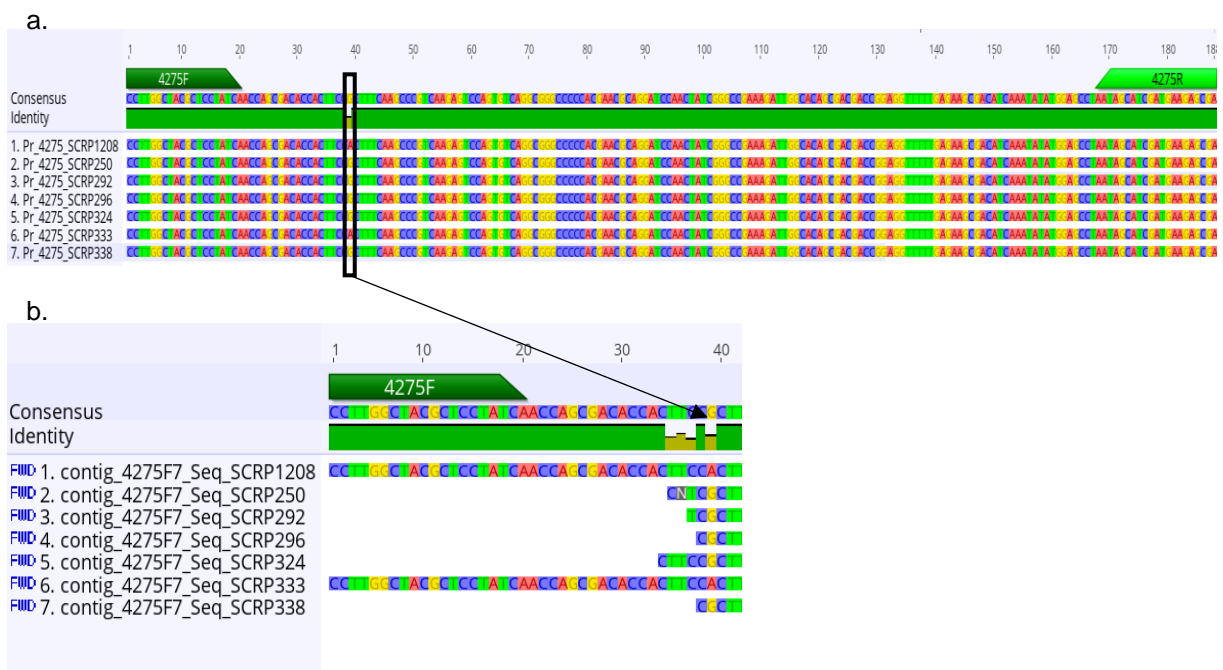


Figure 3. 20. Validation of PenSeq SNPs for SCR333_contig_4275_F7 gene. a. Nucleotide alignment of SCR333_contig_4275_F7 gene a subset of seven *P. rubi* PenSeq isolates on the SCR333_contig_4275_F7 region amplified with designed primers: SCR1208, SCR250, SCR292, SCR296, SCR324, SCR333 and SCR338. Sequences were extracted from PenSeq data and SNP is highlighted (black rectangle, position 39 on alignment). b. Nucleotide sequences extracted from Sanger sequencing for the SCR333_contig_4275_F7 gene for the seven *P. rubi* isolates. SNP at position 39 was confirmed, as pointed by the arrow. Nucleotide alignments were performed in Geneious.

Another interesting *P. rubi* RXLR, SCR333_g19119 (PR003_g20604), was found to be identical in all *P. rubi* isolates (100 % covered at 0 % mm) and absent in three of the *P. fragariae* (Table 3.23, Figure 3.18). SCR333_g19119 top matches in other species were *P. infestans* secreted RXLR PITG_14093 (XP_002899221.1) with 45 % protein identity and *P. sojae* Avr effector, Avh265 (AEK81071.1) with 41 % protein identity, all presenting RXLR-EER motifs.

Two RXLRs were found to be highly conserved between species: BC-16_contig_51_F623 (PF003_g26871) and BC-16_contig_61_RC_R2199 (PF003_g29701) showing 100 % coverage at 0 % mismatch rate across all isolates of both species, except for BC-16_contig_51_F623 gene in SCRP283 (USA, 1987; 93 % coverage) indicating that these two effectors could have an important conserved function (Figure 3.18, Table 3.23). SNPs in the SCRP283 reads mapped to BC-16_contig_51_F623 were located in the 5' region ahead of the gene coding sequence but preventing reads to map the reference (Appendix B, Figure B.7). Using the extracted sequence from 3 % mm mapping revealed that the nucleotide sequence for SCRP283 for RXLR gene BC-16_contig_51_F623 was in fact an exact match to the other isolates (Figure 3.21).

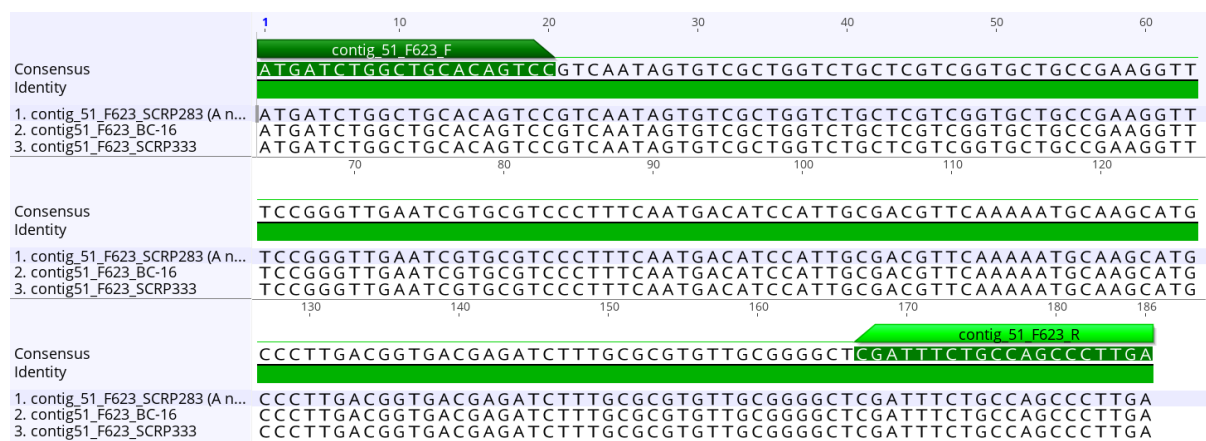


Figure 3. 21. Nucleotide alignment for BC-16_contig_51_F623 RXLR gene. Geneious nucleotide alignment of BC-16_contig_51_F623 for *P. rubi* SCRP283 and SCRP333 and *P. fragariae* BC-16 showing *in silico* primers tested.

Although numerous PenSeq reads will usually overlap and map to the same gene, sequence gaps and SNPs ahead of coding regions can interfere with the mapping and coverage analyses, highlighting the importance of screening at higher mismatch rates and the need for the extraction of sequences and their alignment to truly explore the conservation / variation of genes. BLASTx of BC-16_contig_51_F623 (PF003_g26871) and BC-16_contig_61_RC_R2199 (PF003_g29701) showed that they had equivalent proteins ('hypothetical proteins') in other *Phytophthora* species, like *P. sojae*, *P. cinnamomi*, *P. palmivora*, *P. megakarya*, *P. nicotianae*, and *P. parasitica* for the former (68 % to 83 % identity) and in *P. sojae* for the latter (with a lower match of 45 % to 74 % identity). PCR test of BC-16_contig_51_F623 showed

the anticipated amplification in *P. rubi* and *P. fragariae* and thus also independently validated PenSeq (Figure 3.22).

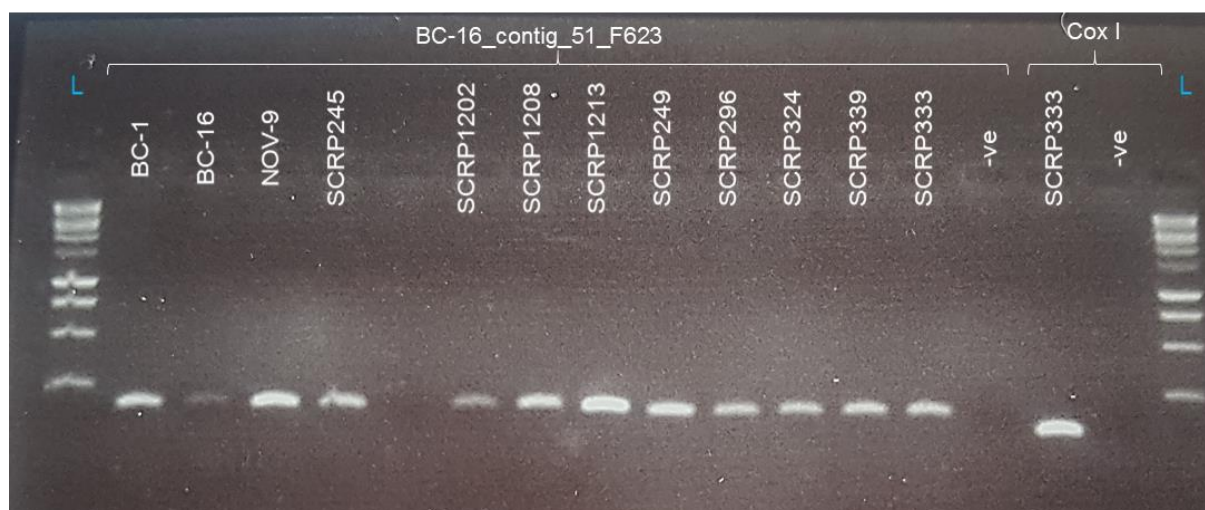


Figure 3. 22. Agarose electrophoresis gel following PCR of BC-16_contig_51_F623. Agarose gel (2 % agarose) tested conserved RXLR gene BC-16_contig_51_F623 primers with Cox I control. BC-16_contig_51_F623 amplicon size is 186 bp and Cox I amplicon size is 127 bp. Blue ladder (L) is 1 kb. Negative control (-ve) using SdW did not show amplification.

3.3.7.4. *P. rubi* PAMP and effectors involved in infections

Apoplastic effectors can also be very interesting indicators of diversifying selection and can be important in limiting host range of pathogens (Hein et al., 2009; Chaparro-Garcia et al., 2011). Here we selected a range of effectors published in other *Phytophthora* species (Tian et al., 2004; Tian et al., 2005; Kanneganti et al., 2006; Ma et al., 2017; Guo et al., 2020; Rocafort et al., 2020), as well as effectors from PenSeq analyses (Table 3.25 and Appendix B, Figure B.8). Apoplastic genes expressed in infection and genes involved in PAMP-triggered immunity responses, such as PaRXLR40, PaRXLR24, EPIC1, EPIC2B, EPIC3 and PsXLP1 had matching genes in *P. rubi* (Table 3.26 and Figure 3.23).

Table 3. 25. Description of eight *P. rubi* apoplastic effector of interest

Effector and accession	PenSeq ID	NCBI <i>P. rubi</i> number ID	Original organism used for BLAST search	Percentage Identity between original and <i>P. rubi</i>	Function / Gene description	References
PaRXLR40 (QMU2486 4.1)	SCR333_g13165	PR003_g14130	<i>P. agathidici da</i>	33.3 %	PaRXLR40 can suppress Avr3a-R3a cell death. Expressed in infection	Guo et al., 2020

Effector and accession	PenSeq ID	NCBI <i>P. rubi</i> number ID	Original organism used for BLAST search	Percentage Identity between original and <i>P. rubi</i>	Function / Gene description	References
PaRXLR24 (QMU2484 8.1)	SCR333_g29010	PR003_g31306	<i>P. agathidici da</i>	55.5 %	PaRXLR24 is similar to PsAvh238 from <i>P. sojae</i> , and pPE4 from <i>P. parasitica</i> . Expressed in infection	Guo et al., 2020
EPIC1 (A1L015)	SCR333_g24119	PR003_g26002	<i>P. infestans</i>	53.8 %	Inhibits host cysteine proteases	Tian et al., 2004; Tian et al., 2005; Rocafort et al., 2020
EPIC2B (D0NBV3)				55.4 %		
EPIC3 (D0NP95)				73.1 %		
PsXLP1 (G4ZHR3)	SCR333_g8655	PR003_g9263	<i>P. sojae</i>	82.5 %	Decoy that protects PsXEG1 from the inhibitory action of a host xyloglucan-specific endoglucanase inhibitor protein	Ma et al., 2017
INF1 (AY830094 .1)	SCR333_g25193	PR003_g27228	<i>P. rubi</i>	91.5 %	Elicitin protein inducing HR (necrosis inducing)	Kaneganti et al., 2006
SCR333_contig_1656_RC_R9	SCR333_contig_1656_RC_R9	PR003_g19542	<i>P. rubi</i>	N/A	<i>P. rubi</i> apoplastic gene showing sequence diversity and variation in coverage amongst <i>P. rubi</i>	
SCR333_g28651	SCR333_g28651	PR003_g30919	<i>P. rubi</i>	N/A	<i>P. rubi</i> unique gene (unknown function), absent from four <i>P. fragariae</i> and present in all 20 <i>P. rubi</i> isolates	
SCR333_contig_1090_RC_R83	SCR333_contig_1090_RC_R83	PR003_g15594	<i>P. rubi</i>	N/A	<i>P. rubi</i> unique apoplastic effector gene, absent from four <i>P. fragariae</i> and present and identical in all 20 <i>P. rubi</i> isolates	

SCR333_contig_1656_RC_R9, an apoplastic effector, appears to be absent from isolates with little apparent links: SCR338, a Canadian isolate from 1987, SCR339, a French one from 1985 and SCR333, a Scottish isolate collected in 1985, but present in all others *P. rubi*, showing high polymorphism (Table 3.26 and Figure 3.23).

Four of the eight apoplastic effectors selected showed complete conservation with identical sequences amongst *P. rubi* isolates but absence or high sequence polymorphism in *P. fragariae* (SCR333_contig_1090_RC_R83/ PR003_g15594; SCR333_g13165/ PR003_14130; SCR333_g24119/ PR003_g26002 and SCR333_g29010/ PR003_g31306) (Table 3.26 and Figure 3.23).

Table 3. 26. Coverage data for eight *P. rubi* genes. Coverage for eight *P. rubi* genes of interest at 0 % and 3 % mismatch mapping rates for all 24 isolates studied.

PenSeq gene ID	SCR333_contig_1090_RC_R83		SCR333_contig_1656_RC_R9		SCR333_g13165		SCR333_g24119		SCR333_g25193		SCR333_g28651		SCR333_g29010		SCR333_g8655	
Gene of interest	P. rubi unique and conserved apoplastic effector		P. rubi apoplastic gene with coverage variation		PaRxLR40		PIEPI1/PIEPI2B/EPIC3		PrINF1		P. rubi unique gene (unknown function)		PaRxLR24		PsXLP1	
Mismatch mapping rate	0%	3%	0%	3%	0%	3%	0%	3%	0%	3%	0%	3%	0%	3%	0%	3%
<i>P. rubi</i>	SCR1202	100.0	100.0	83.5	83.5	100.0	100.0	100.0	100.0	100.0	100.0	100.0	100.0	100.0	100.0	100.0
	SCR1207	100.0	100.0	92.1	92.1	100.0	100.0	100.0	100.0	100.0	100.0	100.0	100.0	100.0	83.2	100.0
	SCR1208	100.0	100.0	57.3	57.3	100.0	100.0	100.0	100.0	100.0	100.0	100.0	100.0	100.0	99.2	100.0
	SCR1212	100.0	100.0	50.0	100.0	100.0	100.0	100.0	100.0	100.0	100.0	100.0	100.0	100.0	100.0	100.0
	SCR1213	100.0	100.0	100.0	100.0	100.0	100.0	100.0	100.0	100.0	100.0	100.0	100.0	100.0	100.0	100.0
	SCR249	100.0	100.0	44.5	64.0	100.0	100.0	100.0	100.0	100.0	100.0	100.0	100.0	100.0	100.0	100.0
	SCR250	100.0	100.0	43.9	43.9	100.0	100.0	100.0	100.0	100.0	100.0	94.0	97.5	100.0	100.0	100.0
	SCR260	100.0	100.0	100.0	100.0	100.0	100.0	100.0	100.0	100.0	100.0	100.0	100.0	100.0	99.6	100.0
	SCR283	100.0	100.0	100.0	100.0	100.0	100.0	100.0	100.0	100.0	100.0	100.0	100.0	100.0	100.0	100.0
	SCR287	100.0	100.0	97.6	100.0	100.0	100.0	100.0	100.0	100.0	100.0	100.0	100.0	100.0	100.0	100.0
	SCR288	100.0	100.0	99.4	100.0	100.0	100.0	100.0	100.0	100.0	100.0	100.0	100.0	100.0	100.0	100.0
	SCR290	100.0	100.0	100.0	100.0	100.0	100.0	100.0	100.0	100.0	100.0	100.0	100.0	100.0	100.0	100.0
	SCR292	100.0	100.0	100.0	100.0	100.0	100.0	100.0	100.0	86.5	100.0	95.0	100.0	100.0	100.0	100.0
	SCR293	100.0	100.0	0.0	27.4	100.0	100.0	100.0	100.0	100.0	100.0	91.5	91.5	100.0	83.7	83.7
	SCR296	100.0	100.0	61.0	61.0	100.0	100.0	100.0	100.0	100.0	100.0	100.0	100.0	100.0	100.0	100.0
	SCR323	100.0	100.0	100.0	100.0	100.0	100.0	100.0	100.0	100.0	100.0	100.0	100.0	100.0	100.0	100.0
	SCR324	100.0	100.0	0.0	26.2	100.0	100.0	100.0	100.0	100.0	100.0	100.0	100.0	100.0	100.0	100.0
SCR333	100.0	100.0	0.0	0.0	100.0	100.0	100.0	100.0	100.0	100.0	100.0	100.0	100.0	100.0	100.0	
SCR338	100.0	100.0	0.0	0.0	100.0	100.0	100.0	100.0	100.0	100.0	100.0	100.0	100.0	100.0	100.0	
SCR339	100.0	100.0	0.0	0.0	100.0	100.0	100.0	100.0	100.0	100.0	100.0	100.0	100.0	100.0	100.0	
<i>P. fragariae</i>	BC-1	0.0	0.0	26.2	26.2	28.0	28.0	0.0	100.0	0.0	100.0	0.0	0.0	0.0	0.0	100.0
	BC-16	0.0	0.0	0.0	93.9	0.0	0.0	0.0	75.0	16.9	100.0	0.0	0.0	0.0	0.0	100.0
	NOV-9	0.0	0.0	0.0	56.7	0.0	0.0	63.8	94.9	0.0	94.7	0.0	0.0	0.0	0.0	100.0
	SCR245	0.0	0.0	0.0	100.0	0.0	0.0	0.0	100.0	0.0	87.1	0.0	0.0	0.0	0.0	100.0

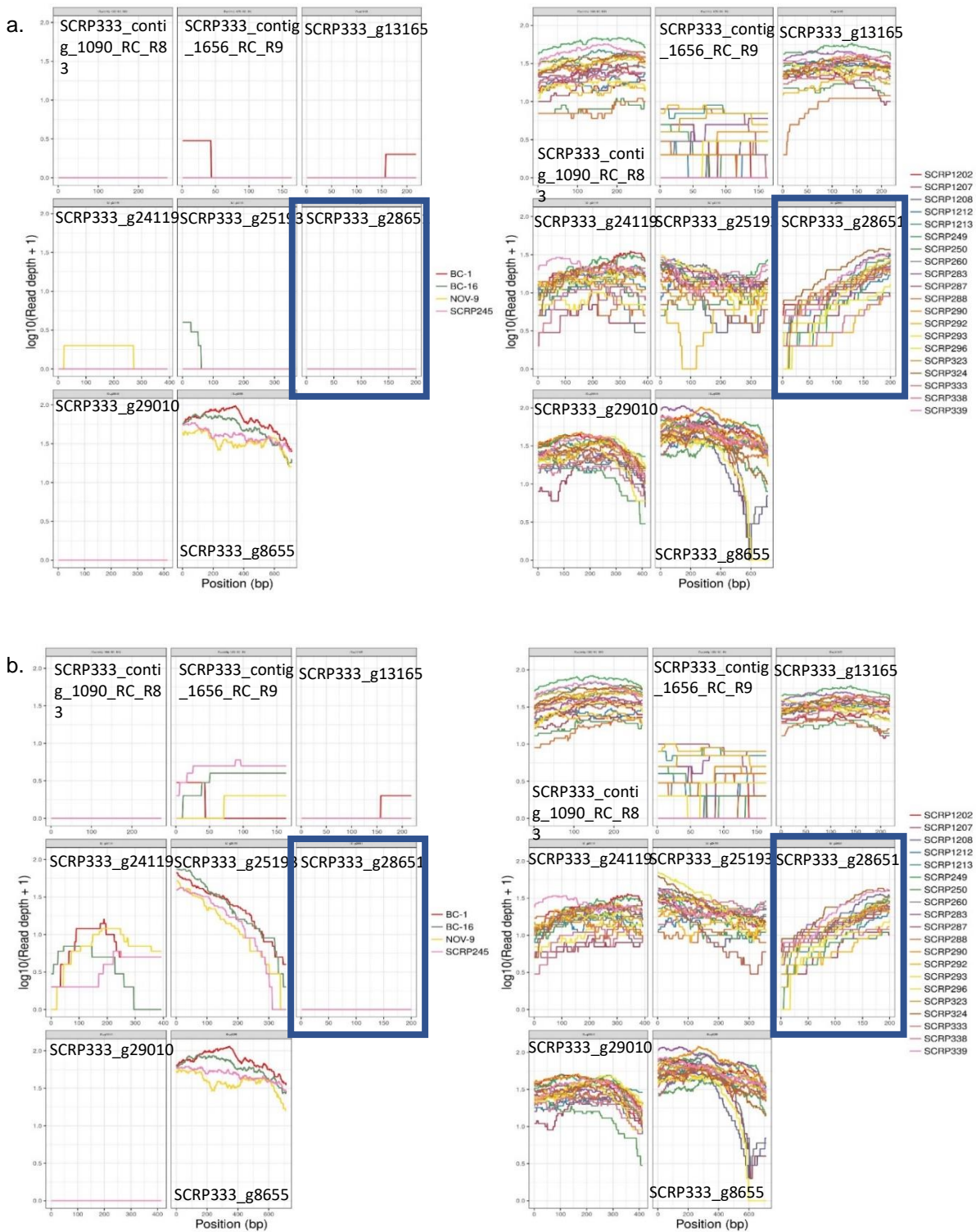


Figure 3. 23. Coverage graph for eight *P. rubi* apoplast genes. Left: *P. fragariae* isolates and right: *P. rubi* isolates at **a.** 0 % and **b.** 3 % mismatch mapping rates. Eight *P. rubi* effector genes were selected and their coverage was retrieved at 0 % (**a.**) and 3 % (**b.**) mismatch mapping rates for the four *P. fragariae* isolates (left) using cross-species mapping and for the 20 *P. rubi* isolates (right) using same-species mapping. Blue rectangle highlights SCRP333_g28651.

A further three of the eight genes showed a coverage difference in less than four of the 20 *P. rubi* isolates (SCR333_g25193/ PR003_g27228; SCR333_g28651/ PR003_g30919 and SCR333_g8655/ PR003_9263).

SCR333_g28651 (PR003_g30919), showing high coverage at 0 % and 3 % mismatch mapping rates for *P. rubi* and 0 % in *P. fragariae* was tested via PCR (Table 3.7). Coverage data showed that SCR333_g28651 should be amplified for all *P. rubi* but not for any of the four *P. fragariae*; which was confirmed *in silico* with primer testing and *in vitro* with PCR and gel electrophoresis (Figures 3.24).

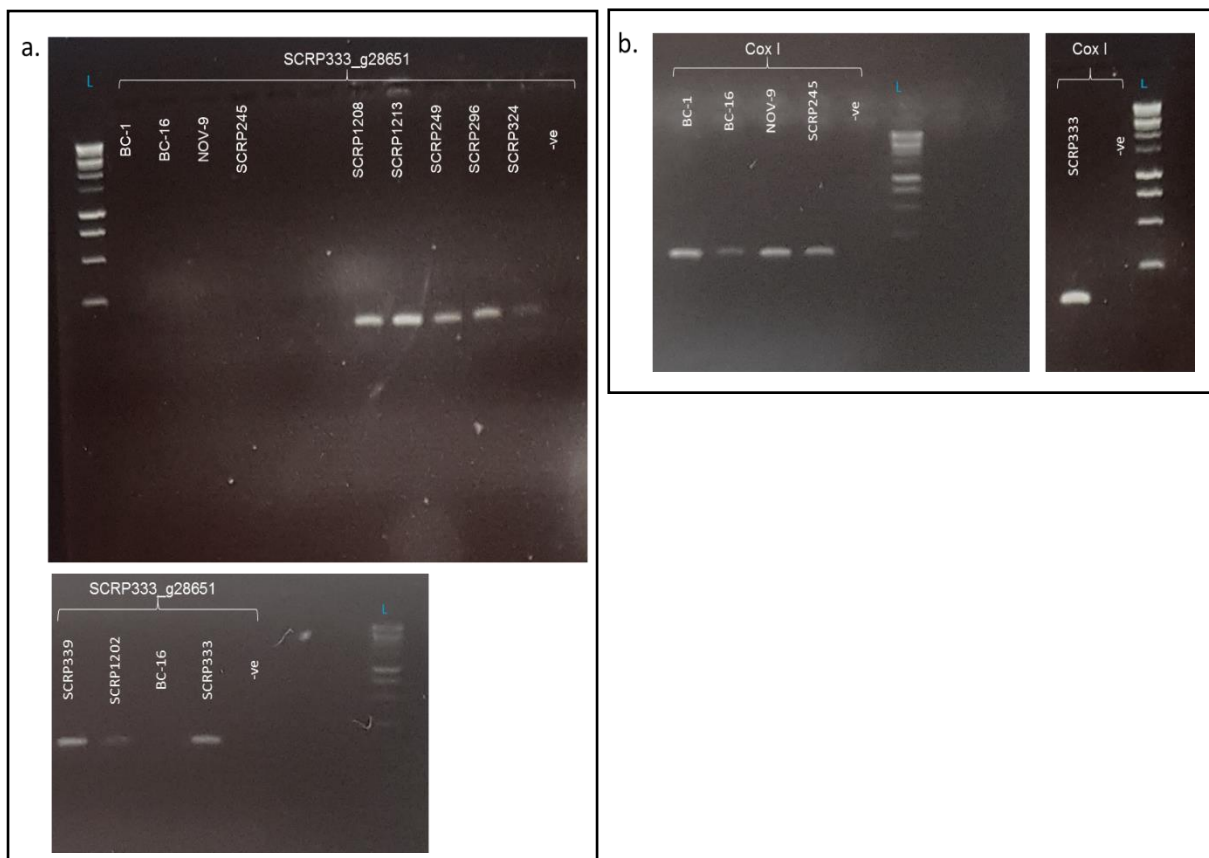


Figure 3. 24. Agarose electrophoresis gels for SCR333_g28651. Agarose electrophoresis gels (2 % agarose) testing *P. rubi* unique gene SCR333_g28651 (a) with *Cox I* control to check presence of DNA in *P. fragariae* templates (b). SCR333_g28651 amplicon size is 111 bp and *Cox I* amplicon size is 127 bp. Gel a. shows amplification of appropriate size amplicons for SCR333_g28651 for all *P. rubi* isolates tested, while *P. fragariae* did not show amplifications. Gel b. shows amplification of all samples for *Cox I*. Blue ladder (L) is 1 kb. Negative control (-ve) using SdW did not show amplification.

Furthermore, nucleotides sequences for SCR333_g28651 were confirmed for a subset of six isolates (SCR1202, SCR1208, SCR1213, SCR249, SCR296 and SCR333). Unfortunately, we were unable to obtain high-quality sequences from more isolates to confirm SNPs of that gene (Figure 3.25).

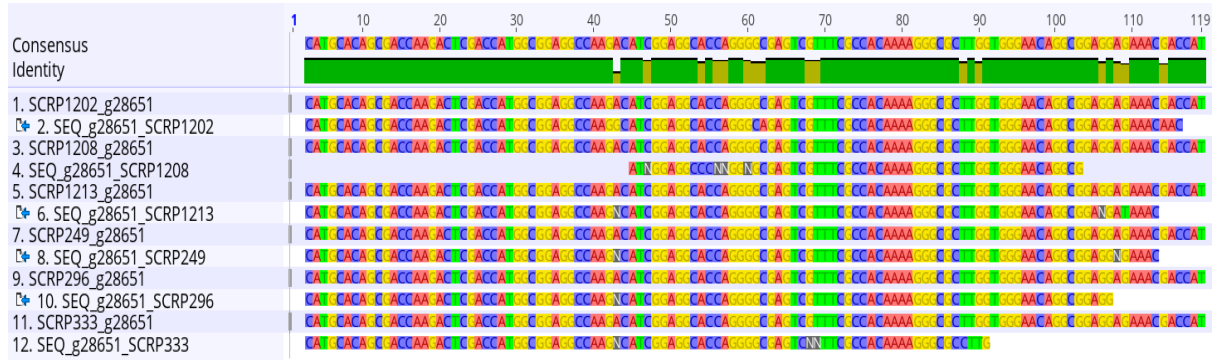


Figure 3. 25. Sequencing to confirm nucleotide sequences for SCR333_g28651. Following SCR333_g28651 conventional PCR, Sanger sequencing was performed. “SEQ_g28651_[isolate]” refers to consensus sequences after Sanger (even rows). Sequences are compared to PenSeq sequences of SCR333_g28651 (“[isolate]_g28651”, odd rows) using nucleotide alignment (Geneious).

Interestingly, SCR333_g8655 (PR003_g9263) identified as a top match for PsXLP1 (which protects PsXEG1 from inhibition). SCR1207, SCR1208, SCR260 and SCR293 showed heterozygous SNPs, explaining the partial coverage of that gene. SCR293 also showed sequence gap, where no reads mapped at 3 % mm (Figure 3.26). In addition, SCR1207 and SCR1208, isolated in Perthshire (farm A) in 2017, showed three SNPs on SCR333_g8655, compared to other *P. rubi* sequences (positions 599, 601 and 605, Figure 3.26).

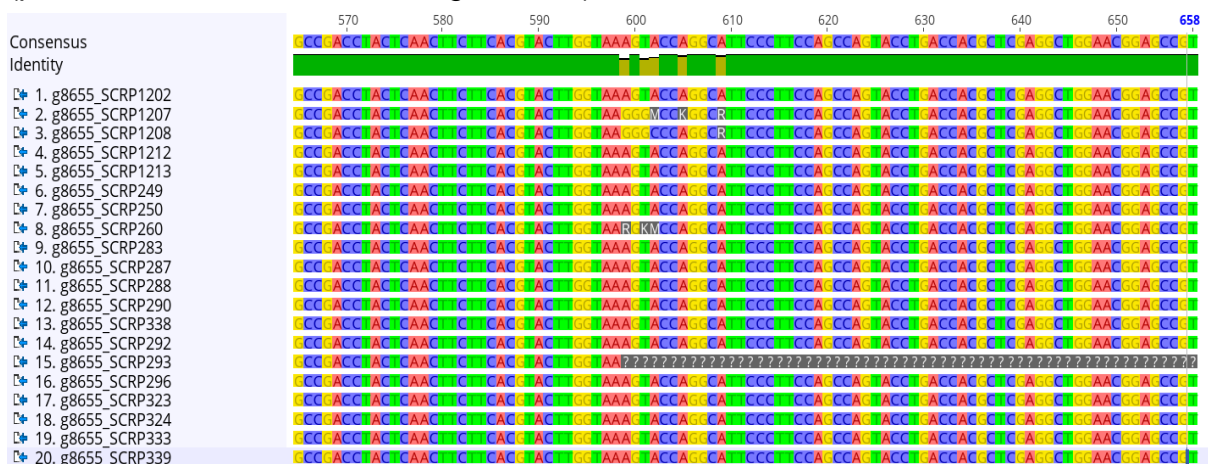


Figure 3. 26. Nucleotide sequences alignment for SCR333_g8655, matching *P. sojae* PsXLP1. Nucleotides sequences from PenSeq were aligned with Geneious for the 20 *P. rubi* isolates. Alignment shows SNPs at positions 599, 601 and 605 for SCR1207 and SCR1208 (isolated in Invergowrie, 2017) compared to other isolates.

PenSeq enabled the rapid identification of both core conserved effectors and effectors under diversifying selection. Here we have carried out a more in-depth study of 32 of those genes, conforming to specific patterns: *P. rubi* or *P. fragariae* genes, species-specific genes, RXLRs, genes expressed *in planta* and orthologs of genes with published functions. Additionally, for six of those genes, presence / absence variations, nucleotide sequences and SNPs that were detected through PenSeq analyses were confirmed with PCR and Sanger sequencing assays.

3.4. Discussion and conclusions

P. rubi and *P. fragariae* are two closely related oomycete species that diverged approximately 10 million years ago. They infect plant species of the same *Rosaceae* family, from the *Rubus* and *Fragariae* genus, that diverged around 57 million years.

The molecular reasons why and how these two pathogens infect two different crops is of interest to both soft fruit growers and molecular plant pathologists alike. This chapter utilises target enrichment sequencing of pathogen sequences (PenSeq) to determine the diversity between species and isolates and use it to try and predict geographical, chronological and race-related relationships in *P. fragariae* and *P. rubi*. PenSeq is a highly robust and representative approach that enables the identification of presence / absence, polymorphism and genetic variants for any and multiple genes of interest. PenSeq enrichment provides good coverage of *P. rubi* and *P. fragariae* isolates for effector, housekeeping and drug target genes, as previously proven by Thilliez et al. (2019). Two isolates with available genome sequences were used as references, *P. rubi* SCRP333 and *P. fragariae* BC-16. PenSeq analyses of these two strains show the highest mapping percentages at 0 % mismatch, as predicted. However, coverage of BC-16 and SCRP333 appeared below 100 % (77.15 % and 69.56 % respectively at 0 % mismatch), indicating diversification in the lab strains. Effector gene loss in lab strains over time has been previously reported, where 16 RXLRs appeared to be missing from the *P. infestans* reference genome (T30-4) after PenSeq, later confirmed by PCR (Thilliez et al., 2019). Correspondingly, this study here identifies genes absent from reference genomes, such as BC-16_contig_38_F2468, present and covered in all *P. fragariae* except for BC-16. The absence of this effector is confirmed via PCR. This can be explained by possible annotation / sequencing mistakes, potential evolution of the pathogen in the lab over time, and / or presence of allelic variation not

reflected during whole genome sequencing (Thilliez et al., 2019). Since numerous RXLR effectors are associated with regions of the genome where many mobile genetic elements reside, genetic rearrangements are not uncommon and gene deletion is not unusual in *Phytophthora* species. Prolonged artificial culturing does appear to induce loss of virulence as lab strains become 'lazy' and gradually lose the ability to infect plants (Judelson and Whittaker, 1995; van der Lee et al., 2001; Sandhu et al., 2004; Jiang et al., 2006; Na et al., 2013; Adams, 2019). It can therefore be expected that not all effectors would be present from isolates recovered from long-term storage (~ 40 years) and may not be identical to the genomes of the same isolates sequenced by other labs.

PenSeq analysis highlights several candidates for further evolutionary and phylogenetic studies. While it is crucial to screen multiple genes to draw evolutionary conclusions, single housekeeping genes are often used in detection tools. Housekeeping gene polymorphism could be useful to generate better and faster detection through PCR, using species-specific primers on highly polymorphic regions of the gene. Diagnostics of *P. rubi* and *P. fragariae* from samples collected in the field is currently based on sequencing of the *Cox1* gene. In this chapter, PenSeq identifies several other housekeeping genes candidates showing high inter-species polymorphism, such as *tigA* and *Hsp90* genes. While variation between species is important in housekeeping genes, and as we speculated at the beginning of the work, a higher resolution into the divergence within species is provided with analyses of effector genes, compared to traditional genes used for phylogenetic analysis of housekeeping genes.

Effectors are an important class of proteins that are needed to overcome the defense responses in plant hosts in order for the pathogen to cause disease and reproduce. Effectors are sensitive to selection pressures making them fast evolving. When conserved across a number of isolates, they are termed core effectors (Evangelisti et al., 2017) and imply an essential function in virulence of the pathogen. This means they cannot easily be mutated or lost without a detrimental effect on the pathogen. Previous studies into genetic comparisons between *P. rubi* and *P. fragariae* by Adams et al. (2019, 2020) have revealed differences in the effector complements between the two species; however, these studies did not identify substantial diversity within in isolates of *P. fragariae*. In addition, work described by Tabima et al. (2018) highlighted

the struggle to detect noticeable differences between *P. rubi* isolates that could help track the spread of the disease and the evolution of virulence of different isolates in the USA. Displaying the PenSeq data as colour-coded coverage tables (Figures 3.8, 3.9 and 3.10) constitute a great visual tool to summarize the genetic diversity for different genes across many isolates. This allows quick comparisons of country, time of isolation and race. Our hypothesis was that diversity in housekeeper genes were not suitable to compare isolates of the same species and that PenSeq provided a wealth of information on the genes families in which we were interested. For any targeted gene (such as housekeeping, drug targets or effectors), the distinction between species is evident. Read coverage of genes mapped to the other species reference genome is significantly decreased at any mismatch mapping rate. Only 3.7 % of all effectors are completely identical between the 24 isolates, 20 *P. rubi* and 4 *P. fragariae*. Compared with identical genes amongst isolates of one species, those values go up to 22 % for *P. rubi* and 43 % for *P. fragariae*. The higher percentage for *P. fragariae* is most probably due to the small number of isolates studied compared to that of *P. rubi*. When considering fast evolving effectors in two distinct but closely related species, this small percentage is not surprising, perhaps stressing the existence of more differences than initially thought between the two organisms. Subsequently, species-specific genes have been identified through PenSeq and confirmed using *in vitro* PCR. These genes could be involved in key stages of pathogenicity and determine host range. PenSeq therefore provides a powerful tool to study the diversity and polymorphism in thousands of effector genes simultaneously and can be used to inform and to estimate the diversity in the effector complements of the examined isolates. A total of 217 effector genes were found to be unique to *P. rubi* and 218 unique to *P. fragariae*. Following Gao et al. (2021) and Schulze-Lefert and Panstruga (2011) studies, we hypothesize that *P. fragariae* isolates have lost effectors that are conserved in *P. rubi* isolates or gained new effectors, in order to infect *Fragaria* species. Therefore, and according to our assumption, some of the 218 *P. fragariae* effectors could have been gained while several the 217 *P. rubi* effectors could have also been lost in parallel to infect *Fragaria* species.

We noticed that overall, housekeeping, drug target and CRNs genes show the lowest level of variation amongst isolates of one species, while RXLR and apoplastic effectors have higher divergence between isolates, which reflects their *in planta* virulence functions and associated evolutionary pressure. Nevertheless, an additional method

bringing all the gene sequencing information together to provide a global view of the relatedness and diversity between isolates is successfully implemented using k-mer. K-mer analyses based on all enriched genes as well as focused on particular gene families provide evidence of clustering between isolates and clearly differentiate the two species. Though there does not appear to be a clear distinction between isolates collected from a particular year, location or predicted race that has been identified thus far, which suggests a high level of plasticity.

Identical RXLR effector genes shared amongst isolates of one species were found to represent 32 % of *P. rubi* and 65 % of *P. fragariae* pool of studied RXLR genes (Table 3.27).

Table 3. 27. Summary table. a. Percentages of identical genes. Percentages of genes that are 100 % covered at 0 % mismatch mapping rate in *P. rubi* and *P. fragariae* for apoplastic, RXLR and CRN effectors and housekeeping / drug target genes. **b.** Percentages of genes absent (0 % covered) in one or more isolate at 5 % mismatch mapping rate in *P. rubi* and *P. fragariae* for apoplastic, RXLR and CRN effectors and housekeeping / drug target genes.

a.	Percentages of identical genes (100 % covered at 0 % mismatch mapping rate)		
	<i>P. fragariae</i>	<i>P. rubi</i>	<i>P. rubi</i> mapped to <i>P. fragariae</i> BC-16
Apoplastic effectors	62.7 %	32.4 %	6.9 %
CRN effectors	68.8 %	23.3 %	0
RXLR effectors (Win et al., 2007; Whisson et al., 2007)	64.7 %	31.6 %	5.1 %
Housekeeping / Drug target genes	35.3 %	16.7 %	0
b.	Percentages of genes absent (0 % covered) in one or more isolate at 5 % mismatch mapping rate		
	<i>P. fragariae</i>	<i>P. rubi</i>	<i>P. rubi</i> mapped to <i>P. fragariae</i> BC-16
Apoplastic effectors	5.8 %	12 %	60.2 %
CRN effectors	0	0	56.9 %
RXLR effectors (Win et al., 2007; Whisson et al., 2007)	3.3 %	5.6 %	63.41 %
Housekeeping / Drug target genes	0	0	53 %

This suggests that the majority of RXLR effectors selected for *P. rubi* are showing some level of polymorphism between isolates that previous studies have failed to identify. Adams (2019) and Tabima et al. (2018) used whole genome sequencing for *de novo* assembly and pathogenomic studies but failed to detect much intra-species differentiation. Here, PenSeq analyses focus on mostly fast evolving effector sequences. PenSeq finds key genes involved in virulence (RXLR, CRN and apoplastic) that are diversifying within the species. This intra-species diversity and sequence polymorphism is even detectable amongst isolates sampled at the same farm and in the same year. Even with populations that are mostly clonal, variation can happen when the pathogen is under pressure or outbreeds under the right conditions. This can create minor random mutations or major variations with sexual recombination, which can then lead to co-infection of a plant by two different strains. This is a possibility for the differences we see through PenSeq on isolates sampled at the same location and time. As discussed in the introduction chapter, *Phytophthora* species form oospores, which can remain in the soil for many years. Thus, it is also possible that several introductions of *P. rubi* happened in one location over the years and that older oospores germinated and infected plants at the same time as newer ones, resulting in the emergence of several strains.

We found that *P. rubi* SCRP324 (Scotland, Perthshire, farm D, 1991) and SCRP1208 (Scotland, Perthshire, farm A, 2017) have the most RXLRs missing (0 % covered at 5 % mm) and the most diversity out of the European isolates. Coverage of effector genes for French 1985 isolate SCRP339, differs from the German 1985 isolate SCRP249, and shows more genes identical to reference genome SCRP333, which was confirmed with k-mer analysis and clustering of SCRP339 and SCRP333, along with SCRP1202 (Netherlands, 2010) and SCRP1213 (Scotland, 2018). The relatedness of these isolates could be an indication of their origin. For *P. fragariae*, the oldest and only UK isolate SCRP245 stands out as the most diverse compared to the reference BC-16. When looking at effector genes in our 24 isolates, PenSeq and k-mer analyses also found that *P. rubi* isolate SCRP290 and *P. fragariae* isolate BC-1 could constitute better reference isolates than SCRP333 and BC-16 respectively.

The intra-species diversity study shows that when looking for patterns amongst isolates driven by geographical or historical variation, more specific genes were found to be uniquely absent rather than present in specific isolates. However, this could also

be an artefact of our analysis as we mapped all reads to a reference genome and did not conduct a *de novo* assembly of unmapped reads. We hypothesize that intra-species diversity is driven not only by effector polymorphism but also by contraction events leading to gene loss.

Finally, sequence variation observed with PenSeq and extracted mapped reads was independently verified with Sanger sequencing of some of the genes of interest, confirming the accuracy and resolution power of PenSeq multiple reads mapping.

In summary, PenSeq is an efficient and cost-effective approach to enrich genes of interest and discover presence / absence variation and polymorphism between and within species. It reveals how diverse *P. rubi* and *P. fragariae* isolates are, focussing on important infectious components. We discovered that *P. rubi* is more diverse than initially thought, showing a significant genetic potential to evolve, to overcome selection pressures for example, and thus its threat to farming should not be underestimated. This information is a pre-requisite for resistance breeding as a single dominant disease resistance gene might be liable to be overcome by the existing pathogen diversity.

CHAPTER 4. HYDROPONIC INFECTION OF RASPBERRIES USING *P. RUBI* EXPRESSING A FLUORESCENT MARKER

4.1. Introduction

Studies of *Phytophthora in planta* have largely focussed on above-ground tissues and mainly utilise model plants that are easier to work with, such as *N. benthamiana* (Maor et al., 1998; Sexton and Howlett, 2001; Chen et al., 2003; Si-Ammour et al., 2003; Li et al., 2011; Njoroge et al., 2011; Dunn et al., 2013; Ochoa et al., 2019). The very nature of soil, the host root architecture and the rich rhizosphere microbiome all present a set of challenges for measuring and monitoring disease progression of a root pathogen while in soil (easy root breakage, several steps of washing, contamination issues etc.).

The methodology for infection assays of raspberry roots with *P. rubi* needs reviewing as, like many clade-7 oomycete species, *P. rubi* fails to sporulate in aseptic culture conditions. Indeed, many rhizosphere *Phytophthoras* require non-sterile flooding solutions made from untreated water, soil solutions or host root exudates to sporulate (Backwell and Waterhouse, 1931; Waterhouse, 1931; Marx and Haasis, 1965; Zentmyer, 1965; Ayers, 1971; Mussel and Fay, 1973; Norman and Hooker, 2000; Chandelier et al., 2006; Acosta-Maspons et al., 2019; Adams, 2019). A great number of factors can add to the success of the sporulation, such as light, temperature (examined in Chapter 2), culturing media, the length of time cultures were left to grow before being flooded with sporulation solutions and the type of solutions (Goode, 1956; Marx and Haasis, 1965; Zentmyer, 1965; Chee and Newhook, 1966; Mussel and Fay, 1973). Furthermore, different isolates may respond differently and produce varying numbers of sporangia.

Infection analyses by Le Berre et al. (2008) and Evangelisti et al (2017) have reported the use of fluorescent isolates of *P. parasitica* and *P. palmivora*, respectively, to follow the progression and formation of infectious structures in root tissue. To date, *P. rubi* and *P. fragariae* have not been reportedly transformed to express fluorescent proteins, and thus never trialled in imaging assays of infected raspberry / strawberry roots.

The first *Phytophthora* transformation protocol was introduced for *P. infestans* by Judelson et al. (1991) and has been well documented for other *Phytophthora* species (Judelson et al., 1991; van West, 1999; McLeod et al., 2008; Dunn et al., 2013; Meng et al., 2015; Chen et al., 2016; Fang and Tyler, 2016). This polyethylene glycol (PEG)-protoplast transformation method starts from sporangia in order to get fresh zoospores. However, as mentioned previously, sporangia production for *P. rubi* can be difficult and requires non-sterile compounds, which can jeopardise the transformation process with contamination and presents a major challenge for this chapter. This study aims at transforming several *P. rubi* and *P. fragariae* isolates to use in infection assays, using a modified version of Judelson's transformation starting from mycelia obtained in aseptic conditions.

In order to better study molecular plant-pathogen interactions, we aim to develop a reliable supply of hydroponically grown raspberry plantlets that can be infected with virulent fluorescently labelled *P. rubi* lines. Laun and Zinkernagel (1997) provide evidence that *P. rubi* zoospores swim towards the root tip to attach, encyst and penetrate at what appears to be the root elongation zone. Hyphae then grows towards and up into the root vascular system (stele). Their study highlighted the importance of keeping roots intact when studying the disease, which can be achieved through hydroponics. An NFT hydroponic system using rockwool plugs was thus trialled to grow raspberry plants hydroponically. Other methods to grow plants for the study of roots have included tissue culture (de Freitas and Germida, 1990; Hussain et al., 2012; Yu et al., 2017; Fenning, 2019; Xu et al., 2019), or artificial transparent growth medium (Zhang et al., 2020), but can be expensive, especially for larger plant species and for infection assays that may take considerably longer. As a consequence, studies of root diseases are often limited to smaller plants that can be used for high throughput screens using media such as the transparent soil (Downie et al., 2015; Zhang et al., 2020). Hydroponic systems offer flexibility and constitute a cheaper and easier method for soil-free plant growth for roots studies. Furthermore, hydroponic systems provide suitable conditions in which to perform plant infection assays and can limit environmental stress on the plants. Previous literature on hydroponics has mostly focused on smaller crops grown commercially, such as lettuce, tomatoes, basil & herbs, carrots, peppers, and strawberries (Benoit and Ceustermans, 1987; Sarooshi and Cresswell, 1994; Arias et al., 2000; Parađiković et al., 2011; Coolong, 2012; Lin et al., 2013; Treftz and Omaye, 2015). At present, indoor vertical farming is a huge

growth area mainly focusing on fast-growing species. Until recently, there has been little commercial interest or scientific research on growing larger crop species in controlled environments using hydroponic systems. Raspberries have a lengthy growth cycle and take years to become commercially viable in terms of fruit yield. Thus, hydroponic production has not been extensively considered by growers. Still, one study by Treft and Omaye (2015) showed that while raspberries grown hydroponically using a drip system have a lower survival rate (33 %) compared to soil-grown raspberries (66 %), the fruit yield per plant was 10 % higher, while the sensory and nutritional analyses showed similar values. This study has demonstrated the feasibility and interest of growing raspberries hydroponically. Furthermore, there is vast potential in supporting research focused on expanding the uses of indoor agriculture to propagate larger crop species out of season for the UK soft fruit sector. This chapter aims to investigate the use of NFT hydroponic system to quickly obtain young raspberry plants for root infection assays, where the pathogen can be tracked *in planta* in both susceptible and resistant cultivars. In susceptible cultivars, we hope to identify oomycete life stages and associated gene expression of life cycle markers and effectors.

To illustrate broad-spectrum resistance (PTI) responses of plants to *P. rubi* PAMPs were assessed through visualisation of hypersensitive response (HR), using leaf infiltration assays. This method of infiltrating leaves is widely used, especially for *Agrobacterium* infiltration (agroinfiltration) for transient expression of genes of interest (Schöb et al., 1997; Goodin et al., 2002; Voinnet et al., 2003; Huitema et al., 2005; Goodin et al., 2008; Rajput et al., 2014; Maximo et al., 2019; Debler et al., 2021). This chapter experiments with leaf infiltrations to observe PTI response to *P. rubi* on susceptible and resistant raspberries and will serve as a foundation for agroinfiltration assays on effectors selected from PenSeq and expression analyses.

Finally, following the study of *P. rubi* infection processes, deploying resistant cultivars is an important step in controlling and managing the disease, as discussed in Chapter 1. Cultivars of raspberries are regularly developed in breeding programs and new strains of *P. rubi* frequently found in the field, leading to a need for rapid resistance screening. Li et al. (2017) developed a fast and effective method to evaluate varieties resistance through a detached-petiole inoculation method. This method is tested with inoculation of *P. rubi* isolates on raspberry cultivars to verify its reliability for further

resistance examination and is used in combination with other methods to investigate the resistance mechanisms to *P. rubi*.

Overall, the aims of this chapter are to:

- Transform *P. rubi* isolates
- Set up hydroponics raspberry plants
- Develop *P. rubi* infection system for raspberry plants
- Monitor disease progression and host responses using confocal microscopy
- Detect gene expression of life markers and effectors *in planta*
- Test leaf infiltrations to observe PTI response to *P. rubi* PAMPs and as a precursor for future agroinfiltration assays

4.2. Material and Methods

4.2.1. Preparation of *P. rubi* for infections

4.2.1.1. Culture of Phytophthora for infection assays

Various isolates of *P. rubi* were used for the different types of infection assays (Table 4.1). Unless specified otherwise, isolates were routinely kept on rye agar with ampicillin in the dark at 18 °C and plugs of mycelia grown on rye agar were transferred onto French bean agar amended with 100 µg/mL of ampicillin for sporulation.

4.2.1.2. P. rubi culture for sporulation assays

P. rubi isolates SCRP333 and SCRP333_tdT (SCRP333 transformed to express the fluorescent protein tdTomato, see 4.2.2) were used to assess sporulation criteria. Single agar plugs from clean rye agar cultures were transferred onto French bean agar plates amended with 100 µg/mL of ampicillin. French bean agar plates were then incubated at 18 °C in the dark for one week unless specified otherwise.

Table 4. 1. List of *P. rubi* isolates used in various infection assays

Species	Isolate name	Race / mating type	Isolation year	Isolation country	Infection	Infection purpose
<i>P. rubi</i>	SCR333_tdT	Race 3	transgenic SCR333 expressing tdTomato fluorescent protein		Hydroponic infection	Real-time observation of <i>P. rubi</i> in its original host, raspberry roots Expression of specific genes
	SCR1207	Unknown	2017	Scotland	Petioles inoculations	Highlighting cultivars differences and / or isolate differences during infection
	SCR333	Race 3	1985	Scotland		
	SCR338	Race 3	1987	Canada	Leaf infiltration	Observing potential HR responses
<i>P. infestans</i>	88069	A1	1988	The Netherlands		

4.2.1.3. Sporulation solutions

Four main solution types were used to test *P. rubi* SCR333 sporulation: 1) rainwater, 2) soil solution, 3) root exudates and 4) sterile distilled water (SDW).

1. Rainwater was collected at The James Hutton Institute site, using an outside 35 L collection container (March 2018), and stored at -20 °C.
2. Soil solutions were generated as described in Chapter 2. Soil solutions were stored undiluted and unsterilized at -20 °C (unless specified otherwise). A range of filtration levels and storage temperatures were tested for a week: room temperature, 4 °C, -20 °C and -80 °C. Solutions referred to as “standard” soil solution indicate soil solution filtered once through Whatman paper (grade 2V).
3. ‘Raspberry mixed root exudates’ were obtained by suspending roots of a susceptible cultivar Glen Moy and a resistant cultivar Latham in 15 L of distilled water overnight in the dark, using a similar volume of roots per cultivar. One litre of the resulting solution was collected in a 1 L autoclaved glass bottle, aliquoted into 50 mL tubes and frozen at -20 °C. Exudates were used as such (unsterilised) to mimic infection conditions.
4. Sterile distilled water (SDW) was used as a control and obtained from The James Hutton Institute media kitchen.

For each sporulation solution, three filtration levels were tested: unsterilised, filtered and autoclaved. Solutions were autoclaved in a standard autoclave (media cycle, 121 °C for 15 mins). When filtered, solutions were passed once or twice through a 0.22 µm Millex filter (Millipore™) using a 50 mL syringe after being initially passed through Whatman paper (grade 2V).

Root exudates to induce sporulation in *P. rubi* SCRP333_tdT were further explored by using susceptible (Glen Moy) and resistant (Latham) cultivars separately. Exudates were collected as mentioned previously using one plant per 1 L of distilled water and used unsterilised.

4.2.1.4. Induction of sporulation

Square plugs (~ 5 mm²) of actively growing mycelia from FBA plates were placed into an empty and sterile 150 mm Petri dish. Ten plugs per 150 mm plate were flooded with the different sporulation solutions (described in 4.2.1.3.). Solutions were changed twice in the following 24 hours as described in Chapter 2 (Mussel and Fay, 1973). Plates were incubated at 15 °C in the dark, unless specified otherwise. Four days later, plates with plugs of agar flooded with sporulation solutions were placed under the microscope and number of sporangia per field of view per plug was recorded for each of the ten plugs per plate (Chapter 2, Figure 2.6).

4.2.1.5. Sporulation assays

Effect of media on sporulation was investigated by transferring rye agar plugs of SCRP333 onto 90 mm Petri dishes of FBA and rye agar, amended with ampicillin (100 µg/mL). Five replicates were used per isolate per medium. After a week's growth at 18 °C in the dark in the various media, the colony diameter of *P. rubi* was measured along two perpendicular axes (Chapter 2, Figure 2.5) and average growth was calculated. Following this, ten plugs of FBA or rye agar (~ 5 mm²) were placed into an empty and sterile 150 mm Petri dish which was then flooded with soil solution as described in 4.2.1.4. One 150 mm plate of plugs and standard solution was used per medium.

Effect of the initial culture's age was tested by incubating FBA plates of SCRP333 and SCRP333_tdT for one and two weeks at 18 °C before being used for sporangia production. After one / two weeks of growth, ten plugs (~ 5 mm²) were placed into a 150 mm Petri dish which was flooded with standard soil solution as described above

and incubated at 15 °C. Two 150 mm plates of plugs were used per isolate and per culture age.

Solution types, filtration and storage were tested on *P. rubi* SCRP333 incubated for one week on FBA with ampicillin to grow (18 °C), before cutting plugs and placing them in 150 mm Petri dishes with sporulation solution, as detailed in 4.2.1.2 and 4.2.1.3. One 150 mm plate of ten plugs was used per solution type and filtration; and two plates of ten plugs each were used per storage temperature. Plates were incubated at 15 °C to induce sporangia.

Separate Glen Moy and Latham root exudates tested the induction of sporangia for *P. rubi* SCRP333_tdT using the same protocol as above, with flooded plates incubated at 15 °C, and two plates of ten plugs were used per solution (Glen Moy root exudates, Latham root exudates, SDW and soil solution).

4.2.1.6. Zoospore release for *P. rubi* and *P. fragariae*

To release zoospores from *P. rubi* and *P. fragariae* sporangia, Petri's solution (Waterhouse and Backwell, 1954) was made with 1 mM KCl, 2 mM Ca(NO₃)₂, 1.2 mM MgSO₄, 1 mM KH₂PO₄ (chemicals from Sigma Aldrich, UK) and autoclaved (121 °C for 15 mins), before being cooled down to 15 °C. Petri dishes (150 mm) of mycelial plugs with sporangia were incubated at 4 °C for 30 minutes, after which 50 mL of Petri's solution was poured in each plate on the sporangia (Mussel and Fay, 1973; Adams, 2019).

4.2.2. *P. rubi* transformation for expression of fluorescent markers

Transformation of *Phytophthora rubi* was performed using two techniques adapted from Judelson et al. (Judelson and Michelmore, 1991; Judelson et al., 1991). Several isolates of *P. rubi* were trialled for genetic transformation (Table 4.2).

4.2.2.1. Preparation of transformation plasmids pTOR-eGFP and pTOR-tdT

This transformation method used already-made *Escherichia coli* plasmids pTOR-eGFP and pTOR-tdT, using pTOR plasmid (Genbank Accession EU257520, Torche, 2004) with transgenes encoding fluorescent proteins eGFP (enhanced Green Fluorescent Protein) and tdTomato (Tandem Dimer Tomato or tdT) cloned between the *Cla*I and *Sac*II restriction sites. The vector contains selection markers where genes for resistance to ampicillin and geneticin (G418, Thermo Fisher Scientific, UK) are

expressed using a bacterial (hsp70) and an oomycete (ham34) promoter respectively, to allow regeneration and selection of mutants. Long term stocks of *E. coli* cultures with vector pTOR-eGFP and pTOR-tdT were kept in 50 % glycerol at -80 °C.

Table 4. 2. List and details of transformations carried out on *P. rubi*

Transformation	Isolates	Method	Fluorescent protein in plasmid	Geneticin dose incorporated in regenerating medium
Previously carried out by L. Welsh	SCR333	method 1	eGFP	3 µg/mL
Previously carried out by L. Welsh	SCR333	method 1	tdT	3 µg/mL
T1	SCR1207	method 1	eGFP and tdT	2 µg/mL
T2	SCR1207	method 1	eGFP and tdT	2 µg/mL
T3	SCR1207	method 2	eGFP and tdT	2 µg/mL
T4	SCR333	method 2	eGFP and tdT	3 µg/mL
T5	SCR1208	method 2	eGFP and tdT	2 µg/mL
T6	SCR1207	method 2	eGFP and tdT	2 µg/mL
T7	SCR333	method 2	eGFP and tdT	3 µg/mL
T8	SCR1202	method 2	eGFP and tdT	3 µg/mL

For plasmid preparation, culture was spread onto two LB (Luria-Bertani) agar plates with 150 µg/mL ampicillin and grown for one day in the dark at 37 °C. Single colonies were each pricked into 50 mL of pre-warmed (37 °C) LB medium containing 1 mg / mL ampicillin, incubated for 24 hrs in a shaking incubator at 37 °C. Each 50 mL culture was used to inoculate two 250 mL flasks of pre-warmed LB with 300 µg/mL ampicillin, which was sealed with foil and incubated overnight in a shaking incubator at 37 °C. Plasmid purification was performed using Qiagen Plasmid Maxi Prep kit (QIAGEN, UK) using the manufacturer's protocol and DNA eluted in 50 µL of molecular grade water (Sigma Aldrich, UK).

4.2.2.2. Pre-screening for *P. rubi* geneticin sensitivity

Prior to transformation, the tolerance of *P. rubi* to geneticin had to be assessed for each isolate using a dose-response analysis with a dilution series of geneticin (G418). The regenerating concentration of geneticin was determined as the lowest concentration at which wild type isolates of *P. rubi* are not able to grow anymore (Table 4.2).

4.2.2.3. *P. rubi* hyphal preparation for transformation method 1

For transformation method 1, *Phytophthora* cultures were grown on 50 x 150 mm rye agar plates containing 100 µg/mL of ampicillin in the dark at 18 °C for two weeks. Each

plate was inoculated with eight plugs of *P. rubi*. Hyphae were scraped from the agar surface using sterile spreader.

4.2.2.4. *P. rubi* hyphal preparation for transformation method 2

For transformation method 2, *Phytophthora* cultures were grown on 10 x 150 mm plates of liquid lima bean media (Bruck et al., 1981) containing 100 µg/mL of ampicillin. Each plate was inoculated with six plugs of *P. rubi* grown in the dark at 18 °C for two weeks. Hyphae were collected by pouring lima bean plates into an autoclavable blender and blended for a few seconds.

4.2.2.5. PEG – protoplast transformation method

Hyphal suspension was poured into 200 mL of lima bean media (Bruck et al., 1981) containing 50 µg/mL ampicillin and 400 µL of vitamin stock filtered through a 0.22 µm Millex filter (Table 4.3), gently swirled once to mix and incubated at 18 °C in the dark for 24 hours (protocol from Steve Whisson, personal communication, 2017).

Table 4. 3. Media used for PEG-protoplasts transformation of *P. rubi*

Medium	Content	Concentrations	Solvent
LBSM (Lima Bean-Sucrose-Mannitol)	1 M mannitol	182 mg/mL	Lima bean broth (Bruck et al., 1981)
	Sucrose	20 mg/mL	
FPB solution (Fry Protoplasting Buffer)	0.4 M mannitol	72.87 mg/mL	Water
	20 mM KCl	1.5 mg/mL	
	20 mM MES pH 5.7 (4-morpholineethane sulfonic acid)	20 mL of 1M MES for 1 L of medium	
	10 mM CaCl ₂	1.5 mg/mL	
Vitamin stock	Biotin	0.6 µg/mL	Water
	Folic acid	0.6 µg/mL	
	Myo-inositol	34 µg/mL	
	Nicotinic acid	0.17 mg/mL	
	Pyridoxine-HCl	51.4 µg/mL	
	Riboflavin	42.9 µg/mL	
	Thiamine-HCl	0.11 mg/mL	
	Coconut milk	50 mL for 300 mL of water	
All chemicals were purchased from Sigma Aldrich, UK			
All media were aliquoted and autoclaved before use			

Uncontaminated liquid lima bean of *P. rubi* cultures were filtered through 70 µm nylon mesh to collect mycelium, washed with 2 x 200 ml of FPB (Fry Protoplasting Buffer) medium (Table 4.3) and transferred to a 50 mL centrifuge tube containing 20 mL of FPM containing protoplasting enzymes (5 mg/mL of Extralyse (Laffort) and 2 mg/mL of cellulase (Sigma Aldrich, UK)) prefiltered through a 0.22 µm Millex filter. Centrifuge tubes were wrapped in foil and shaken gently on a platform for 40 minutes. Digested mycelium was filtered through 100 µm nylon mesh (company) and rinsed with 5 mL FPB. Gentle agitation was used to prevent clogging. Filtered protoplasts were then poured through 35 µm mesh (company) and washed with 5 mL FPB. Protoplasts were then centrifuged in XX mL tube at 700 x g for 4 mins, and supernatant was discarded. The pellet of protoplasts was gently resuspended in 10 mL FPB and centrifuged again at 700 x g, 4 mins. The supernatant was discarded and protoplasts resuspended with the gentle addition of 10 mL of 1:1 MTC10-FPB (Judelson et al., 1991) and centrifuged at 700 x g, 4 mins. The supernatant was discarded, and protoplasts resuspended in 10 mL of MTC10, before final centrifuge at 700x g, 4 mins. The supernatant was discarded, and protoplasts were resuspended in 1 mL MTC10. Resulting protoplasts (1 mL) were transferred to a 20 mL polystyrene universal tube containing 50 µg of plasmid DNA preparation to a final volume of 57.1 µL of molecular grade water (Sigma Aldrich, UK) and 85.7 µL of Lipofectin, gently mixed prior to use (Judelson et al., 1991). The tube was gently mixed for 30 seconds at an angle such that the mixture does not move far up the inside of the tube and left to settle for 5 minutes. One ml of freshly prepared and filter-sterilised 50 % PEG 3350 (using a 0.22 µm Millex filter) was added to protoplasts by slowly pipetting while rolling the tube at an angle. The tube was rotated for an additional 30 seconds before being left to stand for 2 minutes and then slowly inverted and allowed to stand for a further 5 min. Then 2 mL of LBSM (Lima bean sucrose mannitol) solution (recipe?) was added and mixed by inversion before leaving to stand for 2 minutes. Another 6 mL of LBSM was then added and mixed by inversion again, before standing for 3 minutes. Finally, the universal contents were poured into a 90 mm Petri dish containing 12 mL of liquid LBSM with 50 µg/mL of ampicillin and sealed with double layer of parafilm and left to regenerate for 48 to 72 hours. Protoplast / mycelium mixture was then poured into a 50 mL centrifuge tube and the remaining petri dishes were rinsed with 5 mL LBSM, also added to the tube and spun at 700 x g for 5 mins. The supernatant was discarded, and mycelia/protoplast pellets gently resuspended in 2 mL LBSM and spread onto 5 x 150 mm Petri dishes

of rye agar supplemented with geneticin G418 (at the appropriate dose), 50 µg/mL ampicillin, 50 µg/mL vancomycin (Sigma Aldrich, UK) and 5 µg/mL pimarinic acid (in 70 % ethanol, Sigma Aldrich). Plates were sealed, wrapped in foil and incubated at 18 °C in the dark until transformants appeared. Any transformants were isolated onto fresh plates of rye agar with geneticin (G418) and 50 µg/mL of ampicillin before assessing colony growth and fluorescence.

4.2.2.6. Confirmation of *P. rubi* transformation using fluorescent assessment

- Microscopic assessment of transgenic isolates

Mycelium samples from candidate transformants were taken once growth appeared. Hyphae was first confirmed to be non-septate through observation under a standard microscope before assessing the fluorescence with a Zeiss LSM710 fluorescent confocal microscope. The microscope used standard GFP settings (excitation at 466 - 495 nm and emission at 510 - 541 nm) to examine eGFP transformants and RFP (Red Fluorescent Protein) settings to examine tdTomato transformants (excitation at 553 - 578 nm and emission at 582 - 630 nm). Once confirmed, transgenic isolates SCRP333_eGFP and SCRP333_tdT were routinely cultured onto rye agar amended with 100 µg/mL of ampicillin and geneticin (G418) at 10 µg/mL and 15 µg/mL respectively.

- Ability of transgenic isolates to produce sporangia and zoospores

The ability of transgenic isolates to produce sporangia and zoospores was assessed with methods identical to the ones described above.

4.2.3. Plant collection and growth conditions

4.2.3.1. Hydroponic raspberries

- Raspberry plants

Cultures of raspberry (*Rubus idaeus*) cultivars Glen Dee, Glen Fyne, Glen Moy and Latham were obtained from Alison Dolan at The James Hutton Institute (Table 4.4) and tested in a two-years trial (2018, 2019).

Table 4. 4. Raspberry cultivars tested in hydroponic conditions. Four raspberry cultivars, with and without the Rub118b marker and displaying various resistance levels to PRR, were grown for hydroponics systems.

Raspberry cultivar	Rub118b marker	Known level of field resistance to PRR
Latham	Yes	Most resistant
Glen Dee	No	Susceptible
Glen Fyne	Yes	Very susceptible
Glen Moy	No	Most susceptible

Glen Dee was incorporated into the hydroponic raspberries trial from October 2018. Glen Moy and Latham were certified Pre-Basic ('high health') reference cultivars, the highest grade in the EU Certification Scheme for fruit plants. All raspberry plants were grown in autoclaved compost and kept in a glasshouse with 16 hours of artificial lighting (400 W sodium lamps), during which the temperature was set to 20 °C, followed by 8 hours with no artificial lights and a set temperature of 18 °C. Solar radiation (MJ/m²) was measured from a weather station outside the glasshouse (Invergowrie, Scotland). Nutrient Osmacote '3-4-month control release' fertiliser (LBS, Clydeside Trading) was added with 4 plugs per 10 L pot of compost. Vitax fertiliser (NPK 1:1:1, from LBS, Clydeside Trading) was mixed with water and applied as a drench fortnightly on raspberry plants, as per manufacturer's instructions.

- Hydroponic equipment and nutrients

NFT kits were supplied by ProGrow Hydroponics UK. Additional air-pump supplied by Hailea (adjustable air pump ACO9601) with a 192 L / hr output and attached air-stone were placed in the reservoir. Different sizes of rockwool plugs as well as rockwool 'transfer' blocks were used to provide alternative substrate and supplied by ProGrow Hydroponics UK and Great Stuff Hydroponics UK. Several nutrients were used for rockwool plugs and for reservoir solution: Kristalon Red (NPK 1:1:3, from Yara Tera, UK), Solufeed (NPK 1:1:1, from Solufeed, UK), MaxiCrop (original seaweed extract, NPK 5:2:5, from Fargro, UK), Formulex (nutrient designed for hydroponics, NPK 2.7:1:3.8, from Growth Technology, UK), and a Clonex mist solution (Growth Technology).

- Hydroponic technique applied to raspberries

Rockwool plugs were pre-soaked in either water or half-strength nutrient solution with a pH adjusted between 5.2 and 6.1. Raspberry stem cuttings with apical meristem and 2-3 internodes were taken, dipped in Clonex rooting hormone (Growth Technology) before being anchored into previously soaked plugs. Rockwool plugs with fresh cuttings were placed in a mist unit, spraying water for 15 seconds every 20 minutes in daylight hours (6:00 am to 6:00 pm) and every 40 minutes at night (6:00 pm to 6:00 am) on a heat mat (230 V, 2.9 A, 656 W, Hotbox International Ltd, Newport, UK) set at 25 °C. When roots developed, plugs were moved into NFT hydroponic tanks. Hydroponic tanks included water pump, air-stone, and air-pump; and were filled (~16L) with water where a half-strength nutrient solution was added, using Kristalon Red or NPK 1:1:1 nutrients. The pH was adjusted between 6.0 and 6.5. A fibre mat was placed into the channel in the first few weeks to help the nutrient solution spread more evenly. All hydroponics systems and mist units were set up in a glasshouse with 16 hours lighting, during which the temperature was set to 20 °C, followed by 8 hours with no artificial lights and a set temperature of 18 °C.

4.2.3.2. Plant leaves for infiltration assays

Raspberry plants (Glen Dee), *Nicotiana benthamiana* and potato plants were used for leaf infiltration assays. Raspberry plants were grown from sown roots from 'high health' plants for six weeks before being used. *N. benthamiana* plants were grown in a glasshouse set at 22 °C with 16 hours lighting, followed by 8 hours with no artificial lights. *N. benthamiana* plants were grown for 3 weeks before being used.

4.2.4. Hydroponic infection assay

Several plates (150 mm) of sporangia containing ten plugs each were produced, as described in 4.2.1, using standard soil solutions (filtered once) and transgenic *P. rubi* strain SCRP333_tdT (tdTomato, ref fluorescent protein) grown for one week to ten days. Fluorescence of sporangia was checked using the Zeiss LSM710 microscope prior to inducing zoospores release. Zoospores were released as described in 4.2.1.6. Raspberry roots priorly washed in distilled water were dipped in the suspension of sporangia releasing zoospores for a total of six hours (Adams, 2019). On average, one raspberry plant was dipped into the equivalent of 10 plugs of sporangia, in 50 mL of solution. Roots were covered in tin foil and kept at 18 °C during the incubation.

Following the six-hour inoculation, plants were transferred to a tank filled with distilled water, with a similar air-pump and air-stone as the ones used in NFT hydroponic system and air-pump was turned on 7 days after inoculation. Samples were taken regularly: before inoculation (used as controls), 3 dpi (days post-inoculation), 7 dpi, 11 dpi, 14 dpi, 22 dpi, 24 dpi and 30 dpi. Roots were collected for confocal fluorescent microscopy observation and stored in water from their original hydroponic infection tank. Additional root samples were collected at 3 dpi, 7 dpi, 11 dpi and 14 dpi for gene expression study, and immediately frozen in liquid nitrogen and stored at -80 °C before RNA extraction.

A total of nine hydroponic infections were performed over 14 months using available raspberry cultivars grown in hydroponics: January 2019, February 2019, July 2019, August 2019, September 2019, October 2019, December 2019, January 2020 and February 2020.

4.2.5. *P. rubi* PTI leaf infiltration assays

Leaf infiltration assays were performed on raspberries and *N. benthamiana* model plants, grown as described in 4.2.3. Culture filtrates of *P. rubi* SCRP338, SCRP249 and SCRP296, and *P. infestans* 88069 were produced with isolates grown in liquid lima bean with 100 µg/mL ampicillin for two weeks at 18 °C in the dark. Mycelial mats formed were removed and the liquid lima bean was collected and filtered through a 0.22 µm Millex filter (Millipore™) before being stored at -80 °C. Controls used liquid lima bean with ampicillin. The infiltration was carried out as per Wang et al. (2018). Three leaves per plant were infiltrated and two inoculation points were made per leaf, with each of the two isolates and the controls (Figure 4.1). Four plants of the same species were used per assay and per modality. Plants were kept at 18 °C. Leaf lesions were assessed four days after infiltration: if the infiltrated area showed more than 50 % cell death, it was associated with a score of 1 and was considered to be showing a hypersensitive response; if the area affected was below 50 %, it scored 0. The total number of responding infiltrations (of a total of six per plant) were recorded for the four replicate plants and converted into mean percentage of cell death.

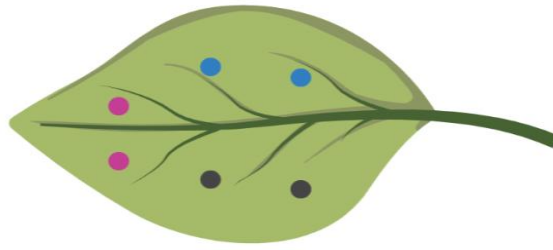


Figure 4. 1. Illustration of leaf infiltration inoculation points. The underside of the leaf was inoculated 6 times: 2 inoculations with lima bean control (pink), 2 inoculation points with *P. rubi* isolate SCRP338 (blue) and 2 inoculation points with *P. infestans* isolate 88069 (black)

4.2.6. Microscopic observation of *P. rubi* infection progression inside raspberry roots

4.2.6.1. Confocal microscopy and calcofluor staining

Collected roots infected with *P. rubi* SCRP333_tdT were kept in water from their original tank until stained and properly mounted onto a microscope slide. Roots were stained with calcofluor white (CFW, Sigma Aldrich, UK) to highlight root cell walls. Samples were dipped in calcofluor for 2-3 minutes and rinsed in distilled water before being placed on a microscope slide (Figure 4.2). Roots were screened with a Zeiss LSM710 fluorescent confocal microscope using different settings: transmission (CHD) along with red fluorescence detector or calcofluor with red fluorescence detectors. Filter emission wavelength was 582 to 630 nm and laser excitation wavelength was 553 - 578 nm to detect red fluorescence from tdTomato. Calcofluor white emission wavelength was between 415 and 455 nm and excitation was ~ 365 nm. Z-stacks (depth) of interesting root sections showing fluorescence were collected and analysed.

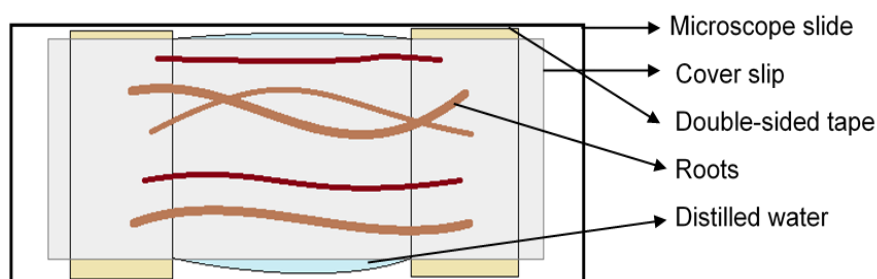


Figure 4. 2. Layout of microscope slides. Schematic representation of microscope slide for the observation of infected raspberry roots under confocal fluorescent microscope.

4.2.6.2. Trypan blue and light microscopy

Additional samples were collected at 6 dpi, 9 dpi and 23 dpi and stained with trypan blue (Sigma Aldrich, UK) as per Koske and Gemma (1989), using 3% potassium

hydroxide (KOH) and 2% hydrochloric acid (HCl). Stained roots were mounted on microscope slides as previously described (Figure 4.2).

4.2.7. RNA extraction from infected raspberry roots (hydroponic infection)

Three methods were tested to extract sufficient yields of RNA from hydroponically grown raspberry roots: a method adapted from the Qiagen RNeasy Plant Mini Kit, using β -mercaptoethanol and Ambion Plant RNA Isolation Aid; a TriReagent method with chloroform and isopropanol; and a CTAB method from Yu et al. (2012a). At least three samples of raspberry roots were trialled for each method. Prior to extraction, mortars and pestles were autoclaved and treated with RNase Zap (Sigma Aldrich, UK). Root samples were ground in liquid nitrogen to make 80-200 mg of starting material, prior to RNA extraction methods. Extracted RNA samples were assayed for purity (DNA contamination) and concentration by NanoDrop (NanoDrop 1000 Thermo Fisher Scientific).

4.2.7.1. TriReagent RNA extraction method

The TriReagent RNA extraction method was used as per the Thermo Fisher Scientific protocol, with the extra steps described in “Troubleshooting: Proteoglycan and polysaccharide contamination”. Chloroform (200 μ L) was added instead of BCP (1-bromo-3-chloropropane), and a mix of salt solution (0.8 M sodium citrate and 1.2 M NaCl in a total volume of 250 μ L) and isopropanol (250 μ L, Sigma Aldrich, UK) were used, as per instructions. The RNA pellet was resuspended in 20 μ L of molecular biology grade (nuclease-free) water (Sigma Aldrich, UK).

4.2.7.2. Qiagen RNeasy Plant Mini Kit RNA extraction method

The second RNA extraction method tested was adapted from the RNeasy Plant Mini Kit (QIAGEN, UK) starting with 80 to 200 mg of frozen raspberry roots and using β -mercaptoethanol (Sigma Aldrich, UK) in buffer RLT (provided in the kit), to which Ambion Plant RNA Isolation Aid (Thermo Fisher Scientific, UK) containing polyvinylpyrrolidone (PVP) was added to remove common plant contaminants (polyphenolics and polysaccharides). The addition of buffer RW1 was split to allow the incorporation of a DNase treatment. RNA extraction was then performed as per manufacturer’s instructions (RNeasy Plant Mini Kit, QIAGEN, UK) and total RNA was eluted twice in 30 μ L of RNase free water.

4.2.7.3. CTAB RNA extraction (Yu et al., 2012a)

A CTAB RNA extraction method from Yu et al. (2012a) was tested. Frozen raspberry roots (approx. 100 to 200 mg) were ground in liquid nitrogen with 0.01 g of polyvinylpolypyrrolidone (PVPP). The frozen powder was carefully transferred to a 2 mL micro-centrifuge tube containing 700 μ L of extraction buffer pre-warmed at 65 °C (3 % CTAB, 100 mM Tris-HCl pH 8.0, 1.4 M NaCl, 20 mM EDTA, 5 % PVP); and 2 μ L/mL of β -mercaptoethanol that was added just before use. All following steps were carried out as described in the Yu et al. (2012a) protocol. Ethanol washes consisted of adding 75 % ethanol and centrifuging 5 minutes at 7500 x g at room temperature twice. Final RNA was re-suspended in 30 μ L of DEPC-treated (Diethyl Pyrocarbonate-treated) water.

4.2.8. Expression of specific genes during hydroponic infection of raspberries

4.2.8.1. Gene selection

Several genes were selected for expression analyses from raspberry roots infected with *P. rubi* SCR333_tdT. Genes included lifecycle markers such as the *P. rubi* orthologs of INF1 (secreted elicitor that triggers cell death, here named *RUB1*), CDC14 (sporulation marker, *PrCDC14*) and Hmp1 (haustorial membrane protein marker, *PrHmp1*). Lifecycle marker genes were retrieved using BLASTp for *P. rubi* genome, with *P. infestans* genes as queries (INF1: AY830094.1; CDC14: AY204881.1; HMP1: EU680858.1). Additionally, SCR333_contig_4275_F7 (PR003_g28352), a *P. rubi* RXLR absent from *P. fragariae* (refer to Chapter 3, Table 3.23) was added to the gene expression study. Moreover, an RNASeq experiment was carried out at The James Hutton Institute using hydroponic raspberries infected with *P. rubi* SCR333_tdT and hydroponic infection methods adapted from the ones described in this study. It identified genes expressed *in planta* at 7 dpi, which were filtered for FPKM value above 5 (Adams, 2019) and as predicted RXLR according to the Whisson et al. (2007) model. The resulting RXLR genes were also included in the qRT-PCR assay. Coverage of selected effector genes was assessed with data obtained from the PenSeq study.

4.2.8.2. Primer design

Primers for genes of interest were designed following the Taqman criteria for qRT-PCR (Table 4.5). Primers for life marker genes were first tested by conventional PCR

with SCRP333 gDNA template (50-250 ng/ μ L), non-infected raspberry cDNA (50-100 ng/ μ L) and water as a negative template control (see Chapter 3 for more details on conventional PCR reagents and settings). The raspberry Actin 2 gene was used as a positive control to check presence of DNA template in the non-infected raspberry sample. Agarose gel electrophoreses (2 % agarose) were used to visualise PCR amplicons and run at 80 V for 50 mins.

Table 4. 5. Details of primers used to screen for genes of interest in qRT-PCR assays

Gene of Interest	Details	PenSeq ID	NCBI <i>P. rubi</i> number ID	primers names	primers sequences 5'-3'	product size (bp)
<i>RUB1</i> (based on <i>P. infestans</i> INF1: AY8300941)	Triggers cell death (HR)	SCRP333_g25193	PR003_g27228	qRT_Pr_INF1_F2	CGGACTCGT CGTTCAACC A	144
				qRT_Pr_INF1_R2	GGTTCAGCG ACACGATCT TG	
<i>PrCDC14</i> (based on <i>P. infestans</i> CDC14: AY204881.1)	Sporulation marker	SCRP333_g17955	PR003_g13389	qRT_Pr_CDC14_F1	GCACGTTTA ATCTGACCA TCTTG	86
				qRT_Pr_CDC14_R1	GTCGAACGT CTTGATGGA GATG	
<i>PrHmp1</i> (base on <i>P. infestans</i> HMP1: EU680858.1)	Haustoria marker (biotrophy)	SCRP333_g2600	PR003_g2773	SCR33_HM_P1.2_F	GGTTGGTCA GCGTCTTCA TC	196
				SCR33_HM_P1.2_R	GTTGTGTCC GCCATTGTC AT	
<i>PrCoxI</i>	Controls (housekeeping)	SCRP333_CoxI	N/A	coxIAB_F	GGGCGCATC ACATGTTTAC T	127
				coxIAB_R	CCTCCCAT AAAGTTGCT AACC	
<i>PrBtub</i>		SCRP333_g4344	PR003_g22653	Betatub_AB_F	AGCACGAAG GAGGTTGAT GA	215
				Betatub_AB_R	GCCTTACGA CGGAACATA GC	
SCRP333_contig_4275_F7	<i>P. rubi</i> RXLR gene absent from 4 <i>P. fragariae</i> and covered in all 20 <i>P. rubi</i> isolates (see Chapter 3)	SCRP333_contig_4275_F7	PR003_g28352	qPCR_Pr_4275_F7_F	GGCTACGCT CCTATCAAC CA	67
				qPCR_Pr_4275_F7_R	GCCTGACAC TGGACTCTT GA	
SCRP333_g22109	<i>P. rubi</i> RXLR gene expressed during infection (SCRP333_tdT, RNASeq)	SCRP333_g22109	PR003_g23841	qPCR_g22109_F	GCACTCCCC AACGATCAC T	75
				qPCR_g22109_R	CGCCAACCTC TCTCCTCTTC T	

Gene of Interest	Details	PenSeq ID	NCBI <i>P. rubi</i> number ID	primers names	primers sequences 5'-3'	product size (bp)
SCR333_g22154	<i>P. rubi</i> RXLR gene expressed during infection (SCR333_tdT, RNASeq + <i>P. rubi</i> equivalent of BC-16_g5824 expressed <i>in planta</i>)	SCR333_g22154	PR003_g23891	qPCR_g22154_F	ATTCTTCTCG TCGGCTCTG A	91
				qPCR_g22154_R	CTC CCG AGG TCA AGA GGT TT	
SCR333_g24428	<i>P. rubi</i> RXLR gene expressed during infection (SCR333_tdT, RNASeq + PenSeq identified as Canadian marker (absent/highly diverse in Canadian and American isolates))	SCR333_g24428	(PR003_g26341)	qPCR_g24428_F	ATGGACCTC AGCAAGAAC CT	82
				qPCR_g24428_R	GCTCCTTGG CTTTCTTCAA CT	

4.2.8.3. cDNA synthesis

RNA from infected time course material extracted with the CTAB method was treated with DNase (TURBO DNA-free kit (ThermoFisher Scientific, UK)). Complementary DNA (cDNA) was synthesised using the Takara cDNA EcoDry Premix kit (Takara Bio Europe) and following the manufacturer's protocol with RNA quantities as close to 1 µg as possible.

4.2.8.4. qRT-PCR

Genes of interest were tested on cDNA from Glen Dee infected material sampled at 3, 7, 11 and 14 dpi during hydroponic infections (February 2019 and September 2019). Uninfected raspberry roots were used as controls. cDNA from infected material was diluted for a final reaction concentration of ~ 50 ng / µL and cDNA from controls was diluted to ~ 20 ng / µL. *Cox1* and *Btub* (beta-tubulin) were used as endogenous control genes. Quantitative PCR was performed using 6.25 µL of Sybr Green, 1 µL of each primer to a final concentration of 300 nM, 3.25 µL molecular grade water and 1 µL template cDNA per 12.5 µL reaction. QPCR cycle was carried out using a StepOnePlus™ Real-Time PCR System machine (Thermo Fisher Scientific, UK). The cycle consisted of a first step to bring the temperature to 50 °C for 2 minutes (UNG activation), followed by initial denaturation at 95 °C for 10 minutes, and 44 cycles of 95 °C for 15 seconds and 60 °C for 1 minute. The melting curve consisted of 95 °C for

15 seconds, 60 °C for 1 minute, and an addition of 0.5 °C to 95 °C every 15 seconds. Analysis of the qPCR CT (cycle threshold) was performed using ANOVA and Tukey's HSD tests. Relative expression using the $\Delta\Delta\text{CT}$ method (Winer et al., 1999; Schmittgen et al., 2000; Livak and Schmittgen, 2001) was calculated comparing the cDNA from infected samples to cDNA from a control sample of SCRP333_tdT sporulating mycelia for endogenous control genes (*CoxI* and *Btub*). Control sample was collected from SCRP333_tdT mycelia with attached sporangia after preparation as described in 4.2.1. using soil solutions. RNA was extracted using the Yu et al. (2012a) method described in 4.2.7.3 and 1 μg was used to make cDNA according to 4.2.8.3.

4.2.9. Statistical analyses

Statistical analyses (ANOVA and Tukey's HSD tests) were performed using R Studio v1.1.383. Statistical differences were considered significant if the p-value was lower than 0.05 (using a 95 % confidence interval). Bar chart graphs were performed in Excel (v. 2102 for Microsoft Office 365). N numbers indicate the numbers samples per modality for the experiment (replicates). Bar chart and line graphs were performed in Excel (v. 2102 for Microsoft Office 365).

4.3. Results

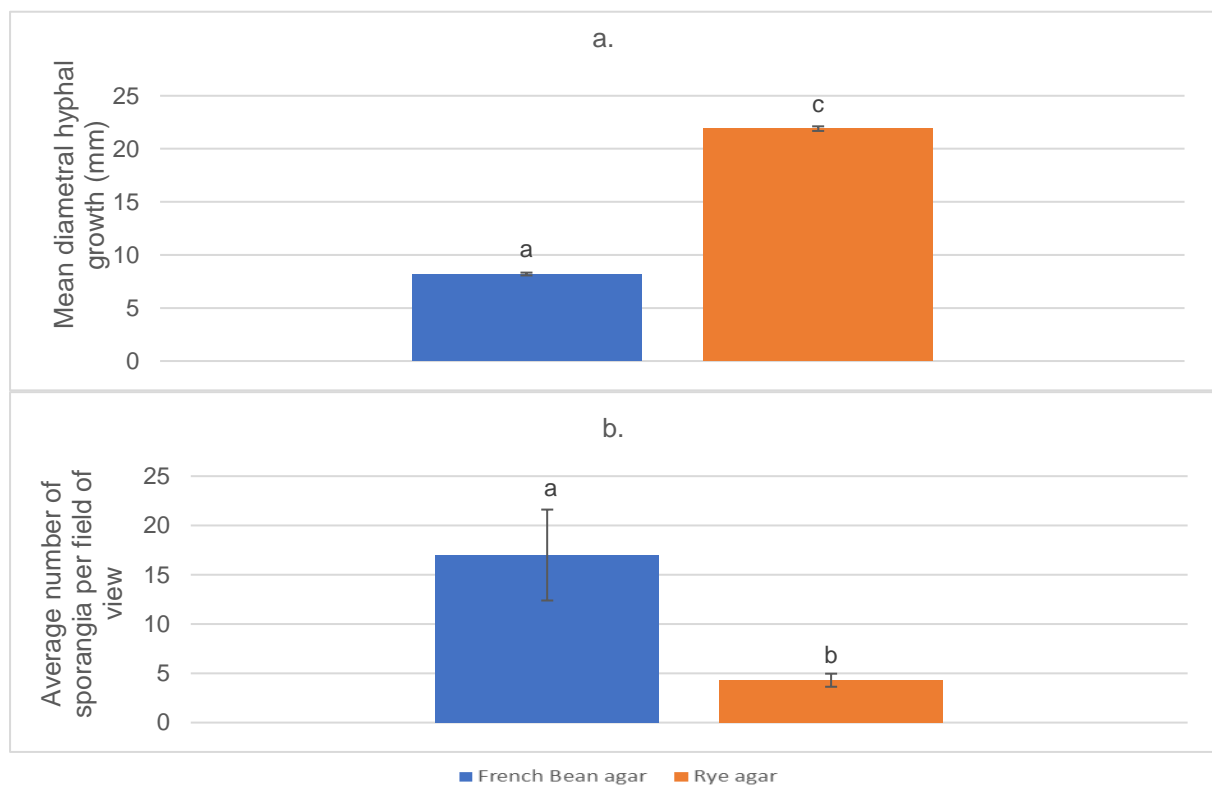
P. rubi optimal conditions for sporulation were investigated and tested on newly transformed isolate, expressing fluorescent proteins. Following production of sporangia and zoospores, the fluorescent *P. rubi* was inoculated on raspberries that had been grown hydroponically, presenting clean and intact roots. Confocal observation of infected roots of susceptible raspberry cultivars (Glen Moy and Glen Dee) showed typical life stages of *P. rubi* at specific time points (hyphae, sporangia, zoospores and oospores). The life stages were confirmed with gene expression. Expression levels of additional RXLR genes of interest were assessed at different time points during infection.

4.3.1. Preparation of *Phytophthora* for inoculation assays

For most *Phytophthora* species, sporangia stage is the most amenable for pathogenicity assays *in planta*. Several studies on clade 7 *Phytophthora* species show that pond / rainwater, soil / compost extract and root exudates can induce sporulation (Chee and Newhook, 1966; Mussel and Fay, 1973; Norman and Hooker, 2000; Acosta-Maspons et al., 2019) and that many other factors could influence the sporulation process (Goode, 1956; Marx and Haasis, 1965; Zentmyer, 1965; Chee and Newhook, 1966; Mussel and Fay, 1973). Therefore, identification of a suitable method to generate adequate number of sporangia for *P. rubi* was necessary.

4.3.1.1. Identifying the most effective sporulation media

Phytophthoras are often grown on a range of media with varying nutrient compositions. *P. rubi* and *P. fragariae* are often cultured on rye or French bean agar (FBA). Here, it was shown that while FBA may be more nutrient rich, rye agar growing medium



induced greater colony growth of *P. rubi* SCRP333 (Figure 4.3 a.), but significantly less sporangia (Figure 4.3 b.), suggesting that a medium reducing *P. rubi* hyphal development might enhance its sporulation.

Figure 4. 3. Effect of medium on growth and sporulation of *P. rubi* SCRP333. a. SCRP333 colony growth on two different media: French bean and rye agar (n = 5). **b.** SCRP333 average number of

sporangia (per field of view) using cultures grown on two different media: French bean and rye agar. One 150 mm Petri dishes of ten plugs each were used per modality (n = 10). Vertical bars represent the standard error of the mean. ANOVA and Tukey's HSD test were performed in R Studio v1.1.383 and statistical differences are given as labelled letters.

4.3.1.2. Younger cultures of *P. rubi* optimized the sporangia production

One-week old and two-weeks old cultures grown on FBA were used to generate sporangia using standard soil solution. It was found that one-week old cultures produced significantly more sporangia than two-weeks old cultures (Figure 4.4).

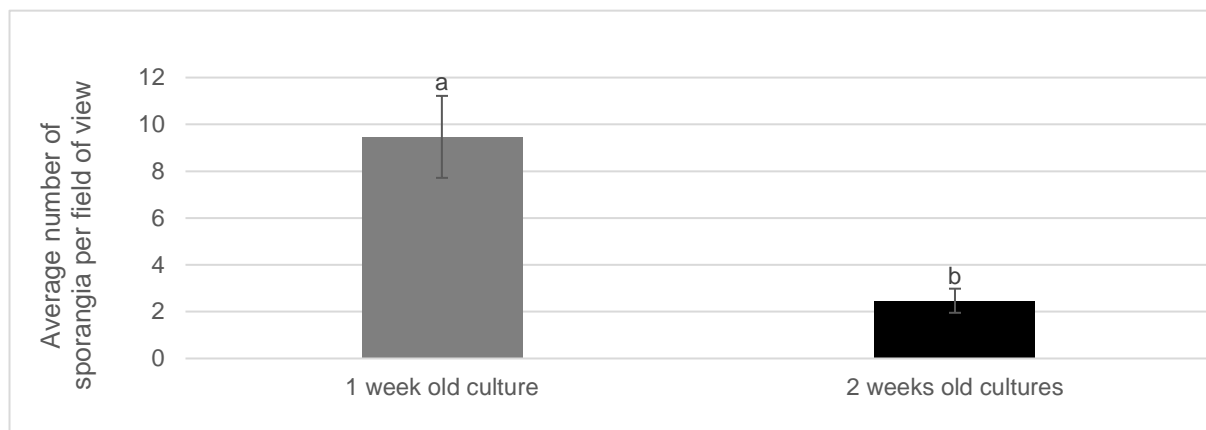


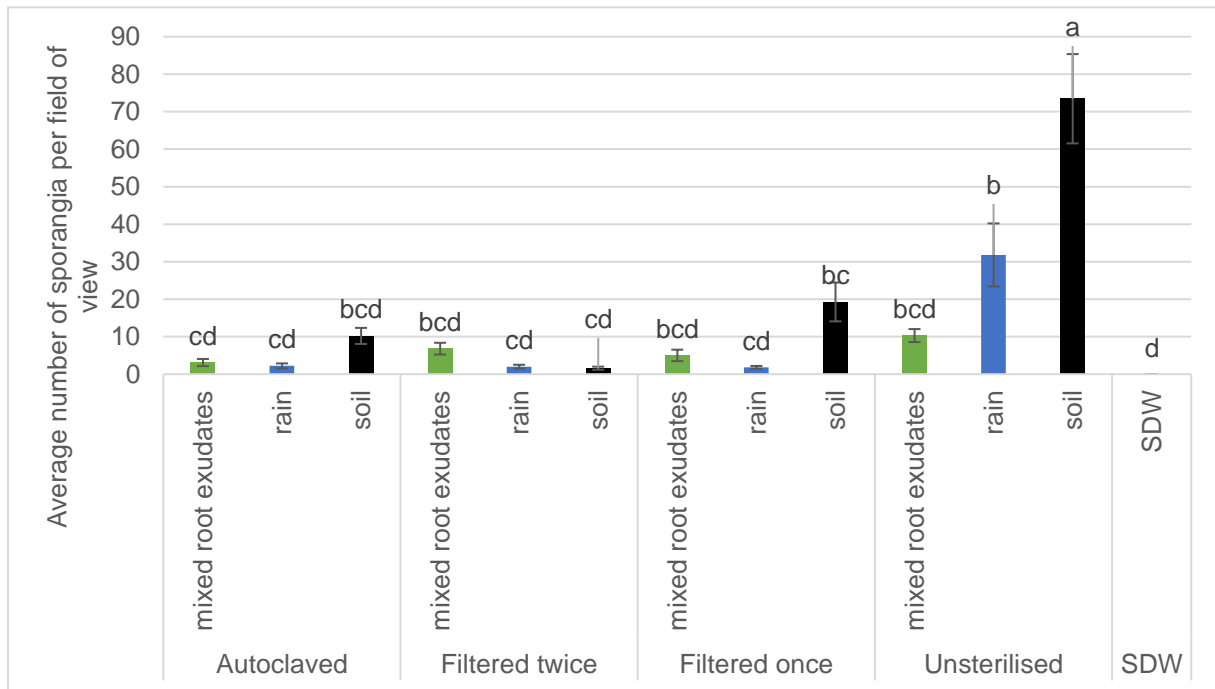
Figure 4. 4. Effect of SCRP333 culture age on sporulation. SCRP333 average number of sporangia (per field of view) using cultures of different ages, grown for one week or two weeks prior to flood in sporulation solutions. Sterile distilled water (SDW) was used as a negative control. One 150 mm Petri dishes of ten plugs each were used per modality (n = 10). Vertical bars represent the standard error of the mean. ANOVA and Tukey's HSD test were performed in R Studio v1.1.383 and statistical differences are given as labelled letters.

4.3.1.3. Identifying the most effective sporulation solution

Preliminary research carried out by L. Welsh at The James Hutton Institute (unpublished data) examined whether diluted soil solution (1 %, 10 %, 25 %, 50 %) could produce sporangia as efficiently as undiluted solution. Unfortunately, it was found that increasingly diluted solution led to a decreasing number of sporangia produced for SCRP333 (Appendix C, Figure C.1). Consequently, soil solutions used for trials and later for infection were never diluted.

FBA plates of *P. rubi* wild type isolate SCRP333 were used to compare various sporulation recipes with various levels of filtration (sterilisation) (Figure 4.5). It was found that unsterilised soil solution was significantly better at inducing the greatest number of sporangia produced by SCRP333. Unsterilized rainwater was also suitable

for sporangia production. In addition, soil solutions always produced the highest number of sporangia when compared to other types of solutions per filtration level,



although it was only significant for unsterilised solutions.

Figure 4. 5. Effect of different solutions on *P. rubi* SCRP333 sporulation. Bar chart of average number of sporangia for *P. rubi* isolate SCRP333 (per field of view per plug) incubated at 15 °C. Rainwater, mixed root exudates and soil solutions that were either autoclaved, filtered once, filtered twice or unsterilised were used to induce sporangia production. Solutions were stored at -20 °C. Sterile distilled water (SDW) was used as a negative control. One 150 mm Petri dishes of ten plugs each were used per modality (n = 10). Vertical bars represent the standard error of the mean. ANOVA and Tukey's HSD test were performed in R Studio v1.1.383 and statistical differences are given as labelled letters.

4.3.1.4. Sporulation soil solutions could be stored at 20 °C or -80 °C prior to use
Storage conditions were tested in collaboration with L. Welsh at The James Hutton Institute, to evaluate whether these lengthy preparation times could be shortened by making solutions in advance and storing them, as opposed to made fresh every time. Storage of filtered soil solutions was examined at room temperature, 4 °C, -20 °C and -80 °C. Freezing at either -20 °C and -80 °C led to a satisfactory number of SCRP333 sporangia, significantly higher than those produced with SDW (Figure 4.6). We subsequently stored all soil solutions aliquoted in 50 mL tubes at -20 °C.

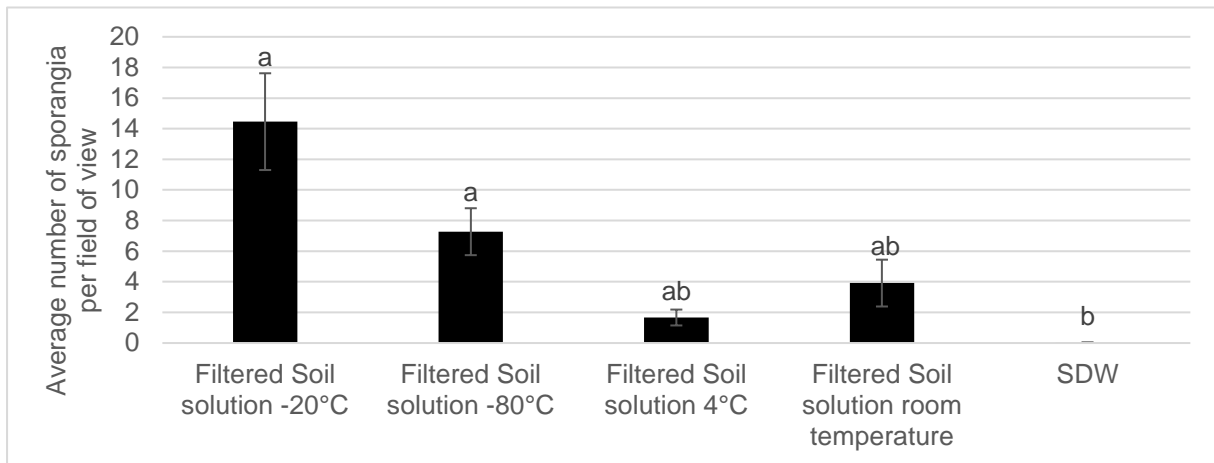


Figure 4. 6. Effect of storage conditions of solutions on sporulation of *P. rubi* SCRP333. Bar chart of average number of sporangia for *P. rubi* isolate SCRP333 (per field of view per plug) induced with standard soil solution incubated at 15 °C. The filtered soil solutions were stored either at -20°C, -80°C, 4°C or at room temperature prior to being used. Sterile distilled water (SDW) was used as a negative control. Two 150 mm Petri dishes of ten plugs each were used per modality (n = 20). Vertical bars represent the standard error of the mean. ANOVA and Tukey's HSD test were performed in R Studio v1.1.383 and statistical differences are given as labelled letters.

4.3.2. *P. rubi* transformation via two PEG-protoplast methods was confirmed

P. rubi isolate SCRP333 had previously been transformed by L. Welsh to express eGFP and tdTomato using mycelia preparation method 1 for transformation. Of the four different *P. rubi* isolates tested through eight transformations, only SCRP333 yielded transformed lines with both methods (L. Welsh and T7, Table 4.2).

Transformants were examined under the scanning confocal microscope to assess whether fluorescent labels could be identified. Both SCRP333 eGFP and tdT lines were expressing adequate levels of the fluorescent tag to use isolates for *in planta* assays (Figure 4.7). Potential negative effects of transformation on colony growth and on the ability to produce sporangia for transgenic *P. rubi* SCRP333_eGFP and SCRP333_tdT were examined to ensure they were still suitable for inoculations and infections. Transgenic isolates grew well and were able to produce sporangia and zoospores with soil solutions in the same conditions than wild type isolate SCRP333 (Figure 4.8).

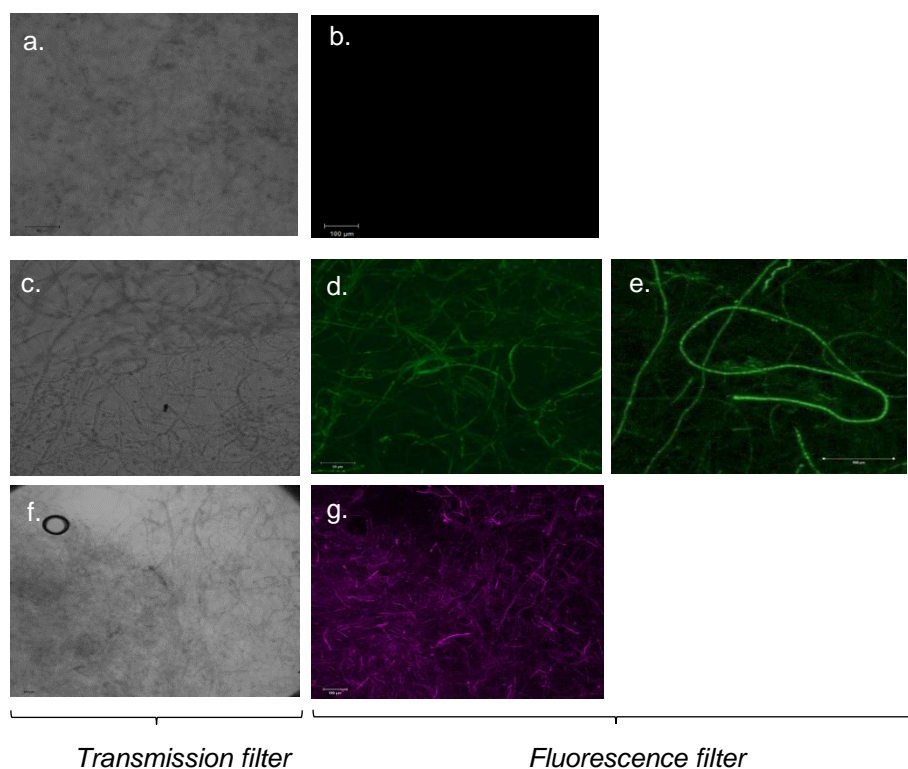


Figure 4. 7. *P. rubi* isolate SCR333 mycelium expressing fluorescent proteins. Microscopic photos of hyphae from agar plates of SCR333 wild type (a) under transmission filters (b) under fluorescence filters; and SCR333 transgenic isolates (c-g). c. SCR333_eGFP transformed with method 1 (described in 5.2.3) under transmission filter; d. SCR333_eGFP transformed with method 1 under eGFP filter; e. SCR333_eGFP transformed with method 2 (5.2.3) under eGFP filter; f. SCR333_tdT transformed with method 1 under transmission filter; g. SCR333_tdT transformed with method 1 under tdT filter. All photos were taken with a Zeiss LSM 710 microscope. Settings for fluorescence are detailed in 4.2.6.

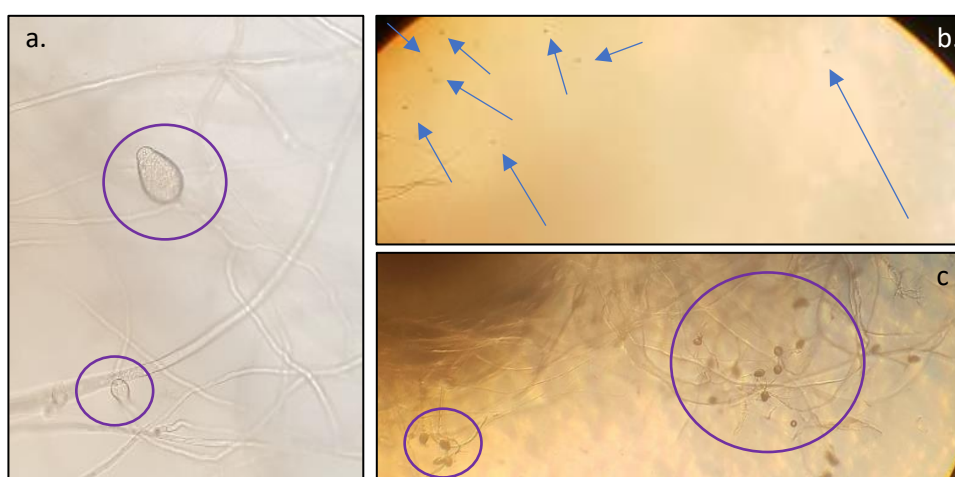


Figure 4. 8. Sporangia and zoospores of transformed *P. rubi* isolates. Microscopic photos of SCR333_tdT sporangia (a, purple circles) and zoospores (b, blue arrows) and SCR333_eGFP sporangia (c, purple circles) produced by transformed *P. rubi* isolates under similar conditions than previously described.

Before selecting the best transformant for infection, background root fluorescence needed evaluation, and could depend on the species, cultivar, and age of the plant. This study has assessed all raspberry cultivars grown in hydroponics (Glen Moy, Glen Dee and Latham) and showed a range of background fluorescence from light orange to light green (data not shown), though the latter is observed more often. With tdTomato fluorescent protein six times brighter than eGFP (Shaner et al., 2004), isolate SCRP333_tdT was thus more appropriate for the infection of raspberry roots.

As transgenic isolates growing on selected media can show slower development than wild type ones, the age of the culture for *P. rubi* SCRP333_tdT was also investigated. Results show that, like its wild type relative, one-week old cultures of SCRP333_tdT produced significantly more sporangia than two-weeks old cultures in the presence of soil solutions (Figure 4.9). In light of those results, *P. rubi* fluorescent transgenic isolate SCRP333_tdT was chosen for infections of raspberry roots.

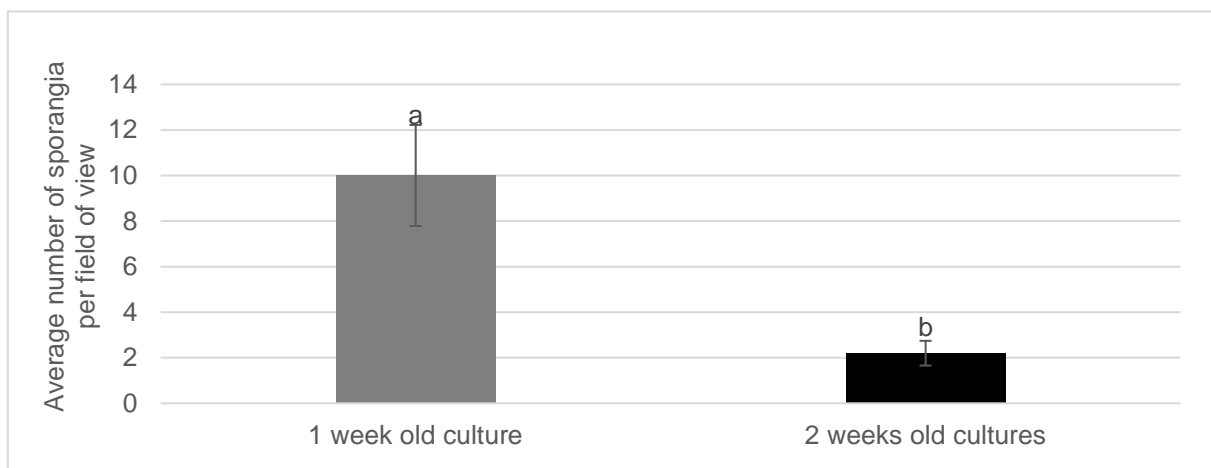


Figure 4. 9. Effect of SCRP333_tdT culture age on sporulation. SCRP333_tdT average number of sporangia (per field of view) using cultures of different ages, grown for one week or two weeks prior to flood in sporulation solutions. Sterile distilled water (SDW) was used as a negative control. One 150 mm Petri dishes of ten plugs each were used per modality (n = 10). Vertical bars represent the standard error of the mean. ANOVA and Tukey's HSD test were performed in R Studio v1.1.383 and statistical differences are given as labelled letters.

Furthermore, during hydroponic infection trials, root exudates from plants would surround *P. rubi*, and the ability of such root exudates from separate susceptible and resistant cultivars to induce sporulation was thus examined (4.2.1.3). Root exudates solutions were used unsterilised, to more accurately mimic conditions of hydroponic infection. Sporangia, zoospores, and a few oospores were observed for SCRP333_tdT

in raspberry root exudates. Both cultivars produced a significantly higher number of sporangia compared to SDW, and root exudates from Glen Dee produced more sporangia than exudates from Latham, though this difference was not statistically significant (Figure 4.10).

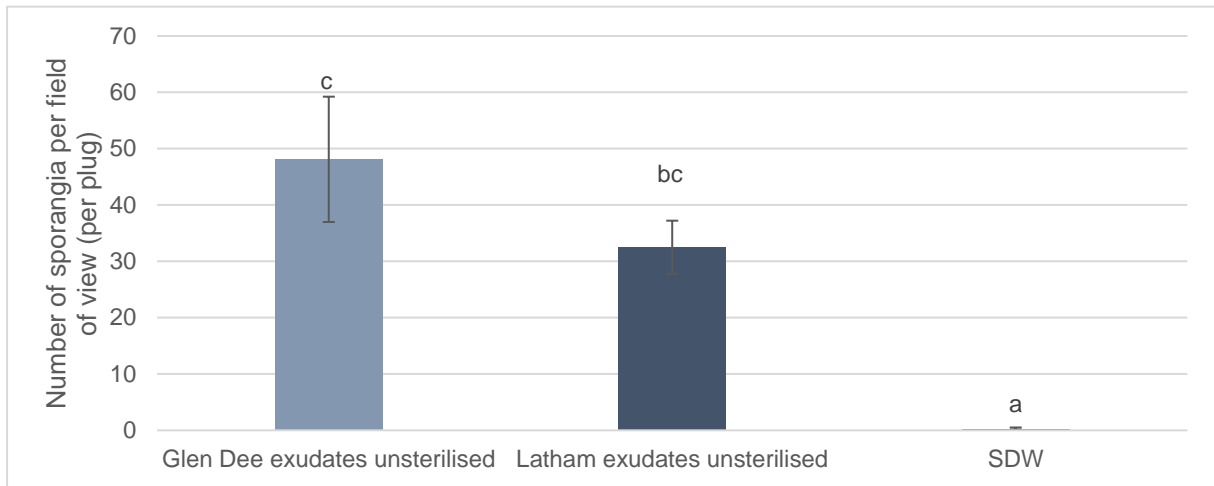


Figure 4. 10. Effect of raspberry root exudates on sporulation for transgenic *P. rubi* SCRP333_tdT. Bar chart of average number of sporangia for *P. rubi* isolate SCRP333_tdT (per field of view per plug) induced with Glen Dee and Latham root exudates. Sterile distilled water (SDW) was used as a negative control. One 150 mm Petri dishes of ten plugs each were used per modality (n = 10). Vertical bars represent the standard error of the mean. ANOVA and Tukey's HSD test were performed in R Studio v1.1.383 and statistical differences are given as labelled letters

4.3.3. Rooting success of raspberry cultivars used for infection assays

In order to provide a number of raspberry cultivars with varying root architectures and resistances to *P. rubi*, raspberries from the 'high health' facility at the James Hutton institute were potted and grown in clean glasshouse to provide source material for cuttings.

Cuttings were taken from the stems of PRR susceptible Glen Fyne, Glen Moy, Glen Dee and PRR resistant Latham raspberry plants (Figure 4.11) to examine rooting success in rockwool plugs pre-soaked in water or in a range of nutrient solutions (Solufeed, Kristalon Red, Formulex and MaxiCrop). The time to root was determined (in terms of number of weeks taken for root to emerge from the plugs) and rooting success was measured as cutting survival (as a percentage of total cuttings taken) over a two-year period (Figure 4.11).



Figure 4. 11. Progress of hydroponic-raspberry cultures. **a.** First rooted plug 31.01.18, 2 weeks after cutting was taken (17.01.2018). **b.** Hydroponic tank on 12.02.18, 3.5 weeks after cuttings taken. **c.** Rooted raspberries on the 12.02.18, 3.5 weeks after cuttings taken. **d.** Rooted raspberries on the 15.02.18, 4 weeks after first cuttings were taken. **e.** Rooted raspberries on the 26.02.18, 5.5 weeks after cuttings taken. **f.** Roots on the 26.03.18, 9.5 weeks after cuttings taken. **g.** Roots before infection on the 11.04.18, 12 weeks after first cuttings were taken. **h.** Foliage of raspberries grown with technique described from a to g. **i.** Rockwool transfer block showing emerging roots from raspberry. **j.** Raspberry grown in transfer block. **k.** Transfer blocks with rooted raspberry in NFT tank. **l.** Photo of the rockwool block in the hydroponic tank channel showing the root mat formed. **m.** Shoots emerging from the root mat on transfer blocks. **n.** Photo of the foliage from hydroponic tank using rockwool transfer blocks: n. taken on the 29.03.18 and o. taken on the 12.06.18.

Glen Fyne showed poor success with a survival rate below 2%. However, Glen Moy, Glen Dee and Latham were successfully grown, and survived once transferred in the NFT after rooting. Nevertheless, great variation was observed in terms of success and timing of root development throughout a year (Figures 4.12 and 4.13).

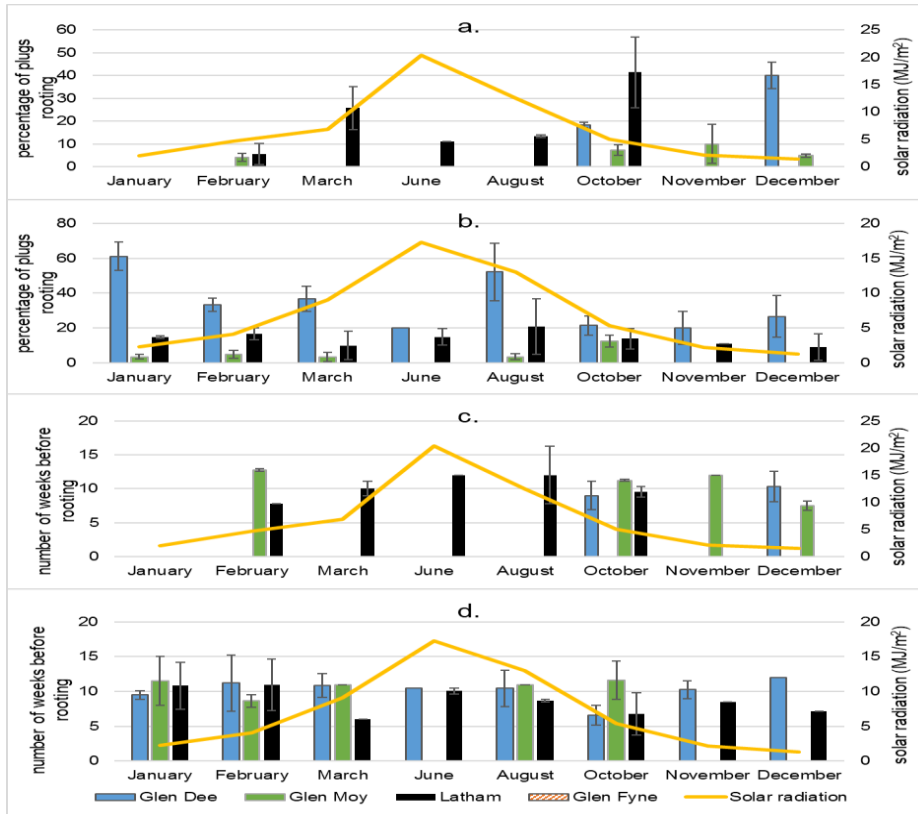


Figure 4. 12. Data for success of hydroponics during the two-years of trials. Cutting survival rate: **a.** during trial 1 (2018), **b.** during trial 2 (2019) and average number of weeks before rooting appeared on rockwool plugs with raspberry cuttings, **c.** during trial 1 (2018), **d.** during trial 2 (2019). Vertical bars represent standard error of the mean.

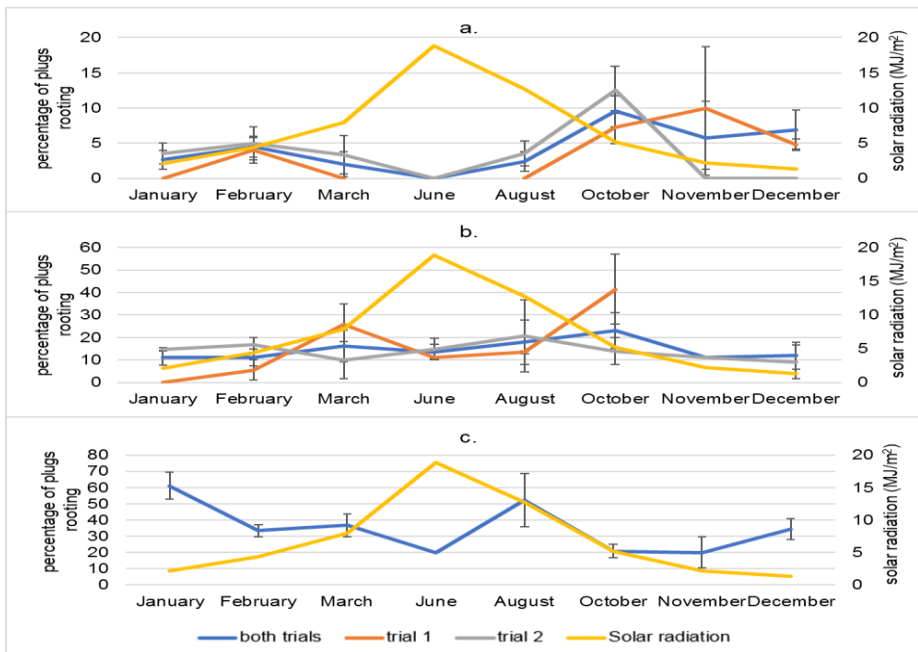


Figure 4. 13. Average percentage of cuttings surviving and rooting over the two-years trial. **a.** Glen Moy; **b.** Latham; **c.** Glen Dee (average for both trials only). The series labelled “both trials” represents the average of trial 1 and 2. The solar radiation represented in a-c is the average natural solar radiation outside the glasshouse over the two years. Vertical bars represent standard error of the means.

The percentage survival of Glen Moy was highest in the winter months (September to March), between 4 and 40 %, as opposed to < 2 % in the summer months (Figure 4.14). This appears to correlate with lower solar radiation.

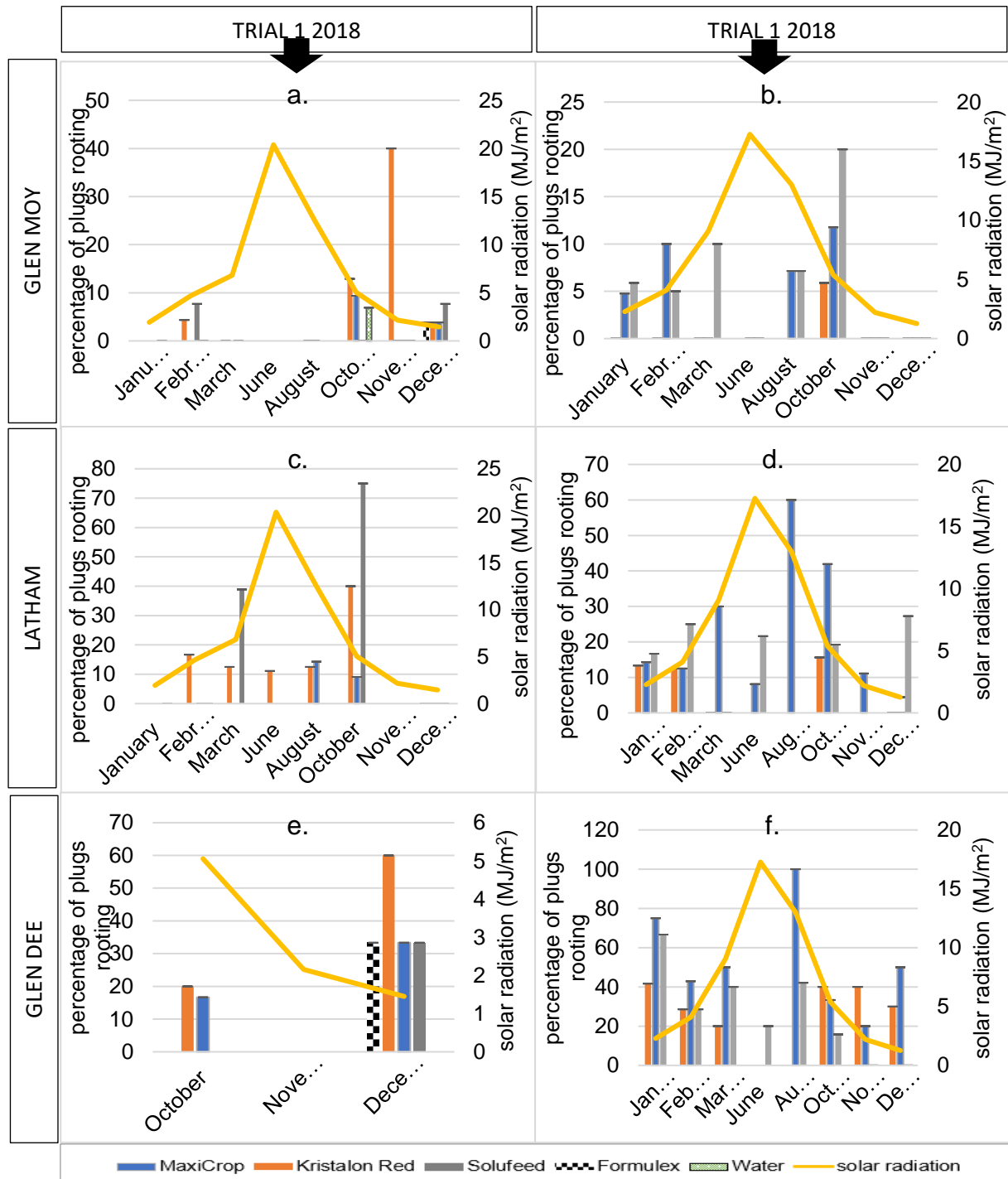


Figure 4. 14. Survival rates of hydroponic raspberries. Average percentages of cuttings surviving and rooting with different nutrients in soaked rockwool plugs (a & b: Glen Moy; c & d: Latham; e & f: Glen Dee) during trial 1 in 2018 (left) for a. Glen Moy, c. Latham and e. Glen Dee; and during trial 2 in 2019 (right) for b. Glen Moy, d. Latham and f. Glen Dee. Nutrient presented (bottom legend) were used to soak the rockwool plugs for the raspberry cuttings. Percentages were calculated using number of surviving plants on total number of cuttings taken.

None of the nutrient solutions tested appeared to be significantly better as cutting survival rates were very similar across cultivars and experimental replicates (Appendix C, Table C.1.a and Figure 4.14). For instance, the best survival rates for Glen Moy were observed using Kristalon Red (10.2 %) in trial 1 but with Solufeed (6 %) in trial 2 (Appendix C, Table C.1.a.). However, overall, Kristalon Red showed the most consistent survival rates. When examining which nutrient solution was the best in terms of promoting the fastest rooting of Glen Moy, Formulex stood out (5.5 weeks), followed by MaxiCrop in both trial 1 and trial 2.

For cv. Latham, the best survival rates were observed using Solufeed (28.5 %) in trial 1 and MaxiCrop (21.2 %) in trial 2 (Figure 4.14 and Appendix C, Table C.2.a.). The overall shortest time to root was observed with MaxiCrop (9.1 weeks) (Appendix C, Table C.2.b.).

Glen Dee was incorporated into the trial from October 2018 and showed promising results quickly, with much better survival rates than Glen Moy. Glen Dee had an overall average of 36 % survival compared to 4 % for Glen Moy (Figure 4.14 and Appendix C, Table C.3). Again, the survival of cuttings was generally higher and more reliable in the winter months (Figure 4.14). MaxiCrop offered the best survival rate (46.8 %) and the shortest time to root (9.2 weeks) (Appendix C, Table C.3).

Due to variability observed during the two-years trial, the reliability of the rooting procedure was assessed in Glen Moy, Glen Dee and Latham. Ratios of number of times where cuttings survival rate is null (0 %) to the total number of attempts were calculated (here referred to as “reliability ratios” where the reliability increases as the ratio decreases). Reliability scores were of 0.53 for Glen Moy, 0.3 for Latham and 0.1 for Glen Dee.

Once rooted through the rockwool medium, raspberries were transferred to the hydroponic (NFT) tank and stayed established and growing until used for infections, proving the suitability of this method. New cuttings from hydroponically grown raspberries showed similar survival rates and number of weeks to root as did cuttings taken from plants grown in pots.

A supplementary study revealed that raspberry cultivars grown in hydroponics could successfully recover from induced dormancy and fruit (Appendix C, Figure C.2).

In summary, all cultivars displayed significant variation in time to rooting in alternative hydroponic-friendly medium, but PRR susceptible cultivars appeared to root most successfully during autumn / winter months (early September to March), as opposed to spring / summer months. Results showed that overall, survival rates and timings were better when nutrients were used to soak rockwool plugs compared to water only but that no particular solution could be recommended overall. Glen Dee (PRR susceptible) was the best performing cultivar and consequently became the most highly utilised for downstream *in planta* infection assays.

4.3.4. *In planta* lifecycle of *P. rubi*

After setting up raspberry plantlets production in hydroponics, infections were started with sporangia and zoospores from our recently transformed transgenic fluorescent *P. rubi* isolate (SCR333_tdT). In the field, raspberries can take months to develop symptoms of root rot while the actual time scale of infection remains unknown. It was hypothesised that *P. rubi* SCR333_tdT should be able to infect susceptible raspberry cultivars Glen Moy and Glen Dee but not resistant cultivar Latham. The aim here was to set up infection assays, determine the speed of the life cycle and assess the suitability for short time-scale glasshouse and lab experiments. A method was adapted from Attard et al. (2010), Evangelisti et al. (2017) and Le Berre et al. (2008).

Confocal images from several biological replicates were combined to highlight *P. rubi in planta* infections structures. At 24 hours post-inoculation, spores were observed attaching to the roots of susceptible cultivar Glen Dee. At 3 days after inoculation, hyphae were visible in the roots of Glen Dee and sporangia (~32–68 µm length x 22–52 µm width) with swimming zoospores were observed on Glen Moy (Figure 4.15). Many *Phytophthora* species have an initial biotrophic phase associated with the development of haustoria to deliver RXLR effectors in host tissue to promote disease. Possible haustoria-like structures were seen during the infection of Glen Dee at 7 dpi, though we believe they might be from secondary *P. rubi* infection (Figure 4.16). Hyphae were also seen ramifying inside both Glen Moy and Glen Dee roots, predominantly in the central vascular cylinder (Figure 4.16). At this timepoint, zoospores were observed swimming around the roots which could indicate that new sporangia had formed from the infected roots. Additionally, oospores (~19 - 40 µm diameter) were observed in both susceptible cultivars.

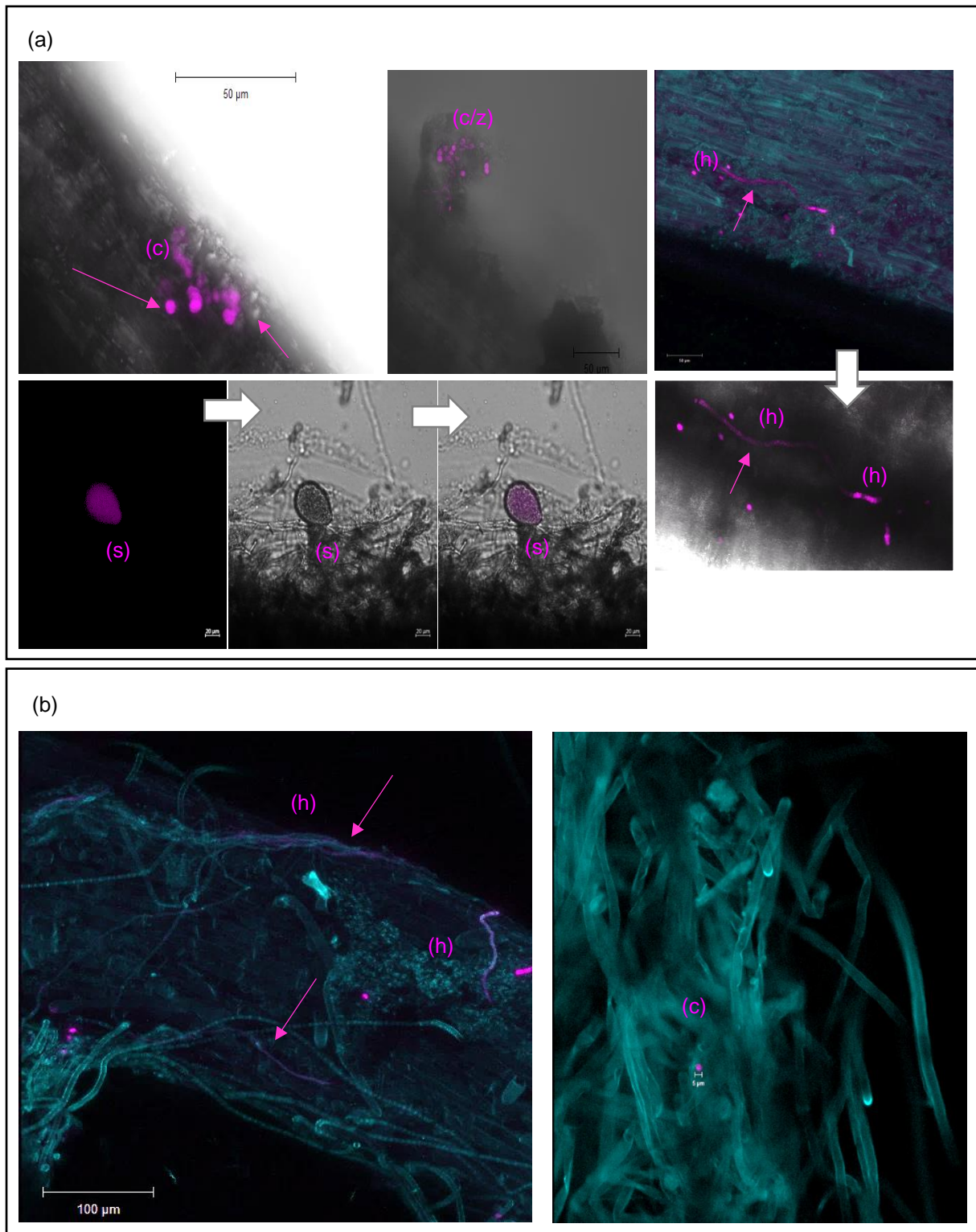


Figure 4. 15. Photos of infected Glen Dee and Glen Moy at 3 dpi. Photos of *P. rubi* red fluorescent structures (tdT) on Glen Moy roots (a) and Glen Dee roots (b): cyst (c), hyphae (h), sporangia (s) and zoospores (z). Photos were taken at 3 dpi from infections carried out in January 2019, February 2019, January 2020 and February 2020. Photo were taken with Zeiss LSM 710.

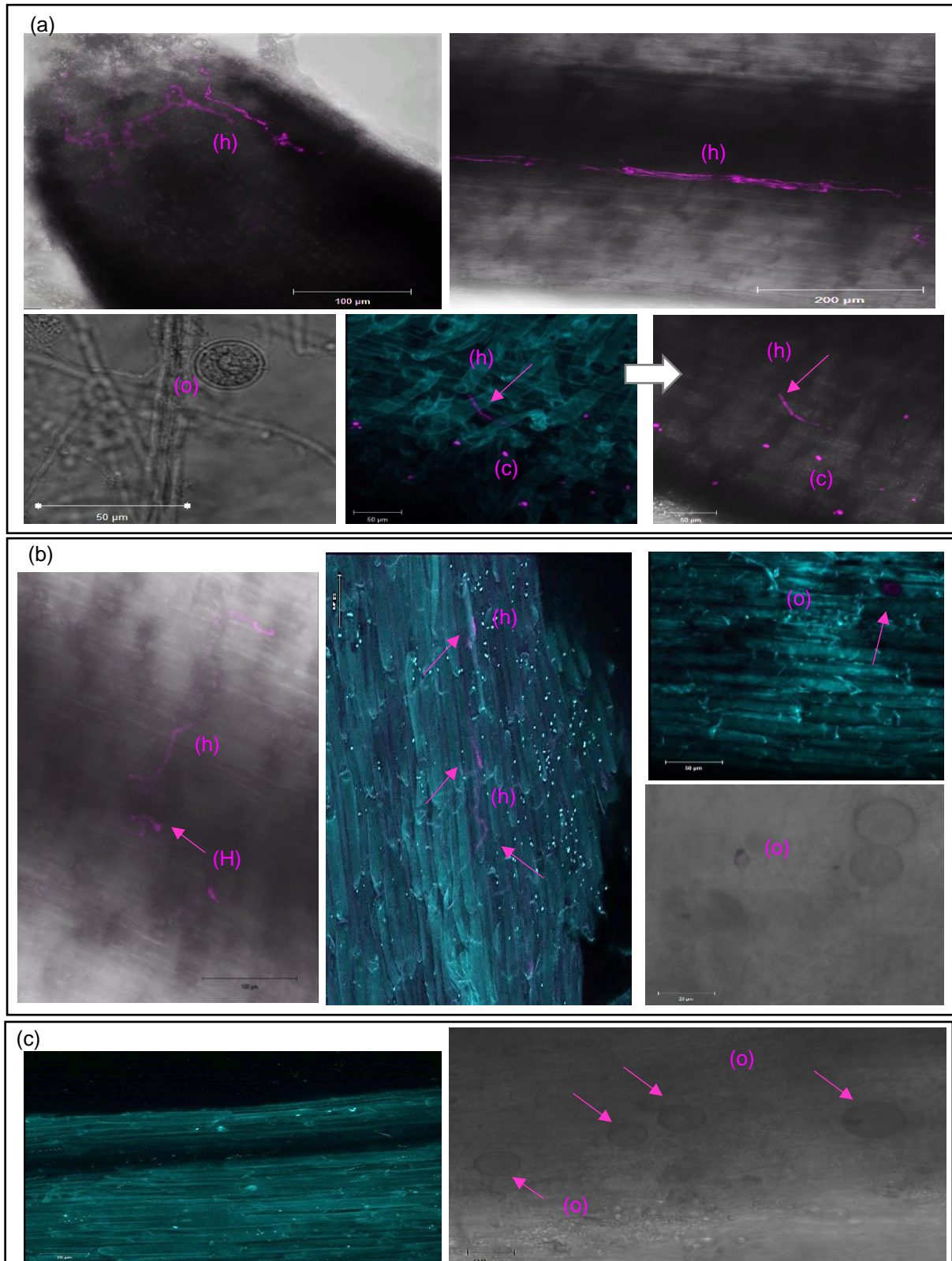


Figure 4. 16. Photos of infected Glen Dee, Glen Moy and Latham at 7 dpi. Photos of *P. rubi* red fluorescent structures (tdT) on Glen Moy (a), Glen Dee (b) and Latham (c) roots: cyst (c), hyphae (h), possible haustoria (H), zoospores (z) and oospores (o). Photos were taken at 7 dpi from infections carried out in February 2019, December 2019, January 2020 and February 2020. Photo were taken with Zeiss LSM 710

At 9 to 11 dpi, more oospores, hyphae and sporangia releasing zoospores were observed in susceptible cultivars (Figures 4.17 and 4.18).

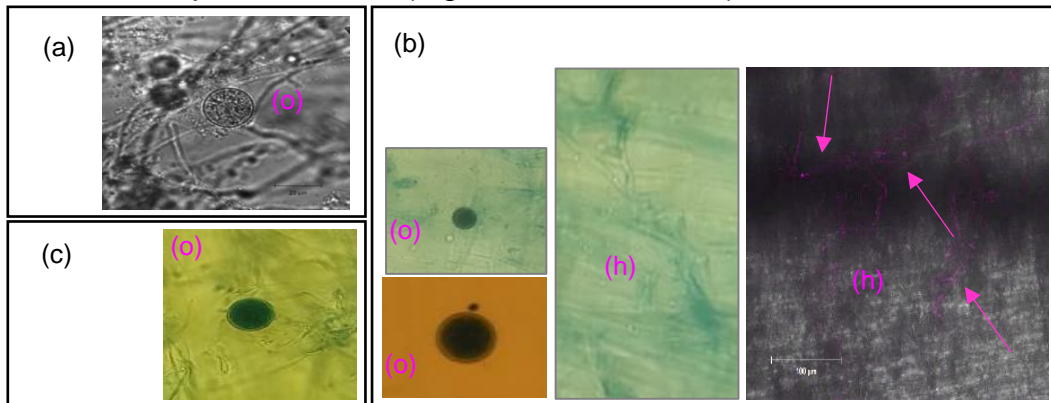


Figure 4.17. Photos of infected Glen Dee, Glen Moy and Latham at 9 and 10 dpi. Photos of *P. rubi* red fluorescent structures (tdT) on Glen Moy (a), Glen Dee (b) and Latham (c) roots: hyphae (h), sporangia (s) and oospores (o). Some roots were stained with Trypan Blue and observed under a standard microscope. Photos were taken at 9 dpi (Trypan Blue stained photos) and 10 dpi from infections carried out in August 2019, September 2019 and February 2020. Photos were taken with Zeiss LSM 710.

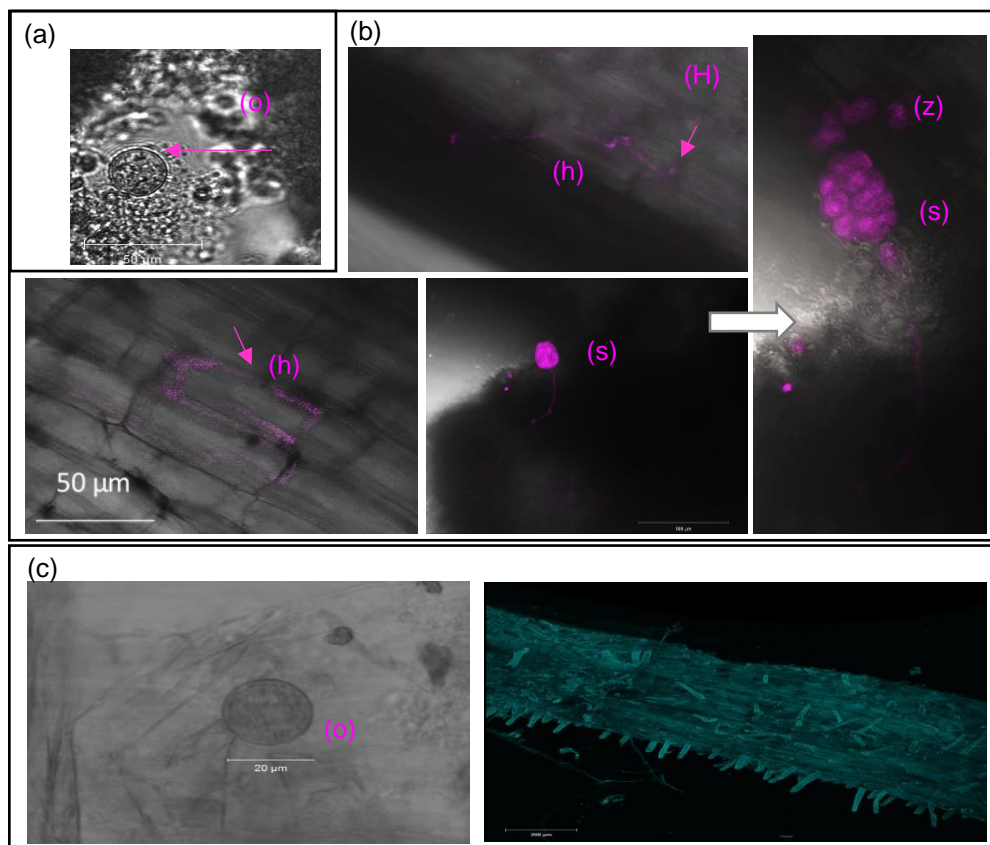


Figure 4.18. Photos of infected Glen Dee, Glen Moy and Latham at 11 dpi. Photos of *P. rubi* red fluorescent structures (tdT) on Glen Moy (a), Glen Dee (b) and Latham (c) roots: hyphae (h), possible haustoria (H), sporangia (s), zoospores (z) and oospores (o). Photos were taken at 11 dpi from infections carried out in February 2019, January 2020 and February 2020. Photos were taken with Zeiss LSM 710.

By 14 dpi, oospores, hyphae, sporangia and possible haustoria were again present in greater numbers and illustrated the extent of infection (Figure 4.19).

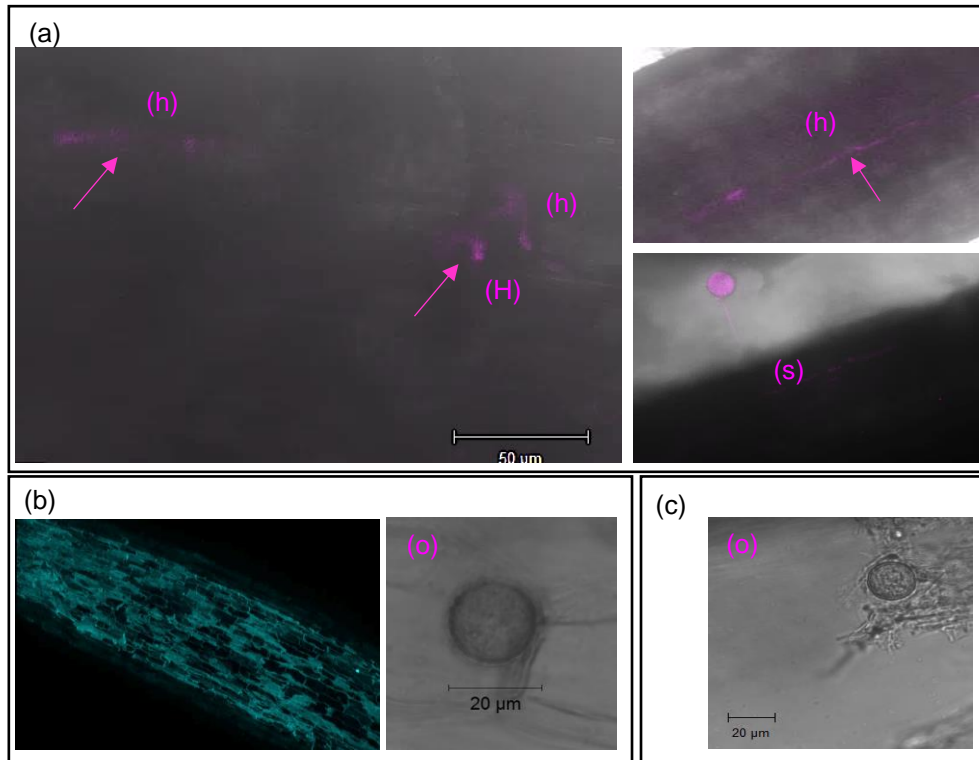


Figure 4. 19. Photos of infected Glen Dee, Glen Moy and Latham at 14 dpi. Photos of *P. rubi* red fluorescent structures (tdT) on Glen Moy (a), Glen Dee (b) and Latham (c) roots: hyphae (h), possible haustoria (H), sporangia (s) and oospores (o). Photos were taken at 14 dpi from infections carried out in February 2019, September 2019 and January 2020. Photo were taken with Zeiss LSM 710.

By 22 dpi, 24 dpi and 30 dpi, sporangia and oospores were still observed but the isolate appeared to have lost its fluorescence in the absence of antibiotic selection (Figure 4.20). The disease symptoms displayed by the whole plants at 30 dpi showed that Glen Moy plants were heavily wilted compared to Glen Dee (Figure 4.21), confirming Glen Moy to be the most susceptible cultivar.

These experiments indicate that the life cycle of *P. rubi* on raspberry roots could be completed in hydroponic conditions within 11-14 days. Glen Dee was the most attractive susceptible raspberry for these infection assays as it grew well in hydroponics and appeared to be susceptible to transgenic *P. rubi* SCRP333_tdT, as expected. A reliable supply of Glen Moy and Latham from hydroponics was more difficult to obtain.

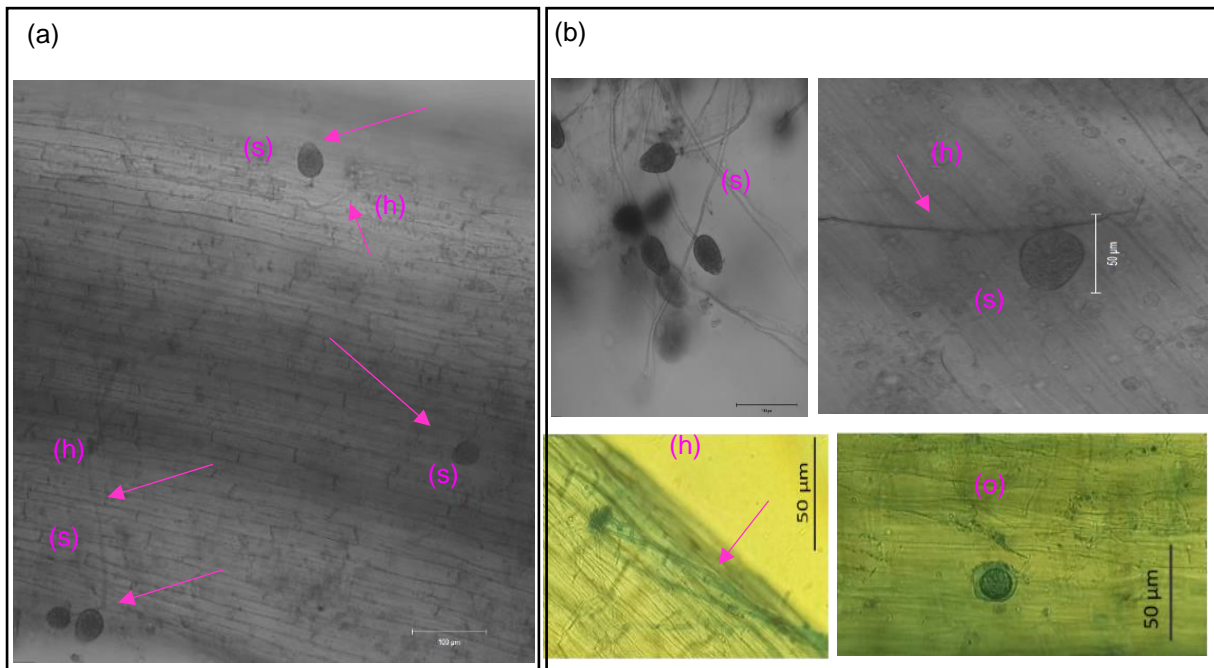


Figure 4. 20. Photos of infected Glen Dee and Glen Moy at 22 and 30 dpi. Photos of *P. rubi* red fluorescent structures (tdT) on Glen Moy (a) and Glen Dee (b) roots: hyphae (h), sporangia (s) and oospores (o). Photos were taken between 22 and 30 dpi from infections carried out in February 2019 and September 2019. Photos were taken with Zeiss LSM 710.



Figure 4. 21. Photos of infected Glen Dee and Glen Moy plants at 30 dpi. Plants were infected with *P. rubi* SCRP333_tdT at 30 dpi in the February 2019 infection assay.

4.3.5. Investigation of resistance in Latham

Latham is known as a root rot resistant cultivar. Genetic studies have identified candidate loci associated with both root vigour and resistance (Graham et al., 2011). Here we examined whether we could distinguish if Latham displays signs of a

resistance mechanism to *P. rubi* or if the root vigour phenotype helps it outgrow the attempted infection.

No *P. rubi* hyphae was detected inside the roots of Latham in any experimental reps (seven infections that included Latham plants). Latham root tissues were stained using Trypan blue (to stain dead or dying cells for both host cells and pathogen hyphae) but results were inconclusive. Several non-fluorescent oospores were, however, observed on the surface of the Latham roots, suggesting that oospores can be formed and bind the roots (Figures 4.16 c), 4.17 c), 4.18 c) and 4.19 c)).

A quick resistance screening test was performed following Li et al. (2017) protocol using detached petioles with 'high health' Glen Moy and Latham plants. Briefly, petioles were inoculated with *P. rubi* isolates SCRP333 and SCRP1207 (as described in Li et al., 2017), and symptoms observed 4 and 11 days after inoculation. This assay only confirmed differences between the cultivars in terms of visible symptoms, as chlorosis of Glen Moy leaves but not Latham happened quickly. However, lesions were not observed on stems and infection were not confirmed, making any further conclusion difficult (data not shown).

Next, we examined whether Latham may induce HR-like lesions in response to *P. rubi* PAMPs. Lima bean containing culture filtrate, left from the liquid culture of *P. rubi* and *P. infestans* isolates, should contain a PAMP cocktail. We observed that *P. rubi* culture filtrate infiltrated into *N. benthamiana* and potato leaves induced HR-like lesions (Figures 4.22 and 23).

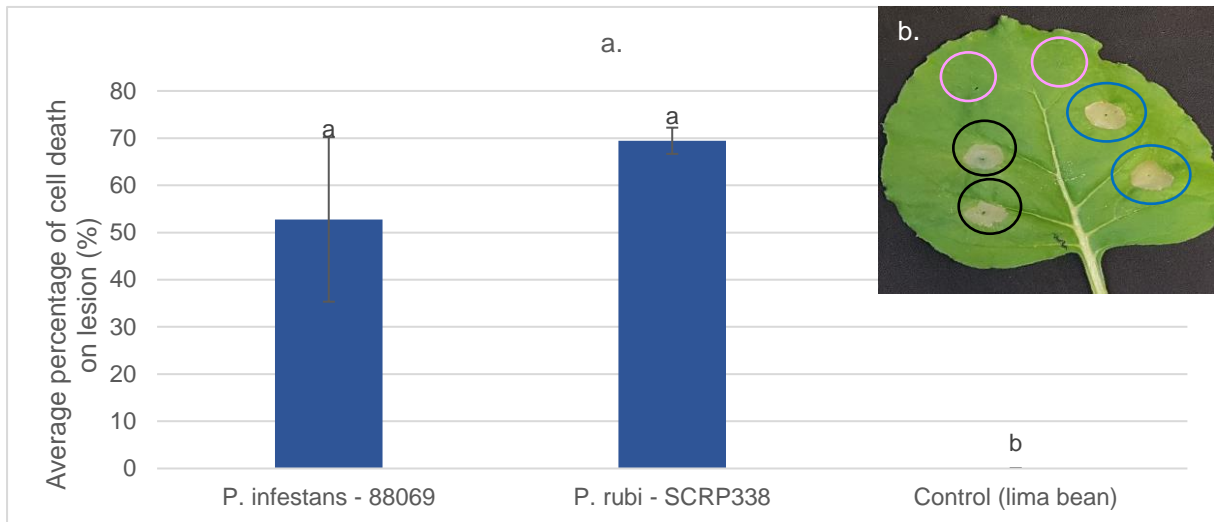


Figure 4. 22. *N. benthamiana* leaf infiltration with *P. rubi* and *P. infestans* culture filtrates. Average percentages of cell death on *N. benthamiana* leaves infiltrated with *P. rubi* isolate SCRP338 and *P. infestans* isolate 88069 and on non-infected leaves (control). **a.** Lesions were assessed 4 days after infiltration. Vertical bars represent the standard error of the mean. ANOVA and Tukey's HSD test were performed in R Studio v1.1.383 and statistical differences are given as labelled letters. **b.** Photos of *N. benthamiana* leaf infiltrated with *P. rubi* isolate SCRP338 (circled blue) and *P. infestans* isolate 88069 (black) showing HR response. Lima bean controls are shown circled in white.

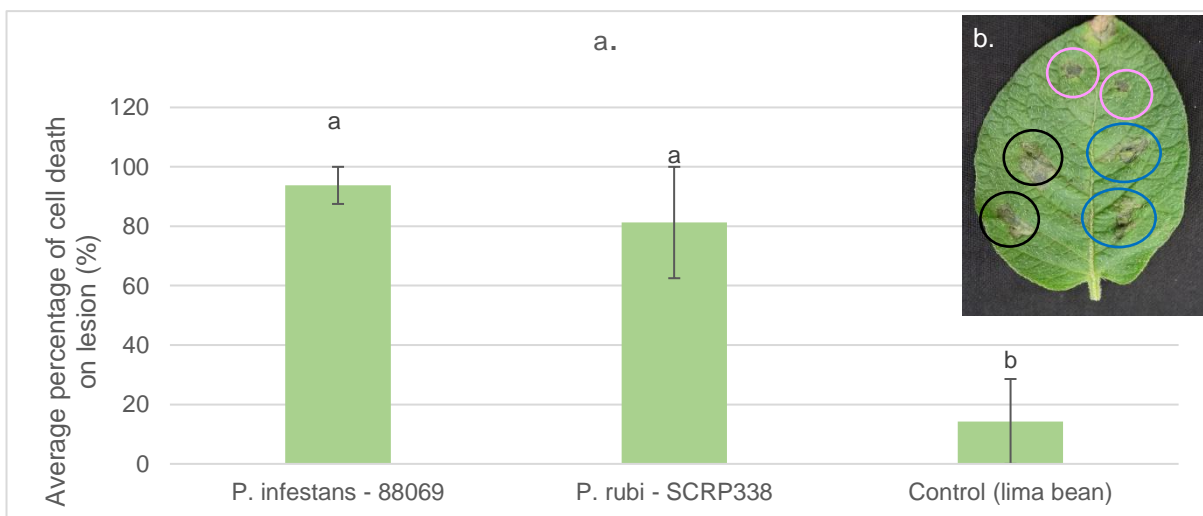


Figure 4. 23. Potato leaf infiltration with *P. rubi* and *P. infestans* culture filtrates. **a.** Average percentages of cell death on potato leaves infiltrated with *P. rubi* isolate SCRP338 and *P. infestans* isolate 88069 and on non-infected leaves (control). Lesions were assessed 4 days after infiltration. Vertical bars represent the standard error of the mean. ANOVA and Tukey's HSD test were performed in R Studio v1.1.383 and statistical differences are given as labelled letters. **b.** Photos of potato leaf infiltrated with *P. rubi* isolate SCRP338 (circled blue) and *P. infestans* isolate 88069 (black) taken at 5 dpi and showing HR response. Lima bean controls are shown circled in white.

Culture filtrates were also inoculated into leaves of resistant (Latham) and susceptible (Glen Dee) raspberry cultivars to assess responses to *P. rubi* PAMP and any potential differences between cultivars and pathogenic isolates. Unfortunately, inoculation process on raspberries was proven very difficult and considerably damaging to the leaves. In addition, lima bean extracts used as controls also induced significant background levels of cell death (Figure 4.24). Therefore, even though we believe similar HR responses than the ones observed in *N. benthamiana* and potato would be seen in raspberry cultivars, we could not conclude whether PTI responses were being induced in Latham by *P. infestans* or *P. rubi* PAMP cocktail.

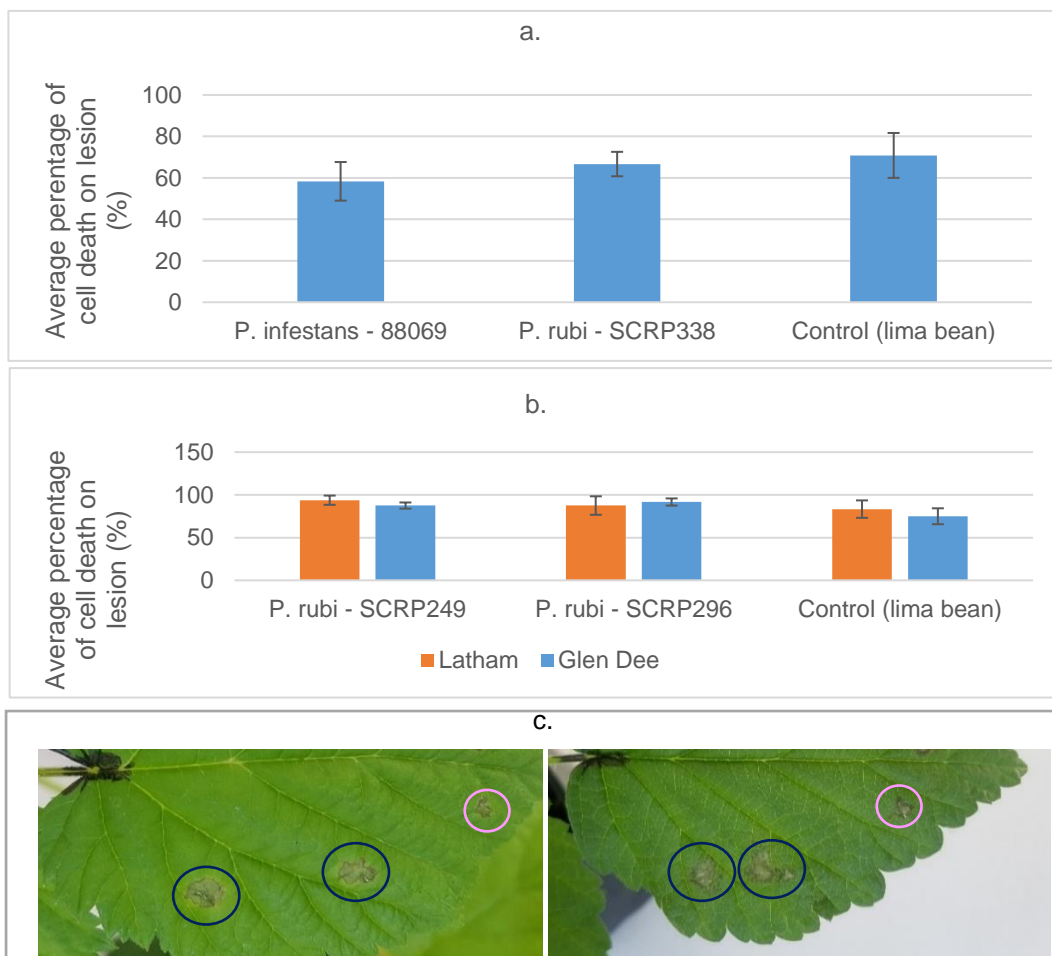


Figure 4. 24. Raspberry leaf infiltration with *P. rubi* and *P. infestans* culture filtrates. Average percentages of cell death on raspberry leaves infiltrated with *P. rubi* and *P. infestans* isolates and on non-infected leaves (control). **a.** Leaf infiltration assay using Glen Dee leaves infiltrated with culture filtrates of *P. infestans* isolate 88069 and *P. rubi* isolate SCRP338. **b.** Leaf infiltration assay using Glen Dee (blue) and Latham (orange) leaves infiltrated with *P. rubi* isolates SCRP296 and SCRP249. Lesions were assessed 4 days after infiltration. Vertical bars represent the standard error of the mean. ANOVA and Tukey's HSD test were performed in R Studio v1.1.383 and no statistical differences were observed. **c.** Photos of raspberry leaves infiltrated with *P. rubi* SCRP249 (circled dark blue) and lima bean (circled pink) showing cell death response. Left: Glen Dee and right: Latham.

4.3.6. *P. rubi* gene expression studies in susceptible raspberry cultivars

RNA was extracted from infected Glen Dee at several time points to study expression of genes of interest, including life markers and RXLR effectors identified by PenSeq. RNA purification from woody plants has proven difficult due to plant biochemicals such as polyphenols or polysaccharides (Dash, 2013). Raspberries are well known to contain particularly high levels of polyphenols like flavonoids (anthocyanins, flavonols etc.) and polysaccharides (Jones et al., 1997). Polyphenols interfere with RNA indirectly when oxidised into quinonic compounds (Mattheus et al., 2003). Polysaccharides have similar properties to nucleic acids and therefore co-precipitate with the RNA, thus contaminating it (Azevedo et al., 2003; Sharma et al., 2003).

4.3.6.1. The CTAB RNA extraction method from Yu et al. (2012) was the most suitable for raspberry root samples

Three RNA extraction techniques from infected roots were tested to find the most suitable one for the assay (Table 4.6). High yield was specifically important as *P. rubi* transcripts are swamped by raspberry transcripts, during *in planta* stages of the life cycle. Only the Yu et al. (2012a) CTAB gave satisfactory yields and considerably higher quality than those obtained from the two other techniques (Table 4.6). Consequently, all further RNA extractions were performed as per Yu et al. (2012a).

Table 4. 6. RNA results from three extraction methods. Average results from NanoDrop (NanoDrop 1000 from Thermo fisher Scientific) using three RNA extraction methods from infected raspberry roots grown in hydroponics

RNA extraction method used	Starting weight	NanoDrop results		
		260/280	260/230	ng/ μ L
Qiagen RNeasy Plant Mini Kit + Ambion Plant RNA Isolation Aid and DNase treatment	~ 50-100 mg	1.37	0.38	18.85
	~ 200 mg	2.08	0.06	9.9
TriReagent	~ 100 mg	1.71	4.15	7.9
Yu et al. (2012)	~ 100 mg	1.76	1.78	350.1

4.3.6.2. Expression of *P. rubi* life markers

To determine and confirm infection progression of *P. rubi in planta*, expression of published lifecycle markers from other *Phytophthora* species were identified. Genes such as *PrHmp1* (linked to biotrophic feeding and secretion structures known as

haustoria), *PrCDC14* (upregulated in sporangia) and *RUB1* (ortholog of *P. infestans* INF1, PAMP elicitor causing necrotic cell death lesions) were assessed during infection. Primers were validated through conventional PCR and electrophoresis gel before using in qRT-PCR assays. Expression levels relative to a control sample of SCRP333_tdT mycelia and sporangia were calculated using *CoxI* and beta-tubulin as endogenous control genes. *CoxI* was the endogenous control chosen for data presented here, as it appeared to be marginally more robust through infection time-courses examined.

- *PrHmp1* expression indicates presence of haustoria development and biotrophic phase

Relative expression for haustorial marker *Hmp1* (*PrHmp1*) during infection of susceptible cultivar Glen Dee showed upregulation during two independent time-course experiments (Figure 4.25). In fact, *PrHmp1* showed a biphasic expression, upregulated at 3 dpi and 11 dpi (February 2019 time-course), but dipped at 7 dpi and 14 dpi, (Figure 4.25). The same expression patterns were observed in the 2nd independent replicate (September 2019, data not shown). This biphasic pattern of haustoria membrane protein expression could suggest the re-infection of roots by fresh zoospores production.

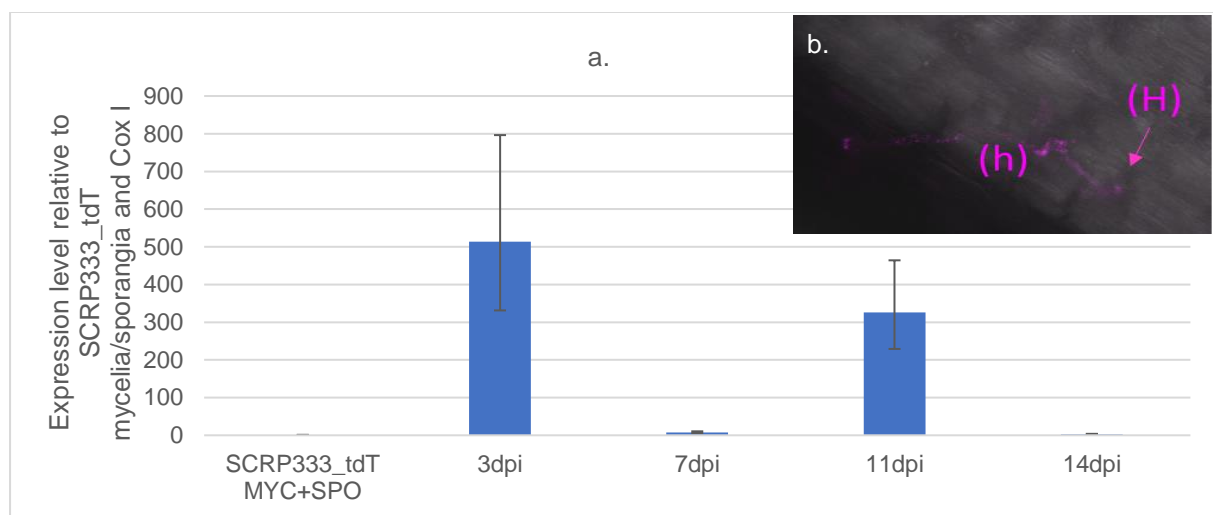


Figure 4. 25. Relative expression of *P. rubi* haustoria-specific membrane protein *PrHmp1*. a. Relative expression of *PrHmp1* during the February 2019 infection of Glen Dee cultivar at several time points. Expression relative to the housekeeping gene *CoxI* and the control sample SCRP333_tdT sporulating mycelia (MYC+SPO) was calculated using the $\Delta\Delta CT$ method. Vertical bars represent the standard error of the mean for three technical replicates. b. Photos from February 2019 infection of Glen Dee at 11 dpi show fluorescent hyphae (h) and possible haustoria (H).

- *PrCDC14* expression confirmed timing of sporangia formation

Relative expression of marker associated with sporangia development, *PrCDC14*, showed statistically higher expression in infected sample at all *in planta* time points during the February 2019 time-course (Figure 4.26.a). It appears the timing of the 2nd biological rep may have been slightly different (September 2019), as much higher relative expression of *PrCDC14* at 14 dpi was identified whereas this marker was under-expressed at 7 dpi (Figure 4.26.b). These findings were supported by detection of sporangia at 11 dpi (Figure 4.26.c).

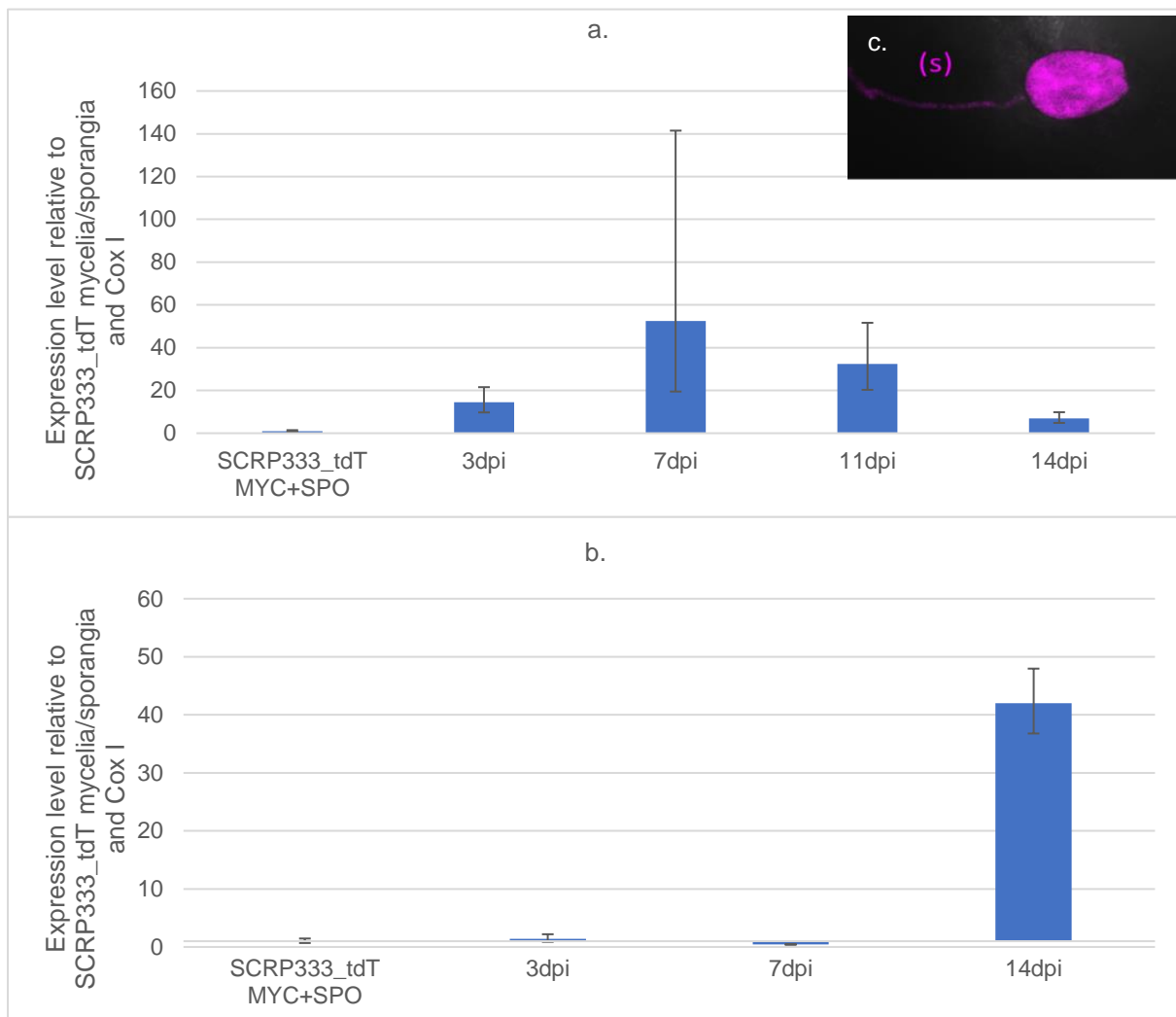


Figure 4. 26. Relative expression of *P. rubi* sporulation marker *PrCDC14*. Relative expression of *PrCDC14* during the February 2019 (a) and September 2019 (b) infection of Glen Dee cultivar at several time points. Expression relative to the housekeeping gene *CoxI* and the control sample SCRP333_tdT sporulating mycelia (MYC+SPO) was calculated using the $\Delta\Delta$ CT method. Vertical bars represent the standard error of the mean for three technical replicates. c. Photo from February 2019 infection of Glen Dee at 11 dpi shows fluorescent sporangia (s).

- Expression levels of *RUB1* indicates increasing necrotrophy over time

Relative expression of *RUB1*, ortholog to *P. infestans* necrotic PAMP elicitor INF1, was found increased during infection from 3 dpi to 11 dpi and upregulated at all time points assessed (Figure 4.27). Unfortunately, the presence of a necrotrophic stage in susceptible cultivars could not be confirmed on infected roots with Trypan Blue.

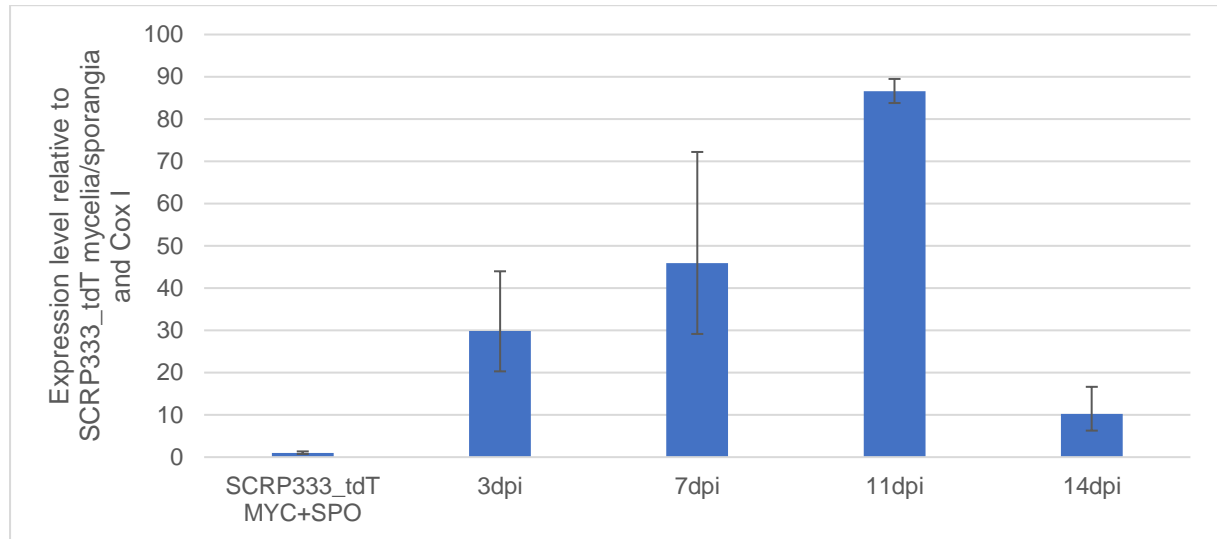


Figure 4. 27. Relative expression of *P. rubi* marker *RUB1*. Relative expression of *RUB1* during the February 2019 infection of Glen Dee cultivar at several time points. Expression relative to the housekeeping gene *CoxI* and the control sample SCRP333_tdT sporulating mycelia (MYC+SPO) was calculated using the $\Delta\Delta CT$ method. Vertical bars represent the standard error of the mean for three technical replicates.

Generally, patterns for expression of these three life markers were confirmed in two independent replicates. These results reinforce confocal observations of simultaneous waves of infection, caused by initial inoculum and second-generation zoospores infecting the roots.

4.3.6.3. Expression of four *P. rubi* RXLR genes in susceptible raspberry roots

Several RXLRs were selected for expression studies and examined during multiple *in planta* infections. SCRP333_contig_4275_F7 (PR003_g28352) gene coverage shows 100 % conservation across all *P. rubi* isolates at 3 % mismatch rate, while coverage remained 0 % in *P. fragariae* isolates examined, thus indicating absence in *P. fragariae* (Chapter 3, Table 3.18). Expression analyses revealed early *in planta* expression, particularly at 3 dpi (September 2019, Figure 4.28). It would be interesting to functionally characterise this unique *P. rubi* RXLR effector, as it may be essential for

virulence and could play a role in early PTI or ETI suppression in raspberries or in determining host range.

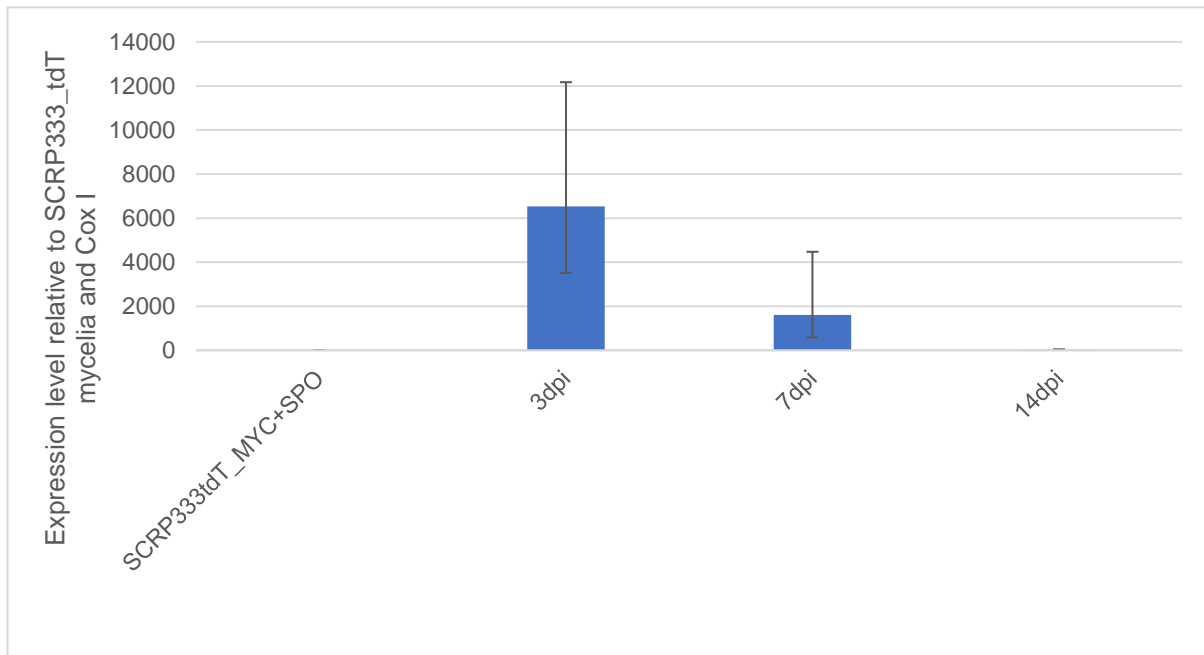


Figure 4. 28. Relative expression of *P. rubi* SCRP333_contig_4275_F7 RXLR gene during the September 2019 infection time course. Relative expression of *P. rubi* SCRP333_contig_4275_F7 RXLR gene from infected raspberry in the September 2019 infection assay. Expression relative to the housekeeping gene *CoxI* and the control sample SCRP333_tdT sporulating mycelia (MYC+SPO) was calculated using the $\Delta\Delta CT$ method. Vertical bars represent the standard error of the mean for three technical replicates.

To narrow down the list of *P. rubi* candidate RXLR genes to select for the expression study *in planta*, an alternative approach was utilised, using an RNASeq experiment. Hydroponic infection of Glen Dee roots inoculated with SCRP333_tdT and sampled after 7 days (performed by fellow PhD student, Raisa Osama) was set up to examine plant transcriptomics. This data was mined here for the presence of *P. rubi* transcripts. Transcripts were filtered for an FPKM value above 5 (Adams, 2019). Reads were mapped to our PenSeq list of 14,295 *P. rubi* genes of interest. Transcripts from 278 apoplastic genes and 25 RXLR effectors. Ten of these RXLR genes were predicted by the Whisson et al. (2007) model. PenSeq derived read coverage for the ten *in planta* expressed Whisson RXLRs candidates were assessed for inter- and intra-species diversity (Table 4.7). Three RXLRs with the highest FPKM values and displaying intra and inter-species polymorphism were selected for qRT-PCR analyses (Table 4.7): SCRP333_g22109 (PR003_g23841), SCRP333_g22154 (PR003_g23891) and SCRP333_g24428 (PR003_g26341).

Table 4. 7. Coverage of 10 *P. rubi* RXLR genes expressed at 7 dpi. Coverage of 10 RXLR genes predicted with the Whisson et al. (2007) model and selected through RNASeq experiment of infected raspberry at 7 dpi showing transcripts with FPKM value >5. Coverage is presented for 0 % and 3 % mismatch mapping rates (mm). Coverage below 100 % at 0 % mm is likely indicating of Single Nucleotide Polymorphism (SNP). Three RXLRs selected for qRT-PCR assays are highlighted (green rectangle).

Genes of interest		SCR333_g13961		SCR333_g22109		SCR333_g22154		SCR333_g24428		SCR333_g5642		SCR333_g14107		SCR333_g14499		SCR333_g20928		SCR333_g25008		SCR333_g4670		
Mismatch rate		0%mm	3%mm	0%mm	3%mm	0%mm	3%mm	0%mm	3%mm	0%mm	3%mm	0%mm	3%mm	0%mm	3%mm	0%mm	3%mm	0%mm	3%mm	0%mm	3%mm	
<i>P. rubi</i>	SCR249	100.0	100.0	57.0	95.4	100.0	100.0	41.9	98.4	100.0	100.0	98.3	100.0	100.0	100.0	99.2	100.0	99.4	100.0	100.0	100.0	
	SCR296	100.0	100.0	100.0	100.0	100.0	100.0	45.4	99.2	100.0	100.0	100.0	100.0	100.0	100.0	100.0	100.0	100.0	100.0	75.8	100.0	
	SCR324	100.0	100.0	100.0	100.0	100.0	100.0	53.0	95.1	100.0	100.0	95.2	100.0	100.0	100.0	100.0	100.0	96.6	100.0	50.3	100.0	
	SCR333	100.0	100.0	100.0	100.0	100.0	100.0	100.0	100.0	100.0	100.0	100.0	100.0	100.0	100.0	100.0	100.0	100.0	100.0	100.0	100.0	
	SCR339	100.0	100.0	100.0	100.0	100.0	100.0	100.0	100.0	100.0	100.0	100.0	100.0	100.0	100.0	100.0	100.0	100.0	100.0	100.0	100.0	100.0
	SCR1202	100.0	100.0	100.0	100.0	100.0	100.0	100.0	100.0	100.0	100.0	100.0	100.0	100.0	100.0	100.0	100.0	100.0	100.0	100.0	100.0	100.0
	SCR1208	100.0	100.0	80.8	100.0	100.0	100.0	100.0	100.0	100.0	97.2	100.0	100.0	100.0	88.2	100.0	100.0	100.0	92.2	100.0	58.7	100.0
	SCR1213	100.0	100.0	100.0	100.0	100.0	100.0	100.0	100.0	100.0	100.0	100.0	100.0	100.0	100.0	100.0	100.0	100.0	100.0	100.0	100.0	100.0
	SCR250	100.0	100.0	100.0	100.0	100.0	100.0	42.7	100.0	100.0	100.0	100.0	99.0	100.0	100.0	100.0	100.0	100.0	91.8	100.0	51.4	100.0
	SCR260	100.0	100.0	88.5	100.0	100.0	100.0	100.0	100.0	100.0	97.2	100.0	100.0	100.0	87.1	100.0	100.0	100.0	90.8	100.0	63.0	100.0
	SCR283	100.0	100.0	100.0	100.0	100.0	100.0	0.0	37.9	61.9	100.0	93.9	100.0	100.0	100.0	100.0	99.8	100.0	96.9	100.0	75.5	100.0
	SCR287	100.0	100.0	100.0	100.0	100.0	100.0	100.0	100.0	100.0	100.0	100.0	100.0	100.0	100.0	100.0	100.0	100.0	100.0	100.0	100.0	100.0
	SCR288	100.0	100.0	64.7	100.0	100.0	100.0	89.7	100.0	100.0	100.0	100.0	100.0	100.0	100.0	100.0	100.0	100.0	95.4	100.0	100.0	100.0
	SCR290	100.0	100.0	100.0	100.0	100.0	100.0	100.0	100.0	100.0	100.0	100.0	100.0	100.0	100.0	100.0	100.0	100.0	96.8	100.0	100.0	100.0
	SCR292	100.0	100.0	68.8	100.0	98.3	100.0	41.6	99.4	67.9	100.0	100.0	100.0	95.7	100.0	100.0	100.0	100.0	100.0	100.0	43.5	98.4
	SCR293	100.0	100.0	97.1	100.0	100.0	100.0	100.0	100.0	100.0	95.3	100.0	100.0	100.0	85.7	100.0	100.0	100.0	91.8	100.0	58.4	100.0
SCR323	100.0	100.0	100.0	100.0	100.0	100.0	44.3	95.1	100.0	100.0	95.9	100.0	100.0	100.0	100.0	100.0	100.0	99.4	100.0	51.6	93.8	
SCR338	100.0	100.0	100.0	100.0	97.8	100.0	0.0	0.0	65.5	100.0	98.8	100.0	100.0	100.0	100.0	98.4	100.0	94.1	100.0	87.0	100.0	
SCR1207	100.0	100.0	99.3	100.0	100.0	100.0	100.0	100.0	100.0	97.9	100.0	100.0	100.0	84.4	100.0	100.0	100.0	89.5	100.0	57.3	100.0	
SCR1212	100.0	100.0	100.0	100.0	100.0	100.0	100.0	100.0	100.0	100.0	100.0	100.0	100.0	100.0	100.0	100.0	100.0	100.0	100.0	100.0	100.0	
<i>P. fragariae</i>	BC-1	78.6	96.9	80.3	100.0	48.7	94.8	0.0	0.0	0.0	30.2	45.8	100.0	23.6	23.6	48.2	48.3	0.0	100.0	0.0	57.3	
	BC-16	32.8	52.8	23.3	71.9	81.5	100.0	0.0	0.0	0.0	1.9	0.0	100.0	17.8	17.8	25.9	25.9	23.6	100.0	27.2	57.1	
	NOV-9	0.0	50.2	25.5	70.2	11.7	94.9	63.3	85.8	42.2	88.4	59.8	100.0	0.0	0.0	26.8	26.8	24.7	100.0	38.0	73.4	
	SCR245	62.9	100.0	26.7	72.4	0.0	98.9	15.1	68.9	51.0	52.9	0.0	100.0	25.4	25.4	39.1	45.7	0.0	100.0	45.1	69.8	
FPKM	452.0		410.0		195.0		172.0		488.0		65.0		126.0		156.0		59.0		43.0			

SCR333_g22109 (PR003_g23841) was found in all *P. rubi* isolates at 3 % mismatch rate but in only one *P. fragariae* isolate (BC-1). SCR333_g22154 (PR003_g23891) shows 100 % coverage at 3 % mm in all *P. rubi* isolates and high coverage in *P. fragariae* (94.8 % to 98.9 %). Evaluation of SCR333_g22154 sequence revealed that it was a close match to *P. fragariae* RXLR effector BC-16_g5824 (PF003_g6480), found to be expressed *in planta* at all time points during strawberry infections (personal communication, Adams, 2019; see Chapter 3, Table 3.19 and Figure 3.12). SCR333_g24428 (PR003_g26341) was identified as a candidate RXLR absent in Canadian isolates (Chapter 3). Gene coverage shows absence in Canadian isolate SCR338 (0 % at any mm) and highly diversified in USA isolate SCR283 (0 % at 0 % mm and only 37.9% at 3 % mm, Table 4.7).

Relative expression for RXLR genes was first confirmed using qRT-PCR on cDNA synthesised from material used in RNASeq infection (Figure 4.29).

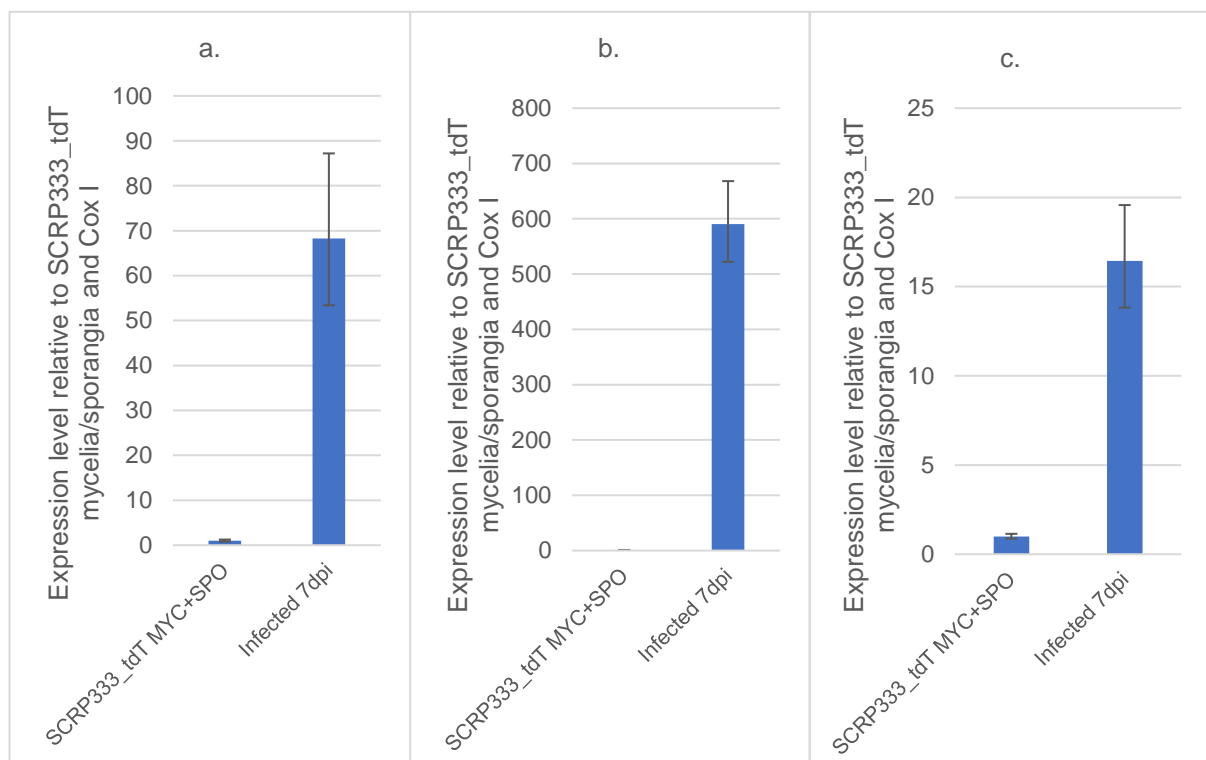


Figure 4. 29. Relative expression of *P. rubi* RXLR genes SCR333_g22109, SCR333_g22154 and SCR333_g24428 at 7 dpi from RNASeq samples. Relative expression of a. SCR333_g22109, b. SCR333_g22154 and c. SCR333_g24428 from infected raspberry sampled at 7 dpi and used for RNASeq data. Expression relative to the housekeeping gene *CoxI* and the control sample SCR333_tdT sporulating mycelia (MYC+SPO) was calculated using the $\Delta\Delta CT$ method. Vertical bars represent the standard error of the mean for three technical replicates.

Two further independent biological replicates of Glen Dee infection time-courses (February 2019; September 2019), used above to examine life stage markers, were used to confirm *in planta* RXLR expressions. SCRP333_g22154, SCRP333_g24428 and SCRP333_g22109 all showed *in planta* expression at most time points during February 2019 time-course (Figure 4.30 a-c) and to a lower extent but also confirmed in September 2019 time-course (Figures 4.30 d-f). Expression data confirms that, as in *P. fragariae* infections of strawberry, *P. rubi* gene SCRP333_g22154 is expressed during infection of raspberry, suggesting an essential and conserved virulence function for both pathogens. We note that expression patterns for these three RxLR genes seems to match expression patterns for sporulation marker *PrCDC14*, with over and under-expression at the same time points. Here, during the September 2019 time course, *PrCDC14* was under-expressed at 7 dpi, similarly to the three RXLR genes. During the February 2019 infection, all genes were over-expressed at all time points studied.

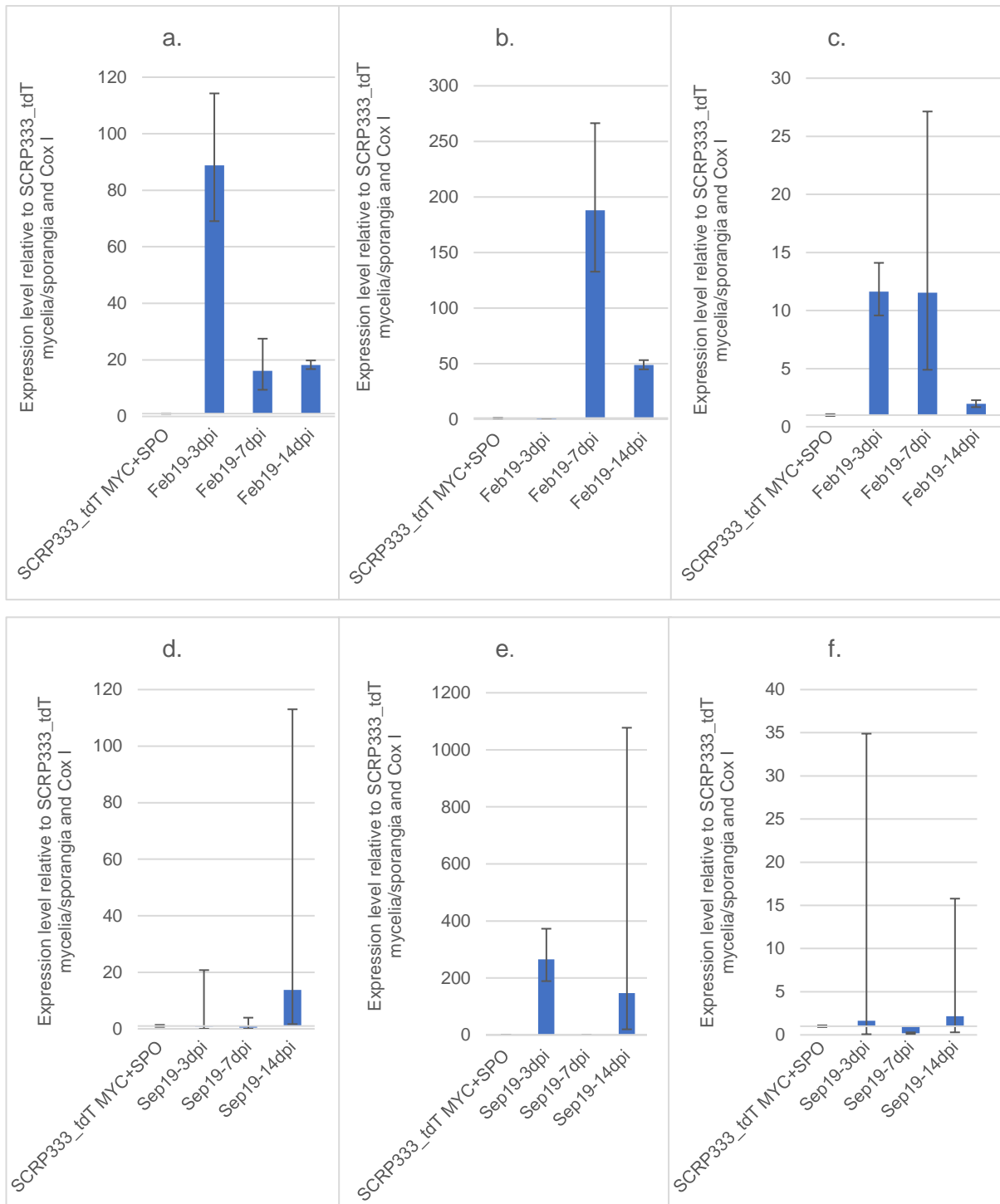


Figure 4. 30. Relative expression of *P. rubi* RXLR genes SCRP333_g22109, SCRP333_g22154 and SCRP333_g24428 in infection time courses from qRT-PCR. Relative expression of SCRP333_g22109 (a,d) , SCRP333_g22154 (b,e) and SCRP333_g24428 (c,f) from infected raspberry sampled at 3, 7 and 14 dpi during the February 2019 (top, a-c) and the September 2019 (bottom, d-f) infection assays using qRT-PCR. Expression relative to the housekeeping gene CoxI and the control sample SCRP333_tdT sporulating mycelia was calculated using the $\Delta\Delta CT$ method. Vertical bars represent the standard error of the mean for three technical replicates.

4.4. Discussion & conclusions

This chapter reviews and updates the methodology regarding *P. rubi* infections of raspberry roots. From the optimization of sporulation to genetic transformation for expression of fluorescent markers, to real-time infections, RNA extraction and gene expression analysis, it provides a comprehensive guide for research of *P. rubi* infection lifecycle.

The most successful *Phytophthora* transformation methods have primarily utilised protoplasts (Judelson et al., 1991). The difficulty in using this stage for transformation of most clade 7 *Phytophthora* species is that sporangia and zoospores production are slow to develop and rely on a number of environmental factors as well as unknown compounds found in non-sterile soil solutions (Waterhouse, 1931; Adams, 2019). Therefore, zoospores production has a huge association with contamination issues. Thus, methods using young mycelial mats for protoplasts liberation have been examined (Dou et al., 2008a; McLeod et al., 2008; Fang and Tyler, 2016; Wang et al., 2019b). Here we report that *P. rubi* isolate SCR333 is successfully transformed to express green and red fluorescent proteins (eGFP and tdTomato respectively) using a PEG-protoplast transformation of tissue derived from young mycelium (Judelson et al., 1991; Judelson et al., 1993; van West, 1999; Champouret and Kamoun, 2004; McLeod et al., 2008). Another difficulty with *Phytophthora* transformations is that not all isolates can be transformed and maintain fluorescence (Ochoa et al., 2019). Unfortunately, and although it was obtained through two methods, the success of initial transformation of SCR333 could not be repeated for other *P. rubi* isolates.

Many transgenic pathogens have been generated to express fluorescent proteins in order to observe *in planta* infection structures (Maor et al., 1998; Dumas et al., 1999; Sexton and Howlett, 2001; Chen et al., 2003; Si-Ammour et al., 2003; Le Berre et al., 2008; Vallad and Subbarao, 2008; Li et al., 2011; Njoroge et al., 2011; Dunn et al., 2013; Evangelisti et al., 2017; Ochoa et al., 2019). Transgenic isolates can display slower *in vitro* growth, and a loss of virulence, demonstrated through smaller lesions or less symptoms (Sexton and Howlett, 2001; Si-Ammour et al., 2003; Riedel et al., 2009; Dunn et al., 2013; Ochoa et al., 2019). Other publications have stated no loss of virulence or pathogenicity after transformation (Bailey et al., 1991; Judelson et al., 1991; Nahalkova and Fatehi, 2003; Visser et al., 2004; Vallad and Subbarao, 2008; Li

et al., 2011). While SCRP333_tdT and SCRP333_eGFP present slowed *in vitro* growth, this study also shows that their ability to produce sporangia, an essential step prior to carrying out infection, is not affected.

A method to reliably induce *P. rubi* sporangia for infection assays has been required for this project and is developed here from a variety of techniques found in the literature (Backwell and Waterhouse, 1931; Waterhouse, 1931; Goode, 1956; Marx and Haasis, 1965; Zentmyer, 1965; Chee and Newhook, 1966; Ayers, 1971; Mussel and Fay, 1973; Chandelier et al., 2006; Adams, 2019). We show that although *P. rubi* grows slower on French Bean agar, it leads to better *P. rubi* sporangia suggesting that different nutrients in these mediums can influence sporulation (Ah Fong and Judelson, 2003; Kim and Judelson, 2003). It was also found that young cultures are best for generating *P. rubi* sporangia, confirming Mussel and Fay conclusions (1973). The type of sporulation solution in which *Phytophthora* plugs are submerged equally plays a crucial role on the efficiency of sporulation. Schmitthenner and Bhat (1994) stated that root-infecting *Phytophthora* sporulate best in liquid, as opposed to on agar, and we have found that *P. rubi* and *P. fragariae* conform to that pattern. As indicated by past studies (Mehrlich, 1934; Marx and Haasis, 1965; Zentmyer, 1965; Chee and Newhook, 1966; Mussel and Fay, 1973), sporangia count for *P. rubi* SCRP333 increases when the sterility of the solution decreases. Soil solution can also be stored at -20 °C, allowing to save considerable time in the preparation of *P. rubi* and *P. fragariae* sporulation. However, there was variation in the success of each soil solution in terms of the number of sporangia. Chee and Newhook (1966) similarly experienced quantitative differences in inducing sporulation using soil extracts, concluding that it was likely due to the production of different stimulants and / or different rates of production of stimulant(s). Root exudates from hydroponically grown susceptible and resistant raspberry cultivars also induce sporangia production of *P. rubi*. It would be interesting to examine whether raspberry exudates induce sporulation of *P. fragariae* too, and to trial strawberry root exudates. The unknown component of the rhizosphere and soil, possibly bacterial, that triggers *P. rubi* and *P. fragariae* sporangia development remains to be determined.

Intact root tips are important for microscopic infection assays of root-infecting oomycetes (Laun and Zinkernagel, 1997). A reliable source of raspberry plants with

clean and unbroken roots (Figure 4.31), ideal for infection assays, has consequently been established using a hydroponic method called nutrient film technique (NFT).

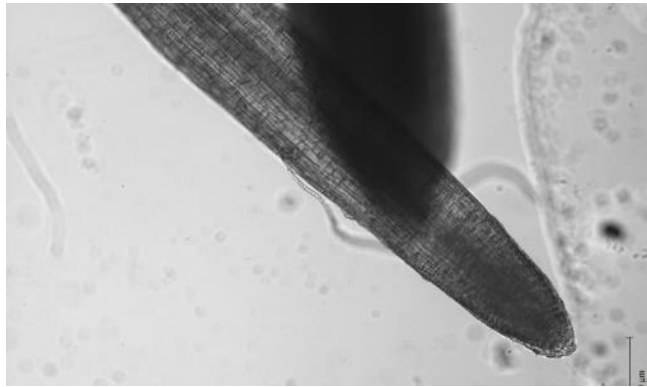


Figure 4. 31. Intact Glen Dee root and root tip (photo taken with ZEISS LSM 710, x10)

The survival and speed of raspberry cuttings rooting through alternative hydroponic-friendly medium vary greatly throughout the season and by cultivar. We found that Glen Dee is the best performing cultivar in hydroponic conditions, and it has therefore been used in infection assays throughout this thesis and in other JHI projects. MaxiCrop appears to be the nutrient solution achieving the most reliable rooting times for all cultivars, but other nutrients have led to very similar conclusions. However, in general, Glen Moy and Latham do not appear to be best suited to propagation in hydroponics using conditions attempted so far.

Interestingly, susceptible cultivars root best during the autumn and winter months (September to March), but this is not observed for Latham, also known for its vigorous root system in soil. In the darker months, lighting has been supplemented in the glasshouse with 400 W sodium lamps and the temperature regulated to 18 - 20 °C. Sodium lamps produce high proportion of light in the green–yellow spectral region and less red and blue spectral regions than natural light (Darko et al., 2014) and so we theorize that the observed differences are due to lighting conditions (Figure 4.32). Root development is known to be influenced by crosstalk between light and phytohormones, e.g. auxin (Kumari and Panigrahi, 2019). As roots typically grow in soil, they are negatively phototropic but are still influenced in many ways by light quality and quantity. For instance, Van Gelderen et al. (2018) review light signalling mechanisms and their impact on root development and physiology. They have shown a strong correlation between natural light and root growth responses. Moreover, Xu et al. (2019) have looked at the effects of composite LED light on the root growth of Chinese

fir (*Cunninghamia lanceolata*) and found that the addition of purple and green to the main red and blue lights promotes the distribution of photosynthates to roots.

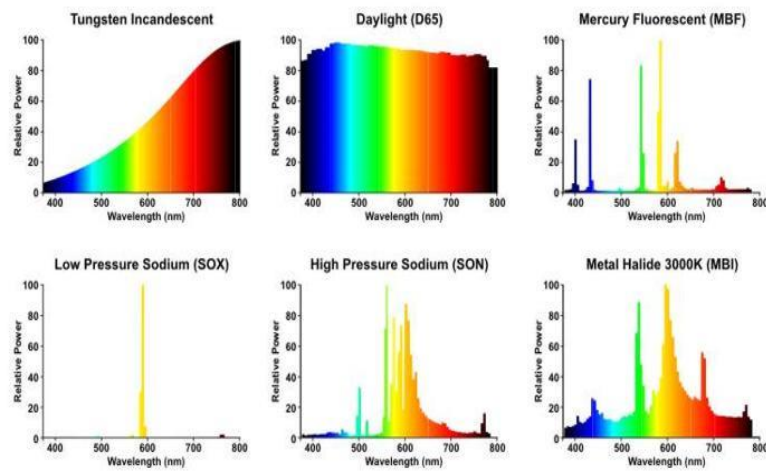


Figure 4. 32. Spectral power distributions of various light sources. Sodium lamps show high proportion of green–yellow region and a lack of red and blue, with an altered red: far red ratio compared to natural daylight (image from lamptech.co.uk).

There is still a lot of research to be done using larger plant species, in terms of how different wavelengths of light regulate different aspects of root growth and development. The solar radiation recorded throughout the year during our hydroponic trials implies that high solar radiation conditions are less conducive for root initiation and cutting survival of PRR susceptible raspberry cv. If raspberry propagation is to become routine in indoor vertical farms, the correct LED light recipes for root initiation, elongation and lateral root development would need to be optimized (Darko et al., 2014).

The following aim of this chapter was to perform infection assays to visualise and localise *P. rubi* inside natural host roots. Infection were set to identify the formation of lifecycle structures, as described by Le Berre et al. (2008) and Evangelisti et al (2017), which will then be confirmed with quantitative gene expression analyses. One problem encountered here was the low apparent *P. rubi* biomass within the root, leading to low transcript abundance of potential genes of interest, compared to plant material, a common issue encountered when looking at pathogen's genes expression *in planta*. However, optimisation steps have led to more reliable infections later in this project, as well as a dependable RNA extraction method producing good yields. The best time-course material for expression studies have been collected in September and February 2019. A second issue appeared to be limitations in the availability of plant

material for infections during summer months, as well as other possible environmental factors leading to variability between infection assays, even in controlled environments (as reported for *P. infestans*, *P. capsici* and *P. rubi*, L. Welsh, personal communication, 2018). Nonetheless, a positive finding was that infection assays were routinely completed in around two weeks. Successful infections show encystment, germination and penetration of the root at 3 days post-inoculation (dpi), hyphae colonizing the central vascular cylinder by 7 dpi, followed by sporangia and oospores after this. In addition, further waves of re-infection are identified by more sporangia, zoospores, oospores, hyphae and possible haustoria-like structures that are detected routinely after 7 dpi. As expected, after 14 dpi and under no antibiotic selection for the transgenic line, *P. rubi* appear to have lost fluorescence. All *P. rubi* structures detected during infection match previous description (Backwell and Waterhouse, 1931; Erwin et al., 1983; Duncan et al., 1987; Wilcox, 1989; Wilcox, 1991; Wilcox et al., 1993; Erwin and Ribeiro, 1996b; Man in't Veld, 2007). We observe that *P. rubi* completes its cycle quicker on Glen Moy compared to Glen Dee, highlighting cultivar variation (Table 4.1). On resistant cv Latham, it is possible that attachment and germination occurs on the root surface but no hyphal progression inside the root has been observed. Oospores are consistently detected at multiple time points which could have derived from surrounding root exudates. Although Pattison et al. (2004; 2007) and Graham et al. (2011) have researched raspberry root rot resistance, the exact mechanisms deployed during *P. rubi* infection on a resistant cultivar are still unclear.

Gene expression analyses confirm the presence of stage specific markers at times that correlate with confocal imaging observations. The haustoria membrane protein (*Hmp1*) gene is associated with initial biotrophic lifecycle stages and as RXLR effectors are delivered through haustoria, their expression profile has been found correlated with this stage (Bos et al., 2006; Whisson et al., 2007; Haas et al., 2009; Oh et al., 2009; Lévesque et al., 2010; Schornack et al., 2010; Gilroy et al., 2011; Liu et al., 2014; Whisson et al., 2016; Wang et al., 2017). Here *PrHmp1* is found significantly expressed at 3 and 11 dpi. *P. rubi* sporulation marker, *PrCDC14*, is also expressed at several time points. We believe further waves of infections occur after 7 dpi, meaning that all infection stages could be detected after this timepoint. The PAMP elicitor *PiINF1* is well documented to associate with the later and more necrotrophic stages of *P. infestans* lifecycle on leaves (Kamoun et al., 1997; Kamoun et al., 1998).

The *PrRUB1* ortholog of *PiINF1* appears to be expressed during *in planta* infection, with transcript abundance increasing over time.

Furthermore, three *P. rubi* RXLR genes, SCRP333_g22154 (PR003_g23891), SCRP333_g24428 (PR003_g26341) and SCRP333_g22109 (PR003_g23841), are confirmed to be expressed *in planta* and correlated with *PrHmp1* and *PrCDC14* expressions. This result implies that *P. rubi* may have a biotrophic phase, that haustoria development should be important for infection and that RXLR genes play an essential role in pathogen virulence. *P. rubi* gene SCRP333_g22154 is an ortholog to BC-16_g5824, which is also expressed during *P. fragariae* infection of strawberry, suggesting that it may play a critical virulence role, such as enhancing the pathogen growth and sporulation during host colonization in both sister species, as reported in other studies (King et al., 2014; Huang et al., 2019). RXLR transcripts of these three genes have also been detected in later infection time points, most probably derived from successive waves of infections in the root tissue sampled. Due to the relative low abundance of *P. rubi* material compared to plant, further work could deploy the use of PenSeq RNA baits library to enrich for RXLR transcripts from cDNA isolated from infection timepoints.

This chapter, along with Chapter 3, highlights interesting RXLR effectors with functions that would benefit from further characterisation in terms of their role in suppressing plant defenses and determining host range. Unfortunately, techniques such as *Agrobacterium*-driven effector over-expression in leaves or host-induced gene silencing (HIGS) in roots may prove extremely difficult in raspberry / strawberry and would not be recommended as the obvious next step.

In conclusion, all the aims of this chapter were successfully attempted to varying degrees of success. A range of methods have been utilised, including triggering sporulation, pathogen transformation, hydroponically grown raspberry plantlets routinely generated, RNA extractions from recalcitrant host roots and root infection assays in hydroponics. This chapter provides a better understanding of the timing of the *P. rubi* lifecycle, lifecycle specific structures and associated transcripts. The mycelial based transformation method has since been used to successfully transform *P. fragariae* isolate NOV-9 expressing red (mCherry, tdT) and green (eGFP) fluorescent proteins (L. Welsh, personal communication, 2020). Furthermore, this work has led to several grant applications on the use of fully controlled indoor farming

to propagate 'high health' soft fruit material by companies such as Liberty Produce. In addition, the James Hutton Institute glasshouse and estates team and the James Hutton Limited breeding teams have both invested in new hydroponic tanks for faster propagation of blueberries (*Vaccinium corymbosum*) and blackcurrant (*Ribes nigrum*) lines.

CHAPTER 5. CONCLUSIONS: ANSWERING QUESTIONS ABOUT RASPBERRY ROOT ROT

5.1. Conclusions on *P. rubi* raspberry root rot

Raspberry root rot, caused by *Phytophthora rubi*, and strawberry red stele, caused by *Phytophthora fragariae*, are two closely related oomycete crop pathogens limited to two *Rosaceae* host species. *P. rubi* has decimated soil grown raspberry production in the UK, parts of the EU and the USA and Canada, as commercial cultivars possess little or no resistance to the disease. Moreover, the limited number of chemical actives licensed for use in soft fruit is steadily diminishing. In the UK, around 70 % of the raspberry production is now in plastic pots with varying substrates, e.g. peat or coir, and grown under hectares of plastic covered polytunnels. The growers are now also facing Brexit related challenges: labour force shortages and trade between UK and EU with a new set of restrictions on import and export of materials, plants and produce.

As *Phytophthora rubi* is a soil and water born pathogen which produces oospores contaminating soil for long periods of time, there is an urgent need to find new methods to control this outbreak. A cleaner and more local way of propagating raspberry cultivars is necessary to prevent large scale import of diseased material. There have been no in-depth studies on how *P. rubi* was introduced to the UK or where it originated. Recent studies on the USA and Canadian *P. rubi* populations have struggled to discern detectable variation between isolates and have thus concluded that the *P. rubi* population structure is likely to be a single clonal lineage. This implies that *P. rubi* may suffer from a lack of intra-species diversity which could impact its evolutionary potential to adapt to environmental stresses.

Chapter 2 was a phenotyping study of a number of *P. rubi* and *P. fragariae* isolates in response to environmental stresses and chemical controls.

- Significant isolate variability in responses to environmental factors was found. Some *P. rubi* grew well in temperatures higher than the standard range of UK soil temperatures, indicating that *P. rubi* has the evolutionary potential to overcome rising temperatures caused by climate change in the future but also

warmer soil temperatures currently found in potted raspberries grown in polytunnels.

- Variation was also detected in both *P. rubi* and *P. fragariae* isolates responses to some long serving and some more recently released chemicals. A significant loss of sensitivity was found to Metalaxyl-M (Mefenoxam) by both *P. rubi* and *P. fragariae*. In the course of this study, we could not identify the mutation responsible for this loss of sensitivity, but this could be achieved with future investment.
- Chapter 2's main finding is that the *P. rubi* population already possesses the potential to adapt to existing chemical control methods and changing climatic conditions. How raspberry growers can control *P. rubi* in the future with current control methods and actives that remain effective must be carefully considered to avoid pushing *P. rubi* to become even more difficult to control through selection pressure. One solution could be regular phenotype monitoring and genetic screening of *P. rubi* populations in the fields for the early detection of new insensitivities.

Chapter 3 utilised an enrichment sequencing method to better study of the diversity within the effector complements (RXLRs, CRNs and apoplastic effectors) of the two very closely related *Phytophthora* species. One of the currently most important questions is “*What is the molecular basis of non-host resistance?*”, as voted by the molecular plant-microbe interaction community (18th IS-MPMI congress in Glasgow, Scotland). As *P. rubi* and *P. fragariae* are sister species with evolutionary related but distinct hosts, it is of key interest to examine the variation in their effector sets and determine genes that are conserved and essential as well as genes that may determine host range. In the past, genome sequencing has failed to detect and identify significant presence / absence variation in effector genes or SNP polymorphisms in or near effectors between same-species isolates (Tabima et al., 2018; Adams et al., 2020). Consequently, there was no evidence found at the genomic level to explain effector variation associated with *P. fragariae* UK1-2-3 races and evidence was provided for gene expression differences linked to race designation (Adams et al., 2020).

- The benefits of the target enrichment sequencing approach were successfully employed here to examine the genetic diversity in key genes under most pressure to evolve.
- Unlike other *P. rubi* and *P. fragariae* genome studies before, intra-species variation was found amongst isolates on effector genes using PenSeq, showing genes under diversifying pressure.
- This study revealed examples of highly conserved core effectors displaying identical nucleotide sequences between all selected isolates and between species. The lack of polymorphism and mutation of these effector genes suggests that they are essential for pathogen virulence, and some were also conserved more widely in other *Phytophthoras*.
- Penseq successfully identified effectors that were unique to either *P. rubi* or *P. fragariae* and could be factors in limiting host range. Here, a total of 217 effectors are thought to be unique for *P. rubi* compared to *P. fragariae*, including 11 RXLRs.
- Penseq also detected effectors with significant SNP polymorphisms in several effector genes confirming and emphasizing species distinction.
- Predictions of *P. rubi* races are based on a 20-year-old unpublished study where a single raspberry breeding accession (EM5605/12) was found to have resistance to only a subset of *P. rubi* isolates. We failed to identify any effector presence / absence variation that could explain race determination. However, many of the more recently collected isolates have not been screened on EM5605/12 and consequently, a number of isolates used in this study are of an unknown race. Provided a successful recovery of currently virus-ridden EM5605/12, an obvious next step would be to screen the currently unknown isolates for virulence on this raspberry accession.

Chapter 4 developed a hydroponic system to produce raspberries and methods to induce sporulation of *P. rubi* in culture to set up and utilise a soil-free infection system in order to analyse the disease in raspberry roots in real time.

- Several cultivars of raspberry were successfully propagated for several months in hydroponics using the nutrient film technique (NFT). Growing raspberries under such conditions allows young plants to form healthy, clean and

accessible roots, for infection assays. This highlights the huge potential for the UK soft fruit industry to propagate their own disease-free material in fully controlled environments instead of relying on expensive and often unhealthy imports from large nurseries overseas. There are currently significant investments in the development of fully controlled environment companies trialling a range of crops under varying light recipes and nutrient solutions. This work supports the Scottish Government's targets to reduce carbon emissions and increase sustainability of food systems. Indeed, this work has promoted the use of hydroponics for propagation of other soft fruit species at The James Hutton Institute and has contributed to a successful Innovate UK Grant with Liberty Produce to optimize propagation of a range of soft fruit species for commercialisation.

- A method to transform *P. rubi* without utilising unsterile sporangia was identified and facilitated the ability to track infections in real-time. However, only one *P. rubi* isolate was effectively transformed and fluorescence was lost towards the end of the infection. Nevertheless, the method adapted and described in this study has been re-used to successfully transform *P. fragariae* isolates. Future efforts should focus on identifying more *P. rubi* stable fluorescence lines and to re-attempt transformation of other, perhaps more recent isolates, identified as of particular interest through this study.
- Transgenic *P. rubi* was still able to successfully sporulate and complete its life cycle on susceptible cultivars of hydroponics raspberries. This was the first report of the use of a fluorescent *P. rubi* strain used for raspberry roots infection assays.
- An infection method developed using transgenic fluorescent *P. rubi* and hydroponically grown raspberries allowed flexibility over cultivars investigated and enabled the real-time detection of the pathogen in the host roots with confocal fluorescent microscopy.
- Successful infections on susceptible raspberry cultivar showed encystment, germination and penetration of the root by 3 days post-inoculation, and invasion of the root with hyphae colonizing the central vascular cylinder by 7 days. It was shortly followed by the formation of sporangia, with second generation

zoospores release, and oospores by 11 days. Confocal microscopy observations were further approved with expression of life markers such as *Hmp1* (linked to biotrophic feeding and secretion structures known as haustoria) or *CDC14* (linked to sporulation). We hypothesize on several successive waves of infections taking place on the infected roots.

- RXLR gene expression has been identified *in planta* using qRT-PCR
 - *P. rubi* SCRP333_g22154, a match of *P. fragariae* BC-16_g5824 that had been found expressed *in planta* through a separate study (Adams, 2019), was also found expressed in raspberry infection, suggesting an essential virulence function of this effector for the two pathogens.
 - Three other RXLR genes were also expressed during raspberry infections: SCRP333_g22109, SCRP333_g24428, a potential Canadian marker gene, and SCRP333_contig_4275_F7, a unique *P. rubi* RXLR, which had high early expression, possibly indicating of a function related to early infection function such as early ETI suppression or host selection. Expression patterns matched other biotrophic life markers expression, such as *Hmp1* or *CDC14*.
- The infection protocol could be adapted to increase *P. rubi* transcripts at earlier time points, however, we struggled to get high quality RNA from samples that were initially pre-screened through confocal microscopy for presence of *P. rubi*, and future improvements would need to be developed.

5.2. Concluding remarks and future work

In a climate where people are encouraged to grow their own and shop locally due to ever increasing carbon dioxide emissions, local and healthy fruits such as raspberries and strawberries are more and more important in the UK, and their production and consumption have largely increased in the last 20 years. Associated pests and pathogens that greatly impact their yields need to be understood in order to develop sustainable control.

Overall, this thesis presents a new comprehensive study of *Phytophthora rubi*, raspberry root rot, with comparison to its close-relative sister species *Phytophthora*

fragariae, causing strawberry red stele. We have attempted to examine all three factors of the disease triangle: environment, pathogen and host. Methods have been improved to study *P. rubi* and *P. fragariae*, which are challenging to work with, such as transformation to express fluorescent proteins, efficacy of sporulation under different conditions, growth of raspberry plants hydroponically as well as techniques for confocal imaging and study of gene expression. These methodology improvements have made vital first steps in establishing a more sustainable approach to propagating raspberries and has helped develop hydroponics for other soft fruit work at our institute and hopefully commercially, as fully controlled environmental farming becomes a more established method to propagate fresh produce all year round despite the changing climate.

Responses to environment as well as genetic studies have confirmed the variation and thus ability for evolution in *P. rubi* and *P. fragariae*. Infection assays have given us insight into the pathogen's behaviour on a real host plant and into the timescale of the infection on susceptible plants.

However, further research is needed to fully understand *P. rubi* and *P. fragariae*:

- Additional life cycle stages, such as sporulation, should be examined during chemical screening. *In vivo* trials using pots should also complete the assessment of chemical effects on *P. rubi* disease. The efficacy of control chemicals should regularly be assessed against several isolates of *P. rubi* and *P. fragariae*, including most recent ones, since we have shown here that resistance can easily and quickly emerged, as previously reported on other *Phytophthora* species. An integrative approach combining different methods should always be adopted for the control of diseases in the field, whilst emphasizing on prevention.
- PenSeq and target enrichment sequencing on cDNA to isolate and enrich for pathogen's transcripts amongst the abundant host transcripts could be used to better examine expression of virulence factors, especially at earlier time points in infection.
- Cloning specific effector genes of interest (such as RXLRs identified here) and expressing them *in planta* through agroinfiltration on a model system initially (e.g. *N. benthamiana*) would be a good way to investigate their localisation, to

identify potential protein interactions in a plant and to predict their possible functions.

- Finally, more research on the third factor of the disease triangle, the host, should be carried out, in order to concurrently study the infection process on both sides. A project utilizing the methods developed in this study (sporulation, infection, hydroponics, and transformation) is currently conducted to evaluate responses of raspberries during infection under various conditions. Parallel transcriptomic and gene expression analyses with assessment of activated plant defenses would complete our knowledge of *P. rubi* infection on raspberry roots.

In conclusion, this work feeds back into further studies on raspberry root rot (*P. rubi*) and strawberry red stele (*P. fragariae*) diseases and contributes to the research towards decreasing crop loss due to pathogens.

REFERENCES

- AABY, K., WROLSTAD, R. E., EKEBERG, D. & SKREDE, G. 2007. Polyphenol Composition and Antioxidant Activity in Strawberry Purees; Impact of Achene Level and Storage. *Journal of Agricultural and Food Chemistry*, 55, 5156-5166.
- AĆIMOVIĆ, S. G., ZENG, Q., MCGHEE, G. C., SUNDIN, G. W. & WISE, J. C. 2015. Control of fire blight (*Erwinia amylovora*) on apple trees with trunk-injected plant resistance inducers and antibiotics and assessment of induction of pathogenesis-related protein genes. *Frontiers in Plant Science*, 6.
- ACOSTA-MASPONS, A., GONZÁLEZ-LEMES, I. & COVARRUBIAS, A. A. 2019. Improved protocol for isolation of high-quality total RNA from different organs of *Phaseolus vulgaris* L. *BioTechniques*, 66, 96-98.
- ADAMS, T. M. 2019. Pathogenomics of *Phytophthora fragariae*, the causal agent of strawberry red core disease. . [Unpublished PhD thesis].
- ADAMS, T. M., ARMITAGE, A. D., SOBCZYK, M. K., BATES, H. J., TABIMA, J. F., KRONMILLER, B. A., TYLER, B. M., GRÜNWARD, N. J., DUNWELL, J. M., NELLIST, C. F. & HARRISON, R. J. 2020. Genomic Investigation of the Strawberry Pathogen *Phytophthora fragariae* Indicates Pathogenicity Is Associated With Transcriptional Variation in Three Key Races. *Frontiers in Microbiology*, 11.
- AH FONG, A. M. V. & JUDELSON, H. S. 2003. Cell cycle regulator Cdc14 is expressed during sporulation but not hyphal growth in the fungus-like oomycete *Phytophthora infestans*. *Molecular Microbiology*, 50, 487-494.
- AHMED, H., HOWTON, T. C., SUN, Y., WEINBERGER, N., BELKHADIR, Y. & MUKHTAR, M. S. 2018a. Network biology discovers pathogen contact points in host protein-protein interactomes. *Nature Communications*, 9, 2312.
- AHMED, M. B., SANTOS, K. C. G. D., SANCHEZ, I. B., PETRE, B., LORRAIN, C., PLOURDE, M. B., DUPLESSIS, S., DESGAGNÉ-PENIX, I. & GERMAIN, H. 2018b. A rust fungal effector binds plant DNA and modulates transcription. *Scientific Reports*, 8, 14718.
- AI, G., XIA, Q., SONG, T., LI, T., ZHU, H., PENG, H., LIU, J., FU, X., ZHANG, M., JING, M., XIA, A. & DOU, D. 2021. A *Phytophthora sojae* CRN effector mediates phosphorylation and degradation of plant aquaporin proteins to suppress host immune signaling. *PLOS Pathogens*, 17, e1009388.
- ALCOCK, N. L. & HOWELLS, D. V. 1936. *The Phytophthora disease of strawberry*.
- ALLEN, R. L., BITTNER-EDDY, P. D., GRENVILLE-BRIGGS, L. J., MEITZ, J. C., REHMANY, A. P., ROSE, L. E. & BEYNON, J. L. 2004. Host-parasite coevolutionary conflict between *Arabidopsis* and Downy mildew. *Science*, 306, 1957-1960.
- ALLEN, R. L., MEITZ, J. C., BAUMBER, R. E., HALL, S. A., LEE, S. C., ROSE, L. E. & BEYNON, J. L. 2008. Natural variation reveals key amino acids in a downy mildew effector that alters recognition specificity by an *Arabidopsis* resistance gene. *Molecular Plant Pathology*, 9, 511-523.
- AMARO, T. M. M., THILLIEZ, G. J. A., MOTION, G. B. & HUITEMA, E. 2017. A Perspective on CRN Proteins in the Genomics Age: Evolution, Classification, Delivery and Function Revisited. *Frontiers in Plant Science*, 8.
- ANANDHAKUMAR, J. & ZELLER, W. 2008. Biological control of red stele (*Phytophthora fragariae* var. *fragariae*) and crown rot (*P. c a c t o r u m*) disease of strawberry with rhizobacteria. *Journal of Plant Diseases and Protection*, 115, 49-56.
- ANDERSON 2017. The impact of brexit on the UK soft fruit industry. *Seasonal Labour Report*. British summer Fruits.
- ARIAS, R., LEE, T. C., SPECCA, D. & JANES, H. 2000. Quality comparison of hydroponic tomatoes (*Lycopersicon esculentum*) ripened on and off vine. *Journal of Food Science*, 65, 545-548.
- ARIF, S., JANG HYUN, A., KIM, M.-R. & OH, S.-K. 2018. Mini-review: oomycete RXLR genes as effector-triggered immunity. *Korean Journal of Agricultural Science*, 45, 561-573.

- ARMITAGE, A. D., LYSØE, E., NELLIST, C. F., LEWIS, L. A., CANO, L. M., HARRISON, R. J. & BRURBERG, M. B. 2018. Bioinformatic characterisation of the effector repertoire of the strawberry pathogen *Phytophthora cactorum*. *PLoS one*, 13, e0202305-e0202305.
- ARMSTRONG, M. R., WHISSON, S. C., PRITCHARD, L., BOS, J. I., VENTER, E., AVROVA, A. O., REHMANY, A. P., BÖHME, U., BROOKS, K., CHEREVACH, I., HAMLIN, N., WHITE, B., FRASER, A., LORD, A., QUAIL, M. A., CHURCHER, C., HALL, N., BERRIMAN, M., HUANG, S., KAMOUN, S., BEYNON, J. L. & BIRCH, P. R. 2005. An ancestral oomycete locus contains late blight avirulence gene *Avr3a*, encoding a protein that is recognized in the host cytoplasm. *Proc Natl Acad Sci U S A*, 102, 7766-71.
- ATTARD, A., GOURGUES, M., CALLEMEYN-TORRE, N. & KELLER, H. 2010. The immediate activation of defense responses in *Arabidopsis* roots is not sufficient to prevent *Phytophthora parasitica* infection. *New Phytologist*, 187, 449-460.
- AVILA-ADAME, C., GÓMEZ-ALPÍZAR, L., ZISMANN, V., JONES, K. M., BUELL, C. R. & RISTAINO, J. B. 2006. Mitochondrial genome sequences and molecular evolution of the Irish potato famine pathogen, *Phytophthora infestans*. *Current Genetics*, 49, 39-46.
- AXTELL, M. J., CHISHOLM, S. T., DAHLBECK, D. & STASKAWICZ, B. J. 2003. Genetic and molecular evidence that the *Pseudomonas syringae* type III effector protein *AvrRpt2* is a cysteine protease. *Molecular Microbiology*, 49, 1537-1546.
- AYERS, W. A. 1971. Induction of sporangia in *Phytophthora cinnamomi* by a substance from bacteria and soil. *Canadian Journal of Microbiology*, 17, 1517-1523.
- AZEVEDO, H., LINO-NETO, T. & TAVARES, R. M. 2003. An improved method for high-quality RNA isolation from needles of adult maritime pine trees. *Plant Molecular Biology Reporter*, 21, 333-338.
- BACKWELL, E. M. & WATERHOUSE, G. M. 1931. Spores and spore germination in the genus *Phytophthora*. *Transactions of the British Mycological Society*.
- BADEL, J. L., CHARKOWSKI, A. O., DENG, W.-L. & COLLMER, A. 2002. A gene in the *Pseudomonas syringae* pv. tomato Hrp pathogenicity island conserved effector locus, *hopPtoA1*, contributes to efficient formation of bacterial colonies in planta and is duplicated elsewhere in the genome. *Molecular Plant-Microbe Interactions*, 15, 1014-1024.
- BAILEY, A. M., MENA, G. L. & HERRERA-ESTRELLA, L. 1991. Genetic transformation of the plant pathogens *Phytophthora capsici* and *Phytophthora parasitica*. *Nucleic Acids Research*, 19, 4273-4278.
- BAILEY, K., ÇEVİK, V., HOLTON, N., BYRNE-RICHARDSON, J., SOHN, K. H., COATES, M., WOODS-TÖR, A., MURAT AKSOY, H., HUGHES, L., BAXTER, L., JONES, J. D. G., BEYNON, J., HOLUB, E. B. & TÖR, M. 2011. Molecular Cloning of *ATR5-Emoy2* from *Hyaloperonospora arabidopsidis*, an Avirulence Determinant That Triggers RPP5-Mediated Defense in *Arabidopsis*. *Molecular Plant-Microbe Interactions*, 24, 827-838.
- BAIN, H. F. & DEMAREE, J. B. 1945. Red stele root disease of the strawberry caused by *Phytophthora fragariae*. *J. Agr. Res.*, 70, 11-30.
- BALDAUF, S. L., ROGER, A. J., WENK-SIEFERT, I. & DOOLITTLE, W. F. 2000. A kingdom-level phylogeny of eukaryotes based on combined protein data. *Science*, 290, 972-977.
- BARKER, A. V. & PILBEAM, D. J. 2007. *Handbook of plant nutrition*, Boca Raton, CRC Press.
- BARRITT, B. H., CRANDALL, P. C. & BRISTOW, P. R. 1979. Breeding for root rot resistance in red raspberry. *Journal of the American Society for Horticultural Science*, 104, 92-98.
- BASU, A., NGUYEN, A., BETTS, N. M. & LYONS, T. J. 2014. Strawberry as a functional food: an evidence-based review. *Crit Rev Food Sci Nutr*, 54, 790-806.
- BASU, A., RHONE, M. & LYONS, T. J. 2010. Berries: emerging impact on cardiovascular health. *Nutr Rev*, 68, 168-77.
- BBC-NEWS. 2011. *Plant pests: The biggest threats to food security?* [Online]. [Accessed Accessible at <https://www.bbc.co.uk/news/science-environment-15623490> (Accessed May 2021)].

- BEAKES, G. W., GLOCKLING, S. L. & SEKIMOTO, S. 2012. The evolutionary phylogeny of the oomycete 'fungi'. *Protoplasma*, 249, 3-19.
- BENOIT, F. & CEUSTERMANS, N. 1987. Some qualitative aspects of tomatoes grown on NFT. *Soiless Culture (Netherlands)*, 3, 3-7.
- BERTIOLI, D. J. 2019. The origin and evolution of a favorite fruit. *Nature Genetics*, 51, 372-373.
- BHATTACHARJEE, S., HILLER, N. L., LIOLIOS, K., WIN, J., KANNEGANTI, T.-D., YOUNG, C., KAMOUN, S. & HALDAR, K. 2006. The malarial host-targeting signal is conserved in the Irish potato famine pathogen. *PLoS Pathogens*, 2(5):e50.
- BIGEARD, J., COLCOMBET, J. & HIRT, H. 2015. Signaling Mechanisms in Pattern-Triggered Immunity (PTI). *Molecular Plant*, 8, 521-539.
- BIRCH, P. R., BOEVINK, P. C., GILROY, E. M., HEIN, I., PRITCHARD, L. & WHISSON, S. C. 2008. Oomycete RXLR effectors: delivery, functional redundancy and durable disease resistance. *Curr Opin Plant Biol*, 11, 373-9.
- BIRCH, P. R., REHMANY, A. P., PRITCHARD, L., KAMOUN, S. & BEYNON, J. L. 2006. Trafficking arms: oomycete effectors enter host plant cells. *Trends Microbiol*, 14, 8-11.
- BLAIR, J. E., COFFEY, M. D., PARK, S.-Y., GEISER, D. M. & KANG, S. 2008. A multi-locus phylogeny for *Phytophthora* utilizing markers derived from complete genome sequences. *Fungal Genetics and Biology*, 45, 266-277.
- BOEVINK, P. C., BIRCH, P. R. J., TURNBULL, D. & WHISSON, S. C. 2020. Devastating intimacy: the cell biology of plant-*Phytophthora* interactions. *New Phytol*, 228, 445-458.
- BOS, J. I., ARMSTRONG, M. R., GILROY, E. M., BOEVINK, P. C., HEIN, I., TAYLOR, R. M., ZHENDONG, T., ENGELHARDT, S., VETUKURI, R. R., HARROWER, B., DIXELIUS, C., BRYAN, G., SADANANDOM, A., WHISSON, S. C., KAMOUN, S. & BIRCH, P. R. 2010. *Phytophthora infestans* effector AVR3a is essential for virulence and manipulates plant immunity by stabilizing host E3 ligase CMPG1. *Proc Natl Acad Sci U S A*, 107, 9909-14.
- BOS, J. I. B., KANNEGANTI, T. D., YOUNG, C., CAKIR, C., HUITEMA, E., WIN, J., ARMSTRONG, M. R., BIRCH, P. R. J. & KAMOUN, S. 2006. The C-terminal half of *Phytophthora infestans* RXLR effector AVR3a is sufficient to trigger R3a-mediated hypersensitivity and suppress INF1-induced cell death in *Nicotiana benthamiana*. *The Plant Journal*, 48, 165-176.
- BOZKURT, T. O., SCHORNACK, S., WIN, J., SHINDO, T., ILYAS, M., OLIVA, R., CANO, L. M., JONES, A. M. E., HUITEMA, E., VAN DER HOORN, R. A. L. & KAMOUN, S. 2011. *Phytophthora infestans* effector AVRblb2 prevents secretion of a plant immune protease at the haustorial interface. *Proceedings of the National Academy of Sciences of the United States of America*, 108, 20832-20837.
- BRASIER, C. 2009. *Phytophthora* biodiversity: how many *Phytophthora* species are there? In: GOHEEN, E. M. & FRANKEL, S. J. (eds.) *Phytophthoras in Forests and Natural Ecosystems*. U.S. Department of Agriculture, Forest Service.
- BROOKS, D. M., BENDER, C. L. & KUNKEL, B. N. 2005. The *Pseudomonas syringae* phytotoxin coronatine promotes virulence by overcoming salicylic acid-dependent defences in *Arabidopsis thaliana*. *Molecular Plant Pathology*, 6, 629-639.
- BRUCK, R. I., FRY, W. E., APPLE, A. E. & MUNDT, C. C. 1981. Effect of protectant fungicides on the developmental stages of *Phytophthora infestans* in potato foliage. *Phytopathology*, 71, 164-166.
- BRUNNER, S., STIRNWEIS, D., DIAZ QUIJANO, C., BUESING, G., HERREN, G., PARLANGE, F., BARRET, P., TASSY, C., SAUTTER, C., WINZELER, M. & KELLER, B. 2012. Transgenic Pm3 multilines of wheat show increased powdery mildew resistance in the field. *Plant Biotechnology Journal*, 10, 398-409.
- BURRA, D. D., BERKOWITZ, O., HEDLEY, P. E., MORRIS, J., RESJÖ, S., LEVANDER, F., LILJEROTH, E., ANDREASSON, E. & ALEXANDERSSON, E. 2014. Phosphite-induced changes of the transcriptome and secretome in *Solanum tuberosum* leading to resistance against *Phytophthora infestans*. *BMC Plant Biology*, 14, 254.

- CAI, G. & SCOFIELD, S. R. 2020. Mitochondrial genome sequence of *Phytophthora sansomeana* and comparative analysis of *Phytophthora* mitochondrial genomes. *PLoS one*, 15, e0231296-e0231296.
- CAILLAUD, M.-C., ASAI, S., RALLAPALLI, G., PIQUEREZ, S., FABRO, G. & JONES, J. D. G. 2013. A Downy mildew effector attenuates salicylic acid-triggered immunity in *Arabidopsis* by interacting with the host mediator complex. *PLoS Biology*, 11, e1001732.
- CAVALIER-SMITH, T. 2018. Kingdom Chromista and its eight phyla: a new synthesis emphasising periplastid protein targeting, cytoskeletal and periplastid evolution, and ancient divergences. *Protoplasma*, 255, 297-357.
- CHAMPOURET, N. & KAMOUN, S. 2004. An improved protocol for the protoplast method of stable DNA transformation of *Phytophthora infestans* <http://www.KamounLab.net>.
- CHAN, L. G. & KWEE, L. T. 1986. Comparative In vitro Sensitivity of Selected Chemicals on *Phytophthora palmivora* from Cocoa and Durian. *Pertanika*, 9 (2), pp. 183-191.
- CHANDELIER, A., ABRAS, S., LAURENT, F., DEBRUXELLES, N. & CAVELIER, M. 2006. Effect of temperature and bacteria on sporulation of *Phytophthora alni* in river water. *Communications in agricultural and applied biological sciences*, 71, 873-880.
- CHANG, Y.-H., YAN, H.-Z. & LIOU, R.-F. 2015. A novel elicitor protein from *Phytophthora parasitica* induces plant basal immunity and systemic acquired resistance. *Molecular Plant Pathology*, 16, 123-136.
- CHAPARRO-GARCIA, A., SCHWIZER, S., SKLENAR, J., YOSHIDA, K., PETRE, B., BOS, J. I. B., SCHORNACK, S., JONES, A. M. E., BOZKURT, T. O. & KAMOUN, S. 2015. *Phytophthora infestans* RXLR-WY effector AVR3a Associates with dynamin-related protein 2 required for endocytosis of the Plant Pattern Recognition Receptor FLS2. *PLoS ONE*, 10, e0137071.
- CHAPARRO-GARCIA, A., WILKINSON, R. C., GIMENEZ-IBANEZ, S., FINDLAY, K., COFFEY, M. D., ZIPFEL, C., RATHJEN, J. P., KAMOUN, S. & SCHORNACK, S. 2011. The receptor-like kinase SERK3/BAK1 is required for basal resistance against the Late blight pathogen *Phytophthora infestans* in *Nicotiana benthamiana*. *PLoS ONE*, 6, e16608.
- CHAPMAN, S., STEVENS, L. J., BOEVINK, P. C., ENGELHARDT, S., ALEXANDER, C. J., HARROWER, B., CHAMPOURET, N., MCGEACHY, K., VAN WEYMERS, P. S. M., CHEN, X., BIRCH, P. R. J. & HEIN, I. 2014. Detection of the virulent form of AVR3a from *Phytophthora infestans* following artificial evolution of potato resistance gene R3a. *PLoS ONE*, 9, e110158.
- CHASE, A. R. 1993. Review of Fungicides for Control of *Phytophthora* and *Pythium* Diseases on Potted Ornamentals. *Central Florida Research and Education Center, Univ. of Fl., CFREC-Apopka Research Report RH-93-3*.
- CHEE, K. H. & NEWHOOK, F. J. 1966. Relationship of micro-Organisms to sporulation of *Phytophthora Cinnamomi* rands. *New Zealand Journal of Agricultural Research*, 9, 32-&.
- CHEN, N., HSIANG, T. & GOODWIN, P. H. 2003. Use of green fluorescent protein to quantify the growth of *Colletotrichum* during infection of tobacco. *Journal of Microbiological Methods*, 53, 113-122.
- CHEN, S., ZHOU, Y., CHEN, Y. & GU, J. 2018. fastp: an ultra-fast all-in-one FASTQ preprocessor. *Bioinformatics*, 34, i884-i890.
- CHEN, X.-R., LI, Y.-P., LI, Q.-Y., XING, Y.-P., LIU, B.-B., TONG, Y.-H. & XU, J.-Y. 2016. SCR96, a small cysteine-rich secretory protein of *Phytophthora cactorum*, can trigger cell death in the Solanaceae and is important for pathogenicity and oxidative stress tolerance. *Molecular Plant Pathology*, 17, 577-587.
- CHEPSEY, J., MOTAUNG, T., RABELO, D. & MOLELEKI, L. 2020. Organize, Don't Agonize: Strategic Success of *Phytophthora* Species. *Microorganisms*, 8.
- CHEUNG, F., WIN, J., LANG, J. M., HAMILTON, J., VUONG, H., LEACH, J. E., KAMOUN, S., ANDRÉ LÉVESQUE, C., TISSERAT, N. & BUELL, C. R. 2008. Analysis of the *Pythium ultimum* transcriptome using Sanger and Pyrosequencing approaches. *BMC Genomics*, 9, 542-542.

- COCK, P. J. A., GRÜNING, B. A., PASZKIEWICZ, K. & PRITCHARD, L. 2013. Galaxy tools and workflows for sequence analysis with applications in molecular plant pathology. *PeerJ* 1:e167.
- COFFEY, M. 1984. Variability in Sensitivity to Metalaxyl of Isolates of *Phytophthora cinnamomi* and *Phytophthora citricola*. *Phytopathology*, 74.
- COHEN, Y. & COFFEY, M. D. 1986. Systemic Fungicides and the Control of Oomycetes. *Annual Review of Phytopathology*, 24, 311-338.
- COLLINGE, D. B. 2009. Cell wall appositions: the first line of defence. *Journal of Experimental Botany*, 60, 351-352.
- CONVERSE, R. H. 1962. Some factors influencing zoosporangium production by *Phytophthora fragariae*. *Phytopathology*, 52.
- COOLONG, T. 2012. *Hydroponic lettuce*. University of Kentucky Cooperative Extension Services.
- D'URBAN-JACKSON, R. 2018. *Phytophthora rubi sporangium releasing zoospores*.
- DALIO, R. J. D., FLEISCHMANN, F., HUMEZ, M. & OSSWALD, W. 2014. Phosphite Protects *Fagus sylvatica* Seedlings towards *Phytophthora plurivora* via Local Toxicity, Priming and Facilitation of Pathogen Recognition. *PLOS ONE*, 9, e87860.
- DAMASCENO, C. M. B., BISHOP, J. G., RIPOLL, D. R., WIN, J., KAMOUN, S. & ROSE, J. K. C. 2008. Structure of the Glucanase Inhibitor Protein (GIP) Family from *Phytophthora* Species Suggests Coevolution with Plant Endo- β -1,3-Glucanases. *Molecular Plant-Microbe Interactions*, 21, 820-830.
- DARKO, E., HEYDARIZADEH, P., SCHOEFS, B. & SABZALIAN, M. R. 2014. Photosynthesis under artificial light: the shift in primary and secondary metabolism. *Philosophical transactions of the Royal Society of London. Series B, Biological sciences*, 369, 20130243-20130243.
- DASH, P. K. 2013. High quality RNA isolation from ployphenol-, polysaccharide- and protein-rich tissues of lentil (*Lens culinaris*). *3 Biotech*, 3, 109-114.
- DE FREITAS, J. R. & GERMIDA, J. J. 1990. A root tissue culture system to study winter wheat-rhizobacteria interactions. *Applied Microbiology and Biotechnology*, 33, 589-595.
- DEBLER, J. W., HENARES, B. M. & LEE, R. C. 2021. Agroinfiltration for transient gene expression and characterisation of fungal pathogen effectors in cool-season grain legume hosts. *Plant Cell Reports*, 40, 805-818.
- DIÉGUEZ-URIBEONDO, J., GARCÍA, M. A., CERENIUS, L., KOZUBÍKOVÁ, E., BALLESTEROS, I., WINDELS, C., WEILAND, J., KATOR, H., SÖDERHÄLL, K. & MARTÍN, M. P. 2009. Phylogenetic relationships among plant and animal parasites, and saprotrophs in *Aphanomyces* (Oomycetes). *Fungal Genetics and Biology*, 46, 365-376.
- DODDS, P. N., RAFIQI, M., GAN, P. H. P., HARDHAM, A. R., JONES, D. A. & ELLIS, J. G. 2009. Effectors of biotrophic fungi and oomycetes: pathogenicity factors and triggers of host resistance. *New Phytologist*, 183, 993-1000.
- DONG, S., QUTOB, D., TEDMAN-JONES, J., KUFLU, K., WANG, Y., TYLER, B. M. & GIJZEN, M. 2009. The *Phytophthora sojae* avirulence locus *Avr3c* encodes a multi-copy RXLR effector with sequence polymorphisms among pathogen strains. *PLoS One*, 4, e5556.
- DONG, S., YU, D., CUI, L., QUTOB, D., TEDMAN-JONES, J., KALE, S. D., TYLER, B. M., WANG, Y. & GIJZEN, M. 2011. Sequence variants of the *Phytophthora sojae* RXLR effector *Avr3a/5* are differentially recognized by *Rps3a* and *Rps5* in soybean. *PLoS One*, 6, e20172.
- DOU, D., KALE, S. D., LIU, T., TANG, Q., WANG, X., ARREDONDO, F. D., BASNAYAKE, S., WHISSON, S., DRENTH, A., MACLEAN, D. & TYLER, B. M. 2010. Different domains of *Phytophthora sojae* effector *Avr4/6* are recognized by soybean resistance genes *Rps4* and *Rps6*. *Mol Plant Microbe Interact*, 23, 425-35.
- DOU, D., KALE, S. D., WANG, X., CHEN, Y., WANG, Q., WANG, X., JIANG, R. H. Y., ARREDONDO, F. D., ANDERSON, R. G., THAKUR, P. B., MCDOWELL, J. M., WANG, Y. & TYLER, B. M. 2008a. Conserved C-terminal motifs required for avirulence and suppression of cell death by *Phytophthora sojae* effector *Avr1b*. *The Plant Cell*, 20, 1118-1133.

- DOU, D., KALE, S. D., WANG, X., JIANG, R. H. Y., BRUCE, N. A., ARREDONDO, F. D., ZHANG, X. & TYLER, B. M. 2008b. RXLR-mediated entry of *Phytophthora sojae* effector Avr1b into soybean cells does not require pathogen-encoded machinery. *The Plant Cell*, 20, 1930-1947.
- DOWNIE, H. F., ADU, M. O., SCHMIDT, S., OTTEN, W., DUPUY, L. X., WHITE, P. J. & VALENTINE, T. A. 2015. Challenges and opportunities for quantifying roots and rhizosphere interactions through imaging and image analysis. *Plant, Cell & Environment*, 38, 1213-1232.
- DU, Y., MPINA, M. H., BIRCH, P. R. J., BOUWMEESTER, K. & GOVERS, F. 2015. *Phytophthora infestans* RXLR Effector AVR1 Interacts with Exocyst Component Sec5 to Manipulate Plant Immunity. *Plant Physiology*, 169, 1975.
- DUMAS, B., CENTIS, S., SARRAZIN, N. & ESQUERRÉ-TUGAYÉ, M.-T. 1999. Use of Green Fluorescent Protein To Detect Expression of an Endopolygalacturonase Gene of *Colletotrichum lindemuthianum* during Bean Infection. *Applied and Environmental Microbiology*, 65, 1769.
- DUNCAN, J. & COOKE, D. 2002. Identifying, diagnosing and detecting *Phytophthora* by molecular methods. *Mycologist*, 16.
- DUNCAN, J. M. 1985. Effect of fungicides on survival, infectivity and germination of *Phytophthora fragariae* oospores. *Transactions of the British Mycological Society*, 85, 585-593.
- DUNCAN, J. M., COOKE, D. E. L., SEEMÜLLER, E., BONANTS, P. & OLSSON, C. 2000. European collaboration on eliminating *Phytophthora fragariae* from strawberry multiplication. *EPPO Bulletin*, 30, 513-517.
- DUNCAN, J. M. & KENNEDY, D. M. 1987. Research at SCRI on *Phytophthora* root rot of raspberry. Bull SCRI.
- DUNCAN, J. M. & KENNEDY, D. M. 1989. The effect of waterlogging on *Phytophthora* root rot of red raspberry. *Plant Pathology*, 38, 161-168.
- DUNCAN, J. M., KENNEDY, D. M. & SEEMULLER, E. 1987. Identities and pathogenicities of *Phytophthora* spp. causing root rot of red raspberry. *Plant Pathology*, 36, 276-289.
- DUNN, A. R., FRY, B. A., LEE, T. Y., CONLEY, K. D., BALAJI, V., FRY, W. E., MCLEOD, A. & SMART, C. D. 2013. Transformation of *Phytophthora capsici* with genes for green and red fluorescent protein for use in visualizing plant-pathogen interactions. *Australasian Plant Pathology*, 42, 583-593.
- EDIRISINGHE, I., BANASZEWSKI, K., CAPPOZZO, J., SANDHYA, K., ELLIS, C. L., TADAPANENI, R., KAPPAGODA, C. T. & BURTON-FREEMAN, B. M. 2011. Strawberry anthocyanin and its association with postprandial inflammation and insulin. *Br J Nutr*, 106, 913-22.
- ELANSKY, S., APRYSHKO, V., MILYUTINA, D. & KOZLOVSKY, B. 2007. Resistance of Russian strains of *Phytophthora infestans* to fungicides metalaxyl and dimethomorph. *Moscow University Biological Sciences Bulletin*, 62, 11-14.
- ELLIS, C. L., EDIRISINGHE, I., KAPPAGODA, T. & BURTON-FREEMAN, B. 2011. Attenuation of meal-induced inflammatory and thrombotic responses in overweight men and women after 6-week daily strawberry (*Fragaria*) intake. A randomized placebo-controlled trial. *J Atheroscler Thromb*, 18, 318-27.
- ELLIS, M. A. 2016. *Phytophthora root rot of raspberry* [Online]. College of Food, Agricultural and Environmental Sciences; the Ohio State University [Accessed May 2018].
- EMERSON, R. 1941. An experimental study of the life cycles and taxonomy of *Allomyces*. *Lloydia*, 4, 77-144.
- EPPO Pathogen sheet - *Phytophthora fragariae*.
- ERWIN, C. D., GARCIA, S. B. & TSAO, P. H. 1983. *Phytophthora*, Saint Paul, Minnesota, USA.
- ERWIN, D. C. & RIBEIRO, O. K. 1996a. *Phytophthora Diseases Worldwide*, St. Paul, MN, APS Press.
- ERWIN, D. C. & RIBEIRO, O. K. 1996b. *Phytophthora infestans* (Mont.) de Bary (1876). . In: ERWIN, D. C. & RIBEIRO, O. K. (eds.) *Phytophthora Diseases Worldwide*. St. Paul, Minnesota: APS Press.
- EULGEM, T. 2005. Regulation of the *Arabidopsis* defense transcriptome. *Trends in Plant Science*, 10, 71-78.

- EVANGELISTI, E., GOGLEVA, A., HAINAUX, T., DOUMANE, M., TULIN, F., QUAN, C., YUNUSOV, T., FLOCH, K. & SCHORNACK, S. 2017. Time-resolved dual transcriptomics reveal early induced *Nicotiana benthamiana* root genes and conserved infection-promoting *Phytophthora palmivora* effectors. *BMC Biol*, 15, 39.
- EVANGELISTI, E., GOVETTO, B., MINET-KEBDANI, N., KUHN, M. L., ATTARD, A., PONCHET, M., PANABIÈRES, F. & GOURGUES, M. 2013. The *Phytophthora parasitica* RXLR effector penetration-specific effector 1 favours *Arabidopsis thaliana* infection by interfering with auxin physiology. *New Phytol*, 199, 476-89.
- FABRO, G., STEINBRENNER, J., COATES, M., ISHAQUE, N., BAXTER, L., STUDHOLME, D. J., KÖRNER, E., ALLEN, R. L., PIQUEREZ, S. J. M., ROUGON-CARDOSO, A., GREENSHIELDS, D., LEI, R., BADEL, J. L., CAILLAUD, M.-C., SOHN, K.-H., VAN DEN ACKERVEKEN, G., PARKER, J. E., BEYNON, J. & JONES, J. D. G. 2011. Multiple candidate effectors from the Oomycete pathogen *Hyaloperonospora arabidopsidis* suppress host plant immunity. *PLoS Pathogens*, 7, e1002348.
- FALLOON, P. G. & GROGAN, R. G. 1991. Effect of root temperature, plant age, frequency and duration of flooding and inoculum placement and concentration on susceptibility of asparagus to *Phytophthora* rot. *New Zealand Journal of Crop and Horticultural Science*, 19, 305-312.
- FANG, J. 2015. Classification of fruits based on anthocyanin types and relevance to their health effects. *Nutrition*, 31, 1301-6.
- FANG, Y. & TYLER, B. M. 2016. Efficient disruption and replacement of an effector gene in the oomycete *Phytophthora sojae* using CRISPR/Cas9. *Molecular Plant Pathology*, 17, 127-139.
- FAO, F. A. A. O. O. T. U. N. 2009. How to Feed the World in 2050 *FAO documents - expert paper*, [http://www.fao.org/fileadmin/templates/wsfs/docs/expert_paper/How to Feed the World in 2050.pdf](http://www.fao.org/fileadmin/templates/wsfs/docs/expert_paper/How_to_Feed_the_World_in_2050.pdf).
- FAWKE, S., DOUMANE, M. & SCHORNACK, S. 2015. Oomycete interactions with plants: infection strategies and resistance principles. *Microbiol Mol Biol Rev*, 79, 263-80.
- FELIX, E. L. 1962. Culture media for sporangial production in *Phytophthora fragariae*. *Phytopathology*, 52.
- FENNING, T. M. 2019. The use of tissue culture and in-vitro approaches for the study of tree diseases. *Plant Cell, Tissue and Organ Culture (PCTOC)*, 136, 415-430.
- FERGUSON, S. D., SALIGA III, R. P. & OMAÏE, S. T. 2014. Investigating the effects of hydroponics media on quality of greenhouse grown leaf greens. *International Journal of Agricultural Extension*, 02, 227-234.
- FORDYCE, W. 1991. Technical note: *Phytophthora* root rot of raspberries. *The Scottish Agricultural College*.
- FRANCESCHETTI, M., MAQBOOL, A., JIMENEZ-DALMARONI, M., PENNINGTON, H., KAMOUN, S. & BANFIELD, M. 2017. Effectors of Filamentous Plant Pathogens: Commonalities amid Diversity. *Microbiology and Molecular Biology Reviews*, 81, e00066-16.
- GAO, R., CHENG, Y., WANG, Y., WANG, Y., GUO, L. & ZHANG, G. 2015. Genome Sequence of *Phytophthora fragariae* var. *fragariae*, a Quarantine Plant-Pathogenic Fungus. *Genome announcements*, 3, e00034-15.
- GAO, R. F., WANG, J. Y., LIU, K. W., YOSHIDA, K., HSIAO, Y. Y., SHI, Y. X., TSAI, K. C., CHEN, Y. Y., MITSUDA, N., LIANG, C. K., WANG, Z. W., WANG, Y., ZHANG, D. Y., HUANG, L., ZHAO, X., ZHONG, W. Y., CHENG, Y. H., JIANG, Z. D., LI, M. H., SUN, W. H., YU, X., HU, W., ZHOU, Z., ZHOU, X. F., YE, C. M., KATO, K., TSAI, W. C., LIU, Z. J., MARTIN, F. & ZHANG, G. M. 2021. Comparative analysis of *Phytophthora* genomes reveals oomycete pathogenesis in crops. *Heliyon*, 7, e06317.
- GAULIN, E., MADOUÏ, M. A., BOTTIN, A., JACQUET, C., MATHE, C., COULOUX, A., WINCKER, P. & DUMAS, B. 2008. Transcriptome of *Aphanomyces euteiches*: new oomycete putative pathogenicity factors and metabolic pathways. *PLoS One*, 3, e1723.
- GHIDIU, G., KUHAR, T., PALUMBO, J. & SCHUSTER, D. 2012. Drip Chemigation of Insecticides as a Pest Management Tool in Vegetable Production. *Journal of Integrated Pest Management*, 3, E1-E5.

- GIJZEN, M., ISHMAEL, C. & SHRESTHA, S. D. 2014. Epigenetic control of effectors in plant pathogens. *Frontiers in plant science*, 5, 638-638.
- GILROY, E. M., BREEN, S., WHISSON, S. C., SQUIRES, J., HEIN, I., KACZMAREK, M., TURNBULL, D., BOEVINK, P. C., LOKOSSOU, A., CANO, L. M., MORALES, J., AVROVA, A. O., PRITCHARD, L., RANDALL, E., LEES, A., GOVERS, F., VAN WEST, P., KAMOUN, S., VLEESHOUWERS, V. G., COOKE, D. E. & BIRCH, P. R. 2011. Presence/absence, differential expression and sequence polymorphisms between PiAVR2 and PiAVR2-like in *Phytophthora infestans* determine virulence on R2 plants. *New Phytol*, 191, 763-76.
- GISI, U. & SIEROTZKI, H. 2008. Fungicide modes of action and resistance in downy mildews. *European Journal of Plant Pathology*, 122, 157-167.
- GÓMEZ-MERINO, F. C. & TREJO-TÉLLEZ, L. I. 2015. Biostimulant activity of phosphite in horticulture. *Scientia Horticulturae*, 196, 82-90.
- GOODE, P. M. 1956. Infection of strawberry roots by zoospores of *Phytophthora fragariae*. *Transactions of the British Mycological Society*, 39, 367-377.
- GOODIN, M. M., DIETZGEN, R. G., SCHICHNES, D., RUZIN, S. & JACKSON, A. O. 2002. pGD vectors: versatile tools for the expression of green and red fluorescent protein fusions in agroinfiltrated plant leaves. *Plant J*, 31, 375-83.
- GOODIN, M. M., ZAITLIN, D., NAIDU, R. A. & LOMMEL, S. A. 2008. *Nicotiana benthamiana*: Its History and Future as a Model for Plant-Pathogen Interactions. *Molecular Plant-Microbe Interactions*[®], 21, 1015-1026.
- GOODWIN, S., GURTOWSKI, J., ETHE-SAYERS, S., DESHPANDE, P., SCHATZ, M. C. & MCCOMBIE, W. R. 2015. Oxford Nanopore sequencing, hybrid error correction, and de novo assembly of a eukaryotic genome. *Genome Res*, 25, 1750-6.
- GOVERNMENT, S. 2019. Pesticide usage - soft fruit crops. Retrieved from <https://www.gov.scot/publications/pesticide-usage-scotland-soft-fruit-crops-2018/pages/13/>.
- GRAHAM, J., HACKETT, C. A., SMITH, K., WOODHEAD, M., MACKENZIE, K., TIERNEY, I., COOKE, D., BAYER, M. & JENNINGS, N. 2011. Towards an understanding of the nature of resistance to *Phytophthora* root rot in red raspberry. *Theoretical and Applied Genetics*, 123, 585-601.
- GRAHAM, K., BECK, B. R., ZASADA, I., SCAGEL, C. F. & WEILAND, J. E. 2020. Growth, sporulation, and pathogenicity of the raspberry pathogen *Phytophthora rubi* under different temperature and moisture regimes. *Plant disease*.
- GREENACRE, M. 2016. Correspondence Analysis in Practice. In: HALL/CRC, R. E. N. Y. C. A. (ed.).
- GROVE, G. G., MADDEN, L. V., ELLIS, M. A. & SCHMITTHENNER, A. F. 1985. Influence of temperature and wetness duration on infection of immature strawberry fruit by *Phytophthora cactorum*. *Phytopathology*, 75, 165-169.
- GROVES, C. T. & RISTAINO, J. B. 2000. Commercial Fungicide Formulations Induce In Vitro Oospore Formation and Phenotypic Change in Mating Type in *Phytophthora infestans*. *Phytopathology*[™], 90, 1201-1208.
- GROVES, E., HOWARD, K., HARDY, G. & BURGESS, T. 2015. Role of salicylic acid in phosphite-induced protection against Oomycetes; a *Phytophthora cinnamomi* - *Lupinus augustifolius* model system. *European Journal of Plant Pathology*, 141, 559-569.
- GUNDESLI, M., KORKMAZ, N. & OKATAN, V. 2019. Polyphenol content and antioxidant capacity of berries: A review. 3, 350-361.
- GUO, Y., DUPONT, P.-Y., MESARICH, C. H., YANG, B., MCDUGAL, R. L., PANDA, P., DIJKWEL, P., STUDHOLME, D. J., SAMBLES, C., WIN, J., WANG, Y., WILLIAMS, N. M. & BRADSHAW, R. E. 2020. Functional analysis of RXLR effectors from the New Zealand kauri dieback pathogen *Phytophthora agathidicida*. *Molecular plant pathology*, 21, 1131-1148.
- HAAS, B. J., KAMOUN, S., ZODY, M. C., JIANG, R. H., HANDSAKER, R. E., CANO, L. M., GRABHERR, M., KODIRA, C. D., RAFFAELE, S., TORTO-ALALIBO, T., BOZKURT, T. O., AH-FONG, A. M., ALVARADO, L., ANDERSON, V. L., ARMSTRONG, M. R., AVROVA, A., BAXTER, L., BEYNON, J., BOEVINK, P. C.,

- BOLLMANN, S. R., BOS, J. I., BULONE, V., CAI, G., CAKIR, C., CARRINGTON, J. C., CHAWNER, M., CONTI, L., COSTANZO, S., EWAN, R., FAHLGREN, N., FISCHBACH, M. A., FUGELSTAD, J., GILROY, E. M., GNERRE, S., GREEN, P. J., GRENVILLE-BRIGGS, L. J., GRIFFITH, J., GRUNWALD, N. J., HORN, K., HORNER, N. R., HU, C. H., HUITEMA, E., JEONG, D. H., JONES, A. M., JONES, J. D., JONES, R. W., KARLSSON, E. K., KUNJETI, S. G., LAMOUR, K., LIU, Z., MA, L., MACLEAN, D., CHIBUCOS, M. C., MCDONALD, H., MCWALTERS, J., MEIJER, H. J., MORGAN, W., MORRIS, P. F., MUNRO, C. A., O'NEILL, K., OSPINA-GIRALDO, M., PINZON, A., PRITCHARD, L., RAMSAHOYE, B., REN, Q., RESTREPO, S., ROY, S., SADANANDOM, A., SAVIDOR, A., SCHORNACK, S., SCHWARTZ, D. C., SCHUMANN, U. D., SCHWESSINGER, B., SEYER, L., SHARPE, T., SILVAR, C., SONG, J., STUDHOLME, D. J., SYKES, S., THINES, M., VAN DE VONDERVOORT, P. J., PHUNTUMART, V., WAWRA, S., WEIDE, R., WIN, J., YOUNG, C., ZHOU, S., FRY, W., MEYERS, B. C., VAN WEST, P., RISTAINO, J., GOVERS, F., BIRCH, P. R., WHISSON, S. C., JUDELSON, H. S. & NUSBAUM, C. 2009. Genome sequence and analysis of the Irish potato famine pathogen *Phytophthora infestans*. *Nature*, 461, 393-8.
- HÄKKINEN, S. T., SEPPÄNEN-LAAKSO, T., OKSMAN-CALDENTY, K.-M. & RISCHER, H. 2015. Bioconversion to Raspberry Ketone is Achieved by Several Non-related Plant Cell Cultures. *Frontiers in Plant Science*, 6.
- HALVORSEN, B. L., HOLTE, K., MYHRSTAD, M. C. W., BARIKMO, I., HVATTUM, E., REMBERG, S. F., WOLD, A.-B., HAFFNER, K., BAUGERØD, H., ANDERSEN, L. F., MOSKAUG, Ø., JACOBS, D. R., JR. & BLOMHOFF, R. 2002. A Systematic Screening of Total Antioxidants in Dietary Plants. *The Journal of Nutrition*, 132, 461-471.
- HARDHAM, A. R. 2005. *Phytophthora cinnamomi*. *Molecular Plant Pathology*, 6, 589-604.
- HARDHAM, A. R. & SHAN, W. 2009. Cellular and molecular biology of *Phytophthora* – Plant interactions. In: HB, D. (ed.) *Plant relationships (a comprehensive treatise on fungi as experimental systems for basic and applied research)*. Berlin Heidelberg, Germany: Springer-Verlag.
- HAVERKORT, A. J., STRUIK, P. C., VISSER, R. G. F. & JACOBSEN, E. 2009. Applied Biotechnology to Combat Late Blight in Potato Caused by *Phytophthora Infestans*. *Potato Research*, 52, 249-264.
- HAYDEN, A. 2006. Aeroponic and Hydroponic Systems for Medicinal Herb, Rhizome, and Root Crops. *HortScience*, 41, 536-538.
- HE, Q., MCLELLAN, H., BOEVINK, P. C. & BIRCH, P. R. J. 2020. All Roads Lead to Susceptibility: The Many Modes of Action of Fungal and Oomycete Intracellular Effectors. *Plant Communications*, 1, 100050.
- HEIBERG, N. 1995. Control of root rot of red raspberries caused by *Phytophthora fragariae* var. *rubi*. *Plant Pathology*, 44, 153-159.
- HEIBERG, N. 1999. Effects of raised beds, black soil mulch and oxadixyl on root rot (*Phytophthora fragariae* var. *rubi*) in red raspberry. *Acta Horticulturae*, 505, 249-255.
- HEIBERG, N., DUNCAN, J. M., KENNEDY, D. M. & SEMB, L. 1989. Raspberry root rot in Norway. *Acta Horticulturae*, 262, 189-191.
- HEIN, I., GILROY, E. M., ARMSTRONG, M. R. & BIRCH, P. R. J. 2009. The zig-zag-zig in oomycete–plant interactions. *Molecular Plant Pathology*, 10, 547-562.
- HENNING, S. M., SEERAM, N. P., ZHANG, Y., LI, L., GAO, K., LEE, R. P., WANG, D. C., ZERLIN, A., KARP, H., THAMES, G., KOTLERMAN, J., LI, Z. & HEBER, D. 2010. Strawberry consumption is associated with increased antioxidant capacity in serum. *J Med Food*, 13, 116-22.
- HENRY, G., THONART, P. & ONGENA, M. 2012. *PAMPs, MAMPs, DAMPs and others: An update on the diversity of plant immunity elicitors*.
- HICKMAN, C. J. 1940. The red core root disease of the strawberry caused by *Phytophthora fragariae* sp. nov. *The Journal of Pomology and Horticultural Society* 18, 89-118.

- HILLER, N. L., BHATTACHARJEE, S., VAN OOIJ, C., LIOLIOS, K., HARRISON, T., LOPEZ-ESTRAÑO, C. & HALDAR, K. 2004. A host-targeting signal in virulence proteins reveals a secretome in malarial infection. *Science*, 306, 1934-7.
- HOGENHOUT, S. A., VAN DER HOORN, R. A. L., TERAUCHI, R. & KAMOUN, S. 2009. Emerging concepts in effector biology of plant-associated organisms. *Molecular Plant-Microbe Interactions*, 22, 115-122.
- HOWLAND, A., KIM, N. & MARKS, A. 2012. Advanced Food Technologies. MIT.
- HU, J., HONG, C., STROMBERG, E. L. & MOORMAN, G. W. 2007. Effects of Propamocarb Hydrochloride on Mycelial Growth, Sporulation, and Infection by *Phytophthora nicotianae* Isolates from Virginia Nurseries. *Plant Disease*, 91, 414-420.
- HUANG, G., LIU, Z., GU, B., ZHAO, H., JIA, J., FAN, G., MENG, Y., DU, Y. & SHAN, W. 2019. An RXLR effector secreted by *Phytophthora parasitica* is a virulence factor and triggers cell death in various plants. *Mol Plant Pathol*, 20, 356-371.
- HUITEMA, E., VLEESHOUWERS, V. G., CAKIR, C., KAMOUN, S. & GOVERS, F. 2005. Differences in intensity and specificity of hypersensitive response induction in *Nicotiana* spp. by INF1, INF2A, and INF2B of *Phytophthora infestans*. *Mol Plant Microbe Interact*, 18, 183-93.
- HUNTER, S., WILLIAMS, N., MCDUGAL, R., SCOTT, P. & GARBELOTTO, M. 2018. Evidence for rapid adaptive evolution of tolerance to chemical treatments in *Phytophthora* species and its practical implications. *PLOS ONE*, 13, e0208961.
- HUNTLEY, A. L. 2009. The health benefits of berry flavonoids for menopausal women: cardiovascular disease, cancer and cognition. *Maturitas*, 63, 297-301.
- HUSSAIN, A., QARSHI, I. A., NAZIR, H. & ULLAH, I. 2012. Plant Tissue Culture: current status and opportunities. *InTech Open*
- IOOS, R., LAUGUSTIN, L., SCHENCK, N., ROSE, S., HUSSON, C. & FREY, P. 2006. Usefulness of single copy genes containing introns in *Phytophthora* for the development of detection tools for the regulated species *P-ramorum* and *P-fragariae*. *European Journal of Plant Pathology*, 116, 171-176.
- JACKSON, K. L., YIN, J., CSINOS, A. S. & JI, P. 2010. Fungicidal activity of fluopicolide for suppression of *Phytophthora capsici* on squash. *Crop Protection*, 29, 1421-1427.
- JASWAL, R., KIRAN, K., RAJARAMMOHAN, S., DUBEY, H., SINGH, P. K., SHARMA, Y., DESHMUKH, R., SONAH, H., GUPTA, N. & SHARMA, T. R. 2020. Effector Biology of Biotrophic Plant Fungal Pathogens: Current Advances and Future Prospects. *Microbiological Research*, 241, 126567.
- JEWORUTZKI, E., ROELFSEMA, M. R. G., ANSCHÜTZ, U., KROL, E., ELZENGA, J. T. M., FELIX, G., BOLLER, T., HEDRICH, R. & BECKER, D. 2010. Early signaling through the Arabidopsis pattern recognition receptors FLS2 and EFR involves Ca²⁺-associated opening of plasma membrane anion channels. *The Plant Journal*, 62, 367-378.
- JIANG, R. H. Y., STAHELIN, R. V., BHATTACHARJEE, S. & HALDAR, K. 2013. Eukaryotic virulence determinants utilize phosphoinositides at the ER and host cell surface. *Trends in Microbiology*, 21, 145-156.
- JIANG, R. H. Y., TRIPATHY, S., GOVERS, F. & TYLER, B. M. 2008. RXLR effector reservoir in two *Phytophthora* species is dominated by a single rapidly evolving superfamily with more than 700 members. *Proceedings of the National Academy of Sciences*, 105, 4874.
- JIANG, R. H. Y., WEIDE, R., VAN DE VONDERVOORT, P. J. I. & GOVERS, F. 2006. Amplification generates modular diversity at an avirulence locus in the pathogen *Phytophthora*. *Genome research*, 16, 827-840.
- JONES, C., IANNETTA, P., WOODHEAD, M., DAVIES, H., MCNICOL, R. & TAYLOR, M. 1997. The Isolation of RNA from Raspberry (*Rubus idaeus*) Fruit. *Molecular Biotechnology*, 8, 219-221.
- JONES, J. D. & DANGL, J. L. 2006. The plant immune system. *Nature*, 444, 323-9.
- JUDELSON, H. S., COFFEY, M. D., ARREDONDO, F. R. & TYLER, B. M. 1993. Transformation of the Oomycete Pathogen *Phytophthora-Megasperma* F-Sp *Glycinea* Occurs by DNA Integration into Single or Multiple Chromosomes. *Current Genetics*, 23, 211-218.

- JUDELSON, H. S. & MICHELMORE, R. W. 1991. Transient expression of genes in the oomycete *Phytophthora infestans* using *Bremia lactucae* regulatory sequences. *Current Genetics*, 19, 453-459.
- JUDELSON, H. S., TYLER, B. M. & MICHELMORE, R. W. 1991. Transformation of the Oomycete pathogen, *Phytophthora-Infestans*. *Molecular Plant-Microbe Interactions*, 4, 602-607.
- JUDELSON, H. S. & WHITTAKER, S. L. 1995. Inactivation of transgenes in *Phytophthora infestans* is not associated with their deletion, methylation, or mutation. *Curr Genet*, 28, 571-9.
- JUPE, F., WITEK, K., VERWEIJ, W., SLIWKA, J., PRITCHARD, L., ETHERINGTON, G. J., MACLEAN, D., COCK, P. J., LEGGETT, R. M., BRYAN, G. J., CARDLE, L., HEIN, I. & JONES, J. D. 2013. Resistance gene enrichment sequencing (RenSeq) enables reannotation of the NB-LRR gene family from sequenced plant genomes and rapid mapping of resistance loci in segregating populations. *Plant J*, 76, 530-44.
- KADOTA, Y., SKLENAR, J., DERBYSHIRE, P., STRANSFELD, L., ASAI, S., NTOUKAKIS, V., JONES, J. D., SHIRASU, K., MENKE, F., JONES, A. & ZIPFEL, C. 2014. Direct regulation of the NADPH oxidase RBOHD by the PRR-associated kinase BIK1 during plant immunity. *Mol Cell*, 54, 43-55.
- KAMOUN, S. 2006. A Catalogue of the Effector Secretome of Plant Pathogenic Oomycetes. *Annual Review of Phytopathology*, 44, 41-60.
- KAMOUN, S. 2007. Groovy times: filamentous pathogen effectors revealed. *Current Opinion in Plant Biology*, 10, 358-365.
- KAMOUN, S., VAN WEST, P., DE JONG, A. J., DE GROOT, K. E., VLEESHOUWERS, V. G. & GOVERS, F. 1997. A gene encoding a protein elicitor of *Phytophthora infestans* is down-regulated during infection of potato. *Molecular plant-microbe interactions : MPMI*, 10, 13-20.
- KAMOUN, S., VAN WEST, P., VLEESHOUWERS, V. G. A. A., DE GROOT, K. E. & GOVERS, F. 1998. Resistance of *Nicotiana benthamiana* to *Phytophthora infestans* Is Mediated by the Recognition of the Elicitor Protein INF1. *The Plant Cell*, 10, 1413-1425.
- KANNEGANTI, T.-D., HUITEMA, E., CAKIR, C. & KAMOUN, S. 2006. Synergistic Interactions of the Plant Cell Death Pathways Induced by *Phytophthora infestans* Nep1-Like Protein PiNPP1.1 and INF1 Elicitor. *Molecular Plant-Microbe Interactions*®, 19, 854-863.
- KANZAKI, H., SAITOH, H., ITO, A., FUJISAWA, S., KAMOUN, S., KATOU, S., YOSHIOKA, H. & TERAUCHI, R. 2003. Cytosolic HSP90 and HSP70 are essential components of INF1-mediated hypersensitive response and non-host resistance to *Pseudomonas cichorii* in *Nicotiana benthamiana*. *Molecular Plant Pathology*, 4, 383-391.
- KENNEDY, D. M. & DUNCAN, J. M. 1993. Occurrence of races in *Phytophthora fragariae* var *rubi* on Raspberry. *Rubus and Ribes*. Acta Horticulture.
- KIM, H.-S., DESVEAUX, D., SINGER, A. U., PATEL, P., SONDEK, J. & DANGL, J. L. 2005. The *Pseudomonas syringae* effector AvrRpt2 cleaves its C-terminally acylated target, RIN4, from Arabidopsis membranes to block RPM1 activation. *Proceedings of the National Academy of Sciences of the United States of America*, 102, 6496-6501.
- KIM, K. S. & JUDELSON, H. S. 2003. Sporangium-specific gene expression in the oomycete phytopathogen *Phytophthora infestans*. *Eukaryotic cell*, 2, 1376-1385.
- KING, S. R., MCLELLAN, H., BOEVINK, P. C., ARMSTRONG, M. R., BUKHAROVA, T., SUKARTA, O., WIN, J., KAMOUN, S., BIRCH, P. R. & BANFIELD, M. J. 2014. *Phytophthora infestans* RXLR effector PexRD2 interacts with host MAPKKK epsilon to suppress plant immune signaling. *Plant Cell*, 26, 1345-59.
- KOPRIVICA, M., DULIC-MARKOVIC, I., JEVTIC, R. & COOKE, D. 2009. Methods for detection of *Phytophthora fragariae* var. *rubi* on raspberry. *Pesticidi i fitomedicina*, 24, 177-184.
- KOSKE, R. E. & GEMMA, J. N. 1989. Staining roots for Arbuscular Mycorrhizal Fungi. *Mycological Research*, 92, 468-488.
- KOZAREWA, I., ARMISEN, J., GARDNER, A. F., SLATKO, B. E. & HENDRICKSON, C. L. 2015. Overview of Target Enrichment Strategies. *Curr Protoc Mol Biol*, 112, 7.21.1-7.21.23.

- KROON, L. P., BROUWER, H., DE COCK, A. W. & GOVERS, F. 2012. The genus *Phytophthora* anno 2012. *Phytopathology*, 102, 348-64.
- KUMARI, S. & PANIGRAHI, K. C. S. 2019. Light and auxin signaling cross-talk programme root development in plants. *Journal of Biosciences*, 44, 26.
- KUŹNIAK, E. & URBANEK, H. 2000. The involvement of hydrogen peroxide in plant responses to stresses. *Acta Physiologiae Plantarum*, 22, 195-203.
- LAMOUR, K. & KAMOUN, S. 2009. *Oomycete genetics and genomics: diversity, interactions and research tools*, Wiley-Blackwell.
- LAMOUR, K. H. 2013. *Phytophthora: a global perspective*, Cambridge, MA, CAB International.
- LANGMEAD, B. & SALZBERG, S. L. 2012. Fast gapped-read alignment with Bowtie 2. *Nature Methods*, 9, 357-359.
- LARROQUE, M., BELMAS, E., MARTINEZ, T., VERGNES, S., LADOUCE, N., LAFITTE, C., GAULIN, E. & DUMAS, B. 2013. Pathogen-associated molecular pattern-triggered immunity and resistance to the root pathogen *Phytophthora parasitica* in *Arabidopsis*. *Journal of Experimental Botany*, 64, 3615-3625.
- LATIJNHOUWERS, M., DE WIT, P. J. G. M. & GOVERS, F. 2003. Oomycetes and fungi: similar weaponry to attack plants. *Trends in Microbiology*, 11, 462-469.
- LATORRE, B. A. & MUÑOZ, R. 1993. Root rot of red raspberry caused by *Phytophthora citricola* and *P. citrophthora* in Chile. *Plant Disease*, 77, 715-718.
- LAUN, N. & ZINKERNAGEL, V. 1997. A Comparison of the Resistance Against *Phytophthora fragariae* var. *rubi*, the Causal Agent of a Raspberry Root Rot. *Journal of Phytopathology*, 145, 197-204.
- LAWRENCE, S. A., ARMSTRONG, C. B., PATRICK, W. M. & GERTH, M. L. 2017. High-Throughput Chemical Screening Identifies Compounds that Inhibit Different Stages of the *Phytophthora agathidicida* and *Phytophthora cinnamomi* Life Cycles. *Front Microbiol*, 8, 1340.
- LE BERRE, J.-Y., ENGLER, G. & PANABIÈRES, F. 2008. Exploration of the late stages of the tomato-*Phytophthora parasitica* interactions through histological analysis and generation of expressed sequence tags. *New Phytologist*, 177, 480-492.
- LEE, T. Y., MIZUBUTI, E. & FRY, W. E. 1999. Genetics of Metalaxyl Resistance in *Phytophthora infestans*. *Fungal Genetics and Biology*, 26, 118-130.
- LEONIAN, L. H. 1934. IDENTIFICATION OF PHYTOPHTHORA SPECIES. *W. Va. Agr. Expt. Sta. Bui.*, 262.
- LÉVESQUE, C. A., BROUWER, H., CANO, L., HAMILTON, J. P., HOLT, C., HUITEMA, E., RAFFAELE, S., ROBIDEAU, G. P., THINES, M., WIN, J., ZERILLO, M. M., BEAKES, G. W., BOORE, J. L., BUSAM, D., DUMAS, B., FERRIERA, S., FUERSTENBERG, S. I., GACHON, C. M. M., GAULIN, E., GOVERS, F., GRENVILLE-BRIGGS, L., HORNER, N., HOSTETLER, J., JIANG, R. H. Y., JOHNSON, J., KRAJAEJUN, T., LIN, H., MEIJER, H. J. G., MOORE, B., MORRIS, P., PHUNTMART, V., PUIU, D., SHETTY, J., STAJICH, J. E., TRIPATHY, S., WAWRA, S., VAN WEST, P., WHITTY, B. R., COUTINHO, P. M., HENRISSAT, B., MARTIN, F., THOMAS, P. D., TYLER, B. M., DE VRIES, R. P., KAMOUN, S., YANDELL, M., TISSERAT, N. & BUELL, C. R. 2010. Genome sequence of the necrotrophic plant pathogen *Pythium ultimum* reveals original pathogenicity mechanisms and effector repertoire. *Genome Biology*, 11, R73-R73.
- LI, C., CHEN, S., ZUO, C., SUN, Q., YE, Q., YI, G. & HUANG, B. 2011. The use of GFP-transformed isolates to study infection of banana with *Fusarium oxysporum* f. sp. *cubense* race 4. *European Journal of Plant Pathology*, 131, 327-340.
- LI, H., HANDSAKER, B., WYSOKER, A., FENNELLS, T., RUAN, J., HOMER, N., MARTH, G., ABECASIS, G. & DURBIN, R. 2009. The Sequence Alignment/Map format and SAMtools. *Bioinformatics*, 25, 2078-9.
- LI, Y., SUN, S., ZHONG, C. & ZHU, Z. 2017. Detached-petiole inoculation method to evaluate *Phytophthora* root rot resistance in soybean plants. *Crop and Pasture Science*, 68, 555.
- LIN, K.-H., HUANG, M.-Y., HUANG, W.-D., HSU, M.-H., YANG, Z.-W. & YANG, C.-M. 2013. The effects of red, blue, and white light-emitting diodes on the growth, development, and edible quality of

- hydroponically grown lettuce (*Lactuca sativa* L. var. *capitata*). *Scientia Horticulturae*, 150, 86-91.
- LINSLEY-NOAKES, G., WILKEN, L. & DE VILLIERS, S. 2006. HIGH DENSITY, VERTICAL HYDROPONICS GROWING SYSTEM FOR STRAWBERRIES. *Acta Horticulturae*, 365-370.
- LIU, T., SONG, T., ZHANG, X., YUAN, H., SU, L., LI, W., XU, J., LIU, S., CHEN, L., CHEN, T., ZHANG, M., GU, L., ZHANG, B. & DOU, D. 2014. Unconventionally secreted effectors of two filamentous pathogens target plant salicylate biosynthesis. *Nature Communications*, 5, 4686.
- LIU, T., YE, W., RU, Y., YANG, X., GU, B., TAO, K., LU, S., DONG, S., ZHENG, X., SHAN, W., WANG, Y. & DOU, D. 2011. Two Host Cytoplasmic Effectors Are Required for Pathogenesis of *Phytophthora sojae* by Suppression of Host Defenses. *Plant Physiology*, 155, 490.
- LIU, W., CHEN, D. & LIU, Z. 2005. High Efficiency Column Culture System in China. *Acta Horticulturae*, 691.
- LIVAK, K. J. & SCHMITTGEN, T. D. 2001. Analysis of Relative Gene Expression Data Using Real-Time Quantitative PCR and the $2^{-\Delta\Delta CT}$ Method. *Methods*, 25, 402-408.
- LOBATO, M. C., MACHINANDIARENA, M. F., TAMBASCIO, C., DOSIO, G. A. A., CALDIZ, D. O., DALEO, G. R., ANDREU, A. B. & OLIVIERI, F. P. 2011. Effect of foliar applications of phosphite on post-harvest potato tubers. *European Journal of Plant Pathology*, 130, 155-163.
- LOBATO, M. C., OLIVIERI, F. P., ALTAMIRANDA, E. A. G., WOLSKI, E. A., DALEO, G. R., CALDIZ, D. O. & ANDREU, A. B. 2008. Phosphite compounds reduce disease severity in potato seed tubers and foliage. *European Journal of Plant Pathology*, 122, 349-358.
- LOBATO, M. C., OLIVIERI, F. P., DALEO, G. R. & ANDREU, A. B. 2010. Antimicrobial activity of phosphites against different potato pathogens. *Journal of Plant Diseases and Protection*, 117, 102-109.
- LÖCHEL, A. & BIRCHMORE, R. J. 1990. Effects of propamocarb on the development of *Phytophthora infestans* on potatoes. Thornton Heath: British Crop Protection Council.
- LU, Y., MCGAVIN, W., COCK, P. J. A., SCHNETTLER, E., YAN, F., CHEN, J. & MACFARLANE, S. 2015. Newly identified RNAs of raspberry leaf blotch virus encoding a related group of proteins. *J Gen Virol*, 96, 3432-3439.
- MA, Z., SONG, T., ZHU, L., YE, W., WANG, Y., SHAO, Y., DONG, S., ZHANG, Z., DOU, D., ZHENG, X., TYLER, B. M. & WANG, Y. 2015. A *Phytophthora sojae* Glycoside Hydrolase 12 Protein Is a Major Virulence Factor during Soybean Infection and Is Recognized as a PAMP. *Plant Cell*, 27, 2057-72.
- MA, Z., ZHU, L., SONG, T., WANG, Y., ZHANG, Q., XIA, Y., QIU, M., LIN, Y., LI, H., KONG, L., FANG, Y., YE, W., WANG, Y., DONG, S., ZHENG, X., TYLER, B. M. & WANG, Y. 2017. A paralogous decoy protects *Phytophthora sojae* apoplastic effector PsXEG1 from a host inhibitor. *Science*, 355, 710.
- MACKEY, D., HOLT, B. F., III, WIIG, A. & DANGL, J. L. 2002. RIN4 interacts with *Pseudomonas syringae* type III effector molecules and is required for RPM1-mediated resistance in *Arabidopsis*. *Cell*, 108, 743-754.
- MALCOLM, P. A. 2013. *History of Raspberry Plants* [Online]. <https://pioneerthinking.com/history-of-raspberry-plants/>. [Accessed July 2021].
- MALONEY, K., WILCOX, W. F. & SANFORD, J. C. 1993. Effects of raised beds and metalaxyl for control of *Phytophthora* root rot of raspberry. *Horticultural Science*, 28, 1106-1108.
- MAN IN'T VELD, W. A. 2007. Gene flow analysis demonstrates that *Phytophthora fragariae* var. *rubi* constitutes a distinct species, *Phytophthora rubi* comb. nov. *Mycologia*, 99, 222-226.
- MAOR, R., PUYESKY, M., HORWITZ, B. A. & SHARON, A. 1998. Use of green fluorescent protein (GFP) for studying development and fungal-plant interaction in *Cochliobolus heterostrophus*. *Mycological Research*, 102, 491-496.
- MARCO-SOLA, S., SAMMETH, M., GUIGÓ, R. & RIBECA, P. 2012. The GEM mapper: fast, accurate and versatile alignment by filtration. *Nat Methods*, 9, 1185-8.

- MARTIN, F. N., BENSASSON, D., TYLER, B. M. & BOORE, J. L. 2007. Mitochondrial genome sequences and comparative genomics of *Phytophthora ramorum* and *P. sojae*. *Current Genetics*, 51, 285-296.
- MARTIN, F. N., BLAIR, J. E. & COFFEY, M. D. 2014. A combined mitochondrial and nuclear multilocus phylogeny of the genus *Phytophthora*. *Fungal Genetics and Biology*, 66, 19-32.
- MARTIN, F. N. & TOOLEY, P. W. 2003. Phylogenetic relationships among *Phytophthora* species inferred from sequence analysis of mitochondrially encoded cytochrome oxidase I and II genes. *Mycologia*, 95, 269-84.
- MARX, D. H. & HAASIS, F. A. 1965. Induction of Aseptic Sporangial Formation in *Phytophthora Cinnamomi* by Metabolic Diffusates of Soil Micro-Organisms. *Nature*, 206, 673-&.
- MATTHEUS, N., EKRAMODDOULLAH, A. K. M. & LEE, S. P. 2003. Isolation of high-quality RNA from white spruce tissue using a three-stage purification method and subsequent cloning of a transcript from the PR-10 gene family. *Phytochemical Analysis*, 14, 209-215.
- MATTHEWS, H. D., GILLETT, N. P., STOTT, P. A. & ZICKFELD, K. 2009. The proportionality of global warming to cumulative carbon emissions. *Nature*, 459, 829-832.
- MAXIMO, H. J., DALIO, R. J. D., DIAS, R. O., LITHOLDO, C. G., FELIZATTI, H. L. & MACHADO, M. A. 2019. PpCRN7 and PpCRN20 of *Phytophthora parasitica* regulate plant cell death leading to enhancement of host susceptibility. *BMC Plant Biology*, 19, 544.
- MCCARTHY, C. G. P. & FITZPATRICK, D. A. 2017. Phylogenomic reconstruction of the Oomycete phylogeny derived from 37 genomes. *Mosphere*, 2.
- MCDONALD, B. A. & STUKENBROCK, E. H. 2016. Rapid emergence of pathogens in agro-ecosystems: Global threats to agricultural sustainability and food security. *Philosophical Transactions of the Royal Society B: Biological Sciences*, 371.
- MCKEEN, W. E. 1958. Red stele root disease of the loganberry and strawberry caused by *Phytophthora fragariae*. *Phytopathology*, 48, 129-132.
- MCLELLAN, H., BOEVINK, P. C., ARMSTRONG, M. R., PRITCHARD, L., GOMEZ, S., MORALES, J., WHISSON, S. C., BEYNON, J. L. & BIRCH, P. R. J. 2013. An RxLR effector from *Phytophthora infestans* prevents re-localisation of two plant NAC transcription factors from the endoplasmic reticulum to the nucleus. *PLoS pathogens*, 9, e1003670-e1003670.
- MCLEOD, A., FRY, B. A., ZULUAGA, A. P., MYERS, K. L. & FRY, W. E. 2008. Toward improvements of oomycete transformation protocols. *J Eukaryot Microbiol*, 55, 103-9.
- MEHRLICH, F. P. 1934. Nonsterile soil leachate stimulating zoosporangia production by *Phytophthora* sp. . *Phytopathology* 24.
- MELOTTO, M., UNDERWOOD, W. & HE, S. Y. 2008. Role of Stomata in Plant Innate Immunity and Foliar Bacterial Diseases. *Annual Review of Phytopathology*, 46, 101-122.
- MENG, Y., ZHANG, Q., ZHANG, M., GU, B., HUANG, G., WANG, Q. & SHAN, W. 2015. The protein disulfide isomerase 1 of *Phytophthora parasitica* (PpPDI1) is associated with the haustoria-like structures and contributes to plant infection. *Front Plant Sci*, 6, 632.
- MESZKA, B. & MICHAŁECKA, M. 2016. Identification of *Phytophthora* spp. isolated from plants and soil samples on strawberry plantations in Poland. *J Plant Dis Prot* 123, 29–36.
- MINK, P. J., SCRAFFORD, C. G., BARRAJ, L. M., HARNACK, L., HONG, C.-P., NETTLETON, J. A. & JACOBS, J. D. R. 2007. Flavonoid intake and cardiovascular disease mortality: a prospective study in postmenopausal women. *The American Journal of Clinical Nutrition*, 85, 895-909.
- MONTGOMERIE, I. G. & KENNEDY, D. M. 1980. The pathogenicity of *Phytophthora* species to red raspberry. *Acta Horticulturae*, 112, 167-176.
- MOSTOWFIZADEH-GHALAMFARSA, R., PANABIÈRES, F., BANIHASHEMI, Z. & COOKE, D. E. L. 2010. Phylogenetic relationship of *Phytophthora cryptogea* Pethybr. & Laff and *P. drechsleri* Tucker. *Fungal Biology*, 114, 325-339.
- MOZAFFARIEH, M., SACU, S. & WEDRICH, A. 2003. The role of the carotenoids, lutein and zeaxanthin, in protecting against age-related macular degeneration: A review based on controversial evidence. *Nutrition Journal*, 2, 20-20.

- MPUSIA, P. T. O. 2006. *Comparison of water consumption between greenhouse and outdoor cultivation*. Master of Science in Geo-information Science and Earth Observation, Specialisation: Advance Use of Remote Sensing, Irrigation and Drainage, International Institute for Geo-Information Science and Earth Observation, Enschede, The Netherlands.
- MUSSEL, H. & FAY, F. 1973. Aseptic Zoospore Production by *Phytophthora fragariae*. *Phytopathology*, 63, 1081-1082.
- NA, R., YU, D., QUTOB, D., ZHAO, J. & GIJZEN, M. 2013. Deletion of the *Phytophthora sojae* avirulence gene *Avr1d* causes gain of virulence on *Rps1d*. *Mol Plant Microbe Interact*, 26, 969-76.
- NAHALKOVA, J. & FATEHI, J. 2003. Red fluorescent protein (DsRed2) as a novel reporter in *Fusarium oxysporum* f. sp. *lycopersici*. *FEMS Microbiology Letters*, 225, 305-309.
- NAVEED, Z. A., WEI, X., CHEN, J., MUBEEN, H. & ALI, G. S. 2020. The PTI to ETI Continuum in *Phytophthora*-Plant Interactions. *Frontiers in Plant Science*, 11.
- NICKERSON, N. L. 1998. Red stele root rot, In Compendium of Strawberry Diseases. *Second Edition*. Maas, J. L. (ed.), APS Press 48-50. .
- NJOROGE, S. M. C., VALLAD, G. E., PARK, S.-Y., KANG, S., KOIKE, S. T., BOLDA, M., BURMAN, P., POLONIK, W. & SUBBARAO, K. V. 2011. Phenological and Phytochemical Changes Correlate with Differential Interactions of *Verticillium dahliae* with Broccoli and Cauliflower. *Phytopathology*, 101, 523-534.
- NOAA 2020. National Centers for Environmental information, Climate at a Glance: Global Time Series. published July 2020, retrieved on July 31, 2020 from <https://www.ncdc.noaa.gov/cag/>.
- NORMAN, J. R. & HOOKER, J. E. 2000. Sporulation of *Phytophthora fragariae* shows greater stimulation by exudates of non-mycorrhizal than by mycorrhizal strawberry roots. *Mycological Research*, 104, 1069-1073.
- NOURISSEAU, J. G. & BAUDRY, A. 1987. Un *Phytophthora* cause de deperissement du framboisier en France. *Phytoma*, 384, 39-41.
- NÜRNBERGER, T., NENNSTIEL, D., JABS, T., SACKS, W. R., HAHLBROCK, K. & SCHEEL, D. 1994. High affinity binding of a fungal oligopeptide elicitor to parsley plasma membranes triggers multiple defense responses. *Cell*, 78, 449-460.
- O'BRIEN, J. A., DAUDI, A., BUTT, V. S. & PAUL BOLWELL, G. 2012. Reactive oxygen species and their role in plant defence and cell wall metabolism. *Planta*, 236, 765-779.
- O'NEILL, B. C., KRIEGLER, E., EBI, K. L., KEMP-BENEDICT, E., RIAHI, K., ROTHMAN, D. S., VAN RUIJVEN, B. J., VAN VUUREN, D. P., BIRKMANN, J., KOK, K., LEVY, M. & SOLECKI, W. 2017. The roads ahead: Narratives for shared socioeconomic pathways describing world futures in the 21st century. *Global Environmental Change*, 42, 169-180.
- OCHOA, J. C., HERRERA, M., NAVIA, M. & ROMERO, H. M. 2019. Visualization of *Phytophthora palmivora* Infection in Oil Palm Leaflets with Fluorescent Proteins and Cell Viability Markers. *The plant pathology journal*, 35, 19-31.
- OH, S.-K., KAMOUN, S. & CHOI, D. 2010. Oomycetes RXLR Effectors Function as Both Activator and Suppressor of Plant Immunity. *Plant Pathology Journal*, 26, 209-215.
- OH, S.-K., YOUNG, C., LEE, M., OLIVA, R., BOZKURT, T. O., CANO, L. M., WIN, J., BOS, J. I. B., LIU, H.-Y., VAN DAMME, M., MORGAN, W., CHOI, D., VAN DER VOSSSEN, E. A. G., VLEESHOUWERS, V. G. A. A. & KAMOUN, S. 2009. In planta expression screens of *Phytophthora infestans* RXLR effectors reveal diverse phenotypes, including activation of the solanum bulbocastanum disease resistance protein *Rpi-blb2*. *The Plant Cell*, 21, 2928-2947.
- OLIVA, R. F., CANO, L. M., RAFFAELE, S., WIN, J., BOZKURT, T. O., BELHAJ, K., OH, S. K., THINES, M. & KAMOUN, S. 2015. A Recent Expansion of the RXLR Effector Gene *Avrblb2* Is Maintained in Global Populations of *Phytophthora infestans* Indicating Different Contributions to Virulence. *Mol Plant Microbe Interact*, 28, 901-12.
- PANDEY, B. & SETO, K. C. 2015. Urbanization and agricultural land loss in India: Comparing satellite estimates with census data. *Journal of Environmental Management*, 148, 53-66.

- PANE, A., LI DESTRI NICOSIA, M. G. & CACCIOLA, S. O. 2001. First Report of *Phytophthora citrophthora* Causing Fruit Brown Rot of Feijoa in Italy. *Plant Dis*, 85, 97.
- PARAĐIKOVIĆ, N., VINKOVIĆ, T., VINKOVIĆ VRČEK, I., ŽUNTAR, I., BOJIĆ, M. & MEDIĆ-ŠARIĆ, M. 2011. Effect of natural biostimulants on yield and nutritional quality: an example of sweet yellow pepper (*Capsicum annuum* L.) plants. *Journal of the Science of Food and Agriculture*, 91, 2146-2152.
- PARRA, G. & RISTAINO, J. B. 2001. Resistance to Mefenoxam and Metalaxyl Among Field Isolates of *Phytophthora capsici* Causing *Phytophthora* Blight of Bell Pepper. *Plant Dis*, 85, 1069-1075.
- PATTISON, J., WILCOX, W. & WEBER, C. 2004. Assessing the Resistance of Red Raspberry (*Rubus idaeus* L.) Genotypes to *Phytophthora fragariae* var. *rubi* in Hydroponic Culture. *HortScience: a publication of the American Society for Horticultural Science*, 39.
- PATTISON, J. A., SAMUELIAN, S. K. & WEBER, C. A. 2007. Inheritance of *Phytophthora* root rot resistance in red raspberry determined by generation means and molecular linkage analysis. *Theoretical and Applied Genetics*, 115, 225-236.
- PEPIN, H. S. 1967. Susceptibility of members of the Rosaceae to races of *Phytophthora fragariae*. *Phytopathology*, 57, 782-784.
- PÉREZ, W., LARA, J. & FORBES, G. A. 2009. Resistance to metalaxyl-M and cymoxanil in a dominant clonal lineage of *Phytophthora infestans* in Huánuco, Peru, an area of continuous potato production. *European Journal of Plant Pathology*, 125, 87-95.
- PETERS, J. & WOODHALL, J. 2014. Raspberry: detection and quantification of *Phytophthora rubi* in soil and plant tissue. Agriculture and Horticulture Development Board.
- PETRE, B. & KAMOUN, S. 2014. How Do Filamentous Pathogens Deliver Effector Proteins into Plant Cells? *PLoS biology*, 12, e1001801.
- PINKERTON, J. N., BRISTOW, P. R., WINDOM, G. E. & WALTERS, T. W. 2009. Soil solarization as a component of an integrated program for control of raspberry root rot. *Plant Disease*, 93, 452-458.
- PONDER, A. & HALLMANN, E. 2019. The effects of organic and conventional farm management and harvest time on the polyphenol content in different raspberry cultivars. *Food Chemistry*, 301, 125295.
- QI, R., WANG, T., ZHAO, W., LI, P., DING, J. & GAO, Z. 2012. Activity of Ten Fungicides against *Phytophthora capsici* Isolates Resistant to Metalaxyl. *Journal of Phytopathology*, 160.
- QUINLAN, A. R. & HALL, I. M. 2010. BEDTools: a flexible suite of utilities for comparing genomic features. *Bioinformatics*, 26, 841-842.
- QUTOB, D., TEDMAN-JONES, J., DONG, S., KUFLU, K., PHAM, H., WANG, Y., DOU, D., KALE, S. D., ARREDONDO, F. D., TYLER, B. M. & GIJZEN, M. 2009. Copy number variation and transcriptional polymorphisms of *Phytophthora sojae* RXLR effector genes *Avr1a* and *Avr3a*. *PLoS One*, 4, e5066.
- RAFFLE, S. & ALLEN, J. 2007. *Phytophthora* root rot of raspberry and other cane fruits. *Horticultural Development Council*, Fact Sheet.
- RAJPUT, N. A., ZHANG, M., RU, Y., LIU, T., XU, J., LIU, L., MAFURAH, J. J. & DOU, D. 2014. *Phytophthora sojae* Effector PsCRN70 Suppresses Plant Defenses in *Nicotiana benthamiana*. *PLOS ONE*, 9, e98114.
- RAMÍREZ GÓMEZ, H., SANDOVAL-VILLA, M., CARRILLO-SALAZAR, A. & MURATALLA-LÚA, A. 2012. Comparison of Hydroponic Systems in the Strawberry Production. *Acta horticulturae*, 947, 165-172.
- RANDALL, E., YOUNG, V., SIEROTZKI, H., SCALIET, G., BIRCH, P. R. J., COOKE, D. E. L., CSUKAI, M. & WHISSON, S. C. 2014. Sequence diversity in the large subunit of RNA polymerase I contributes to Mefenoxam insensitivity in *Phytophthora infestans*. *Molecular plant pathology*, 15, 664-676.
- REHMANY, A. P., GORDON, A., ROSE, L. E., ALLEN, R. L., ARMSTRONG, M. R., WHISSON, S. C., KAMOUN, S., TYLER, B. M., BIRCH, P. R. J. & BEYNON, J. L. 2005. Differential recognition of highly

- divergent Downy mildew avirulence gene alleles by RPP1 resistance genes from two *Arabidopsis* lines. *The Plant Cell*, 17, 1839-1850.
- REKANOVIĆ, E., POTOČNIK, I., MILIJAŠEVIĆ-MARČIĆ, S., STEPANOVIĆ, M., TODOROVIĆ, B. & MIHAJLOVIĆ, M. 2012. Toxicity of metalaxyl, azoxystrobin, dimethomorph, cymoxanil, zoxamide and mancozeb to *Phytophthora infestans* isolates from Serbia. *Journal of Environmental Science and Health, Part B*, 47, 403-409.
- RESH, H. M. 2012. *Hydroponic food production: a definitive guidebook for the advanced home gardener and the commercial hydroponic grower*, Boca Raton, CRC Press.
- RHOADS, A. & AU, K. F. 2015. PacBio Sequencing and Its Applications. *Genomics, Proteomics & Bioinformatics*, 13, 278-289.
- RIDLEY, L., MACE, A., PARRISH, G., BARKER, I., MACARTHUR, R., RAINFORD, J. & GARTHWAITE, D. 2018. PESTICIDE USAGE SURVEY REPORT 285 SOFT FRUIT IN THE UNITED KINGDOM 2018 DEFRA.
- RIEDEL, M., CALMIN, G., BELBAHRI, L., LEFORT, F., GÖTZ, M., WAGNER, S. & WERRES, S. 2009. Green Fluorescent Protein (GFP) as a Reporter Gene for the Plant Pathogenic Oomycete *Phytophthora ramorum*. *Journal of Eukaryotic Microbiology*, 56, 130-135.
- ROCAFORT, M., FUDAL, I. & MESARICH, C. H. 2020. Apoplastic effector proteins of plant-associated fungi and oomycetes. *Current Opinion in Plant Biology*, 56, 9-19.
- ROSE, D. C. & CHILVERS, J. 2018. Agriculture 4.0: Broadening Responsible Innovation in an Era of Smart Farming. *Frontiers in Sustainable Food Systems*, 2.
- ROSE, J. K. C., HAM, K.-S., DARVILL, A. G. & ALBERSHEIM, P. 2002. Molecular cloning and characterization of glucanase inhibitor proteins: coevolution of a counterdefense mechanism by plant pathogens. *The Plant Cell*, 14, 1329-1345.
- SAMOUCHA, Y. & COHEN, Y. 1990. Toxicity of propamocarb to the late blight fungus on potato. *Phytoparasitica*, 18, 27.
- SANDHU, D., GAO, H., CIANZIO, S. & BHATTACHARYYA, M. K. 2004. Deletion of a Disease Resistance Nucleotide-Binding-Site Leucine-Rich- Repeat-like Sequence Is Associated With the Loss of the *Phytophthora* Resistance Gene *Rps4* in Soybean. *Genetics*, 168, 2157-2167.
- SARIBURUN, E., ŞAHIN, S., DEMIR, C., TÜRK BEN, C. & UYLAŞER, V. 2010. Phenolic Content and Antioxidant Activity of Raspberry and Blackberry Cultivars. *Journal of Food Science*, 75, C328-C335.
- SAROOSHI, R. A. & CRESSWELL, G. C. 1994. Effects of hydroponic solution composition, electrical conductivity and plant spacing on yield and quality of strawberries. *Australian Journal of Experimental Agriculture*, 34, 529-535.
- SAVARY, S., FICKE, A., AUBERTOT, J.-N. & HOLLIER, C. 2012. Crop losses due to diseases and their implications for global food production losses and food security. *Food Security*, 4, 519-537.
- SAVARY, S., WILLOCQUET, L., PETHYBRIDGE, S. J., ESKER, P., MCROBERTS, N. & NELSON, A. 2019. The global burden of pathogens and pests on major food crops. *Nat Ecol Evol*, 3, 430-439.
- SAVILLE, A., GRAHAM, K., GRÜN WALD, N. J., MYERS, K., FRY, W. E. & RISTAINO, J. B. 2015. Fungicide Sensitivity of U.S. Genotypes of *Phytophthora infestans* to Six Oomycete-Targeted Compounds. *Plant Disease*, 99, 659-666.
- SCANU, B., LINALDEDDU, B. T., DEIDDA, A. & JUNG, T. 2015. Diversity of *Phytophthora* Species from Declining Mediterranean Maquis Vegetation, including Two New Species, *Phytophthora crassamura* and *P. ornamentata* sp. nov. *PLOS ONE*, 10, e0143234.
- SCHAEFFER, J. 2013. Latest scoop on berries: Harvard study shows heart health benefits for young women. *Today's Dietitian*, 15, 16.
- SCHENA, L. & COOKE, D. E. L. 2006. Assessing the potential of regions of the nuclear and mitochondrial genome to develop a "molecular tool box" for the detection and characterization of *Phytophthora* species. *Journal of Microbiological Methods*, 67, 70-85.
- SCHENA, L., DUNCAN, J. M. & COOKE, D. E. L. 2007. Development and application of a PCR-based 'molecular tool box' for the identification of *Phytophthora* species damaging forests and natural ecosystems. *Plant Pathology*

- SCHMITTGEN, T. D., ZAKRAJSEK, B. A., MILLS, A. G., GORN, V., SINGER, M. J. & REED, M. W. 2000. Quantitative Reverse Transcription–Polymerase Chain Reaction to Study mRNA Decay: Comparison of Endpoint and Real-Time Methods. *Analytical Biochemistry*, 285, 194-204.
- SCHMITTHENNER, A. F. & BHAT, R. G. 1994. Useful Method for studying *Phytophthora* in the laboratory. *Plant Pathology, Ohio Agricultural Research and Development Center*.
- SCHÖB, H., KUNZ, C. & MEINS, F., JR. 1997. Silencing of transgenes introduced into leaves by agroinfiltration: a simple, rapid method for investigating sequence requirements for gene silencing. *Mol Gen Genet*, 256, 581-5.
- SCHORNACK, S., HUITEMA, E., CANO, L. M., BOZKURT, T. O., OLIVA, R., VAN DAMME, M., SCHWIZER, S., RAFFAELE, S., CHAPARRO-GARCIA, A., FARRER, R., SEGRETIN, M. E., BOS, J., HAAS, B. J., ZODY, M. C., NUSBAUM, C., WIN, J., THINES, M. & KAMOUN, S. 2009. Ten things to know about oomycete effectors. *Mol Plant Pathol*, 10, 795-803.
- SCHORNACK, S., VAN DAMME, M., BOZKURT, T. O., CANO, L. A. M., SMOKER, M., THINES, M., GAULIN, E., KAMOUN, S. & HUITEMA, E. 2010. Ancient class of translocated oomycete effectors targets the host nucleus. *Proceedings of the National Academy of Sciences of the United States of America*, 107, 17421-17426.
- SCHULZE-LEFERT, P. & PANSTRUGA, R. 2003. Establishment of biotrophy by parasitic fungi and reprogramming of host cells for disease resistance. *Annual Review of Phytopathology*, 41, 641-667.
- SCHULZE-LEFERT, P. & PANSTRUGA, R. 2011. A molecular evolutionary concept connecting nonhost resistance, pathogen host range, and pathogen speciation. *Trends in Plant Science*, 16, 117-125.
- SEEMÜLLER, E., DUNCAN, J. M., KENNEDY, D. M. & RIEDEL, M. 1986. *Phytophthora* sp. als Ursache einer Wurzelfäule an Himbeere. *Nachrichtenbl. Dtsch. Pflanzenschutz*, 38, 17-21.
- SEGRETIN, M. E., PAIS, M., FRANCESCHETTI, M., CHAPARRO-GARCIA, A., BOS, J. I., BANFIELD, M. J. & KAMOUN, S. 2014. Single amino acid mutations in the potato immune receptor R3a expand response to *Phytophthora* effectors. *Mol Plant Microbe Interact*, 27, 624-37.
- SESSO, H. D., GAZIANO, J. M., JENKINS, D. J. & BURING, J. E. 2007. Strawberry intake, lipids, C-reactive protein, and the risk of cardiovascular disease in women. *J Am Coll Nutr*, 26, 303-10.
- SEXTON, A. C. & HOWLETT, B. J. 2001. Green fluorescent protein as a reporter in the Brassica–*Leptosphaeria maculans* interaction. *Physiological and Molecular Plant Pathology*, 58, 13-21.
- SHAN, W., CAO, M., LEUNG, D. & TYLER, B. M. 2004. The Avr1b locus of *Phytophthora sojae* encodes an elicitor and a regulator required for avirulence on soybean plants carrying resistance gene Rps1b. *Mol Plant Microbe Interact*, 17, 394-403.
- SHANER, N. C., CAMPBELL, R. E., STEINBACH, P. A., GIEPMANS, B. N., PALMER, A. E. & TSIEN, R. Y. 2004. Improved monomeric red, orange and yellow fluorescent proteins derived from *Discosoma* sp. red fluorescent protein. *Nat Biotechnol*, 22, 1567-72.
- SHARMA, A. D., GILL, P. K. & SINGH, P. 2003. RNA isolation from plant tissues rich in polysaccharides. *Analytical Biochemistry*, 314, 319-321.
- SHEN, D., LIU, T., YE, W., LIU, L., LIU, P., WU, Y., WANG, Y. & DOU, D. 2013. Gene Duplication and Fragment Recombination Drive Functional Diversification of a Superfamily of Cytoplasmic Effectors in *Phytophthora sojae*. *PLOS ONE*, 8, e70036.
- SI-AMMOUR, A., MAUCH-MANI, B. & MAUCH, F. 2003. Quantification of induced resistance against *Phytophthora* species expressing GFP as a vital marker: β -aminobutyric acid but not BTH protects potato and Arabidopsis from infection. *Molecular Plant Pathology*, 4, 237-248.
- SILVA, O. C., SANTOS, H. A. A., DALLA PRIA, M. & MAY-DE MIO, L. L. 2011. Potassium phosphite for control of downy mildew of soybean. *Crop Protection*, 30, 598-604.
- SNODDERLY, D. M. 1995. Evidence for protection against age-related macular degeneration by carotenoids and antioxidant vitamins. *The American Journal of Clinical Nutrition*, 62, 1448S-1461S.

- SNODDERLY, D. M., HANDELMAN, G. J. & ADLER, A. J. 1991. Distribution of individual macular pigment carotenoids in central retina of macaque and squirrel monkeys. *Investigative Ophthalmology & Visual Science*, 32, 268-279.
- SONG, T., MA, Z., SHEN, D., LI, Q., LI, W., SU, L., YE, T., ZHANG, M., WANG, Y. & DOU, D. 2016. An Oomycete CRN Effector Reprograms Expression of Plant HSP Genes by Targeting their Promoters. *PLOS Pathogens*, 11, e1005348.
- SPENCER, J. P. E. 2010. The impact of fruit flavonoids on memory and cognition. *British Journal of Nutrition*, 104, S40-S47.
- SPERSCHNEIDER, J., DODDS, P. N., SINGH, K. B. & TAYLOR, J. M. 2018. ApoplastP: prediction of effectors and plant proteins in the apoplast using machine learning. *New Phytol*, 217, 1764-1778.
- STAM, R., JUPE, J., HOWDEN, A. J. M., MORRIS, J. A., BOEVINK, P. C., HEDLEY, P. E. & HUITEMA, E. 2013. Identification and Characterisation CRN Effectors in *Phytophthora capsici* Shows Modularity and Functional Diversity. *PLOS ONE*, 8, e59517.
- STEWART, J. E., KROESE, D., TABIMA, J. F., LARSEN, M. M., FIELAND, V. J., PRESS, C. M., ZASADA, I. A. & GRÜNWARD, N. J. 2014. Pathogenicity, fungicide resistance, and genetic variability of *Phytophthora rubi* isolates from raspberry (*Rubus idaeus*) in the western United States. *Plant Disease*, 98, 1702-1708.
- STONER, G. D. & MUKHTAR, H. 1995. Polyphenols as cancer chemopreventive agents. *Journal of Cellular Biochemistry*, 59, 169-180.
- TABIMA, J. F., COFFEY, M. D., ZASADA, I. A. & GRUNWALD, N. J. 2018. Populations of *Phytophthora rubi* Show Little Differentiation and High Rates of Migration Among States in the Western United States. *Mol Plant Microbe Interact*, 31, 614-622.
- TABIMA, J. F., KRONMILLER, B. A., PRESS, C. M., TYLER, B. M., ZASADA, I. A. & GRUNWALD, N. J. 2017. Whole Genome Sequences of the Raspberry and Strawberry Pathogens *Phytophthora rubi* and *P. fragariae*. *Mol Plant Microbe Interact*, 30, 767-769.
- TAKANORI, T. 2012. Dietary anthocyanin-rich plants: Biochemical basis and recent progress in health benefits studies. *Molecular Nutrition & Food Research*, 56, 159-170.
- TAYLOR, F. J. R. 1978. Problems in the development of an explicit hypothetical phylogeny of the lower eukaryotes. *Biosystems*, 10, 67-89.
- THILLIEZ, G. J. A., ARMSTRONG, M. R., LIM, T.-Y., BAKER, K., JOUET, A., WARD, B., VAN OOSTERHOUT, C., JONES, J. D. G., HUITEMA, E., BIRCH, P. R. J. & HEIN, I. 2019. Pathogen enrichment sequencing (PenSeq) enables population genomic studies in oomycetes. *New Phytologist*, 221, 1634-1648.
- THOMASSET, S., BERRY, D. P., CAI, H., WEST, K., MARCZYLO, T. H., MARSDEN, D., BROWN, K., DENNISON, A., GARCEA, G., MILLER, A., HEMINGWAY, D., STEWARD, W. P. & GESCHER, A. J. 2009. Pilot Study of Oral Anthocyanins for Colorectal Cancer Chemoprevention. *Cancer Prevention Research*, 2, 625-633.
- TIAN, M., BENEDETTI, B. & KAMOUN, S. 2005. A second Kazal-like protease inhibitor from *Phytophthora infestans* inhibits and interacts with the apoplastic pathogenesis-related protease P69B of tomato. *Plant Physiology*, 138, 1785-1793.
- TIAN, M., HUITEMA, E., DA CUNHA, L., TORTO-ALALIBO, T. & KAMOUN, S. 2004. A Kazal-like extracellular serine protease inhibitor from *Phytophthora infestans* targets the tomato pathogenesis-related protease P69B. *J Biol Chem*, 279, 26370-7.
- TIAN, M., WIN, J., SONG, J., VAN DER HOORN, R., VAN DER KNAAP, E. & KAMOUN, S. 2007. A *Phytophthora infestans* cystatin-like protein targets a novel tomato papain-like apoplastic protease. *Plant Physiology*, 143, 364-377.
- TILMAN, D., BALZER, C., HILL, J. & BEFORT, B. L. 2011. Global food demand and the sustainable intensification of agriculture. *Proceedings of the National Academy of Sciences*, 108, 20260-20264.

- TÖFOLI, J., DOMINGUES, R., JR, W. & TORTOLO, M. 2016. Ametoctradin: a new fungicide for potato late blight control. *Arquivos do Instituto Biológico*, 83.
- TOLLEFSON, J. 2020. How hot will Earth get by 2100? *Nature*, News feature
- TOQUIN, V., BARJA, F., SIRVEN, C. & BFFA, R. 2007. Fluopicolide, a new Anti-oomycetes Fungicide with a New Mode of Action inducing Perturbation of a Spectrin-like Protein. *Modern Crop Protection Compounds*.
- TORTO, T. A., LI, S., STYER, A., HUITEMA, E., TESTA, A., GOW, N. A. R., VAN WEST, P. & KAMOUN, S. 2003. EST mining and functional expression assays identify extracellular effector proteins from the plant pathogen *Phytophthora*. *Genome Research*, 13, 1675-1685.
- TOULIATOS, D., DODD, I. C. & MCAINSH, M. 2016. Vertical farming increases lettuce yield per unit area compared to conventional horizontal hydroponics. *Food and energy security*, 5, 184-191.
- TREFTZ, C. & OMAYE, S. T. 2015. Comparison between hydroponic- and soil-grown raspberries (*Rubus idaeus*): viability and sensory traits. *Food and Nutrition Sciences*, 6, 1533-1540.
- TULIPANI, S., ALVAREZ-SUAREZ, J. M., BUSCO, F., BOMPADRE, S., QUILES, J. L., MEZZETTI, B. & BATTINO, M. 2011. Strawberry consumption improves plasma antioxidant status and erythrocyte resistance to oxidative haemolysis in humans. *Food Chem*, 128, 180-6.
- UKRI-NERC, N. E. R. C. 2016. Agriculture and Forestry Climate Change Impacts. *Report Card 2016*.
- VALLAD, G. E. & SUBBARAO, K. V. 2008. Colonization of Resistant and Susceptible Lettuce Cultivars by a Green Fluorescent Protein-Tagged Isolate of *Verticillium dahliae*. *Phytopathology*[®], 98, 871-885.
- VAN DAMME, M., BOZKURT, T. O., CAKIR, C., SCHORNACK, S., SKLENAR, J., JONES, A. M. E. & KAMOUN, S. 2012. The Irish Potato Famine Pathogen *Phytophthora infestans* Translocates the CRN8 Kinase into Host Plant Cells. *PLOS Pathogens*, 8, e1002875.
- VAN DE WEG, W. E. 1997. Gene-for-gene relationships between strawberry and the causal agent of red stele root rot, *Phytophthora fragariae* var. *fragariae*. *PhD thesis, University of Wageningen, The Netherlands*, 93 p
- VAN DEN BERG, N., CHRISTIE, J. B., AVELING, T. A. S. & ENGELBRECHT, J. 2018. Callose and β -1,3-glucanase inhibit *Phytophthora cinnamomi* in a resistant avocado rootstock. *Plant Pathology*, 67, 1150-1160.
- VAN DER LEE, T., TESTA, A., VAN 'T KLOOSTER, J., VAN DEN BERG-VELTHUIS, G. & GOVERS, F. 2001. Chromosomal deletion in isolates of *Phytophthora infestans* correlates with virulence on R3, R10, and R11 potato lines. *Mol Plant Microbe Interact*, 14, 1444-52.
- VAN GELDEREN, K., KANG, C. & PIERIK, R. 2018. Light Signaling, Root Development, and Plasticity. *Plant physiology*, 176, 1049-1060.
- VAN POPPEL, P. M., GUO, J., VAN DE VONDERVOORT, P. J., JUNG, M. W., BIRCH, P. R., WHISSON, S. C. & GOVERS, F. 2008. The *Phytophthora infestans* avirulence gene *Avr4* encodes an RXLR-dEER effector. *Mol Plant Microbe Interact*, 21, 1460-70.
- VAN WEST, P. 1999. Green fluorescent protein (GFP) as a reporter gene for the plant pathogenic oomycete *Phytophthora palmivora*. *FEMS Microbiology Letters*, 178, 71-80.
- VAN WEST, P. 2006. *Saprolegnia parasitica*, an oomycete pathogen with a fishy appetite: new challenges for an old problem. *Mycologist*, 20, 99-104.
- VANNINI, A. & VETTRAINO, A. 2011. *Phytophthora cambivora*. *Forest Phytophthoras*, 1.
- VAWDREY, L., GRICE, K., PETERSON, R. A. & DEFAVERI, J. 2004. The use of metalaxyl and potassium phosphonate, mounds, and organic and plastic mulches, for the management of *Phytophthora* root rot of papaya in far northern Queensland. *Australasian Plant Pathology - AUSTRALAS PLANT PATHOL*, 33.
- VISSER, M., GORDON, T. R., WINGFIELD, B. D., WINGFIELD, M. J. & VILJOEN, A. 2004. Transformation of *Fusarium oxysporum* f. sp. *cubense*, causal agent of *Fusarium* wilt of banana, with the green fluorescent protein (GFP) gene. *Australasian Plant Pathology*, 33, 69-75.
- VLEESHOUWERS, V. G. A. A., RAFFAELE, S., VOSSEN, J. H., CHAMPOURET, N., OLIVA, R., SEGRETIN, M. E., RIETMAN, H., CANO, L. M., LOKOSSOU, A., KESSEL, G., PEL, M. A. & KAMOUN, S. 2011.

- Understanding and Exploiting Late Blight Resistance in the Age of Effectors. *Annual Review of Phytopathology*, 49, 507-531.
- VLEESHOUWERS, V. G. A. A., RIETMAN, H., KRENEK, P., CHAMPOURET, N., YOUNG, C., OH, S.-K., WANG, M., BOUWMEESTER, K., VOSMAN, B., VISSER, R. G. F., JACOBSEN, E., GOVERS, F., KAMOUN, S. & VAN DER VOSSEN, E. A. G. 2008. Effector genomics accelerates discovery and functional profiling of potato disease resistance and phytophthora infestans avirulence genes. *PLoS one*, 3, e2875-e2875.
- VOINNET, O., RIVAS, S., MESTRE, P. & BAULCOMBE, D. 2003. An enhanced transient expression system in plants based on suppression of gene silencing by the p19 protein of tomato bushy stunt virus. *Plant J*, 33, 949-56.
- WALADKHANI, A. & CLEMENS, M. 1998. Effect of dietary phytochemicals on cancer development (review). *International Journal of Molecular Medicine*, 1, 747-800.
- WALLACE, T. C. 2011. Anthocyanins in cardiovascular disease. *Adv Nutr*, 2, 1-7.
- WANG, H., CHEN, Y., WU, X., LONG, Z., SUN, C., WANG, H., WANG, S., BIRCH, P. & TIAN, Z. 2018. A potato STRUBBELIG-RECEPTOR FAMILY member, StLRPK1, associates with StSERK3/BAK1 and activates immunity. *Journal of experimental botany*, 69.
- WANG, S., BOEVINK, P. C., WELSH, L., ZHANG, R., WHISSON, S. C. & BIRCH, P. R. J. 2017. Delivery of cytoplasmic and apoplastic effectors from *Phytophthora infestans* haustoria by distinct secretion pathways. *New Phytol*, 216, 205-215.
- WANG, S., MCLELLAN, H., BUKHAROVA, T., HE, Q., MURPHY, F., SHI, J., SUN, S., VAN WEYMERS, P., REN, Y., THILLIEZ, G., WANG, H., CHEN, X., ENGELHARDT, S., VLEESHOUWERS, V., GILROY, E. M., WHISSON, S. C., HEIN, I., WANG, X., TIAN, Z., BIRCH, P. R. J. & BOEVINK, P. C. 2019a. *Phytophthora infestans* RXLR effectors act in concert at diverse subcellular locations to enhance host colonization. *Journal of Experimental Botany*, 70, 343-356.
- WANG, W., XUE, Z., MIAO, J., CAI, M., ZHANG, C., LI, T., ZHANG, B., TYLER, B. M. & LIU, X. 2019b. PcMuORP1, an Oxathiapiprolin-Resistance Gene, Functions as a Novel Selection Marker for *Phytophthora* Transformation and CRISPR/Cas9 Mediated Genome Editing. *Frontiers in microbiology*, 10, 2402-2402.
- WASHINGTON, W. S. 1988. *Phytophthora cryptogea* as a cause of root rot of raspberry cultivars and control with fungicides. *Plant Pathology*, 37.
- WATERHOUSE, G. M. 1931. The production of conidia in the genus *Phytophthora*. *Transactions of the British Mycological Society*.
- WATERHOUSE, G. M. 1956. *The genus Phytophthora, Diagnoses (or descriptions) and Figures from the Original Papers*.
- WATERHOUSE, G. M. 1963. Key to the species of *Phytophthora* de Bary. *Mycological Papers*, 92, 1-22.
- WATERHOUSE, G. M. & BACKWELL, E. M. 1954. Key to the species of *Phytophthora* recorded in the British Isles. *Mycological papers*, 57.
- WATERSON, J. M. 1937. A note on the association of a species of *Phytophthora* with a 'dieback' disease of the raspberry. *Transactions of the Royal Society of Edinburgh*, 32, 251-259.
- WEDGWOOD, E. & WOODHALL, J. 2013. *Phytophthora rubi* research, AHDB Projects SF 123: Efficacy of novel products and SF 130: Detection and quantification.
- WEILAND, J. E., BENEDICT, C., ZASADA, I. A., SCAGEL, C. R., BECK, B. R., DAVIS, A., GRAHAM, K., PEETZ, A., MARTIN, R. R., DUNG, J. K., REYES GAIGE, A. & THIESSEN, L. 2018. Late-summer disease symptoms in Western Washington red raspberry fields associated with co-occurrence of *Phytophthora rubi*, *Verticillium dahliae*, and *Pratylenchus penetrans*, but not Raspberry bushy dwarf virus. *Plant Disease*, 102, 938-947.
- WHISSON, S. C., BOEVINK, P. C., MOLELEKI, L., AVROVA, A. O., MORALES, J. G., GILROY, E. M., ARMSTRONG, M. R., GROUFFAUD, S., VAN WEST, P., CHAPMAN, S., HEIN, I., TOTH, I. K., PRITCHARD, L. & BIRCH, P. R. 2007. A translocation signal for delivery of oomycete effector proteins into host plant cells. *Nature*, 450, 115-8.

- WHISSON, S. C., BOEVINK, P. C., WANG, S. & BIRCH, P. R. J. 2016. The cell biology of late blight disease. *Current Opinion in Microbiology*, 34, 127-135.
- WILCOX, W. F. 1989. Identity, virulence, and isolation frequency of seven *Phytophthora* spp. causing root rot of red raspberry in New York. *Phytopathology*, 79, 93-101.
- WILCOX, W. F. 1991. *Phytophthora* root rot. In: ELLIS, M. A., CONVERSE, R. H., WILLIAMS, R. N. & WILLIAMSON, B. (eds.) *Compendium of Raspberry and Blackberry Diseases and Insects*. St Paul, MN: American Phytopathological Society.
- WILCOX, W. F. & LATORRE, B. A. 2002. Identities and geographic distributions of *Phytophthora* spp. causing root rot of red raspberry in Chile. *Plant Disease*, 86, 1357-1362.
- WILCOX, W. F., PRITTS, M. P. & KELLY, M. J. 1999. Integrated control of *Phytophthora* root rot of red raspberry. *Plant Disease*, 83, 1149-1154.
- WILCOX, W. F., SCOTT, P. H., HAMM, P. B., KENNEDY, D. M., DUNCAN, J. M., BRASIER, C. M. & HANSEN, E. M. 1993. Identity of a *Phytophthora* species attacking raspberry in Europe and North America. *Mycological Research*, 97, 817-831.
- WIN, J., MORGAN, W., BOS, J., KRASILEVA, K. V., CANO, L. M., CHAPARRO-GARCIA, A., AMMAR, R., STASKAWICZ, B. J. & KAMOUN, S. 2007. Adaptive evolution has targeted the C-terminal domain of the RXLR effectors of plant pathogenic oomycetes. *Plant Cell*, 19, 2349-69.
- WINER, J., JUNG, C. K., SHACKEL, I. & WILLIAMS, P. M. 1999. Development and validation of real-time quantitative reverse transcriptase-polymerase chain reaction for monitoring gene expression in cardiac myocytes in vitro. *Anal Biochem*, 270, 41-9.
- WU, J., XUE, Z., MIAO, J., ZHANG, F., GAO, X. & LIU, X. 2020. Sensitivity of Different Developmental Stages and Resistance Risk Assessment of *Phytophthora capsici* to Fluopicolide in China. *Frontiers in Microbiology*, 11.
- WWF 2017. Eating for 2 degrees: new and updated Livewell Plates. *Summary Report, revised edition*.
- XIANG, Y., HUANG, C.-H., HU, Y., WEN, J., LI, S., YI, T., CHEN, H., XIANG, J. & MA, H. 2016. Evolution of Rosaceae Fruit Types Based on Nuclear Phylogeny in the Context of Geological Times and Genome Duplication. *Molecular biology and evolution*, 34.
- XU, Y., LIANG, Y. & YANG, M. 2019. Effects of Composite LED Light on Root Growth and Antioxidant Capacity of *Cunninghamia lanceolata* Tissue Culture Seedlings. *Scientific Reports*, 9, 9766.
- YANG, X., TYLER, B. M. & HONG, C. 2017. An expanded phylogeny for the genus *Phytophthora*. *IMA Fungus*, 8, 355-384.
- YIN, W., DONG, S., ZHAI, L., LIN, Y., ZHENG, X. & WANG, Y. 2013. The *Phytophthora sojae* Avr1d Gene Encodes an RxLR-dEER Effector with Presence and Absence Polymorphisms Among Pathogen Strains. *Molecular Plant-Microbe Interactions*®, 26, 958-968.
- YOSHIDA, K., SCHUENEMANN, V. J., CANO, L. M., PAIS, M., MISHRA, B., SHARMA, R., LANZ, C., MARTIN, F. N., KAMOUN, S., KRAUSE, J., THINES, M., WEIGEL, D. & BURBANO, H. A. 2013. The rise and fall of the *Phytophthora infestans* lineage that triggered the Irish potato famine. *eLife*, 2, e00731.
- YU, C., KARLIN, D. G., LU, Y., WRIGHT, K., CHEN, J. & MACFARLANE, S. 2013. Experimental and bioinformatic evidence that raspberry leaf blotch emaravirus P4 is a movement protein of the 30K superfamily. *Journal of General Virology*, 94, 2117-2128.
- YU, D., TANG, H., ZHANG, Y., DU, Z., YU, H. & CHEN, Q. 2012a. Comparison and Improvement of Different Methods of RNA Isolation from Strawberry (*Fragria × ananassa*). *Journal of Agricultural Science*, 4.
- YU, J., LIU, W., LIU, J., QIN, P. & XU, L. 2017. Auxin Control of Root Organogenesis from Callus in Tissue Culture. *Frontiers in Plant Science*, 8.
- YU, X., TANG, J., WANG, Q., YE, W., TAO, K., DUAN, S., LU, C., YANG, X., DONG, S., ZHENG, X. & WANG, Y. 2012b. The RxLR effector Avh241 from *Phytophthora sojae* requires plasma membrane localization to induce plant cell death. *New Phytologist*, 196, 247-260.
- ZENTMYER, G. A. 1965. Bacterial Stimulation of Sporangium Production in *Phytophthora cinnamomi*. *Science*, 150, 1178-1179.

- ZHANG, D., BURROUGHS, A. M., VIDAL, N. D., IYER, L. M. & ARAVIND, L. 2016. Transposons to toxins: the provenance, architecture and diversification of a widespread class of eukaryotic effectors. *Nucleic Acids Research*, 44, 3513-3533.
- ZHANG, M., LI, Q., LIU, T., LIU, L., SHEN, D., ZHU, Y., LIU, P., ZHOU, J.-M. & DOU, D. 2015. Two Cytoplasmic Effectors of *Phytophthora sojae* Regulate Plant Cell Death via Interactions with Plant Catalases. *Plant Physiology*, 167, 164.
- ZHANG, S.-D., JIN, J.-J., CHEN, S.-Y., CHASE, M. W., SOLTIS, D. E., LI, H.-T., YANG, J.-B., LI, D.-Z. & YI, T.-S. 2017. Diversification of Rosaceae since the Late Cretaceous based on plastid phylogenomics. *New Phytologist*, 214, 1355-1367.
- ZHANG, W., GU, X., ZHONG, W., MA, Z. & DING, X. 2020. Review of transparent soil model testing technique for underground construction: Ground visualization and result digitalization. *Underground Space*.
- ZHAO, L., ZHANG, X., ZHANG, X., SONG, W., LI, X., FENG, R., YANG, C., HUANG, Z. & ZHU, C. 2018. Crystal structure of the RxLR effector PcRxLR12 from *Phytophthora capsici*. *Biochem Biophys Res Commun*, 503, 1830-1835.
- ZHAO, Y., THILMONEY, R., BENDER, C. L., SCHALLER, A., HE, S. Y. & HOWE, G. A. 2003. Virulence systems of *Pseudomonas syringae* pv. tomato promote bacterial speck disease in tomato by targeting the jasmonate signaling pathway. *The Plant Journal*, 36, 485-499.
- ZHOU, Y., ZHOU, H., LIN-WANG, K., VIMOLMANGKANG, S., ESPEY, R. V., WANG, L., ALLAN, A. C. & HAN, Y. 2014. Transcriptome analysis and transient transformation suggest an ancient duplicated MYB transcription factor as a candidate gene for leaf red coloration in peach. *BMC Plant Biology*, 14, 388.
- ZHU, G.-N., HUANG, F.-X., FENG, L.-X., QIN, B.-X., YANG, Y.-H., CHEN, Y.-H. & LU, X.-H. 2008. Sensitivities of *Phytophthora infestans* to Metalaxyl, Cymoxanil, and Dimethomorph. *Agricultural Sciences in China*, 7, 831-840.
- ZHU, S., LI, Y., VOSSEN, J. H., VISSER, R. G. F. & JACOBSEN, E. 2012. Functional stacking of three resistance genes against *Phytophthora infestans* in potato. *Transgenic Research*, 21, 89-99.
- ZHU, Y., CHEN, H., FAN, J., WANG, Y., LI, Y., CHEN, J., FAN, J., YANG, S., HU, L., LEUNG, H., MEW, T. W., TENG, P. S., WANG, Z. & MUNDT, C. C. 2000. Genetic diversity and disease control in rice. *Nature*, 406, 718.

APPENDICES

Appendix A. PHENOTYPIC STUDIES OF *P. RUBI* AND *P. FRAGARIAE*: ASSESSING RESPONSES TO AGRICULTURALLY IMPORTANT FACTORS – Chapter 2

Table A. 1. Molarity (in μM , in bold) of the different chemical used at several doses in the screening assay

Chemical	Formula	Atomic Weight (g/mol)	ppm			
			0.1	1	10	100
Fluazinam	C ₁₃ H ₄ Cl ₂ F ₆ N ₄ O ₄	464.9	0.24	2.37	21.51	215.10
Fluopicolide	C ₁₄ H ₈ Cl ₃ F ₃ N ₂ O	383.35	0.29	2.87	26.09	260.86
Propamocarb	C ₉ H ₂₀ N ₂ O ₂	188	0.59	5.85	53.19	531.91
Ametoctradin	C ₁₅ H ₂₅ N ₅	275	0.40	4.00	36.36	363.64
Phosphite	H ₂ PO ₃ ⁻	80.97	1.36	13.59	123.50	1235.03
Dimethomorph	C ₂₁ H ₂₂ ClNO ₄	387.45	0.28	2.84	25.81	258.10
Metalaxyl-M	C ₁₅ H ₂₁ NO ₄	279	0.39	3.94	35.84	358.42

Table A. 2. Compost mix used for sporulation soil solution, ordered from ICL (Gretna, Scotland)

Peat	1.2 m ³
Sand	100 L
Osmocote Exact Start	1.5 kg
Osmocote Exact Mini/3-4 month/10-12 month	3.5 kg
Lime Ca and Mg	2.5 kg
ZEBA	0.5 kg
Perlite	100 L
Intercept/Exemptor	280 g / 390 g

**Appendix B. *P. RUBI* AND *P. FRAGARIAE* EFFECTOR GENES DIVERSITY
STUDIED THROUGH PENSEQ – Chapter 3**

Table B.1. Numbers and proportion of read counts and mapped reads at several Bowtie mismatch mapping rates (0 %, 3 % and 5 %) for *P. rubi* and *P. fragariae* isolates mapped to same-species reference genomes.

Species	Isolate	Reads count	Reference mapped to	Bowtie mismatch mapping rate	Total reads mapped	Percentage of reads mapped
<i>P. rubi</i>	SCRP1208	874620	<i>P. rubi</i> SCR333	0	505104	57.75
<i>P. rubi</i>	SCRP1208	874620		3	787600	90.05
<i>P. rubi</i>	SCRP1208	874620		5	806453	92.21
<i>P. rubi</i>	SCRP1213	1131707		0	756624	66.86
<i>P. rubi</i>	SCRP1213	1131707		3	1017021	89.87
<i>P. rubi</i>	SCRP1213	1131707		5	1038063	91.73
<i>P. rubi</i>	SCRP1202	1121686		0	767144	68.39
<i>P. rubi</i>	SCRP1202	1121686		3	1016184	90.59
<i>P. rubi</i>	SCRP1202	1121686		5	1037037	92.45
<i>P. rubi</i>	SCRP249	1499947		0	912265	60.82
<i>P. rubi</i>	SCRP249	1499947		3	1327752	88.52
<i>P. rubi</i>	SCRP249	1499947		5	1361592	90.78
<i>P. rubi</i>	SCRP296	1117692		0	686270	61.40
<i>P. rubi</i>	SCRP296	1117692		3	995634	89.08
<i>P. rubi</i>	SCRP296	1117692		5	1020467	91.30
<i>P. rubi</i>	SCRP324	1021039		0	597245	58.49
<i>P. rubi</i>	SCRP324	1021039		3	910019	89.13
<i>P. rubi</i>	SCRP324	1021039		5	933517	91.43
<i>P. rubi</i>	SCRP333	1095654		0	762182	69.56
<i>P. rubi</i>	SCRP333	1095654		3	991193	90.47
<i>P. rubi</i>	SCRP333	1095654		5	1010260	92.21
<i>P. rubi</i>	SCRP339	1481653		0	1015305	68.53
<i>P. rubi</i>	SCRP339	1481653		3	1334224	90.05
<i>P. rubi</i>	SCRP339	1481653		5	1359914	91.78
<i>P. rubi</i>	SCRP1207	928357		0	503917	54.28
<i>P. rubi</i>	SCRP1207	928357		3	847131	91.25
<i>P. rubi</i>	SCRP1207	928357		5	869700	93.68
<i>P. rubi</i>	SCRP1212	1236866		0	796669	64.41
<i>P. rubi</i>	SCRP1212	1236866		3	1142551	92.37
<i>P. rubi</i>	SCRP1212	1236866		5	1168077	94.44
<i>P. rubi</i>	SCRP250	839966	0	475379	56.60	
<i>P. rubi</i>	SCRP250	839966	3	767259	91.34	
<i>P. rubi</i>	SCRP250	839966	5	788373	93.86	
<i>P. rubi</i>	SCRP260	1385768	0	758351	54.72	

Species	Isolate	Reads count	Reference mapped to	Bowtie mismatch mapping rate	Total reads mapped	Percentage of reads mapped	
<i>P. rubi</i>	SCR260	1385768		3	1270648	91.69	
<i>P. rubi</i>	SCR260	1385768		5	1304895	94.16	
<i>P. rubi</i>	SCR283	1775713		0	956688	53.88	
<i>P. rubi</i>	SCR283	1775713		3	1617365	91.08	
<i>P. rubi</i>	SCR283	1775713		5	1665989	93.82	
<i>P. rubi</i>	SCR287	1504466		0	1026998	68.26	
<i>P. rubi</i>	SCR287	1504466		3	1403711	93.30	
<i>P. rubi</i>	SCR287	1504466		5	1431423	95.14	
<i>P. rubi</i>	SCR288	1267092		0	605760	47.81	
<i>P. rubi</i>	SCR288	1267092		3	945029	74.58	
<i>P. rubi</i>	SCR288	1267092		5	969783	76.54	
<i>P. rubi</i>	SCR290	1730989		0	1109867	64.12	
<i>P. rubi</i>	SCR290	1730989		3	1599166	92.38	
<i>P. rubi</i>	SCR290	1730989		5	1636251	94.53	
<i>P. rubi</i>	SCR292	1233448		0	634010	51.40	
<i>P. rubi</i>	SCR292	1233448		3	1108743	89.89	
<i>P. rubi</i>	SCR292	1233448		5	1142545	92.63	
<i>P. rubi</i>	SCR293	1078844		0	581353	53.89	
<i>P. rubi</i>	SCR293	1078844		3	984332	91.24	
<i>P. rubi</i>	SCR293	1078844		5	1011380	93.75	
<i>P. rubi</i>	SCR323	1339034		0	755759	56.44	
<i>P. rubi</i>	SCR323	1339034		3	1226477	91.59	
<i>P. rubi</i>	SCR323	1339034		5	1259995	94.10	
<i>P. rubi</i>	SCR338	1485901		0	790613	53.21	
<i>P. rubi</i>	SCR338	1485901		3	1348662	90.76	
<i>P. rubi</i>	SCR338	1485901		5	1388888	93.47	
<i>P. fragariae</i>	BC-16	1120168		<i>P. fragariae</i> BC-16	0	864193	77.15
<i>P. fragariae</i>	BC-16	1120168			3	1038335	92.69
<i>P. fragariae</i>	BC-16	1120168	5		1047243	93.49	
<i>P. fragariae</i>	BC-1	1182473	0		886729	74.99	
<i>P. fragariae</i>	BC-1	1182473	3		1077333	91.11	
<i>P. fragariae</i>	BC-1	1182473	5		1086799	91.91	
<i>P. fragariae</i>	NOV-9	865044	0		667024	77.11	
<i>P. fragariae</i>	NOV-9	865044	3		784500	90.69	
<i>P. fragariae</i>	NOV-9	865044	5		790774	91.41	
<i>P. fragariae</i>	SCR245	1103774	0		753190	68.24	
<i>P. fragariae</i>	SCR245	1103774	3		1017155	92.15	
<i>P. fragariae</i>	SCR245	1103774	5		1029044	93.23	

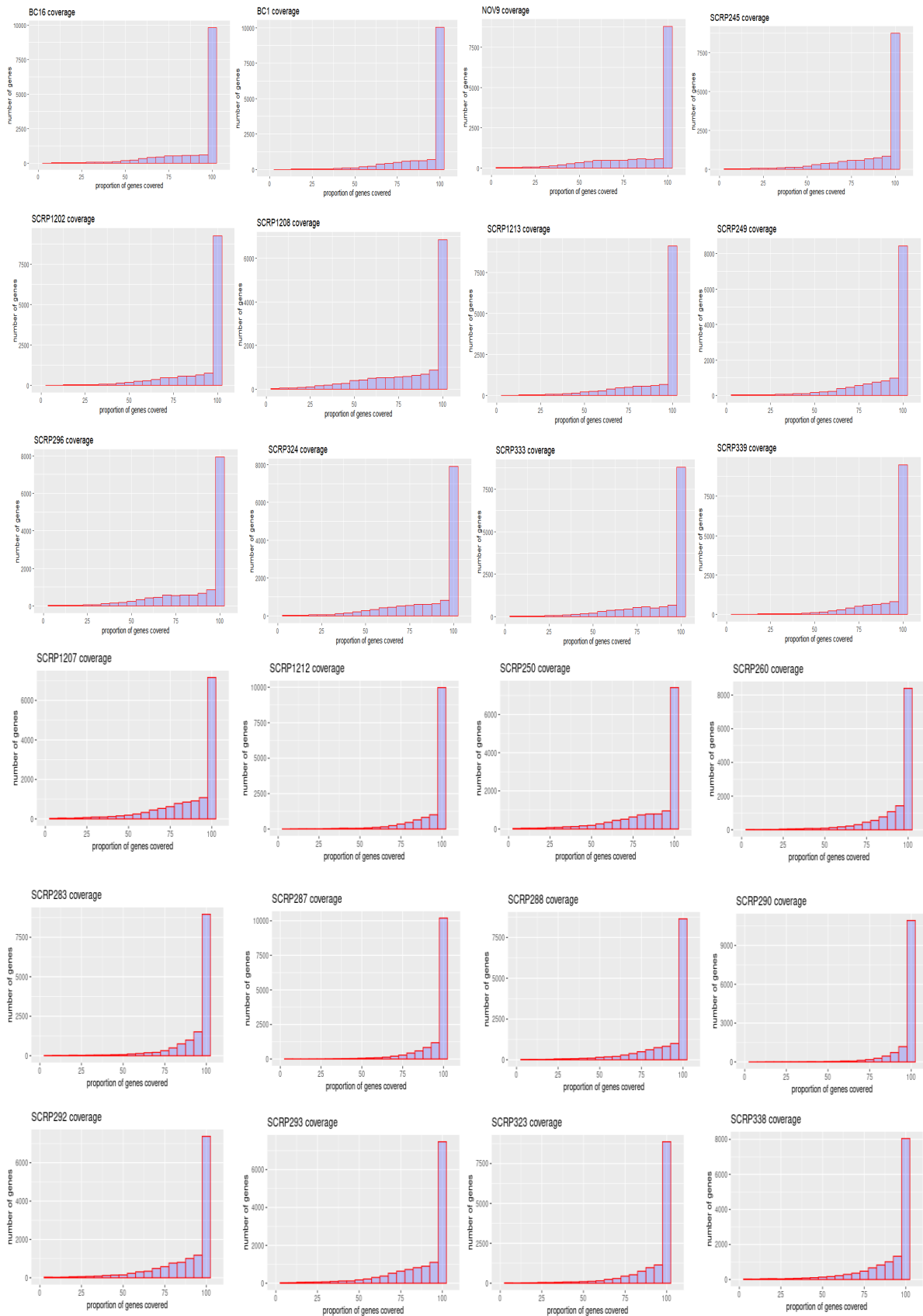


Figure B. 1. Coverage graphs for *P. rubi* and *P. fragariae* isolates from mapping at 0 % mismatch mapping rate. Number of genes covered are represented on the y-axis and proportion of gene covered (in percentage) is represented on the x-axis. Each graph corresponds to one isolate.

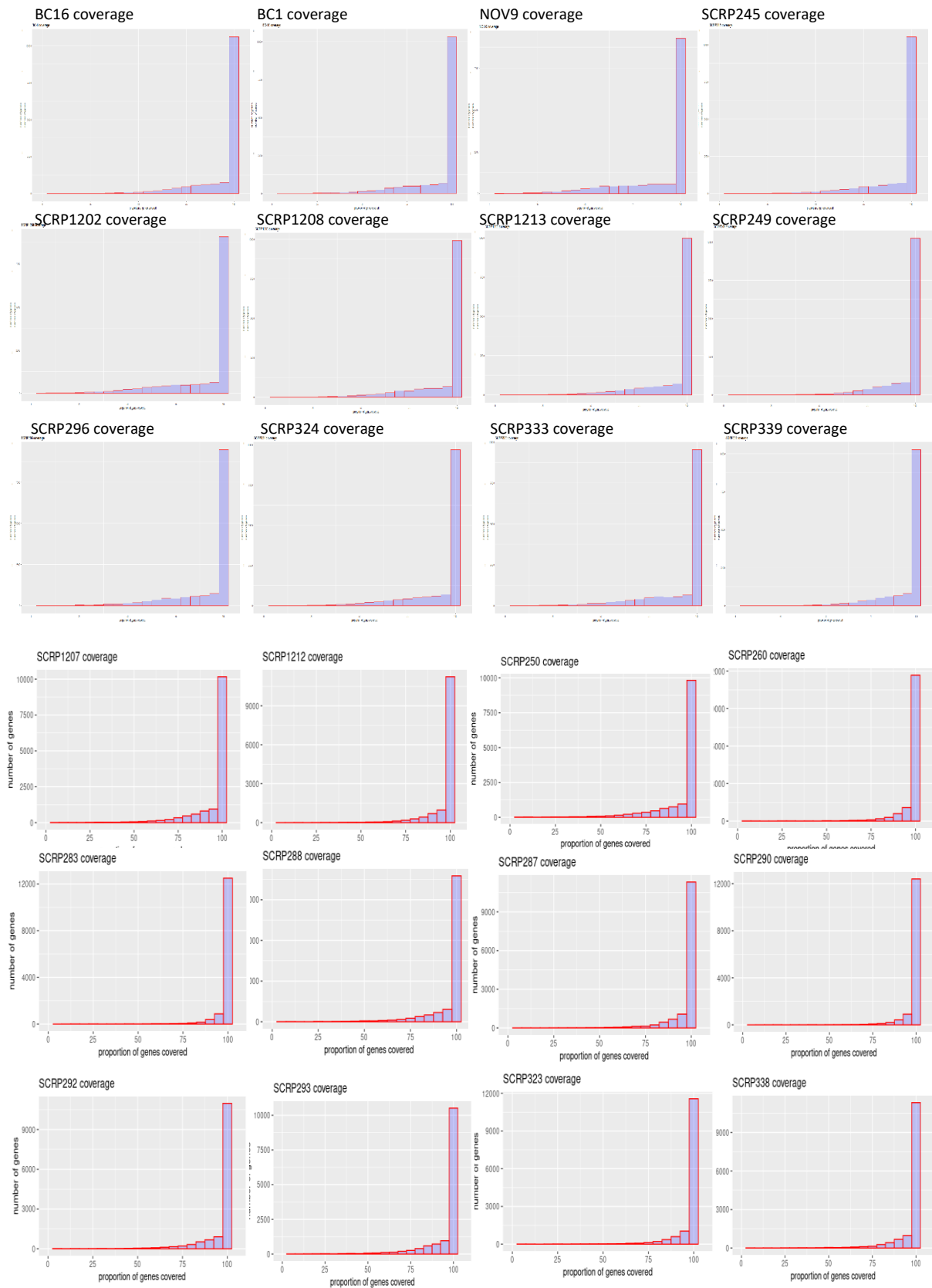


Figure B. 2. Coverage graphs for *P. rubi* and *P. fragariae* isolates from mapping at 3 % mismatch mapping rate. Number of genes covered are represented on the y-axis and proportion of gene covered (in percentage) is represented on the x-axis. Each graph corresponds to one isolate.

Table B. 2. Average coverage of *P. rubi* and *P. fragariae* isolates at 0 %, 3 % and 5 % mismatch mapping rates for the 14,295 and 14,958 enriched genes respectively.

Species	Isolate	Reference mapped to	Average Coverage		
			Bowtie mismatch mapping rate		
			0%	3%	5%
<i>P. rubi</i>	SCRP249	<i>P. rubi</i> SCR333	88.93	93.81	93.96
<i>P. rubi</i>	SCRP296		85.52	90.46	90.61
<i>P. rubi</i>	SCRP324		84.91	90.79	90.90
<i>P. rubi</i>	SCRP333		87.69	90.24	90.34
<i>P. rubi</i>	SCRP339		91.71	93.77	93.85
<i>P. rubi</i>	SCRP1202		90.05	92.28	92.35
<i>P. rubi</i>	SCRP1208		80.64	87.79	87.96
<i>P. rubi</i>	SCRP1213		89.23	91.80	91.89
<i>P. rubi</i>	SCRP250		84.77	92.44	92.79
<i>P. rubi</i>	SCRP260		90.06	96.97	97.22
<i>P. rubi</i>	SCRP283		91.74	98.02	98.19
<i>P. rubi</i>	SCRP287		94.67	96.71	96.82
<i>P. rubi</i>	SCRP288		89.04	94.71	94.96
<i>P. rubi</i>	SCRP290		95.93	98.21	98.32
<i>P. rubi</i>	SCRP292		86.01	95.24	95.54
<i>P. rubi</i>	SCRP293		85.93	94.40	94.70
<i>P. rubi</i>	SCRP323		90.40	96.73	96.94
<i>P. rubi</i>	SCRP338		88.72	96.20	96.49
<i>P. rubi</i>	SCRP1207		84.95	93.59	93.92
<i>P. rubi</i>	SCRP1212		93.47	96.24	96.38
<i>P. rubi</i>	averages		88.72	94.02	94.21
<i>P. fragariae</i>	BC-1	<i>P. fragariae</i> BC16	90.87	92.73	92.81
<i>P. fragariae</i>	BC-16		89.58	91.42	91.50
<i>P. fragariae</i>	NOV-9		85.32	87.15	87.23
<i>P. fragariae</i>	SCRP245		87.16	92.01	92.17
<i>P. fragariae</i>	averages		88.23	90.83	90.93

Table B. 3. Numbers and proportion of read counts and mapped reads at several Bowtie mismatch mapping rates (0 %, 3 % and 5 %) for *P. rubi* and *P. fragariae* isolates mapped to the other species reference genomes.

Species	Isolate	Reads count	Reference mapped to	Bowtie mismatch mapping rate	Total reads mapped	Percentage of reads mapped
<i>P. rubi</i>	SCRP1208	874620	<i>P. fragariae</i> BC-16	0	142237	16.26
<i>P. rubi</i>	SCRP1208	874620		3	622063	71.12
<i>P. rubi</i>	SCRP1208	874620		5	688027	78.67
<i>P. rubi</i>	SCRP1213	1131707		0	181954	16.08
<i>P. rubi</i>	SCRP1213	1131707		3	791736	69.96
<i>P. rubi</i>	SCRP1213	1131707		5	874463	77.27
<i>P. rubi</i>	SCRP1202	1121686		0	200767	17.9
<i>P. rubi</i>	SCRP1202	1121686		3	805737	71.83
<i>P. rubi</i>	SCRP1202	1121686		5	889843	79.33
<i>P. rubi</i>	SCRP249	1499947		0	260956	17.4
<i>P. rubi</i>	SCRP249	1499947		3	1046632	69.78
<i>P. rubi</i>	SCRP249	1499947		5	1155613	77.04
<i>P. rubi</i>	SCRP296	1117692		0	188395	16.86
<i>P. rubi</i>	SCRP296	1117692		3	782352	70
<i>P. rubi</i>	SCRP296	1117692		5	865190	77.41
<i>P. rubi</i>	SCRP324	1021039		0	164157	16.08
<i>P. rubi</i>	SCRP324	1021039		3	726117	71.12
<i>P. rubi</i>	SCRP324	1021039		5	802085	78.56
<i>P. rubi</i>	SCRP333	1095654		0	186389	17.01
<i>P. rubi</i>	SCRP333	1095654		3	776602	70.88
<i>P. rubi</i>	SCRP333	1095654		5	857883	78.3
<i>P. rubi</i>	SCRP339	1481653		0	256627	17.32
<i>P. rubi</i>	SCRP339	1481653		3	1050964	70.93
<i>P. rubi</i>	SCRP339	1481653		5	1161015	78.36
<i>P. rubi</i>	SCRP1207	928357		0	135756	14.62
<i>P. rubi</i>	SCRP1207	928357		3	663499	71.47
<i>P. rubi</i>	SCRP1207	928357		5	734686	79.16
<i>P. rubi</i>	SCRP1212	1236866		0	175389	14.18
<i>P. rubi</i>	SCRP1212	1236866		3	873295	70.61
<i>P. rubi</i>	SCRP1212	1236866		5	967002	78.18
<i>P. rubi</i>	SCRP250	839966		0	124474	14.82
<i>P. rubi</i>	SCRP250	839966		3	602271	71.7
<i>P. rubi</i>	SCRP250	839966		5	667224	79.43
<i>P. rubi</i>	SCRP260	1385768		0	201317	14.53
<i>P. rubi</i>	SCRP260	1385768		3	993523	71.69
<i>P. rubi</i>	SCRP260	1385768		5	1100420	79.41
<i>P. rubi</i>	SCRP283	1775713		0	274141	15.44
<i>P. rubi</i>	SCRP283	1775713		3	1287688	72.52
<i>P. rubi</i>	SCRP283	1775713		5	1425365	80.27
<i>P. rubi</i>	SCRP287	1504466		0	250621	16.66

Species	Isolate	Reads count	Reference mapped to	Bowtie mismatch mapping rate	Total reads mapped	Percentage of reads mapped
<i>P. rubi</i>	SCRP287	1504466		3	1092050	72.59
<i>P. rubi</i>	SCRP287	1504466		5	1206816	80.22
<i>P. rubi</i>	SCRP288	1267092		0	148967	11.76
<i>P. rubi</i>	SCRP288	1267092		3	748590	59.08
<i>P. rubi</i>	SCRP288	1267092		5	829547	65.47
<i>P. rubi</i>	SCRP290	1730989		0	274297	15.85
<i>P. rubi</i>	SCRP290	1730989		3	1235757	71.39
<i>P. rubi</i>	SCRP290	1730989		5	1367534	79
<i>P. rubi</i>	SCRP292	1233448		0	178275	14.45
<i>P. rubi</i>	SCRP292	1233448		3	865491	70.17
<i>P. rubi</i>	SCRP292	1233448		5	957854	77.66
<i>P. rubi</i>	SCRP293	1078844		0	154011	14.28
<i>P. rubi</i>	SCRP293	1078844		3	764630	70.87
<i>P. rubi</i>	SCRP293	1078844		5	846655	78.48
<i>P. rubi</i>	SCRP323	1339034		0	192437	14.37
<i>P. rubi</i>	SCRP323	1339034		3	966489	72.18
<i>P. rubi</i>	SCRP323	1339034		5	1070051	79.91
<i>P. rubi</i>	SCRP338	1485901		0	222000	14.94
<i>P. rubi</i>	SCRP338	1485901		3	1065981	71.74
<i>P. rubi</i>	SCRP338	1485901		5	1180676	79.46
<i>P. fragariae</i>	BC-16	1120168	<i>P. rubi</i> SCP333	0	176976	15.8
<i>P. fragariae</i>	BC-16	1120168		3	796997	71.15
<i>P. fragariae</i>	BC-16	1120168		5	890234	79.47
<i>P. fragariae</i>	BC-1	1182473		0	187769	15.88
<i>P. fragariae</i>	BC-1	1182473		3	827780	70
<i>P. fragariae</i>	BC-1	1182473		5	922444	78.01
<i>P. fragariae</i>	NOV-9	865044		0	155388	17.96
<i>P. fragariae</i>	NOV-9	865044		3	609741	70.49
<i>P. fragariae</i>	NOV-9	865044		5	678999	78.49
<i>P. fragariae</i>	SCRP245	1103774		0	162618	14.73
<i>P. fragariae</i>	SCRP245	1103774		3	777111	70.4
<i>P. fragariae</i>	SCRP245	1103774		5	869709	78.79

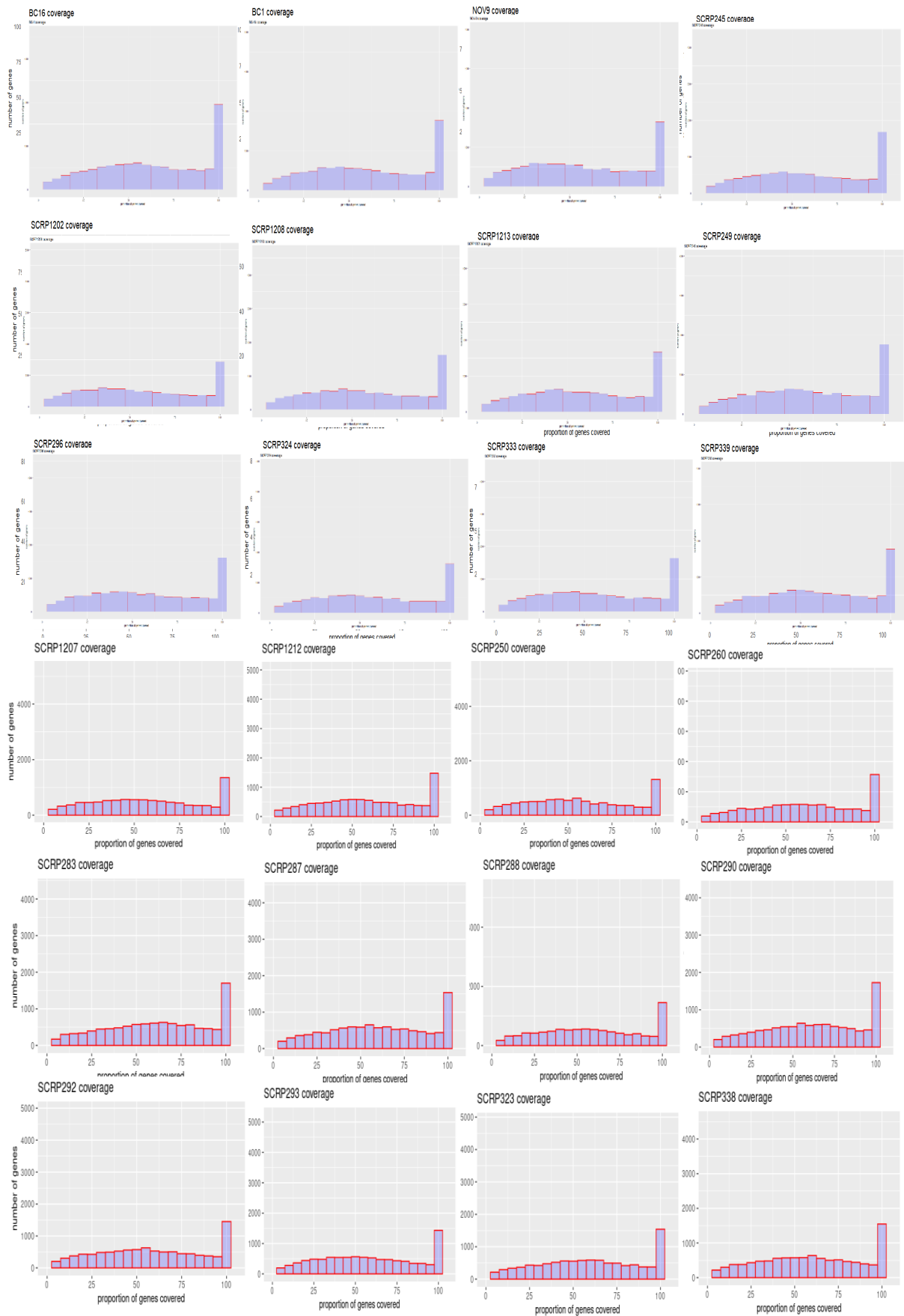


Figure B. 3. Coverage graphs for *P. rubi* and *P. fragariae* isolates from cross-species mapping at 0 % mismatch mapping rate. Number of genes covered are represented on the y-axis and proportion of gene covered (in percentage) is represented on the x-axis. Each graph corresponds to one isolate.

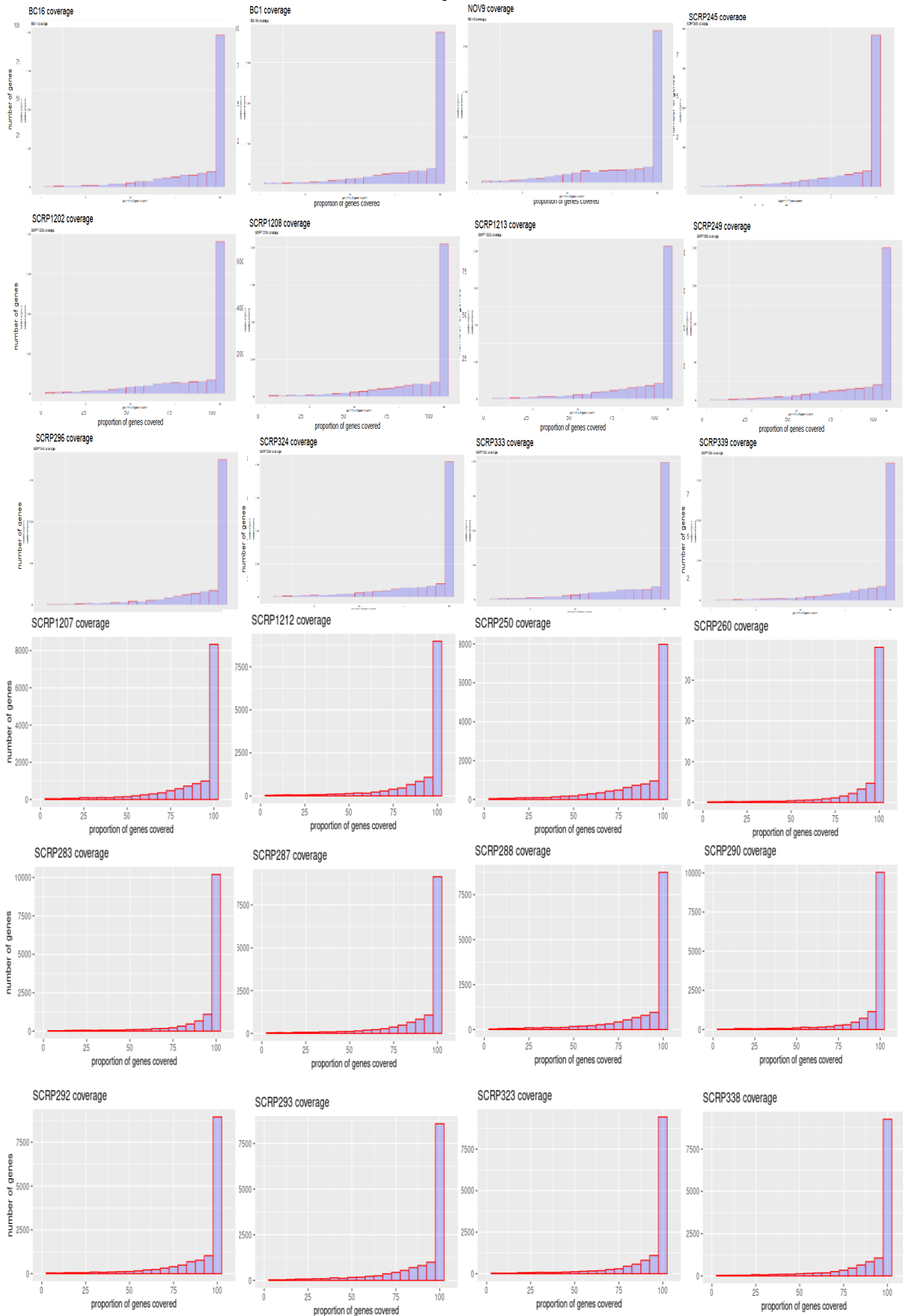


Figure B. 4. Coverage graphs for *P. rubi* and *P. fragariae* isolates from cross-species mapping at 3 % mismatch mapping rate. Number of genes covered are represented on the y-axis and proportion of gene covered (in percentage) is represented on the x-axis. Each graph corresponds to one isolate.

Table B.4. Average coverage of *P. rubi* and *P. fragariae* isolates at 0 %, 3 % and 5 % mismatch cross-species mapping rates for the 14,295 and 14,958 enriched genes respectively.

Species	Isolate	Reference mapped to	Average Coverage		
			Bowtie mismatch mapping rate		
			0%	3%	5%
<i>P. rubi</i>	SCRP249	<i>P. fragariae</i> BC16	44.29	85.17	89.20
<i>P. rubi</i>	SCRP296		40.70	81.69	85.86
<i>P. rubi</i>	SCRP324		39.38	81.77	86.01
<i>P. rubi</i>	SCRP333		40.81	80.78	84.88
<i>P. rubi</i>	SCRP339		43.99	84.33	88.41
<i>P. rubi</i>	SCRP1202		41.74	82.90	87.03
<i>P. rubi</i>	SCRP1208		37.48	79.07	83.32
<i>P. rubi</i>	SCRP1213		40.22	82.31	86.48
<i>P. rubi</i>	SCRP250		35.90	81.93	86.56
<i>P. rubi</i>	SCRP260		40.70	87.03	91.38
<i>P. rubi</i>	SCRP283		43.90	88.26	92.45
<i>P. rubi</i>	SCRP287		42.44	86.27	90.50
<i>P. rubi</i>	SCRP288		37.41	84.20	88.78
<i>P. rubi</i>	SCRP290		44.14	88.16	92.36
<i>P. rubi</i>	SCRP292		39.03	85.11	89.71
<i>P. rubi</i>	SCRP293		37.57	84.18	88.68
<i>P. rubi</i>	SCRP323		40.19	86.71	91.12
<i>P. rubi</i>	SCRP338		41.19	86.38	90.75
<i>P. rubi</i>	SCRP1207		36.79	83.49	41.03
<i>P. rubi</i>	SCRP1212	39.03	85.37	89.91	
<i>P. rubi</i>	averages		40.35	84.26	86.22
<i>P. fragariae</i>	BC16	<i>P. rubi</i> SCR333	43.30	81.42	85.45231
<i>P. fragariae</i>	BC1		46.43	83.39	87.24787
<i>P. fragariae</i>	NOV9		41.59	77.28	81.37201
<i>P. fragariae</i>	SCRP245		41.49	82.13	86.44214
<i>P. fragariae</i>	averages		43.21	81.05	85.12858

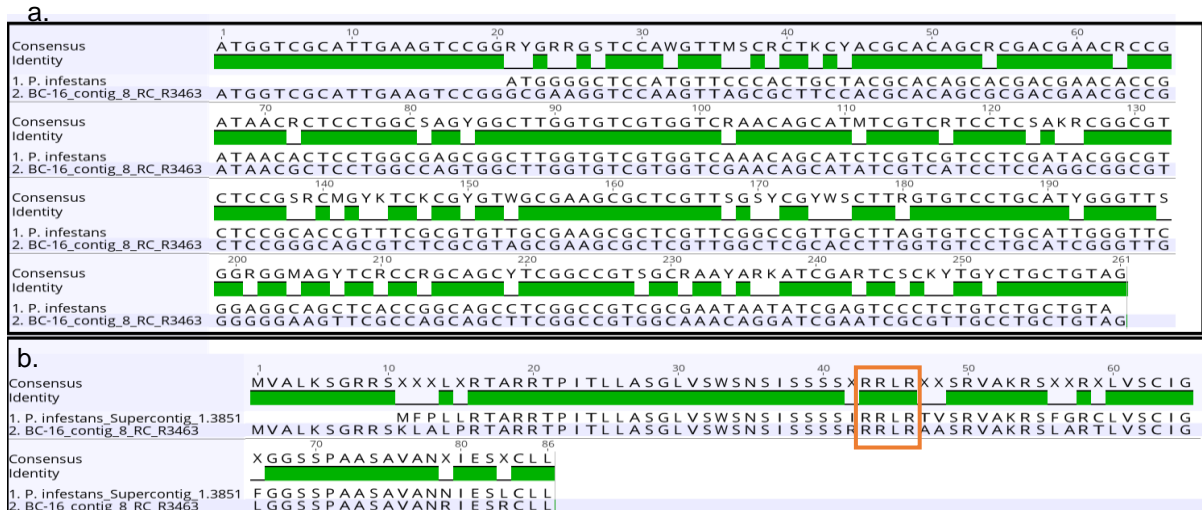


Figure B.5. Sequences alignment between RXLR BC-16_contig_8_RC_R3463 and matching *P. infestans* RXLR effector. a. Nucleotide alignment and b. protein alignment between RXLR BC-16_contig_8_RC_R3463 (Win et al., 2007) and *P. infestans* T30-4 (accession XP_002909763.1). Nucleotide alignment shows 77.1 % identity and protein alignment 83 % identity. RXLR motifs are highlighted in orange. Mapping and alignments performed with Geneious.

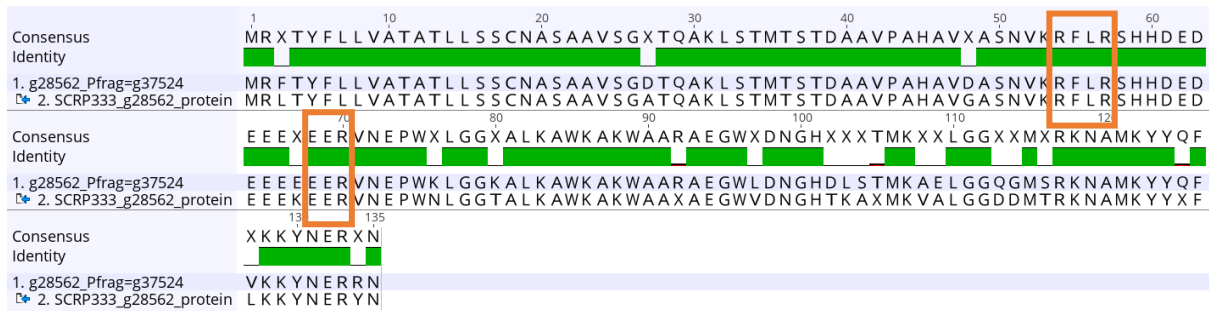


Figure B.6. Protein sequences alignment between *P. rubi* RXLR SCRP333_g28562 and matching RXLR effectors. Protein alignment for *P. rubi* SCRP333_g28562 and *P. fragariae* PF003_g37524. RXLR-EER motifs are highlighted in orange. Drawn with Geneious using sequences from BLASTx searches (NCBI).

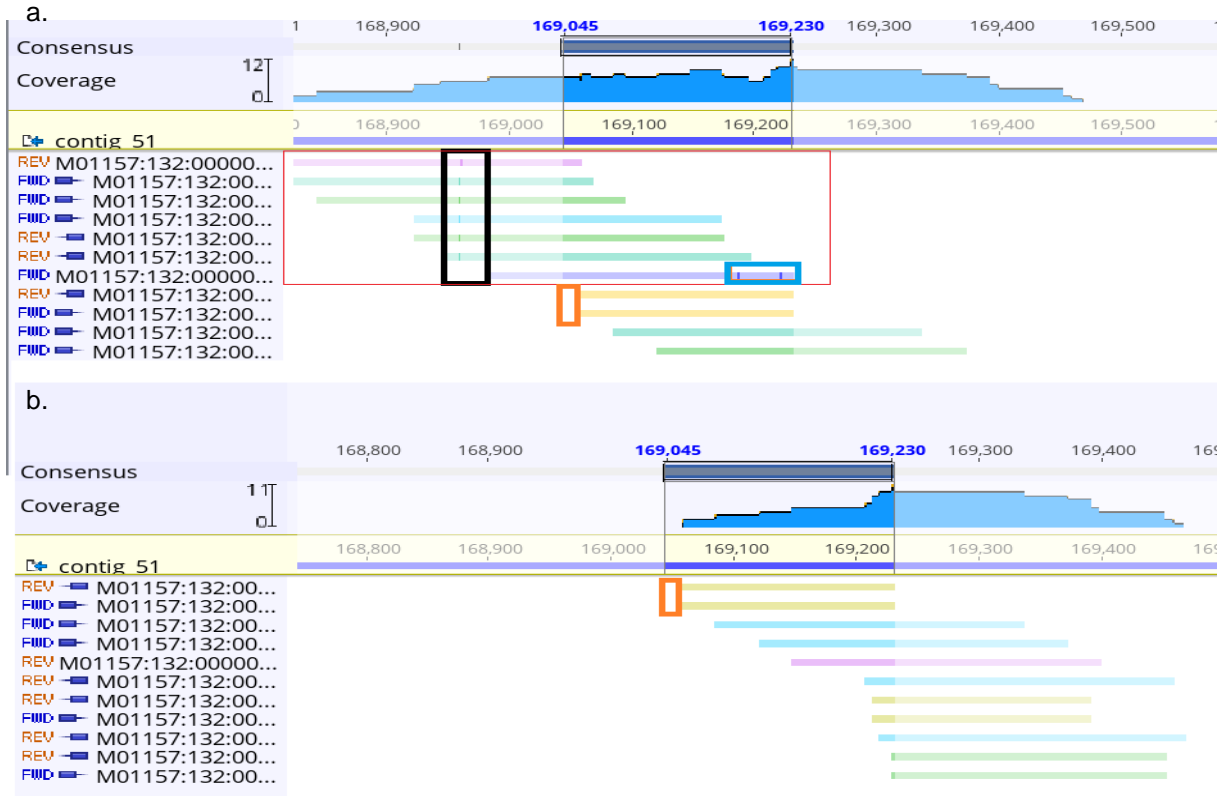


Figure B.7. PenSeq reads from SCRP283 for BC-16_contig_51_F623 RXLR gene. BC-16_contig_51_F623 is highlighted on the consensus (169,045-169,230). **a.** Reads mapped to contig_51 at 3 % mm mapping rate. **b.** Reads mapped to contig_51 at 0 % mm mapping rate. Dark and blue boxes highlight the SNPs on the reads, thus preventing the reads (in red box) from successfully mapping at 0 %mm and leaving a sequence gap (orange boxes). Gap is filled by reads (red box) mapped at 3 %mm. Blue box highlights a heterozygous SNP, where other reads matched to the contig. Graphs made with Geneious.

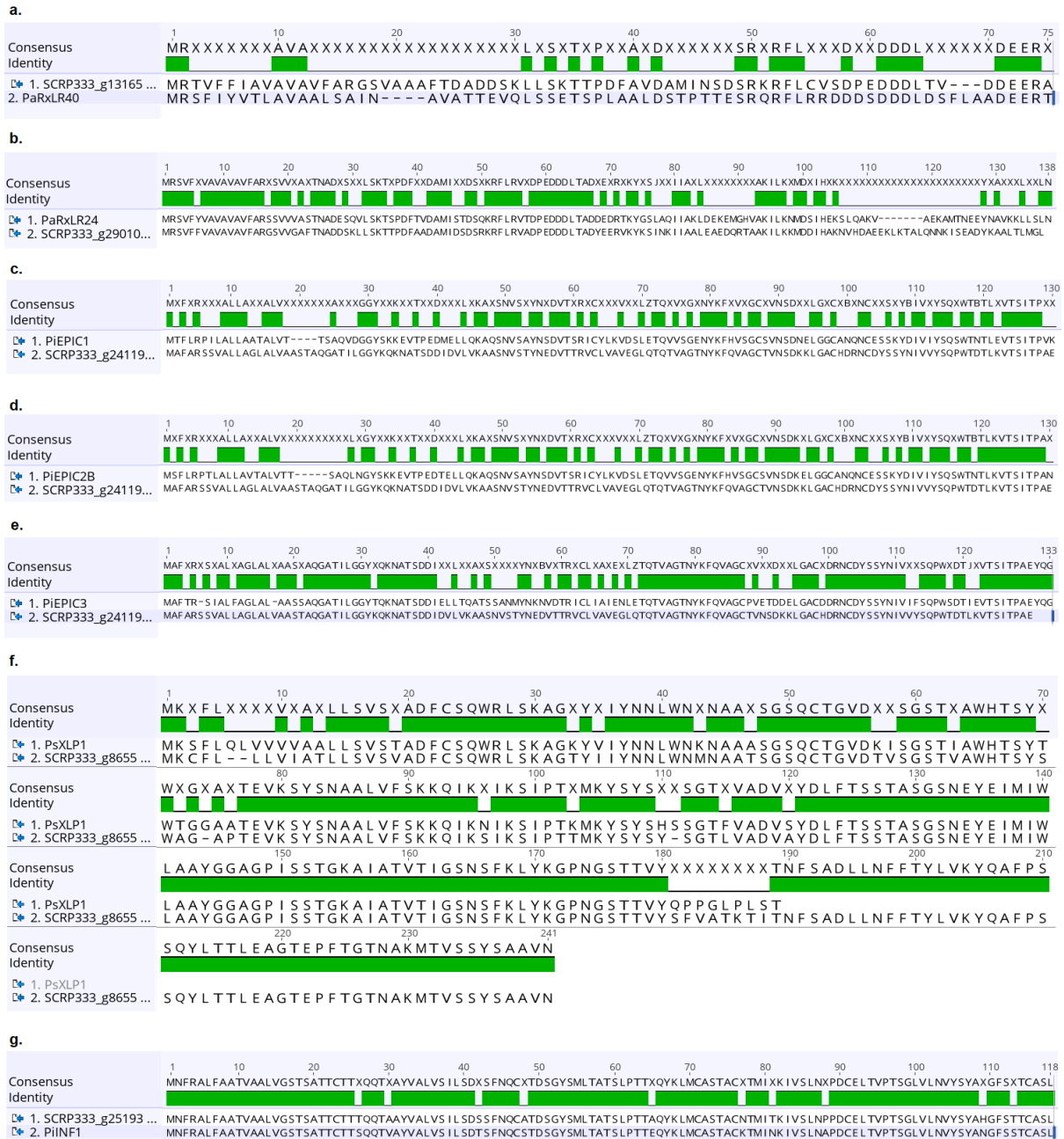


Figure B.8. Protein sequences alignment for PAMPs and apoplastic effectors. Protein alignments between published effectors and matching *P. rubi* proteins found through BLASTx and BLASTp searches (NCBI). a. *P. agathidicida* RXLR effector PaRxLR40 and *P. rubi* SCRP333_g13165. b. *P. agathidicida* RXLR effector PaRxLR24 and *P. rubi* SCRP333_g29010. c. *P. infestans* EPIC1 and *P. rubi* SCRP333_g24119. d. *P. infestans* EPIC2B and *P. rubi* SCRP333_g24119. e. *P. infestans* EPIC3 and *P. rubi* SCRP333_g24119. f. *P. sojae* XLP1 and *P. rubi* SCRP333_g8655. g. *P. infestans* INF1 and *P. rubi* SCRP333_g25193. Alignments drawn with Geneious.

Appendix C. HYDROPONIC INFECTION OF RASPBERRIES – Chapter 4

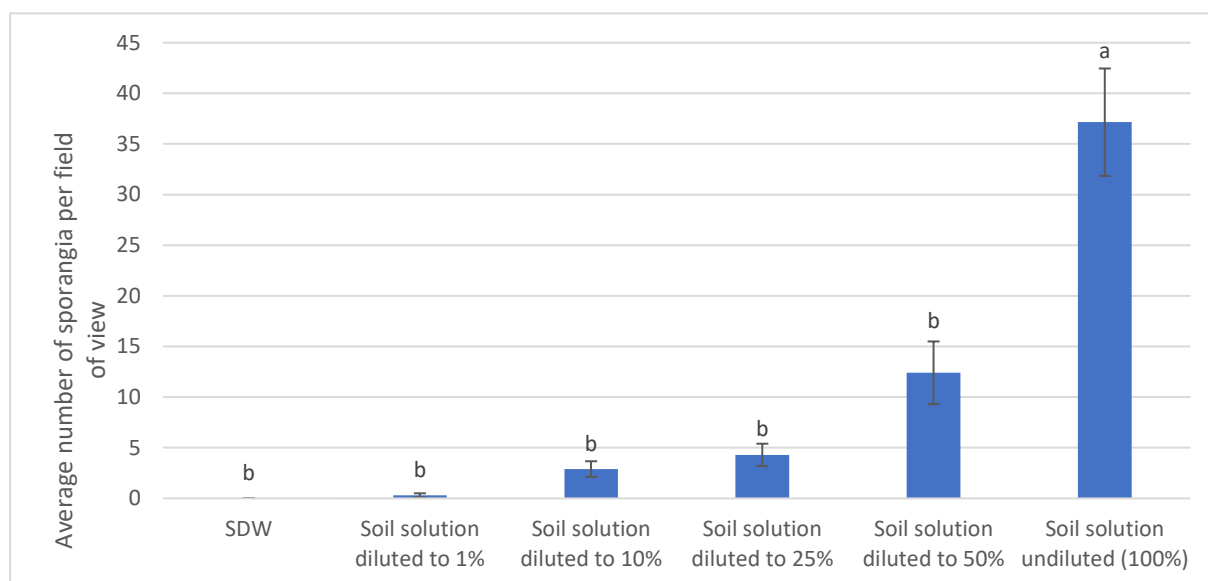


Figure C. 1. Bar chart of average number of sporangia for *P. rubi* isolate SCRP333 (per field of view per plug) incubated at 15 °C. Standard soil solution was diluted to 1%, 10%, 25%, 50% and undiluted. Sterile distilled water (SDW) was used as a negative control. One 150 mm Petri dishes of ten plugs each were used per modality (n = 10). Vertical bars represent the standard error of the mean. ANOVA and Tukey's HSD test were performed in R Studio v1.1.383 and statistical differences are given as labelled letters.

Table C.1. Results for cultivar Glen Moy grown hydroponically. a. Average percentage of cuttings surviving and rooting; b. average number of weeks for cuttings to root. Data in red in table a. indicate the best nutrient. Darkened cells in table b. indicate no data on weeks to root due to 0% of cuttings surviving.

a.						
Year	Month	MaxiCrop	Kristalon Red	Solufeed	Formulex	Water
2018	January					0.0
	February		4.3	7.7		0.0
	March		0.0	0.0		
	June					
	August	0.0	0.0			
	October	9.4	12.9	0.0		6.9
	November	0.0	40.0	0.0		0.0
	December	3.8	3.8	7.7	3.8	
trial 1 averages		3.3	10.2	3.1	3.8	1.7
2019	January	4.8	0.0	5.9		
	February	10.0	0.0	5.0		
	March	0.0	0.0	10.0		
	June	0.0		0.0		
	August	7.1		7.1		
	October	11.8	5.9	20.0		
	November	0.0	0.0	0.0		
	December	0.0	0.0	0.0		
trial 2 averages		4.2	1.0	6.0		
Overall averages		3.9	5.6	4.9	3.8	1.7
b.						
Year	Month	MaxiCrop	Kristalon Red	Solufeed	Formulex	Water
2018	January					
	February		13.0	12.5		
	March					
	June					
	August					
	October	11.0	11.25			12.0
	November		12.0			
	December	7.5	9.5	7.5	5.5	
trial 1 averages		9.3	11.4	10.0	5.5	12.0
2019	January	8.0		15.0		
	February	7.75		9.5		
	March			11.0		
	June					
	August	11.0		11.0		
	October	11.5	15.0	8.3		
	November					
	December					
trial 2 averages		9.6	15.0	11.0		
Overall averages		9.5	12.2	10.7	5.5	12.0

Table C.2. Results for cultivar Latham grown hydroponically. a. Average percentage of cuttings surviving and rooting; b. average number of weeks for cuttings to root. Data in red in table a. indicate the best nutrient. Darkened cells in table b. indicate no data on weeks to root due to 0% of cuttings surviving.

a.						
Year	Month	MaxiCrop	Kristalon Red	Solufeed	Formulex	Water
2018	January					0.0
	February		16.7	0.0		0.0
	March		12.5	38.9		
	June		11.1			
	August	14.3	12.5			
	October	9.1	40.0	75.0		
	November					
	December	0.0	0.0	0.0	0.0	
trial 1 averages		7.8	15.5	28.5	0.0	0.0
2019	January	14.3	13.3	16.7		
	February	12.5	12.5	25.0		
	March	30.0	0.0	0.0		
	June					
	August	60.0	0.0			
	October	42.0	15.6	19.2		
	November	11.1				
	December	0.0	0.0	27.3		
trial 2 averages		21.2	5.9	14.7	0	
Overall averages		17.6	10.3	20.2	0	0
b.						
Year	Month	MaxiCrop	Kristalon Red	Solufeed	Formulex	Water
2018	January					
	February		7.8			
	March		8.5	11.6		
	June		12.0			
	August	6.0	18.0			
	October	11.0	10.0	7.7		
	November					
	December					
trial 1 averages		8.5	11.3	9.7		
2019	January	10.8	6.8	15.0		
	February	16.0	9.5	7.3		
	March	6.0				
	June	9.7		10.4		
	August	8.8				
	October	5.1	4.8	5.2		
	November	8.5				
	December			7.2		
trial 2 averages		9.3	7.0	9.0		
Overall averages		9.1	9.7	9.2		

Table C.3. Results for cultivar Glen Dee grown hydroponically. a. Average percentage of cuttings surviving and rooting; b. average number of weeks for cuttings to root. Data in red in table a. indicate the best nutrient. Darkened cells in table b. indicate no data on weeks to root due to 0% of cuttings surviving.

a.					
Year	Months	MaxiCrop	Kristalon Red	Solufeed	Formulex
2018	October	16.7	20.0		
	December	33.3	60.0	33.3	33.3
2019	January	75.0	41.7	66.7	
	February	42.9	28.6	28.6	
	March	50.0	20.0	40.0	
	June			20.0	
	August	100.0		42.1	
	October	33.3	40.0	15.8	
	November	20.0	40.0	0.0	
	December	50.0	30.0	0.0	
Averages		46.8	35.0	27.4	
b.					
Year	Months	MaxiCrop	Kristalon Red	Solufeed	Formulex
2018	October	6	12		
	December	6	5.9	16	13.5
2019	January	10.2	9.5	8.75	
	February	13.3	14.8	5.5	
	March	9.7	13.2	9.6	
	June			10.5	
	August			8.7	
	October	9.75	8.75	5.9	
	November	7.4	9		
	December	11.5	12		
Averages		9.2	10.6	9.3	13.5

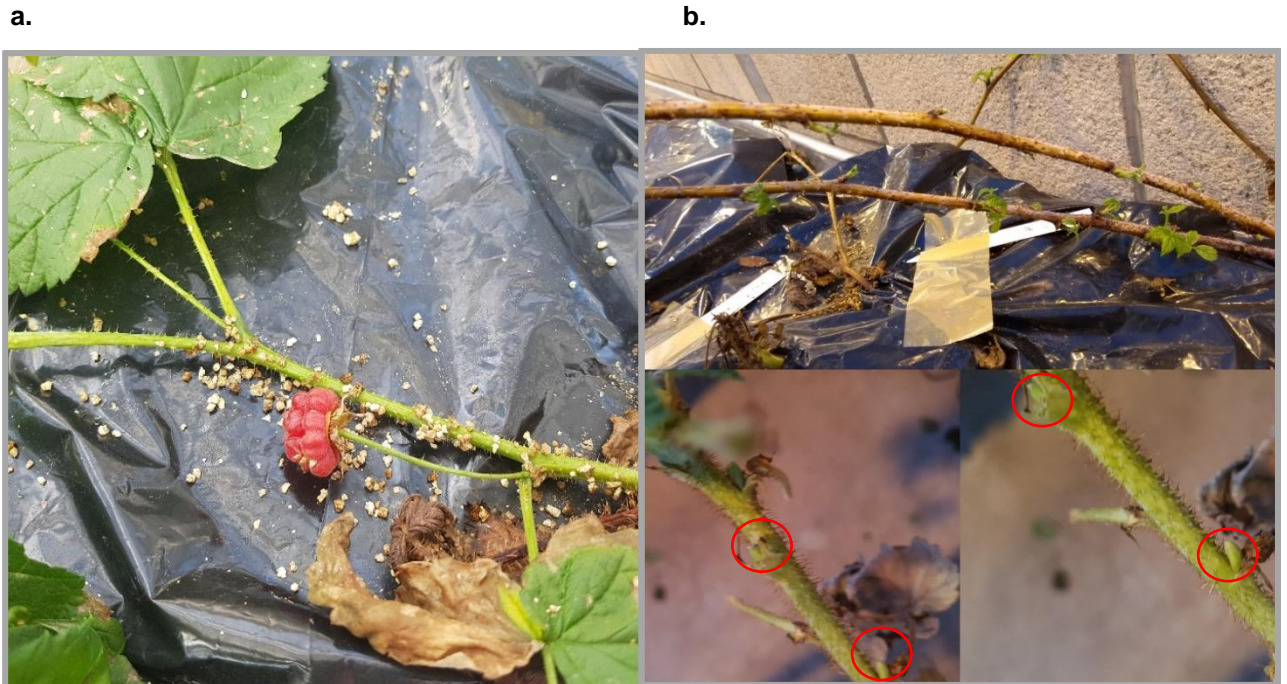


Figure C.2. a. Fruits and b. buds seen on raspberry plants following induced dormancy. Buds (b) were observed after 3 weeks stored in the cold glasshouse. Red circles show the buds on the raspberry canes. Fruits (a) were observed on the plants left to grow over the winter. The NFT tank of hydroponically grown raspberries was moved to a cold glasshouse for four weeks, (not heated) and thus subjected to outdoor temperatures in October and November 2018, ranging from $-1.9\text{ }^{\circ}\text{C}$ to $15.3\text{ }^{\circ}\text{C}$, with an average of $9.6\text{ }^{\circ}\text{C}$ in October and $7.7\text{ }^{\circ}\text{C}$ in November. After four weeks, they were moved to a $4\text{ }^{\circ}\text{C}$ dark cold store with the hydroponic system disconnected. After another seven weeks in the cold store, plants in the hydroponic tank were brought back to normal hydroponic growth temperatures progressively: a first week at $10\text{ }^{\circ}\text{C}$ was followed by another week where temperature was set at $15\text{ }^{\circ}\text{C}$ before plants were finally placed back at $18\text{--}20\text{ }^{\circ}\text{C}$.